Aerial vehicle guidance problem through the Pontryagin Maximum Principle and Hamilton Jacobi Bellman approach

Veljko Aškovic

École doctorale Science Mathématiques de Paris Centre (ED nº 386)

Doctorat Sorbonne Université

THÈSE

pour obtenir le grade de docteur délivré par

Sorbonne Université

Spécialité doctorale "Mathématiques Appliquées"

présentée et soutenue publiquement par

Veljko AŠKOVIĆ

le 18 décembre 2023

Aerial vehicle guidance problem through the Pontryagin Maximum Principle and Hamilton Jacobi Bellman approach

Directeur de thèse : **Emmanuel TRÉLAT**
Co-Directrice de thèse : **Hasnaa ZIDANI**

Jury

Joseph Gergaud	Professeur	Rapporteur
Maria do Rosario de Pinho	Professeur	Rapporteur
Mario Sigalotti	Directeur de recherche Inria	Examinateur
Frédéric Jean	Professeur	Examinateur
Max Cerf	Ingénieur ArianeGroup	Examinateur
Stéphane L. M.	Ingénieur Mbda	Examinateur

Laboratoire Jacques Louis Lions
CNRS UMR 7598, 4 place Jussieu, 75005 France

Remerciements

Je tiens à adresser mes remerciements en tout premier lieu à mes deux directeurs de thèse Emmanuel Trélat et Hasnaa Zidani qui ont su diriger mes travaux avec beaucoup de compétence, patience et gentillesse pendant ces années de thèse.

Je remercie Emmanuel pour son expertise scientifique, sa grande disponibilité, sa bienveillance, ses constants encouragements et enfin une pédagogie exceptionnelle. Je souhaite souligner ici son immense culture mathématique mais également son pragmatisme et ouverture d'esprit permettant d'appréhender la spécificité des problèmes rencontrés en ingénierie.

Je remercie Hasnaa de m'avoir chaleureusement accueilli à l'Unité de Mathématiques Appliquées de l'ENSTA Paris et de m'avoir fait confiance pour débuter cette thèse. Je rends hommage à la qualité de l'encadrement scientifique qu'elle a assuré durant la première partie mes travaux, mais également à la pertinence de ses remarques et conseils prodigués tout au long de mes recherches. J'en profite pour remercier deux membres de son équipe, Anya Désilles et Olivier Bokanowski, pour leur compétence scientifique et l'aide qu'ils ont su m'apporter.

Je remercie Mme Maria do Rosario de Pinho, Professeur à l'Université de Porto, ainsi que M. Joseph Gergaud, Professeur à l'Université de Toulouse, pour m'avoir fait l'honneur d'être rapporteurs de ma thèse, ainsi que M. Mario Sigalotti, Directeur de recherche Inria, M. Stéphane L. M., Ingénieur Mbda et M. Max Cerf, Ingénieur ArianeGroup pour avoir accepté d'en être examinateurs. Je suis très honoré que M. Frédéric Jean, Professeur à ENSTA ParisTech, m'ait fait l'honneur de présider le jury de thèse.

Cette thèse n'aurait pas vu le jour sans le support d'Alexandre K., mon responsable hiérarchique à MBDA France. Alexandre, merci infiniment de ton soutien indéfectible et de ta résilience afin que ce projet puisse aller à son terme. Je remercie également Stéphane avec qui les premiers contacts ont été établis en vue de ce projet. Enfin, j'exprime ma gratitude à Bénédicte, qui a oeuvré en interne afin que les techniques étudiées dans cette thèse puissent être présentées au sein de l'entreprise.

Je voudrais ré-itérer ma gratitude à Frédéric Jean de m'avoir accueilli au laboratoire et mis dans les conditions idéales pour réaliser la première partie de mon doctorat. J'en profite pour remercier pour leur gentillesse les personnes du laboratoire avec qui j'ai eu la chance d'échanger: Anne-Sophie Bonnet Ben Dhia, Maryna Kachanovska, Laurent Bourgeois, Laure Giovangigli, Christophe Hazard, Nicolas Kielbasiewicz, Zacharie Alès, Sourour Elloumi, Jean François Mercier, Jérôme Perez, Pierre Carpentier, Benjamin Bonrepaux, Maurice Diamantini, Tof, Tatiana Grard (scolarité) et bien d'autres que j'oublie certainement. Enfin, comment ne pas citer ici Corinne Chen, l'assistante du département sans qui le laboratoire ressemblerait à une piste sans danseurs ou pire-une chanson sans accords majeurs!

J'ai une pensée pour tous ceux que j'ai pu croiser (ou pas!) au cours de cette aventure et qui ont contribué de près ou de loin à la rendre encore plus agréable: Nidhal, Othmane, Senan, Didier, Dogmaster, Tochiba, le Renard Argenté, Yoyo, Audrey Lamy, le Chou farci, Dominique, Adrien, Nana, Prigo et Vlad The Great...

Je remercie mes fils Lucas et Marco, ma compagne Elisa et mon chat Lilypute pour leur patience. J'ai une pensée pour mon frère Marko.

Enfin, je dédie ce manuscrit à la mémoire de mes chers parents Andja et Radomir.

Contents

Contents 5

List of Figures 9

List of Tables 11

General Introduction 13
- 0.1 Two-term large-time expansion of the value fonction for general nonlinear optimal control problems . . . 13
  - 0.1.1 State of the art . . . 13
  - 0.1.2 Contributions of the thesis . . . 14
  - 0.1.3 Linear Quadratic (LQ) case . . . 15
  - 0.1.4 The general nonlinear case . . . 15
- 0.2 Numerical methods in aerial vehicle guidance problem . . . 16
  - 0.2.1 State of the art . . . 17
  - 0.2.2 Analysis of the problem, difficulties and contributions of the thesis . . . 17

1 Value function expansion in large time optimal control problems 19
- 1.1 Introduction . . . 20
  - 1.1.1 Turnpike phenomenon . . . 20
  - 1.1.2 Value function behavior . . . 22
- 1.2 Linear quadratic case . . . 24
  - 1.2.1 Setting . . . 24
  - 1.2.2 Main result . . . 24
  - 1.2.3 The steady optimisation problem . . . 25
  - 1.2.4 Proof of the main result . . . 26
  - 1.2.5 Numerical example . . . 29
- 1.3 Dissipative nonlinear systems . . . 31
  - 1.3.1 Setting of the problem . . . 31
  - 1.3.2 Assumptions . . . 32
  - 1.3.3 Comments . . . 33
  - 1.3.4 Main result . . . 34
  - 1.3.5 Some useful lemmas . . . 34
  - 1.3.6 Proof of the main result . . . 36

2 Missile guidance problem 41
- 2.1 Introduction . . . 42
- 2.2 Guidance principles . . . 42
- 2.3 Surface to air missile . . . 43
- 2.4 Cruise missile . . . 43
  - 2.4.1 Presentation . . . 43
  - 2.4.2 Mission data preparation . . . 44
- 2.5 Equations of the motion and environment model . . . 44

2.5.1 Assumptions and Coordinate systems . . . 44
2.5.2 Kinematic equations . . . 45
2.5.3 Dynamic equations . . . 46
2.5.4 Flight in the vertical plane . . . 47
2.5.5 Discussion of the equations of motion . . . 48
2.5.6 Atmosphere model . . . 49
2.6 Context of the study . . . 50
2.7 Global trajectory optimization . . . 51
2.8 Mathematical setting . . . 51
2.9 Numerical values . . . 52

3 Numerical solving of the guidance problem 55
3.1 Optimal control in finite dimension . . . 57
3.1.1 General setting . . . 57
3.1.2 Pontryagin maximum principle . . . 58
3.2 Numerical methods in optimal control . . . 59
3.2.1 Context . . . 59
3.2.2 Direct methods . . . 60
3.2.3 Indirect methods . . . 60
3.2.4 Methods implemented in the thesis . . . 61
3.3 Continuation methods . . . 62
3.3.1 Existence results and discrete continuation . . . 62
3.3.2 Numerical tracking of the zero paths . . . 62
3.4 Dubins-Fuller problem . . . 64
3.4.1 Motivation and definition of the model . . . 64
3.4.2 Dubins case $(k_0, k_1) = (1,0)$ . . . 65
3.4.2.1 State of the art . . . 65
3.4.2.2 Direct method . . . 66
3.4.2.3 Shooting method . . . 67
3.4.2.4 Numerical implementation . . . 68
3.4.2.5 Numerical tests . . . 68
3.4.3 Fuller case $(k_0, k_1) = (0,1)$ . . . 69
3.4.3.1 Direct method . . . 69
3.4.3.2 Comments . . . 70
3.4.3.3 Optimal synthesis in the Fuller case . . . 71
3.4.4 Dubins-Fuller case, $k_0 > 0$, $k_1 > 0$ . . . 72
3.4.4.1 Formal analysis . . . 72
3.4.4.2 Direct method . . . 73
3.4.4.3 Numerical solving strategy: L^2 regularization and shooting method . . . 76
3.4.4.4 Continuation at step 1 . . . 78
3.4.4.5 Well posedness of the shooting method . . . 78
3.4.4.6 Optimal solution for $\lambda_1 = 1.0$ . . . 79
3.4.4.7 Continuation at step 2 . . . 80
3.4.4.8 Comments . . . 81
3.5 The missile guidance problem . . . 82
3.5.1 Parametrized dynamics . . . 82
3.5.2 Numerical solving strategy . . . 82
3.5.3 The minimum time problem . . . 83
3.5.4 The “bunt” case . . . 85
3.5.4.1 Continuation at step 1 . . . 86
3.5.4.2 Continuation at step 2 . . . 88
3.5.4.3 Comments and perspectives . . . 90
3.5.5 Computation of a quasi optimal trajectory by a reduced shooting method . . . 90

4 Hamilton Jacobi Bellman approach **93**
4.1 A global approach . . . 94
4.1.1 Introduction . . . 94
4.1.2 Dynamic Programming Principle . . . 94
4.1.3 Theoretical elements related to the Hamilton Jacobi Bellman (HJB) approach 95
4.1.4 Minimum time trajectories reconstruction from the value function . . . 96
4.2 An application: reachable sets for the vehicle in level flight . . . 97
4.2.1 Minimum time problem . . . 97
4.2.2 Numerical Hamiltonian . . . 98
4.2.3 Spatial grid . . . 98
4.2.4 Reachable sets . . . 98
4.2.5 Minimum time trajectories . . . 99
4.3 HJB approach for optimal control problems with state constraints . . . 101
4.3.1 Motivation . . . 101
4.3.2 Mathematical setting . . . 101
4.3.3 Assumptions . . . 101
4.3.4 General considerations and notations . . . 102
4.3.5 Time variable change . . . 102
4.3.6 State constrained case . . . 104
4.3.7 A particular case: the target capture bassin . . . 105
4.3.8 Optimal trajectories reconstruction from the value function . . . 106
4.3.9 Numerical scheme . . . 106
4.4 An application: optimisation of a glider trajectory . . . 106
4.4.1 Setting . . . 106
4.4.2 HJB equation . . . 107
4.4.3 Numerical Hamiltonian . . . 108
4.4.4 Computation domain and numerical results . . . 108
4.4.5 Comments . . . 110

Conclusion and perspectives **111**

A Appendix **113**
A.1 Some useful results . . . 113
A.2 On the need of viscosity solutions in the HJB framework . . . 115
A.3 Computation of the Jacobian of the shooting function . . . 116
A.4 Solving Dubins-Fuller (DF) with multiple shooting . . . 118
A.5 Guidance problem with the control in dimension 2 . . . 119
A.6 Existence, regularity and uniqueness of the solution to the HJB equation . . . 122
A.6.1 Definition . . . 122
A.6.2 Regularity . . . 122
A.6.3 Existence . . . 123
A.6.4 Uniqueness . . . 125

B Acronym List **127**

List of Figures

1 Turnpike illustration: (a) small time case (b) large time case . . . 14

1.1 Highway to Hell . . . 21
1.2 Optimal trajectory . . . 23
1.3 Turnpike phenomenon . . . 23
1.4 Optimal triple for some values of T . . . 29
1.5 Value function expansion error . . . 30
1.6 Construction of an admissible trajectory for $\left(\mathscr{P}^{x,z}_{[0,\mathrm{T}]}\right)$ . . . 38

2.1 Artist view of the M 51 ballistic missile . . . 42
2.2 Guidance principle . . . 43
2.3 Coordinate systems . . . 45
2.4 Forces acting on the vehicle in flight . . . 47
2.5 Atmospheric air density and pressure function of h . . . 49
2.6 A-Profile typical trajetory . . . 50
2.7 B-Profile typical trajetory . . . 50

3.1 Continuation with linear prediction . . . 64
3.2 Illustration of optimal paths . . . 66
3.3 Optimal state, costate & control for $(k_0,k_1)=(1,0)$ . . . 67
3.4 Optimal solution . . . 69
3.5 Optimal state, costate & control for $(k_0,k_1)=(0,1)$ . . . 70
3.6 Chattering phenomenon . . . 71
3.7 Optimal synthesis for the Fuller's problem . . . 72
3.8 Optimal state, costate & control for $k_0=1$, $k_1=0.1$ . . . 74
3.9 Optimal state, costate & control for $k_0=1$, $k_1=1$ . . . 74
3.10 Optimal state, costate & control for $k_0=1$, $k_1=10$ . . . 75
3.11 Optimal state, costate & control for $k_0=1$, $k_1=100$ . . . 75
3.12 Singular values of the Jacobian for different values of k_2 . . . 79
3.13 Optimal state, control and adjoint state for $\lambda_1=1$ . . . 80
3.14 Optimal state, control and adjoint state for $\lambda_2=1$ . . . 81
3.15 Trajectory, control & switching function samples . . . 84
3.16 Shooting vs direct method comparison on minimum time problem . . . 85
3.17 Samples of optimal trajectory and control . . . 87
3.18 Optimal state, control and adjoint state for $\lambda=1$ . . . 88
3.19 Optimal state, control and adjoint state for $\delta=1$ . . . 89
3.20 State and control: Shooting vs direct method . . . 92

4.1 Illustration of the Dynamic Programming Principle . . . 94
4.2 Reachable sets . . . 99
4.4 Glider range optimisation: case 1 . . . 109
4.5 Glider range optimisation: case 2 . . . 109

A.1 Value function . . . 115

A.2 Non uniqueness of lipschitzian solutions 116
A.3 Multiple shooting for the Dubins-Fuller problem 118
A.4 Samples of optimal state & control (continuation) 120
A.5 Final optimal state, costate & control 120

List of Tables

2.1 Numerical values for the guidance problem 52

3.1 Final accuracy of the shooting (step 1) 80
3.2 Final accuracy of the shooting (step 2) 81
3.3 Final accuracy 85
3.4 Final accuracy of the shooting (step 1) 88
3.5 Final accuracy of the shooting (step 2) 90

A.1 Final shooting accuracy with the control in dimension 2 121

General Introduction

Control theory can be defined as the way of acting on systems in order to steer them from an initial state to a final state. To park a car, to heat a room, etc., the possibilities of applications are at least as numerous as the ways to describe things that happen in real life. This makes it a field at the interface between various fields (aeronautics, biology, structural calculation, economics, etc.) by mixing fundamental and more applied mathematics. In a world that is increasingly competitive and in search of performance, the question of optimizing the action on a system naturally arises and the optimal control theory aims at providing precise answers. In parallel with the progress made in functional and numerical analysis, it is becoming easier to describe mathematically what we observe in reality. This thesis is part of the broad field of optimal control of ordinary differential equations, both from a theoretical and numerical point of view and is divided into two main contributions. First, we study the asymptotic behavior of the value function associated to an optimal control problem within the class of *dissipative* dynamical systems. Second, the question of implementing efficient numerical methods for aerial vehicle guidance has led us to exploit both direct and indirect numerical methods. Amongst the latter, we focus on the shooting method based on the Pontryagin Maximum Principle (PMP) and its implementation by using continuations. Finally the last part is devoted to some numerical experiments based on the Hamilton Jacobi Bellman (HJB) approach.

0.1 Two-term large-time expansion of the value fonction for general nonlinear optimal control problems

0.1.1 State of the art

The question of the asymptotic behavior of the value function has been widely studied from the Partial Differential Equations (PDE) point of view, mainly within the frame of HJB ([56], [38], [65]) or ergodic theory ([11]). For instance in Chapter VII of [56], the authors consider the infinite time horizon optimal control problem with discounted Lagrange cost. To characterize the ergodic behavior of the value function, the authors pass to the limit as the discount factor tends to zero and characterize the limit value function as the viscosity solution of the limit equation. In [38], under suitable assumptions amongst which some periodicity assumptions on the Hamiltonian, the authors characterize the large time behavior of the solution of the first-order HJB equation as the solution of a stationary HJB equation. The extension of the results to the deterministic zero-sum differential games with two conflicting controllers has been studied for instance in [65]. It can be noticed that more general results exist, for instance in [69], where the authors show that, under adequate assumptions, there is at most one possible accumulation point of the values (in the uniform convergence topology), when the time horizon of the Cesaro means converges to infinity or the discount factor of the Abel means converges to zero.

From a classical optimal control point of view, the large time behavior of the value function is usually deduced as a consequence of a property that is satisfied by a wide class of optimal control problems and arises when the time horizon is sufficiently large. This is the so-called *turnpike property*, which reflects the fact that, for suitable optimal control problems in a sufficiently large time horizon, any optimal solution thereof remains, most of the time, close to the optimal solution

of an associated *static optimization* problem. This optimal static solution is referred to as the turnpike (the name stems from the idea that a turnpike is the fastest route between two points which are far apart, even if it is not the most direct route, see Figure 1).

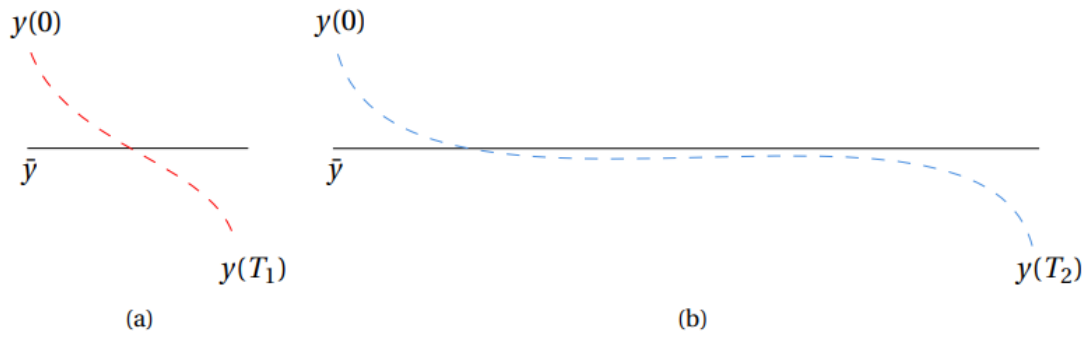

Figure 1: Turnpike illustration: (a) small time case (b) large time case

The turnpike phenomenon was first observed and investigated by economists for discrete-time optimal control problems (see [68], [63]). There are several possible notions of turnpike properties, some of them being stronger than the others (see [88]). Exponential turnpike properties have been established in [48], [9], [8], [29] and [30] for the optimal triple resulting of the application of PMP, ensuring that the extremal solution (state, adjoint and control) remains exponentially close to the optimal solution of the corresponding static controlled problem, except at the beginning and at the end of the time interval, as soon as the time horizon T is large enough. As unravelled in [29], this phenomenon is closely related to hyperbolicity properties of the Hamiltonian flow. For discrete-time problems it has been shown for instance in [78], [50] that the exponential turnpike property is also closely related to a strict dissipativity property. Measure-turnpike is a weaker notion of turnpike, meaning that any optimal solution, along the time frame, remains close to the optimal static solution except along a subset of times of small Lebesgue measure. It has been proved in [79], [28] that measure turnpike follows from strict dissipativity or from strong duality properties.

Based on the turnpike property, an equivalent as $T \to +\infty$ of the value function has been derived for instance in [8] or [29].

To our knowledge, the most advanced result related to the asymptotic expansion of the value function in large time has been obtained in [18]. In this paper, the authors consider the LQ problem with prescribed initial state x and free final state. A terminal cost is added to the running quadratic cost. By denoting $v(.)$ the value function, it is proved that

$$v(T,x) \underset{T\to+\infty}{\approx} T.\bar{v} + W(x) + \lambda \tag{1}$$

where $\bar{v}$ is the minimum of the static optimization problem, $W(x)$ is the cost to stabilize the system from the initial point x towards the turnpike and $\lambda = \lim_{T\to+\infty} V(T,\bar{y}) - \bar{v}.T$. We mention that the above result is proved by exploiting the exponential turnpike inequality enjoyed by the dynamical system.

0.1.2 Contributions of the thesis

In our framework, we consider the finite-dimensional optimal control problem consisting of minimizing the cost functional:

$$J_{T,x,z}(u) = \int_0^T f^0(y(t),u(t))\,dt \tag{2}$$

over the time interval $[0,\mathrm{T}]$, $\mathrm{T}>0$ being fixed under the dynamical constraints:

$$\dot{y}(t) = f(y(t),u(t)) \tag{3a}$$
$$y(0) = x \text{ and } y(\mathrm{T}) = z \tag{3b}$$

where $y(t)\in\mathbb{R}^n$ and $u(t)\in\mathbb{R}^p$. The value function of the optimal control problem (2)- (3) is defined by:

$$v(\mathrm{T},x,z) := \min_{u(.)\in\mathscr{U}_\mathrm{T}} \mathrm{J}_{\mathrm{T},x,z}(u) \tag{4}$$

where $\mathscr{U}_\mathrm{T} := \mathrm{L}^\infty([0,\mathrm{T}],\Omega)$ with Ω compact subset of $\mathbb{R}^p$. Moreover, we assume the existence and uniqueness of the solution (denoted by $(\bar{y},\bar{u})$) to the *static optimization problem*:

$$\bar{v} := \min_{f(y,u)=0} f^0(y,u) \tag{5}$$

The contributions of the thesis are the following (hereafter we give only the main results, the exhaustive list of assumptions, explanations and comments will be provided in chapter 1):

0.1.3 LQ case

We consider the linear quadratic case, that is:

$$\begin{aligned} f(y,u) &:= \mathrm{A}y+\mathrm{B}u \\ f^0(y,u) &:= \frac{1}{2}(u-d)^*\mathrm{U}(u-d)+\frac{1}{2}(y-c)^*\mathrm{Q}(y-c) \end{aligned} \tag{6}$$

The analysis is based on the Hamiltonian nature of the extremal equations of the PMP and some classical results of the LQ theory. We provide the expansion of $\frac{1}{\mathrm{T}}.v(\mathrm{T},.)$ at order one in $1/\mathrm{T}$ and we identify precisely all the terms of the expansion. We highlight that we assume neither the existence of the turnpike nor the exponential inequality (which is a stronger assumption). Even better, the latter appears as an intermediate result.

We prove the following value function expansion:

$$v(\mathrm{T},x,z) \underset{\mathrm{T}\to+\infty}{=} \mathrm{T}.\bar{v} + \underbrace{\mathrm{F}(x)+\langle\bar{\lambda},\bar{y}-x\rangle}_{\text{Initial cost}} + \underbrace{\mathrm{B}(z)+\langle\bar{\lambda},z-\bar{y}\rangle}_{\text{Final cost}} + \mathrm{o}(1) \tag{7}$$

where:

$$\begin{cases} \mathrm{F}(x) := \min\limits_{\tilde{u}_1(.)} \dfrac{1}{2}\displaystyle\int_0^{+\infty} \left(\|\tilde{u}_1(t)-\bar{u}\|_\mathrm{U}^2 + \|\tilde{y}_1(t)-\bar{y}\|_\mathrm{Q}^2\right) dt \\ \dot{\tilde{y}}_1 = \mathrm{A}\tilde{y}_1+\mathrm{B}\tilde{u}_1, \quad \tilde{y}_1(0)=x \end{cases} \tag{8}$$

and

$$\begin{cases} \mathrm{B}(z) := \min\limits_{\tilde{u}_2(.)} \dfrac{1}{2}\displaystyle\int_0^{+\infty} \left(\|\tilde{u}_2(t)-\bar{u}\|_\mathrm{U}^2 + \|\tilde{y}_2(t)-\bar{y}\|_\mathrm{Q}^2\right) dt \\ \dot{\tilde{y}}_2 = -\mathrm{A}\tilde{y}_2-\mathrm{B}\tilde{u}_2, \quad \tilde{y}_2(0)=z \end{cases} \tag{9}$$

$\bar{\lambda}$ being the optimal Lagrange multiplier in the steady optimization problem (5).

0.1.4 The general nonlinear case

In the nonlinear case, the key assumption is the *strict dissipativity* property enjoyed by (2)-(3a). This concept, first introduced in [86], is defined in a general setting, alongside associated concepts such as the available storage and the supply rate function. When a system is dissipative with a given supply rate function, the question of finding a storage function has been extensively studied. This question is similar to the problem of finding a suitable Lyapunov function in the Lyapunov second method ensuring the stability of a system. A precise mathematical definition will be given

in the chapter 1. At this step, we mention that strict dissipativity was used in the literature (see [78], [49], [79], [50] and [28]) to derive turnpike properties.

We generalize the previous result within the class of *dissipative* nonlinear dynamical systems by proving the following result

$$v(\mathrm{T},x,z) \underset{\mathrm{T}\to+\infty}{=} \mathrm{T}.\bar{v} + v_f(x) + v_b(z) + \mathrm{o}(1) \tag{10}$$

where

$$\begin{aligned} v_f(x) &:= \min_{u(.)} \int_0^{+\infty} w(y(t),u(t))dt \\ \dot{y}(t) &= f(y(t),u(t)), \quad y(0) = x \end{aligned} \tag{11}$$

and

$$\begin{aligned} v_b(z) &:= \min_{u(.)} \int_0^{+\infty} w(y(t),u(t))dt \\ \dot{y}(t) &= -f(y(t),u(t)), \quad y(0) = z \end{aligned} \tag{12}$$

with $w(y,u) := f^0(y,u) - f^0(\bar{y},\bar{u})$.

0.2 Numerical methods in aerial vehicle guidance problem

Our objective is to design an algorithm able to solve automatically the problem of guidance of an aerial vehicle with prescribed initial and terminal conditions. The aerial vehicle is modelled as a single input control-affine dynamical system in dimension 5 with a constraint on the control. The trajectory is considered in the vertical plane and is controlled through the angle of attack. More precisely, the optimal control problem is the following:

$$(\mathbf{OCP})_0 \begin{cases} \min\limits_{(t_f,\alpha\in\mathscr{A})} \mathrm{J}_0(t_f,\alpha) := \displaystyle\int_0^{t_f} \left(k_0 + k_1.\frac{(h(s)-h_c)^2}{h_c^2}\right) ds \\ \dot{\xi}(s) = f(\xi(s),\alpha(s)) \qquad \forall s\in[0,t_f] \\ \alpha(.)\in\mathscr{A} \\ \xi(0) = \xi_0, \quad \xi(t_f) = \xi_f \end{cases} \tag{13}$$

where:

- $\mathscr{A}$ is a set of admissible control strategies defined as $\mathscr{A} := \{\alpha : [0,+\infty[\to \mathrm{A}\}$ with A compact subset of $\mathbb{R}$
- $f(\xi,\alpha) := \begin{pmatrix} v.\cos\gamma \\ v.\sin\gamma \\ \dfrac{\mathrm{T}_{\max}.(1+\mathrm{C}_s.v) - \mathrm{D}(h,v,\alpha)}{m} - g.\sin\gamma \\ \dfrac{\mathrm{L}(h,v,\alpha_2)}{m.v} - \dfrac{g.\cos\gamma}{v} \\ -\mathrm{C}_s.\mathrm{T}_{\max} \end{pmatrix}$ is the dynamics
- ξ_0 and ξ_f are the prescribed initial and final states.
- $(k_0,k_1)\in\mathbb{R}^+\times\mathbb{R}^+$ is the weight couple in the performance index. k_0 and k_1 weight respectively the time of flight and the deviation to the cruise altitude.

All the terms of the above setting will be precised in chapter 2.

The originality of the problem and its link with the theoretical part of the thesis is the appearance, when the time horizon T is large enough, of a middle partial turnpike arc (meaning a turnpike only on some state coordinates but not all of them) which is quasi-singular in a sense to be made precise. A trajectory arc is *singular* when the linearized system along this arc is not controllable (see chapter 3 or [82], [32]).

0.2.1 State of the art

It is usual to distinguish between two main types of numerical methods for solving optimal control problems: indirect methods and direct methods (see e.g. [16], [83]). The direct methods consist of discretizing the state and the control and thus of reducing the problem to a nonlinear optimization problem (nonlinear programming) with constraints. The indirect methods consist of numerically solving a boundary value problem obtained by applying the PMP, by means of a (single or multiple) shooting method . Roughly speaking, the advantages of the indirect methods are their execution speed and their numerical accuracy whereas the advantages of the direct methods are the simplicity of the implementation and their relative robustness to the initialization.

The main difficulty of shooting methods (which rely on a Newton type resolution) is to initialize them successfully. It is well known that in general they have to be combined with other theoretical or numerical approaches (see [83]), such as continuation method, which is a very powerful tool to be combined with the PMP. The idea of numerical continuation, or homotopy method, is to solve a difficult problem step by step by starting from a simpler problem by parameter deformation. A general presentation of homotopic methods can be found for instance in [42]. In [57], [80], [67] or [43] the continuation method is used to solve challenging orbit transfer problems. In [46], [6], [5] several continuations are used to introduce the atmospheric effects and the path constraints related terms for solving the endo-atmospheric launch vehicle ascent problem starting from a nearly analytic solution.

0.2.2 Analysis of the problem, difficulties and contributions of the thesis

Even though we implement direct methods, we focus in this thesis on the shooting method combined with various continuations. The main reasons for this choice are the enhanced accuracy and its potential to compute almost instantaneously a solution compliant with the real time implementation. These requirements cannot, in general, be met with direct methods as soon as the problem becomes too much complex. We hightlight here that the optimal control problem $(\mathbf{OCP})_0$ is already simplified with respect to more sophisticated models.

The originality of our approach is to first study a simpler optimal control problem in dimension 3 that we call the DF case, which is a meaningful reduction of the initial problem $(\mathbf{OCP})_0$. More precisely, (DF) is defined as:

$$\begin{aligned} &\min_{t_f,\alpha(.)} \mathrm{J}_{k_0,k_1}(t_f,\alpha) := \int_0^{t_f} k_0 + k_1 . \left(\frac{h(s)-h_c}{h_c} \right)^2 ds, \quad k_0 \geqslant 0, \quad k_1 \geqslant 0 \\ &\dot{x} = v.\cos\gamma, \quad \dot{h} = v.\sin\gamma, \quad \dot{\gamma} = \alpha, \quad |\alpha| \leqslant 1, \text{ with boundary conditions} \end{aligned} \tag{14}$$

where $v > 0$ is the longitudinal speed, assumed to be fixed. (x, h, γ) are the state variables defining respectively the position and the pitch angle of the vehicle. We aim at finding the optimal solution connecting prescribed initial and final states.

First we analyse and solve this interesting case and then we use some appropriate numerical continuations in order to "connect" it with the initial guidance problem.

Difficulties: First, the Hamiltonian of the system being linear in the control, the optimal structure arising from the application of the PMP may not be continuous, more precisely may be a succession of bang and singular arcs. The implementation of the shooting method is a challenge in such conditions (see e.g. [32]). We mention here that, even if a direct method remains an interesting alternative, singular arcs, when they occur, are in general not accurately computed by this method as illustrated in the chapter 3.

Second, as mentioned before, we infer (from direct method simulations) the appearance of a partial turnpike arc in the middle of the optimal trajectory. This raises a question of efficient implementation of the shooting method when the time horizon T is large (see for instance the numerical example in dimension 2 in [29]).

Finally, another major difficulty we encounter is the appearance of the chattering phenomenon when $k_1 \longrightarrow +\infty$. Chattering means that the control switches an infinite number of times over a compact time interval. These phenomena have been widely studied in the literature (see for instance [37], [61], [58]). Note that chattering raises serious issues for the convergence of numerical methods. According to [64], the difficulty is in particular due to the numerical integration of the discontinuous Hamiltonian system because the chattering solutions worsen the approximation and error estimates for standard numerical integration method.

Contributions of the thesis:

1. Qualitative study of the optimal control structure of the (DF) case when $(k_0, k_1) \in \mathbb{R}^+ \times \mathbb{R}^+$. More precisely, we study:
   (a) the Dubins (D) case (i.e. $k_0 = 1$, $k_1 = 0$), where we use the deep theoretical result on the optimal control synthesis (which is in a generic case: circular arc-straight line-circular arc, see [25]) in order to implement an efficient shooting method combined with a numerical continuation.
   (b) the Fuller (F) case (i.e. $k_0 = 0$, $k_1 = 1$), where the optimal control structure is of bang-bang- -singular- -bang-bang nature with chattering phenomenon at the junctions with the singular arc (i.e., an infinite number of switchings at the two junctions with the middle singular arc, see [37], [61]).
   (c) the (DF) case with $k_0 > 0$ and $k_1 > 1$, which can be understood as a weighted interpolation between the (D) and (F) cases. The optimal control structure is of bang-bang--singular- -bang-bang nature and the number of bang arcs increases as $k_1 \longrightarrow +\infty$. We regularize the cost with an additional L^2 control term. This is a classical approach in optimal control problems (refer for instance to [32], [80] or [67]). Then we combine two successive continuations with variants of the shooting method in order to compute a solution.
2. We exploit the numerical strategies studied on the reduced optimal control problem in order to solve the original optimal control problem $(\mathbf{OCP})_0$ by implementing:
   (a) the continuation connecting the (D) case with the vehicle minimum time guidance problem.
   (b) the continuation connecting the (DF) case with the vehicle guidance problem.
   (c) for even greater time horizons T, a continuation combined to a *reduced shooting* which computes a quasi-optimal solution and reduces drastically the computation time.
3. Finally, in the chapter 4, we aim at evaluating numerically another approach based on the HJB theory. After recalling the theoretical background (see [56]) and based on recent results (see [3], [4]), we exploited the *ROC-HJ* solver library (see [1]) in order to:
   (a) compute reachable sets and time optimum trajectories for a propelled aerial vehicle model (dimension 3).
   (b) compute optimal trajectories for a glider (non-propelled aerial vehicle) problem and in presence of state constraints (dimension 4).

Chapter 1

Value function expansion in large time optimal control problems

“ The problem with the world is that the intelligent people are full of doubts, while the stupid ones are full of confidence. ”

Charles Bukowski

Sommaire

1.1 Introduction 20
1.1.1 Turnpike phenomenon 20
1.1.2 Value function behavior 22
1.2 Linear quadratic case 24
1.2.1 Setting 24
1.2.2 Main result 24
1.2.3 The steady optimisation problem 25
1.2.4 Proof of the main result 26
1.2.5 Numerical example 29
1.3 Dissipative nonlinear systems 31
1.3.1 Setting of the problem 31
1.3.2 Assumptions 32
1.3.3 Comments 33
1.3.4 Main result 34
1.3.5 Some useful lemmas 34
1.3.6 Proof of the main result 36

1.1 Introduction

In this chapter we study the large-time behavior of the value function associated to an optimal control problem. The subject has been widely studied from the partial differential equations point of view, for instance, within the frame of Hamilton Jacobi Bellman ([56], [38], [65]) or ergodic theory ([11]).

We consider the problem of determining an optimal strategy minimizing the cost functional:

$$J_{T,x,z}(u) = \int_0^T f^0(y(t),u(t))\,dt \tag{1.1}$$

over the time interval $[0,T]$, $T>0$ being fixed and under the constraints:

$$\dot{y}(t) = f(y(t),u(t)), \quad y(0)=x \text{ and } y(T)=z \tag{1.2}$$

where $y(t)\in\mathbb{R}^n$ and $u(t)\in\mathbb{R}^p$. We associate to the optimal control problem (1.1)-(1.2) its value function:

$$v(T,x,z) := \min_{u(\cdot)\in\mathscr{U}_T} J_{T,x,z}(u) \tag{1.3}$$

where $\mathscr{U}_T := L^\infty([0,T],\Omega)$ with Ω compact subset of $\mathbb{R}^p$. We introduce as well the static optimization problem, independent on time, and we denote:

$$\bar{v} := \min_{f(y,u)=0} f^0(y,u) \tag{1.4}$$

This is a usual optimization problem settled in $\mathbb{R}^n\times\mathbb{R}^p$ with a nonlinear equality constraint. We assume that this minimization problem has at least one solution $(\bar{y},\bar{u})$. Note that the minimizer exists and is unique whenever f is linear in y and u for instance, and f^0 is a positive definite quadratic form in (y,u). In what follows, we assume that there is a unique couple $(\bar{y},\bar{u})$ satisfying (1.4).

Let us assume that the optimal solution of (1.1)-(1.2) remains most of the time "close" to $(\bar{y},\bar{u})$. Then, when the time horizon T is large enough and by assuming some controllability properties of the dynamical system (1.2) (that will be precised later on), one understands intuitively that the value function satisfies asymptotically (when $\bar{v}\neq 0$):

$$v(T,x,z) \underset{T\to+\infty}{\sim} \bar{v}.T \tag{1.5}$$

Actually, the above described property, called *turnpike property* is well known in the literature (see for instance [68], [23], [29]).

1.1.1 Turnpike phenomenon

The *turnpike* property is a general phenomenon which holds for a large class of optimal control problems. We say that an optimal control problem enjoys the turnpike property if, when the time horizon becomes large, the optimal solution remains, most of the time, "close" to a steady value which appears to be the optimum of a static optimization problem.

The origin of the term *turnpike* is in the interpretation that Samuelson did of this phenomenon in [68] (Chapter 12): *suppose we want to travel from city A to city B by car, the best way to do it, the optimal way, is to take the highway (namely the turnpike) as near as we can from city A, and leave it when we are close to B. So, except nearby A and B, we are expected to be on the highway: in other words, the turnpike of the problem.*

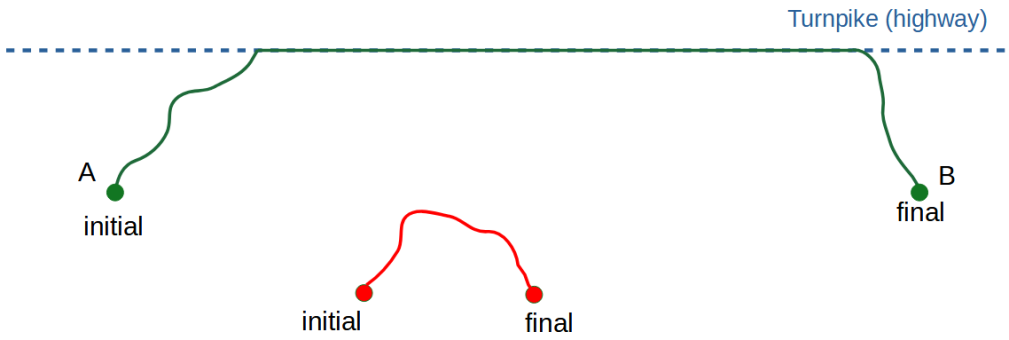

Figure 1.1: Highway to Hell

In [23], the authors proposed an interpretation of the turnpike property in the linear quadratic case and affine-in-control dynamics by remarking that, when the time horizon T is large, the optimal trajectory can be seen as a concatenation of two optimal trajectories over infinite time horizons, one forward in time and the other backward in time.

In [29], the authors precised the turnpike phenomenon through a so-called *exponential turnpike* inequality. We briefly provide some related elements hereafter: let us consider the optimal control problem (1.1)-(1.2)-(1.3) and for sake of simplicity we assume that:

- for T large enough, there exists a unique optimal solution denoted by $(y^\star(\cdot), p^\star(\cdot), u^\star(\cdot))$, the triplet being obtained by the application of the PMP (refer to chapter 3 for detailed description).
- the extremal lift $(y^\star(\cdot), p^\star(\cdot), p^0, u^\star(\cdot))$ is not abnormal thus that we can take $p^0 = -1$.

The turnpike phenomenon stipulates that, when the final time T is large enough, the optimal solution $(y^\star(\cdot), p^\star(\cdot), u^\star(\cdot))$ of (1.1)-(1.2)-(1.3) remains, along the time interval $[0, \mathrm{T}]$, except around the initial time $t = 0$ and around the final time $t = \mathrm{T}$ essentially close to some static point $(\bar{y}, \bar{p}, \bar{u}) \in \mathbb{R}^n \times \mathbb{R}^n \times \mathbb{R}^p$. Moreover, $(\bar{y}, \bar{p}, \bar{u})$ is the solution of the minimization problem (1.4).

The main result proved in [29] states an *exponential turnpike* property, which can be summarized under adequate assumptions by the following inequality: there exists $\mathrm{C} > 0$, $\nu > 0$ and $\mathrm{T}_0 > 0$ such that if $\mathrm{T} \geqslant \mathrm{T}_0$, then:

$$\|y^\star(t) - \bar{y}\| + \|p^\star(t) - \bar{p}\| + \|u^\star(t) - \bar{u}\| \leqslant \mathrm{C}\left(e^{-\nu.t} + e^{-\nu.(\mathrm{T}-t)}\right) \ \forall t \in [0, \mathrm{T}] \tag{1.6}$$

This result, proved locally (provided that the initial and terminal conditions are close enough to the turnpike triple) in [29] states the exponential nature of the closedness of the optimal extremal to the turnpike triple $(\bar{y}, \bar{p}, \bar{u})$. Moreover, under some additional assumptions (amongst which the strict dissipativity), it has been extended globally in [84]. We will discuss the strict dissipativity in section 1.3.

Let us now remind another interesting result proved in [84] which can be understood as a variant of the exponential turnpike. Writing down the state as $\xi(t) = (x(t), y(t))$, consider the following

optimal control problem:

$$\dot{x}(t) = f(x(t),\alpha(t)) \tag{1.7a}$$
$$\dot{y}(t) = g(x(t),\alpha(t)) \tag{1.7b}$$
$$x(0) = x_0, \quad x(\mathrm{T}) = x_f, \quad y(0) = y_0, \quad y(\mathrm{T}) = y_\mathrm{T} \tag{1.7c}$$
$$\min_{\alpha} \int_0^\mathrm{T} f^0(x(t),\alpha(t))dt \tag{1.7d}$$

In comparison to (1.2), the state $\xi(\cdot)$ has been "split" into two coordinates $(x(\cdot), y(\cdot))$, with the associated dynamics (f,g) only depending on x and α. The instantaneous cost function f^0 also does not depend on y. We introduce the "turnpike -static" optimal control problem:

$$\min\{f^0(x,\alpha) \mid (x,\alpha) \in \mathbb{R}^n \times \Omega, f(x,\alpha) = 0, \quad \dot{y}(t) = g(x,\alpha), \quad y(0) = y_0 \text{ and } y(\mathrm{T}) = y_\mathrm{T}\} \tag{1.8}$$

We assume that (1.8) admits a unique optimal solution $(\bar{x}^\mathrm{T}, \bar{y}^\mathrm{T}(\cdot), \bar{p}_x^\mathrm{T}, \bar{p}_y^\mathrm{T}, \bar{\alpha}^\mathrm{T})$ depending on T. Under the previously mentioned and some additional assumptions (please refer to [84] for detailed analysis), there exists $\mathrm{C} > 0$, $\nu > 0$ and $\mathrm{T}_0 > 0$ such that for any $\mathrm{T} \geqslant \mathrm{T}_0$, for any $t \in [0,\mathrm{T}]$:

$$\|x^\star(t) - \bar{x}^\mathrm{T}\| + \|p_x^\star(t) - \bar{p}_x^\mathrm{T}\| + \|\alpha^\star(t) - \bar{\alpha}^\mathrm{T}\| \leqslant \mathrm{C}\left(\frac{1}{\mathrm{T}} + e^{-\nu.t} + e^{-\nu.(\mathrm{T}-t)}\right) \tag{1.9a}$$
$$\|y^\star(t) - \bar{y}^\mathrm{T}(t)\| \leqslant \mathrm{C}, \ \|p_y^\star(t) - \bar{p}_y^\mathrm{T}\| \leqslant \frac{\mathrm{C}}{\mathrm{T}} \tag{1.9b}$$

Clearly speaking, one is able to bound the discrepancies $x^\star(t) - \bar{x}^\mathrm{T}$, $p_x^\star(t) - \bar{p}_x^\mathrm{T}$ and $\alpha^\star(t) - \bar{\alpha}^\mathrm{T}$ by $1/\mathrm{T}$ which tends to 0 as $\mathrm{T} \to +\infty$ but slower than exponentially. At the same time, the distance between $\bar{y}^\mathrm{T}(.)$ and the $y^\star(.)$ remains bounded uniformly with respect to the time horizon T. This turnpike property is thus weaker than the exponential turnpike property presented earlier and is called *linear turnpike* property.

1.1.2 Value function behavior

At the light of what precedes, in the case where the dynamical system enjoys the turnpike property, the optimal trajectory consists of three pieces:

1. a first transient arc leading the state from the initial point x to a vicinity of the turnpike $\bar{y}$.
2. a (long) "midway" arc during which the optimal trajectory-control couple remains essentially close to $(\bar{y},\bar{u})$.
3. a final transient arc during which the trajectory leaves the neighbourhood of $\bar{y}$ to join the final prescribed state z.

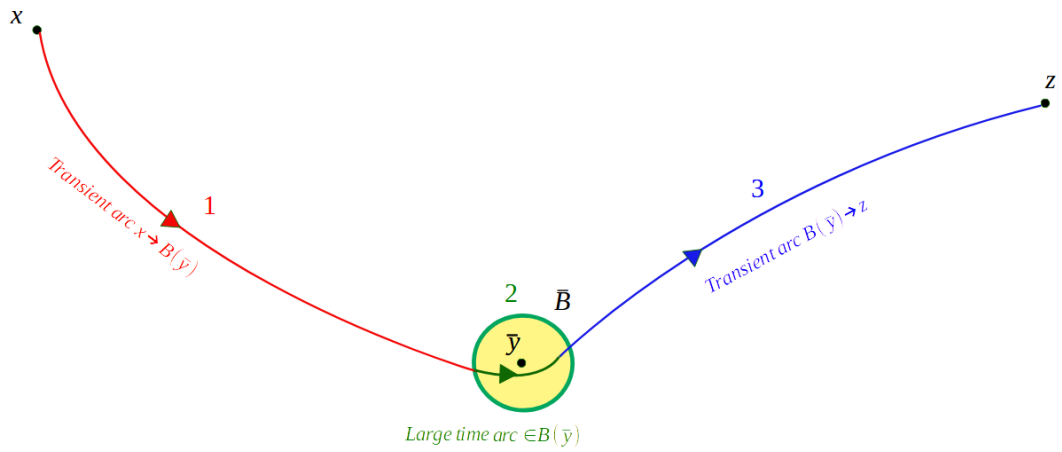

Figure 1.2: Optimal trajectory

In one dimensional state-space, the optimal trajectory can be illustrated as follows:

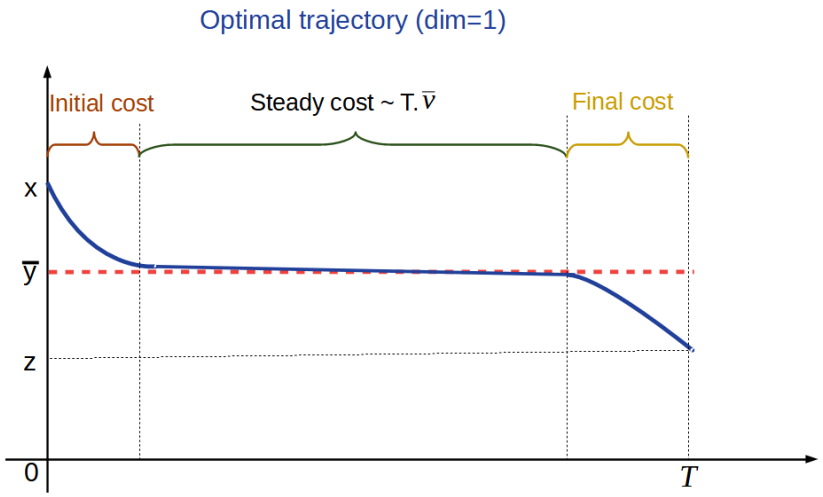

Figure 1.3: Turnpike phenomenon

One expects the asymptotic expansion of the value function v to be of the following form:

$$v(\mathrm{T},x,z) \underset{\mathrm{T}\to+\infty}{\approx} \bar{v}.\mathrm{T} + \underbrace{\text{Initial cost}}_{\text{to the turnpike}}(x) + \underbrace{\text{Final cost}}_{\text{from the turnpike}}(z) \tag{1.10}$$

Intuitively, the underlying result of what precedes is that a quasi-optimal trajectory is the concatenation of three arcs:

1. the transient arc from the initial state to the turnpike
2. the "large-in-time" arc on the turnpike

3. the transient arc from the turnpike to the terminal state

The chapter is organized as follows:

1. we first prove the asymptotic expansion in the linear quadratic (LQ) case
2. we generalize the result to a class of *dissipative* dynamical systems with rather a general cost

1.2 Linear quadratic case

1.2.1 Setting

In the linear quadratic case, one has:

$$\begin{aligned} f(y,u) &:= \mathrm{A}y + \mathrm{B}u \\ f^0(y,u) &:= \frac{1}{2}(u-d)^*\mathrm{U}(u-d) + \frac{1}{2}(y-c)^*\mathrm{Q}(y-c) \end{aligned} \tag{1.11}$$

with $\mathrm{A} \in \mathscr{M}_{n,n}(\mathbb{R})$ and $\mathrm{B} \in \mathscr{M}_{n,p}(\mathbb{R})$, $y \in \mathbb{R}^n$, $u \in \mathbb{R}^p$. U is an $p \times p$ symmetric positive definite matrix, Q is an $n \times n$ symmetric positive definite matrix. The vectors $d \in \mathbb{R}^p$ and $c \in \mathbb{R}^n$ are arbitrarily given. In the LQ case, one can take $\mathscr{U}_\mathrm{T} := \mathrm{L}^2\left([0,\mathrm{T}],\mathbb{R}^p\right)$. In what follows we denote:

$$\|u\|_\mathrm{U}^2 := u^*\mathrm{U}u \text{ and } \|y\|_\mathrm{Q}^2 := y^*\mathrm{Q}y$$

1.2.2 Main result

Theorem 1.2.2.1 *If* (A,B) *satisfies the Kalman condition, the value function* (1.3) *satisfies*

$$v(\mathrm{T},x,z) \underset{\mathrm{T}\to+\infty}{=} \bar{v}.\mathrm{T} + \underbrace{\mathrm{F}(x) + \langle \bar{\lambda}, \bar{y} - x\rangle}_{\textit{Initial cost}} + \underbrace{\mathrm{B}(z) + \langle \bar{\lambda}, z - \bar{y}\rangle}_{\textit{Final cost}} + \mathrm{o}(1) \tag{1.12}$$

where:

$$(\mathscr{F}_x) \begin{cases} \mathrm{F}(x) := \min\limits_{u_1(\cdot)} \dfrac{1}{2}\displaystyle\int_0^{+\infty} \left(\|u_1(t)\|_\mathrm{U}^2 + \|y_1(t)\|_\mathrm{Q}^2\right) dt \\ \dot{y}_1 = \mathrm{A}y_1 + \mathrm{B}u_1, \quad y_1(0) = x - \bar{y} \end{cases} \tag{1.13}$$

and

$$(\mathscr{B}_z) \begin{cases} \mathrm{B}(z) := \min\limits_{u_2(\cdot)} \dfrac{1}{2}\displaystyle\int_0^{+\infty} \left(\|u_2(t)\|_\mathrm{U}^2 + \|y_2(t)\|_\mathrm{Q}^2\right) dt \\ \dot{y}_2 = -\mathrm{A}y_2 - \mathrm{B}u_2, \quad y_2(0) = z - \bar{y} \end{cases} \tag{1.14}$$

with $\bar{\lambda}$ *being the optimal Lagrange multiplier in the steady optimization problem* (1.4) *viewed as a constrained optimization problem (see next paragraph for details).*

Remark 1.2.2.1 *:* $(\mathscr{F}_x)$ *and* $(\mathscr{B}_z)$ *can be equivalently formulated in the following ways:*

$$(\widetilde{\mathscr{F}}_x) \begin{cases} \min\limits_{\tilde{u}_1(\cdot)} \dfrac{1}{2}\displaystyle\int_0^{+\infty} \left(\|\tilde{u}_1(t) - \bar{u}\|_\mathrm{U}^2 + \|\tilde{y}_1(t) - \bar{y}\|_\mathrm{Q}^2\right) dt \\ \dot{\tilde{y}}_1 = \mathrm{A}\tilde{y}_1 + \mathrm{B}\tilde{u}_1, \quad \tilde{y}_1(0) = x \end{cases} \tag{1.15}$$

and

$$(\widetilde{\mathscr{B}}_z) \begin{cases} \min\limits_{\tilde{u}_2(\cdot)} \dfrac{1}{2}\displaystyle\int_0^{+\infty} \left(\|\tilde{u}_2(t) - \bar{u}\|_\mathrm{U}^2 + \|\tilde{y}_2(t) - \bar{y}\|_\mathrm{Q}^2\right) dt \\ \dot{\tilde{y}}_2 = -\mathrm{A}\tilde{y}_2 - \mathrm{B}\tilde{u}_2, \quad \tilde{y}_2(0) = z \end{cases} \tag{1.16}$$

Under the latter formulation, it appears that:

- $\mathrm{F}(x)$ *is the optimal cost of the infinite time linear quadratic stabilization problem starting from* x *towards the turnpike* $(\bar{u},\bar{y})$ *forward in time.*
- $\mathrm{B}(z)$ *is the optimal cost of the infinite time linear quadratic stabilization problem starting from* z *towards the turnpike* $(\bar{u},\bar{y})$ *backward in time.*

By analogy with (1.10), we remark that the initial (resp. final) cost is actually a sum of two terms one of which being $\mathrm{F}(x)$ (resp. $\mathrm{B}(z)$).

1.2.3 The steady optimisation problem

The constraint $f(y,u)=0$ defining a closed, convex non-empty subset of $\mathbb{R}^n\times\mathbb{R}^p$ and f^0 being a continuous, strictly convex function of its arguments, it proves the existence and the uniqueness of the steady control-state pair $(\bar{y},\bar{u})$ of (1.4).

According to the Karush Kuhn Tucker (KKT) optimality conditions, there exists a unique Lagrange multiplier $\bar{\lambda}\in\mathbb{R}^n$ s.t.:

$$\begin{cases} \bar{u}-d-\mathrm{U}^{-1}\mathrm{B}^\star\bar{\lambda}=0\\ \mathrm{Q}\bar{y}-\mathrm{A}^\star\bar{\lambda}-\mathrm{Q}.c=0\\ \mathrm{A}\bar{y}+\mathrm{B}\bar{u}=0 \end{cases} \tag{1.17}$$

which can be written in a more compact way as follows:

$$\begin{cases} \bar{u}=d+\mathrm{U}^{-1}\mathrm{B}^*\bar{\lambda}\\ \mathrm{M}\begin{pmatrix}\bar{y}\\ \bar{\lambda}\end{pmatrix}=\begin{pmatrix}-\mathrm{B}.d\\ \mathrm{Q}.c\end{pmatrix} \end{cases} \tag{1.18}$$

where

$$\mathrm{M}:=\begin{pmatrix}\mathrm{A} & \mathrm{B}\mathrm{U}^{-1}\mathrm{B}^*\\ \mathrm{Q} & -\mathrm{A}^*\end{pmatrix} \tag{1.19}$$

We give the key property at the heart of our proof (refer to [73], [29]).

Proposition 1.2.3.1 (Dichotomy transformation) *Assume that* (A,B) *satisfies the Kalman condition, there exists:*

$$\mathrm{L}:=\begin{pmatrix}\mathrm{I}_n & \mathrm{I}_n\\ \mathrm{N} & \mathrm{P}\end{pmatrix}\in\mathrm{GL}_{2n}(\mathbb{R}) \tag{1.20}$$

where P *(resp.* N*) is the symmetric definite positive (resp. the symmetric definite negative) solution of the Riccati algebraic equation (unknown* K*):*

$$\mathrm{A}^*\mathrm{K}+\mathrm{K}\mathrm{A}+\mathrm{K}\mathrm{B}\mathrm{U}^{-1}\mathrm{B}^*\mathrm{K}-\mathrm{Q}=\mathrm{O}_n \tag{1.21}$$

such that:

$$\mathrm{M}=\mathrm{L}\mathrm{D}\mathrm{L}^{-1} \tag{1.22}$$

where:

$$\mathrm{D}:=\begin{pmatrix}\mathrm{A}+\mathrm{B}\mathrm{U}^{-1}\mathrm{B}^*\mathrm{N} & \mathrm{O}_n\\ \mathrm{O}_n & \mathrm{A}+\mathrm{B}\mathrm{U}^{-1}\mathrm{B}^*\mathrm{P}\end{pmatrix} \tag{1.23}$$

Moreover, the eigenvalues of $\mathrm{A}_-:=\mathrm{A}+\mathrm{B}\mathrm{U}^{-1}\mathrm{B}^*\mathrm{N}$ *have negative real parts and the eigenvalues* $\mathrm{A}_+:=\mathrm{A}+\mathrm{B}\mathrm{U}^{-1}\mathrm{B}^*\mathrm{P}$ *are the negative of those of* A_-.

We set $\Delta\mathrm{E}:=\mathrm{P}-\mathrm{N}$. Using Proposition 1.2.3.1, one can calculate the unique solution of (1.18). Firstly, we remark that:

$$\mathrm{L}^{-1}=\begin{pmatrix}\Delta\mathrm{E}^{-1}\mathrm{P} & -\Delta\mathrm{E}^{-1}\\ -\Delta\mathrm{E}^{-1}\mathrm{N} & \Delta\mathrm{E}^{-1}\end{pmatrix} \tag{1.24}$$

From (1.23), we know that M is invertible, thus:

$$\begin{pmatrix}\bar{y}\\ \bar{\lambda}\end{pmatrix}=\mathrm{M}^{-1}\begin{pmatrix}-\mathrm{B}.d\\ \mathrm{Q}.c\end{pmatrix}=\mathrm{L}\mathrm{D}^{-1}\mathrm{L}^{-1}\begin{pmatrix}-\mathrm{B}.d\\ \mathrm{Q}.c\end{pmatrix}$$

and finally, we obtain:

$$\begin{aligned}
\bar{y} &= (\mathrm{A}_+^{-1} - \mathrm{A}_-^{-1})\Delta\mathrm{E}^{-1}\mathrm{Q}.c - (\mathrm{A}_-^{-1}.\Delta\mathrm{E}^{-1}\mathrm{P} - \mathrm{A}_+^{-1}\Delta\mathrm{E}^{-1}.\mathrm{N})\mathrm{B}.d \\
\bar{\lambda} &= (\mathrm{P}\mathrm{A}_+^{-1} - \mathrm{N}\mathrm{A}_-^{-1})\Delta\mathrm{E}^{-1}\mathrm{Q}.c - (\mathrm{N}\mathrm{A}_-^{-1}.\Delta\mathrm{E}^{-1}\mathrm{P} - \mathrm{P}\mathrm{A}_+^{-1}\Delta\mathrm{E}^{-1}.\mathrm{N})\mathrm{B}.d \\
\bar{u} &= d + \mathrm{U}^{-1}\mathrm{B}^*\bar{\lambda}
\end{aligned} \tag{1.25}$$

We can now prove the main result.

1.2.4 Proof of the main result

It is well known (classical LQ theory, see [82] for instance) that $(\mathscr{F}_x)$ can be explicitly solved and that the optimal trajectory, adjoint, control and cost are given by:

$$\widehat{y}_f(t) = e^{\mathrm{A}_- t}(x - \bar{y}), \quad \widehat{\lambda}_f(t) = \mathrm{N}.\widehat{y}_f(t) \tag{1.26a}$$

$$\widehat{u}_f(t) = \mathrm{U}^{-1}\mathrm{B}^*\widehat{\lambda}_f(t), \quad \mathrm{F}(x) = -\frac{1}{2}(x - \bar{y})^*\mathrm{N}(x - \bar{y}) \tag{1.26b}$$

Similarly for $(\mathscr{B}_z)$, the optimal state, adjoint state, control and cost are given by:

$$\widehat{y}_b(t) = e^{-\mathrm{A}_+ t}(z - \bar{y}), \quad \widehat{\lambda}_b(t) = -\mathrm{P}.\widehat{y}_b(t) \tag{1.27a}$$

$$\widehat{u}_b(t) = -\mathrm{U}^{-1}\mathrm{B}^*\widehat{\lambda}_b(t), \quad \mathrm{B}(z) = \frac{1}{2}(z - \bar{y})^*\mathrm{P}(z - \bar{y}) \tag{1.27b}$$

Under the Kalman assumption, the problem (1.1)-(1.2)-(1.3) admits a unique solution. According to the PMP ([55]), there exists an optimal triple $(\widehat{y}_\mathrm{T}(.), \widehat{\lambda}_\mathrm{T}(.), \widehat{u}_\mathrm{T}(\cdot))$ such that, for almost every $t \in [0, \mathrm{T}]$:

$$\dot{\widehat{\lambda}}_\mathrm{T}(t) = -\frac{\partial \mathrm{H}}{\partial y}(\widehat{y}_\mathrm{T}(t), \widehat{\lambda}_\mathrm{T}(t), \widehat{u}_\mathrm{T}(t)) \tag{1.28a}$$

$$\dot{\widehat{y}}_\mathrm{T}(t) = \frac{\partial \mathrm{H}}{\partial \lambda}(\widehat{y}_\mathrm{T}(t), \widehat{\lambda}_\mathrm{T}(t), \widehat{u}_\mathrm{T}(t)) \tag{1.28b}$$

$$\frac{\partial \mathrm{H}}{\partial u}(\widehat{y}_\mathrm{T}(t), \widehat{\lambda}_\mathrm{T}(t), \widehat{u}_\mathrm{T}(t)) = 0 \tag{1.28c}$$

where the Hamiltonian H is defined by:

$$\mathrm{H}(y, \lambda, u) := \langle \lambda, \mathrm{A}y + \mathrm{B}u \rangle + \frac{\lambda_0}{2}\left(\|u - d\|_\mathrm{U}^2 + \|y - c\|_\mathrm{Q}^2\right) \tag{1.29}$$

In the LQ case, under the Kalman condition, the extremal lift is normal thus we take $\lambda_0 = -1$ and denoting $\Theta := \begin{pmatrix} \widehat{y}_\mathrm{T} \\ \widehat{\lambda}_\mathrm{T} \end{pmatrix}$, and $\Pi := \begin{pmatrix} \mathrm{B}.d \\ -\mathrm{Q}.c \end{pmatrix}$, (1.28) can be written:

$$\begin{aligned}
\widehat{u}_\mathrm{T}(t) &= d + \mathrm{U}^{-1}\mathrm{B}^*\widehat{\lambda}_\mathrm{T}(t) \\
\dot{\Theta}(t) &= \mathrm{M}.\Theta + \Pi
\end{aligned} \tag{1.30}$$

with M given by (1.19). Now we set $\Theta := \mathrm{L}.\Theta_1$ with $\Theta_1 := \begin{pmatrix} \widehat{w}_\mathrm{T} \\ \widehat{\eta}_\mathrm{T} \end{pmatrix}$. From the dichotomy transformation (1.22), (1.23) and (1.30), we get:

$$\dot{\Theta}_1 = \begin{pmatrix} \mathrm{A}_- & \mathrm{O}_n \\ \mathrm{O}_n & \mathrm{A}_+ \end{pmatrix}\Theta_1 + \mathrm{L}^{-1}\Pi \tag{1.31}$$

which is equivalent to:

$$\dot{\widehat{w}}_\mathrm{T}(t) = \mathrm{A}_-.\widehat{w}_\mathrm{T}(t) + \Delta\mathrm{E}^{-1}.(\mathrm{Q}.c + \mathrm{P}.\mathrm{B}.d) \tag{1.32}$$

$$\dot{\widehat{\eta}}_\mathrm{T}(t) = \mathrm{A}_+.\widehat{\eta}_\mathrm{T}(t) - \Delta\mathrm{E}^{-1}.(\mathrm{Q}.c + \mathrm{N}.\mathrm{B}.d) \tag{1.33}$$

Thanks to the previous transformation, we can explicitly integrate (1.32) forward in time and (1.33) backward in time, and we obtain for any $t \in [0,\mathrm{T}]$:

$$\begin{aligned}\widehat{w}_{\mathrm{T}}(t) &= e^{\mathrm{A}_- t}.\widehat{w}_{\mathrm{T}}(0) - \mathrm{A}_-^{-1}(\mathrm{I}_n - e^{\mathrm{A}_- t})\Delta\mathrm{E}^{-1}.(\mathrm{Q}.c + \mathrm{P}.\mathrm{B}.d)\\ \widehat{\eta}_{\mathrm{T}}(t) &= e^{-\mathrm{A}_+(\mathrm{T}-t)}.\widehat{\eta}_{\mathrm{T}}(\mathrm{T}) + \mathrm{A}_+^{-1}(\mathrm{I}_n - e^{-\mathrm{A}_+(\mathrm{T}-t)})\Delta\mathrm{E}^{-1}.(\mathrm{Q}.c + \mathrm{N}.\mathrm{B}.d)\end{aligned} \tag{1.34}$$

The prescribed initial and final conditions imply that:

$$\begin{pmatrix} x \\ z \end{pmatrix} = \underbrace{\begin{pmatrix} \mathrm{I}_n & e^{-\mathrm{A}_+\mathrm{T}} \\ e^{\mathrm{A}_-\mathrm{T}} & \mathrm{I}_n \end{pmatrix}}_{\mathrm{R}} \begin{pmatrix} \widehat{w}_{\mathrm{T}}(0) \\ \widehat{\eta}_{\mathrm{T}}(\mathrm{T}) \end{pmatrix} + \begin{pmatrix} k_1 \\ k_2 \end{pmatrix} \tag{1.35}$$

where $\begin{pmatrix} k_1 \\ k_2 \end{pmatrix} = \begin{pmatrix} \mathrm{A}_+^{-1}(\mathrm{I}_n - e^{-\mathrm{A}_+\mathrm{T}})\Delta\mathrm{E}^{-1}.(\mathrm{Q}.c + \mathrm{N}.\mathrm{B}.d) \\ -\mathrm{A}_-^{-1}(\mathrm{I}_n - e^{\mathrm{A}_-\mathrm{T}})\Delta\mathrm{E}^{-1}.(\mathrm{Q}.c + \mathrm{P}.\mathrm{B}.d) \end{pmatrix}$.

By inverting R we obtain:

$$\mathrm{R}^{-1} = \begin{pmatrix} (\mathrm{I}_n - \chi(\mathrm{T}))^{-1} & -(\mathrm{I}_n - \chi(\mathrm{T}))^{-1} e^{-\mathrm{A}_+\mathrm{T}} \\ -e^{\mathrm{A}_-\mathrm{T}}(\mathrm{I}_n - \chi(\mathrm{T}))^{-1} & \mathrm{I}_n + e^{\mathrm{A}_-\mathrm{T}}(\mathrm{I}_n - \chi(\mathrm{T}))^{-1} e^{-\mathrm{A}_+\mathrm{T}} \end{pmatrix} \tag{1.36}$$

with $\chi(\mathrm{T}) := e^{-\mathrm{A}_+\mathrm{T}}.e^{\mathrm{A}_-\mathrm{T}}$.

In what follows, all the remainder terms are to be understood as $\mathrm{T} \to +\infty$. Taking into account that $\chi(\mathrm{T}) \longrightarrow \mathrm{O}_n$ as $\mathrm{T} \to +\infty$, at first order:

$$\mathrm{R}^{-1} = \begin{pmatrix} \mathrm{I}_n + \mathrm{O}(\chi(\mathrm{T})) & -(\mathrm{I}_n + \mathrm{O}(\chi(\mathrm{T})).e^{-\mathrm{A}_+\mathrm{T}} \\ -e^{\mathrm{A}_-\mathrm{T}}(\mathrm{I}_n + \mathrm{O}(\chi(\mathrm{T}))) & \mathrm{I}_n + e^{\mathrm{A}_-\mathrm{T}}(\mathrm{I}_n + \mathrm{O}(\chi(\mathrm{T}))e^{-\mathrm{A}_+\mathrm{T}} \end{pmatrix} \tag{1.37}$$

From (1.35) and (1.37), taking into account that $e^{-\mathrm{A}_+\mathrm{T}} \longrightarrow \mathrm{O}_n$, $e^{\mathrm{A}_-\mathrm{T}} \longrightarrow \mathrm{O}_n$, $\chi(\mathrm{T}) = \mathrm{O}(e^{-\mathrm{A}_+\mathrm{T}})$ and $\chi(\mathrm{T}) = \mathrm{O}(e^{\mathrm{A}_-\mathrm{T}})$ as $\mathrm{T} \to +\infty$:

$$\begin{aligned}\widehat{w}_{\mathrm{T}}(0) &= x - \mathrm{A}_+^{-1}.\Delta\mathrm{E}^{-1}.(\mathrm{Q}.c + \mathrm{N}.\mathrm{B}.d) + \mathrm{O}\left(e^{-\mathrm{A}_+\mathrm{T}}\right)\\ \widehat{\eta}_{\mathrm{T}}(\mathrm{T}) &= z + \mathrm{A}_-^{-1}.\Delta\mathrm{E}^{-1}.(\mathrm{Q}.c + \mathrm{P}.\mathrm{B}.d) + \mathrm{O}\left(e^{\mathrm{A}_-\mathrm{T}}\right)\end{aligned}$$

We can now explicitly calculate $\widehat{w}_{\mathrm{T}}(\cdot)$ and $\widehat{\eta}_{\mathrm{T}}(\cdot)$, and we "recognize" the optimal trajectories given by (1.26a) and (1.27a):

$$\widehat{w}_{\mathrm{T}}(t) = \widehat{y}_f(t) - \mathrm{A}_-^{-1}\Delta\mathrm{E}^{-1}(\mathrm{Q}.c + \mathrm{P}.\mathrm{B}.d) + \mathrm{O}\left(e^{-\mathrm{A}_+\mathrm{T}}\right) \tag{1.39}$$

$$\widehat{\eta}_{\mathrm{T}}(t) = \widehat{y}_b(\mathrm{T}-t) + \mathrm{A}_+^{-1}\Delta\mathrm{E}^{-1}(\mathrm{Q}.c + \mathrm{N}.\mathrm{B}.d) + \mathrm{O}\left(e^{\mathrm{A}_-\mathrm{T}}\right) \tag{1.40}$$

This allows us to "re-construct" the optimal trajectory:

$$\widehat{y}_{\mathrm{T}}(t) = \widehat{y}_f(t) + \widehat{y}_b(\mathrm{T}-t) + \bar{y} + \mathrm{O}\left(e^{-\mathrm{A}_+\mathrm{T}}\right) + \mathrm{O}\left(e^{\mathrm{A}_-\mathrm{T}}\right) \tag{1.41}$$

the optimal adjoint state:

$$\begin{aligned}\widehat{\lambda}_{\mathrm{T}}(t) =& \mathrm{N}.\widehat{w}_{\mathrm{T}}(t) + \mathrm{P}.\widehat{\eta}_{\mathrm{T}}(t)\\ =& \widehat{\lambda}_f(t) - \widehat{\lambda}_b(\mathrm{T}-t) + \bar{\lambda} + \mathrm{O}\left(e^{-\mathrm{A}_+\mathrm{T}}\right) + \mathrm{O}\left(e^{\mathrm{A}_-\mathrm{T}}\right)\end{aligned} \tag{1.42}$$

and finally the optimal control:

$$\begin{aligned}\widehat{u}_{\mathrm{T}}(t) &= d + \mathrm{B}^*\widehat{\lambda}_{\mathrm{T}}(t)\\ &= \widehat{u}_f(t) + \widehat{u}_b(\mathrm{T}-t) + \bar{u} + \mathrm{O}\left(e^{-\mathrm{A}_+\mathrm{T}}\right) + \mathrm{O}\left(e^{\mathrm{A}_-\mathrm{T}}\right)\end{aligned} \tag{1.43}$$

We deduce from (1.26a), (1.27a) and from Proposition 1.2.3.1 that for any $t \in [0,\mathrm{T}]$:

$$\|\widehat{y}_f(t)\| \leqslant \|x - \bar{y}\|.e^{-\mathrm{C}.t} \tag{1.44}$$

$$\|\widehat{y}_b(\mathrm{T}-t)\| \leqslant \|z - \bar{y}\|.e^{-\mathrm{C}.(\mathrm{T}-t)} \tag{1.45}$$

where $C := -\max\left\{Re(\mu) \mid \mu \in Sp(A_-)\right\} > 0$.

Consequently for T large enough, we get from (1.41), (1.42) and (1.43):

$$\|\widehat{y}_T(t) - \bar{y}\| \leqslant K_1.\left(e^{-C.t} + e^{-C.(T-t)}\right) \tag{1.46}$$
$$\|\widehat{\lambda}_T(t) - \bar{\lambda}\| \leqslant K_2.\left(e^{-C.t} + e^{-C.(T-t)}\right) \tag{1.47}$$
$$\|\widehat{u}_T(t) - \bar{u}\| \leqslant K_3.\left(e^{-C.t} + e^{-C.(T-t)}\right) \tag{1.48}$$

where:

$$\begin{aligned}
K_1 &:= \max\left(\|x - \bar{y}\|, \|z - \bar{y}\|\right)\\
K_2 &:= \max(\|N\|.\|x - \bar{y}\|, \|P\|.\|z - \bar{y}\|)\\
K_3 &:= \|U^{-1}\|.\|B^*\|.\max(\|N\|.\|x - \bar{y}\|, \|P\|.\|z - \bar{y}\|)
\end{aligned}$$

We have thus recovered the exponential turnpike property stated in [29].

By denoting by $\epsilon(T) := O\left(e^{-A_+T}\right) + O\left(e^{A_-T}\right)$, and taking into account (1.41), (1.42) and (1.43), $v(\cdot)$ can be decomposed as follows:

$$\begin{aligned}
v(T,x,z) &= \frac{1}{2}\int_0^T \left(\|\widehat{u}_T(t) - d\|_U^2 + \|\widehat{y}_T(t) - c\|_Q^2\right) dt\\
&= V_1 + V_2 + V_3 + V_4 + V_5 + V_6 + V_\epsilon
\end{aligned}$$

where:

$$\begin{aligned}
V_1 &= \frac{1}{2}\int_0^T \left(\|\widehat{u}_f(t)\|_U^2 + \|\widehat{y}_f(t)\|_Q^2\right) dt\\
V_2 &= \frac{1}{2}\int_0^T \left(\|\widehat{u}_b(T-t)\|_U^2 + \|\widehat{y}_b(T-t)\|_Q^2\right) dt\\
V_3 &= \frac{1}{2}\int_0^T \left(\|\bar{u} - d\|_U^2 + \|\bar{y} - c\|_Q^2\right) dt = \bar{v}.T\\
V_4 &= \int_0^T \left(\langle \widehat{u}_f(t), U(\bar{u} - d)\rangle + \langle \widehat{y}_f(t), Q(\bar{y} - c)\rangle\right) dt\\
V_5 &= \int_0^T \left(\langle \widehat{u}_b(T-t), U(\bar{u} - d)\rangle + \langle \widehat{y}_b(T-t), Q(\bar{y} - c)\rangle\right) dt\\
V_6 &= \int_0^T \left(\langle \widehat{u}_f(t), U\widehat{u}_b(T-t)\rangle + \langle \widehat{y}_f(t), Q\widehat{y}_b(T-t)\rangle\right) dt
\end{aligned}$$

and V_ϵ is the sum of all the terms that are multiplied by $\epsilon(T)$. It is easy to see that, as $\epsilon(T) \longrightarrow 0$ exponentially as $T \to +\infty$, we have $V_\epsilon \longrightarrow 0$ as $T \to +\infty$.

Let us treat the other terms: clearly, from (1.13) (resp. (1.14)), $V_1 \longrightarrow F(x)$ (resp. $V_2 \longrightarrow B(z)$) as $T \to +\infty$.

The terms V_4 and V_5 can be explicitly calculated from (1.26) and (1.27) and we obtain:

$$\begin{aligned}
V_4 &= \left\langle (e^{A_-T} - I_n)(x - \bar{y}), \bar{\lambda}\right\rangle \longrightarrow \left\langle \bar{y} - x, \bar{\lambda}\right\rangle \text{ as } T \to +\infty\\
V_5 &= \left\langle (I_n - e^{-A_+T})(z - \bar{y}), \bar{\lambda}\right\rangle \longrightarrow \left\langle z - \bar{y}, \bar{\lambda}\right\rangle \text{ as } T \to +\infty
\end{aligned}$$

Finally we have:

$$\begin{aligned}
V_6 &\leqslant \int_0^T \|U\|.\|\widehat{u}_f(t)\|.\|\widehat{u}_b(T-t)\| + \|Q\|.\|\widehat{y}_f(t)\|.\|\widehat{y}_b(T-t)\| dt\\
&\leqslant 2\max\left(\|B\|^2\|P\|.\|N\|\|U^{-1}\|, \|Q\|\right).\|x - \bar{y}\|.\|z - \bar{y}\|.T.e^{-C.T}
\end{aligned}$$

Consequently, $V_6 \longrightarrow 0$ exponentially as $T \to +\infty$ and the main result is proved □.

1.2.5 Numerical example

Let us illustrate numerically the value function expansion. Consider the one-dimensional linear dynamics:

$$\dot{y}(t) = y(t) + 2u(t), \quad y(0) = x, \quad y(\mathrm{T}) = z \tag{1.49}$$

to which we associate the value function:

$$v(\mathrm{T}, x, z) = \min_{u \in \mathscr{U}_\mathrm{T}} \frac{1}{2} \int_0^\mathrm{T} \frac{4}{3}(y(t) - 3)^2 + 3(u(t) + 1)^2 dt \tag{1.50}$$

The optimal triple of the associated steady optimization problem is easily calculated and one has: $\bar{y} = \dfrac{66}{25}$, $\bar{u} = -\dfrac{33}{25}$, $\bar{\lambda} = -\dfrac{12}{25}$ and $\bar{v} = \dfrac{6}{25}$.

Thus we have $\mathrm{F}(x) = \left(x - \dfrac{66}{25}\right)^2$ and $\mathrm{B}(z) = \dfrac{1}{4}\left(z - \dfrac{66}{25}\right)^2$.

For $(x, z) \in [-2, 2] \times [-2, 2]$, and some values of T, the optimal trajectory has been calculated using the shooting method.

The figure below displays the optimal triple in the case: $x = -1$, $z = -2$, T increasing from 1 to 10 by step of 1.

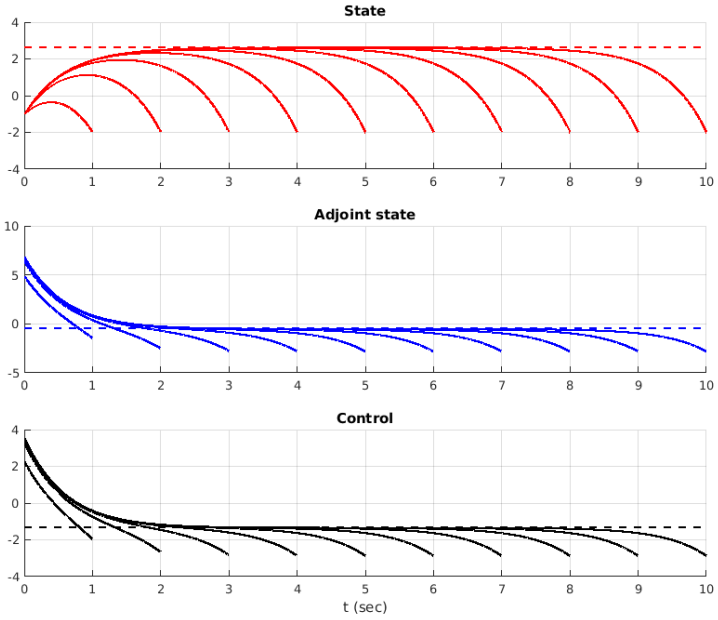

Figure 1.4: Optimal triple for some values of T

Once the optimal trajectory is calculated, the associated cost is numerically estimated. The following figure displays the value of the difference:

$$\epsilon(\mathrm{T}, x, z) = v(\mathrm{T}, x, z) - \bar{v}.\mathrm{T} - \mathrm{F}(x) - \mathrm{B}(z) - \langle \bar{\lambda}, z - x \rangle \tag{1.51}$$

over a grid of fixed initial and final states.

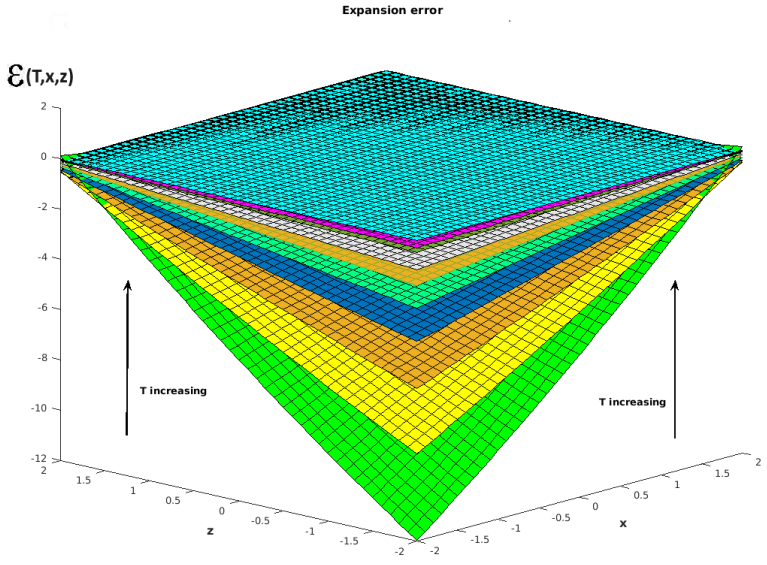

Figure 1.5: Value function expansion error

Each layer corresponds to the difference at a certain fixed time horizon T. The layer at the bottom corresponds to the shortest time horizon and the layer at the top to the largest time horizon.

1.3 Dissipative nonlinear systems

1.3.1 Setting of the problem

In this section we establish a theorem valid for a specific class of nonlinear control systems. We consider the general dynamics (1.2), where $f : \mathbb{R}^n \times \mathbb{R}^p \longrightarrow \mathbb{R}^n$ is of class C^1. We consider the optimal control problem of determining a control $u \in \mathscr{U}_T^\Omega := L^\infty([0,T],\Omega)$, Ω being a fixed compact set of $\mathbb{R}^p$, minimizing the cost functional (1.1), where $f^0 : \mathbb{R}^n \times \mathbb{R}^p \longrightarrow \mathbb{R}$ is of class C^1.

Remark 1.3.1.1 *As Ω does not depend on T for any $T > 0$, the space of controls does neither depend on T (indeed, beyond time horizon T the controls can be trivially extended within Ω) and will consequently be denoted by $\mathscr{U}^\Omega$.*

In the sequel, we assume that $\Omega \subset \overline{B}(0,c)$ for some $c > 0$.

We assume that for $T > 0$ large enough, (1.1)-(1.2)-(1.3) admits an optimal solution, denoted by $(\widehat{y}_T(\cdot), \widehat{u}_T(\cdot))$. The conditions ensuring the existence of such a solution are well known (see for instance [82], [19]). For instance, if the set of velocities $\{f(y,u) \mid u \in \Omega\}$ is a convex subset of $\mathbb{R}^n$ for any $y \in \mathbb{R}^n$, with mild growth at infinity and if the epigraph of f^0 is convex, then there exists at least one optimal solution. These conditions are for example satisfied if the dynamics are control-affine and if the cost functional is convex with respect to u.

If we assume here $\Omega = \mathbb{R}^p$, then by the PMP ([82]-[55]), there exist $\lambda^0 \leqslant 0$ and an absolutely continuous mapping $\widehat{\lambda}_T : [0,T] \longrightarrow \mathbb{R}^n$ (called adjoint vector) satisfying $(\widehat{\lambda}_T(\cdot), \lambda^0) \neq (0,0)$ such that

$$\begin{aligned} \dot{\widehat{y}}_T(t) &= \frac{\partial H}{\partial \lambda}\left(\widehat{y}_T(t), \widehat{\lambda}_T(t), \lambda^0, \widehat{u}_T(t)\right) \\ \dot{\widehat{\lambda}}_T(t) &= -\frac{\partial H}{\partial y}\left(\widehat{y}_T(t), \widehat{\lambda}_T(t), \lambda^0, \widehat{u}_T(t)\right) \\ \frac{\partial H}{\partial u}\left(\widehat{y}_T(t), \widehat{\lambda}_T(t), \lambda^0, \widehat{u}_T(t)\right) &= 0 \end{aligned} \tag{1.52}$$

for almost every $t \in [0,T]$. The Hamiltonian H is defined by

$$H(y,\lambda,\lambda^0,u) := \langle \lambda, f(y,u)\rangle + \lambda^0 f^0(y,u) \tag{1.53}$$

here $\langle , \rangle$ is the Eucledian scalar product in $\mathbb{R}^n$. We will assume that the abnormal case does not occur, thus we set $\lambda^0 = -1$.

By the KKT optimality conditions, there exists $\bar{\lambda} \in \mathbb{R}^n$ such that

$$\begin{aligned} & f(\bar{y},\bar{u}) = 0 \\ & -\frac{\partial f^0}{\partial y}(\bar{y},\bar{u}) + \langle \bar{\lambda}, \frac{\partial f}{\partial y}(\bar{y},\bar{u})\rangle = 0 \\ & -\frac{\partial f^0}{\partial u}(\bar{y},\bar{u}) + \langle \bar{\lambda}, \frac{\partial f}{\partial u}(\bar{y},\bar{u})\rangle = 0 \end{aligned} \tag{1.54}$$

In the Hamiltonian formalism, the first-order optimality system (1.54) is equivalent to

$$\begin{aligned} & \frac{\partial H}{\partial \lambda}(\bar{y},\bar{\lambda},-1,\bar{u}) = 0 \\ & -\frac{\partial H}{\partial y}(\bar{y},\bar{\lambda},-1,\bar{u}) = 0 \\ & \frac{\partial H}{\partial u}(\bar{y},\bar{\lambda},-1,\bar{u}) = 0 \end{aligned} \tag{1.55}$$

We assume that the triple $(\bar{y},\bar{\lambda},\bar{u})$ is unique and we keep the definition (1.4) of $\bar{v}$.

Because of the turnpike property, since it is expected that the dominating term in the asymptotic expansion of $v(\cdot)$ is equal to $T.\bar{v}$, we "absorb" it by subtracting it to the cost $J_{T,x,z}$ and consider the "shifted" optimal control problem, denoted by $\left(\mathscr{P}^{x,z}_{[0,T]}\right)$

$$\min_{u(\cdot)\in\mathscr{U}^\Omega} C_T(u,x,z) := \min_{u(\cdot)\in\mathscr{U}^\Omega} \int_0^T w(y(t),u(t))dt \tag{1.56a}$$

$$\dot{y}(t) = f(y(t),u(t)), \quad \forall t\in[0,T] \tag{1.56b}$$

$$y(0) = x, \ y(T) = z \tag{1.56c}$$

where $w(\cdot)$ is the "shifted cost" defined by

$$w(y,u) := f^0(y,u) - f^0(\bar{y},\bar{u}) \tag{1.57}$$

The readers acquainted with the notion of dissipativity in nonlinear optimal control will recognize in (1.57) a classical storage function. This is where the link with disspativity appears.

We introduce as well the following shifted infinite-time optimal control problem denoted respectively by $(\mathscr{P}^x_{\infty f})$

$$\begin{aligned} v_f(x) &:= \min_{u(\cdot)\in\mathscr{U}^\Omega} \int_0^{+\infty} w(y(t),u(t))dt \\ \dot{y}(t) &= f(y(t),u(t)), \quad y(0) = x \end{aligned} \tag{1.58}$$

and $(\mathscr{P}^z_{\infty b})$

$$\begin{aligned} v_b(z) &:= \min_{u(\cdot)\in\mathscr{U}^\Omega} \int_0^{+\infty} w(y(t),u(t))dt \\ \dot{y}(t) &= -f(y(t),u(t)), \quad y(0) = z \end{aligned} \tag{1.59}$$

In our notations, the index “f” stands for “forward” while the index “b” stands for “backward”.

We assume the existence of optimal solutions to $(\mathscr{P}^x_{\infty f})$ and $(\mathscr{P}^z_{\infty b})$ with a finite cost.

1.3.2 Assumptions

Assumptions of global nature:

(A_1): (*Regularity of f and f^0*): We assume that f and f^0 are of class C^1.

(A_2): (*Existence and uniqueness of optimal solutions*): There exists $T_0 > 0$ such that for any $T \geqslant T_0$ each of the optimal control problems $\left(\mathscr{P}^{x,z}_{[0,T]}\right)$, $(\mathscr{P}^x_{\infty f})$ and $(\mathscr{P}^z_{\infty b})$ admits a unique optimal solution denoted respectively by $(\widehat{y}_T(\cdot),\widehat{u}_T(\cdot))$, $\left(\widehat{y}_{\infty f}(\cdot),\widehat{u}_{\infty f}(\cdot)\right)$ and $(\widehat{y}_{\infty b}(\cdot),\widehat{u}_{\infty b}(\cdot))$.

(A_3): (*Boundedness of the optimal trajectories*): The optimal trajectories of $\left(\mathscr{P}^{x,z}_{[0,T]}\right)$, $(\mathscr{P}^x_{\infty f})$ and $(\mathscr{P}^z_{\infty b})$ are bounded uniformly with respect to $T \geqslant T_0$:

$$\exists b > 0, \quad | \quad \forall t \geqslant 0, \|\widehat{y}(t)\| \leqslant b \tag{1.60}$$

(A_4): (*Boundedness of the optimal costs*): The optimal costs of $(\mathscr{P}^{x,z}_{0,T})$, $(\mathscr{P}^x_{\infty f})$ and $(\mathscr{P}^z_{\infty b})$ are bounded uniformly with respect to $T \geqslant T_0$.

(A_5): The minimizer $(\bar{y},\bar{u})$ of (1.4) is unique and there exists a unique $\bar{\lambda}$, assumed to be normal, such that (1.54) is satisfied. Moreover, we assume that $\bar{u}\in\overset{\circ}{\Omega}$.

(A_6): (*Strict dissipativity property*): The family of optimal control problems (1.56a)-(1.56b) indexed by T is strictly dissipative at $(\bar{y},\bar{u})$ with respect to the supply rate function w defined by (1.57) with a storage function S.

The notion of strict dissipativity was introduced in [86] and already used in [78], [49], [79] and [50] to derive turnpike properties.

We recall that (1.56a)-(1.56b) is *dissipative* at the static point $(\bar{y},\bar{u})$ with respect the the supply rate function w if there exists a bounded function $\mathrm{S}:\mathbb{R}^n \longrightarrow \mathbb{R}$, called *storage function* such that for any admissible pair $(y(\cdot),u(\cdot))$ and any $\mathrm{T}>0$:

$$\mathrm{S}(y(0))+\int_0^{\mathrm{T}} w(y(t),u(t))dt \geqslant \mathrm{S}(y(\mathrm{T})) \tag{1.61}$$

The system is *strictly dissipative* if, in addition, there exists some function $\alpha(\cdot)$ of class $\mathscr{K}$ (i.e. $\alpha:[0,+\infty)\longrightarrow[0,+\infty)$ continuous, increasing and such that $\alpha(0)=0$) such that for any $\mathrm{T}>0$ we have:

$$\mathrm{S}(y(0))+\int_0^{\mathrm{T}} w(y(t),u(t))dt \geqslant \mathrm{S}(y(\mathrm{T}))+\int_0^{\mathrm{T}} \alpha\left(\left\| \begin{array}{c} y(t)-\bar{y} \\ u(t)-\bar{u} \end{array} \right\|\right) dt \tag{1.62}$$

Assumption of local nature:

(A_7): Setting $\mathrm{A}:=\dfrac{\partial f}{\partial y}(\bar{y},\bar{u})$, $\mathrm{B}:=\dfrac{\partial f}{\partial u}(\bar{y},\bar{u})$, the pair (A,B) satisfies the Kalman rank condition i.e, the linearized system at $(\bar{y},\bar{u})$ is controllable.

(A_8): (*Local boundedness of the minimum time trajectories and controls near the turnpike*): There exists $r>0$ such that for any $x\in\bar{\mathrm{B}}(\bar{y},r)$ the minimum time trajectory to $\bar{y}$ starting from x, denoted by $y_x^{\tau_f}(\cdot)$ and the associated control, denoted by $u^{\tau_f}(\cdot)$ remain in the neighbourhood of respectively $\bar{y}$ and $\bar{u}$ uniformly with respect to x that is to say:

$$\exists r \text{ and } \mathrm{K}_r>0 \quad | \quad \forall x\in\bar{\mathrm{B}}(\bar{y},r),\ \forall t\in[0,\tau_f(x)],\ \|y_x^{\tau_f}(t)-\bar{y}\|+\|u^{\tau_f}(t)-\bar{u}\|\leqslant \mathrm{K}_r \tag{1.63}$$

where $\tau_f(\cdot)$ is the minimum time function to reach $\bar{y}$ with the dynamics f.

1.3.3 Comments

The assumption "admissible controls remain in Ω" can be weakened to "optimal controls remain in Ω". This is for example usually the case for control-affine systems with quadratic cost.

The assumptions (A_1) and (A_7) together imply that there exists $r>0$ such that for any $x\in\mathrm{B}(\bar{y},r)$, there exists an admissible trajectory steering the control system from x to $\bar{y}$ in finite time. Thus the minimum time function $\tau_f(\cdot)$ is well defined on $\mathrm{B}(\bar{y},r)$ and continuous at $\bar{y}$. This is classical result that can be found, for instance, in [56]. The result remains true for the minimum time function associated to the backward-in-time dynamics $-f$, denoted by $\tau_{-f}(\cdot)$.

The assumption (A_8) requires the local boundedness of the minimum time trajectories and controls for any trajectory starting in the previously defined neighbourhood of the turnpike. This assumption is satisfied if the minimum time function is C^1 in the neighbourhood of $\bar{y}$. We highlight here that the regularity of the minimum time function has been widely studied in the literature: it is well known that under appropriate controllability type conditions the minimum time function has an open domain of definition and is locally Lipschitz on it, see for instance [56]-[36]. Thus, it is differentiable almost everywhere on its domain. The value function fails in general to be differentiable at points that are reached by at least two minimum time trajectories and its differentiability at a point does not guarantee continuous differentiability around this point. In [40], the authors show that, under some assumptions on the regularity and target smoothness (which excludes the singleton case), the nonemptiness of the proximal subdifferential of the minimum time function at a point implies its continuous differentiability in a neighborhood of this point. An analogous result has been proved for the value function of the Bolza problem in [66] in the case where the initial state is a prescribed point and the final state is let free. In [75], the author gives a survey of results on the regularity of the minimum time map for control-affine systems with prescribed initial and final points. Finally, for results on the set where the value function is differentiable, we refer the reader to [44], [33], [34], [53], [54] and references therein.

The (strict) dissipativity property (A_6) is certainly the less intuitive assumption to check in practice. In general, when the system is dissipative, storage functions are closely related to viscosity solutions of partial differential inequalities called Hamilton-Jacobi inequalities. We refer the reader to the Chapter 4 of [15] for more details on this subject. One can remark that, under suitable regularity and boundedness assumptions on the dynamics and the cost, the value function (its opposite more precisely) can be taken as a storage function, and the dissipativity inequality is then deduced from the Dynamic Programming Principle (DPP).

The strict dissipativity inequality (1.62) remains true for the dynamics $-f$, provided that one switches the initial and final states. The corresponding storage function is $-S(\cdot)$.

1.3.4 Main result

Theorem 1.3.4.1 *: Under Assumptions $(A_1)-(A_8)$, the value function (1.3) satisifes*

$$v(T,x,z) = T.\bar{v} + v_f(x) + v_b(z) + o(1) \tag{1.64}$$

as $T \to +\infty$.

Remark 1.3.4.1 *In the LQ case, one can prove that*

- $v_f(x) = F(x) + \langle \bar{\lambda}, \bar{y} - x \rangle$
- $v_b(z) = B(z) + \langle \bar{\lambda}, z - \bar{y} \rangle$

where $F(\cdot)$ and $B(\cdot)$ are respectively given by (1.13) and (1.14). This observation unifies the linear and non linear case.

Remark 1.3.4.2 *: The strict dissipativity assumption being at the heart of the theorem in the general case, one can show that is it automatically satisfied in the linear quadratic case (see the proposition A.1.0.1 in the Annex).*

In order to prove the Theorem 1.3.4.1, we need some preliminary lemmas.

1.3.5 Some useful lemmas

Lemma 1.3.5.1 *The optimal trajectory $\hat{y}_T(\cdot)$ of $\left(\mathscr{P}^{x,z}_{[0,T]}\right)$ satisfies*

$$\exists\, t(T) \in [0,T] \quad | \quad \hat{y}_T(t(T)) \longrightarrow \bar{y} \text{ as } T \to +\infty \tag{1.65}$$

Proof: The strict dissipativity inequality applied to the optimal pair $(\hat{y}_T(\cdot), \hat{u}_T(\cdot))$ implies

$$\begin{aligned} f^0(\bar{y},\bar{u}) \leqslant \frac{1}{T}\int_0^T f^0(\hat{y}_T(s),\hat{u}_T(s))ds + \frac{S(x)-S(z)}{T} \\ - \frac{1}{T}\int_0^T \alpha\left(\left\| \begin{array}{c} \hat{y}_T(s)-\bar{y} \\ \hat{u}_T(s)-\bar{u} \end{array} \right\|\right) ds \end{aligned} \tag{1.66}$$

Let us prove that

$$\frac{1}{T}\int_0^T \alpha\left(\left\| \begin{array}{c} \hat{y}_T(s)-\bar{y} \\ \hat{u}_T(s)-\bar{u} \end{array} \right\|\right) ds \longrightarrow 0 \text{ as } T \to +\infty \tag{1.67}$$

Let us assume by contradiction that this is not true: then there exists $\eta > 0$ and a sequence $T_k \longrightarrow +\infty$ such that

$$\frac{1}{T_k}\int_0^{T_k} \alpha\left(\left\| \begin{array}{c} \hat{y}_{T_k}(s)-\bar{y} \\ \hat{u}_{T_k}(s)-\bar{u} \end{array} \right\|\right) ds \geqslant \eta \tag{1.68}$$

By multiplying the inequality (1.66) by T_k one gets

$$\int_0^{T_k} \alpha\left(\left\| \begin{array}{c} \hat{y}_{T_k}(s)-\bar{y} \\ \hat{u}_{T_k}(s)-\bar{u} \end{array} \right\|\right) ds \leqslant \int_0^{T_k} w(\hat{y}_{T_k}(s),\hat{u}_{T_k}(s))ds + S(x) - S(z) \tag{1.69}$$

which implies from (1.68)

$$\mathrm{T}_k.\eta \leqslant \int_0^{\mathrm{T}_k} w(\widehat{y}_{\mathrm{T}_k}(s),\widehat{u}_{\mathrm{T}_k}(s))ds + \mathrm{S}(x) - \mathrm{S}(z) \tag{1.70}$$

Assumption (A_4) leads to a contradiction in the above inequality when $k \to +\infty$.

Then we have $\frac{1}{\mathrm{T}}\int_0^{\mathrm{T}} \alpha\left(\left\| \begin{array}{c} \widehat{y}_{\mathrm{T}}(t)-\bar{y} \\ \widehat{u}_{\mathrm{T}}(t)-\bar{u} \end{array} \right\|\right) ds \geqslant \frac{1}{\mathrm{T}}\int_0^{\mathrm{T}} \alpha\left(\|\widehat{y}_{\mathrm{T}}(t)-\bar{y}\|\right) ds \longrightarrow 0$ as $\mathrm{T} \to +\infty$ which implies, from the mean value theorem

$$\exists t(\mathrm{T}) \in [0,\mathrm{T}] \quad | \quad \alpha\left(\|\widehat{y}_{\mathrm{T}}(t(\mathrm{T}))-\bar{y}\|\right) \longrightarrow 0 \text{ as } \mathrm{T} \to +\infty \tag{1.71}$$

From the properties of $\alpha(\cdot)$, this leads to

$$\widehat{y}_{\mathrm{T}}\left(t(\mathrm{T})\right) \longrightarrow \bar{y} \text{ as } \mathrm{T} \to +\infty \tag{1.72}$$

Remark 1.3.5.1 *As proved in [84], if one makes the change of variable* $s = \dfrac{t}{\mathrm{T}}$, *in* (1.67) *then*

$$\frac{1}{\mathrm{T}}\int_0^{\mathrm{T}} \alpha\left(\left\| \begin{array}{c} \widehat{y}_{\mathrm{T}}(t)-\bar{y} \\ \widehat{u}_{\mathrm{T}}(t)-\bar{u} \end{array} \right\|\right) dt = \int_0^1 \alpha\left(\left\| \begin{array}{c} \widehat{y}_{\mathrm{T}}(\mathrm{T}.s)-\bar{y} \\ \widehat{u}_{\mathrm{T}}(\mathrm{T}.s)-\bar{u} \end{array} \right\|\right) ds \longrightarrow 0 \text{ as } \mathrm{T} \to +\infty$$

which implies, from the converse Lebesgue theorem (see [17] p. 58, Theorem IV.9) that there exists an increasing sequence of time horizons $(\mathrm{T}_k)_{k\in\mathbb{N}}$ *such that* $\widehat{y}_{\mathrm{T}_k}(\mathrm{T}_k.s) \longrightarrow \bar{y}$ *and* $\widehat{u}_{\mathrm{T}_k}(\mathrm{T}_k.s) \longrightarrow \bar{u}$ *as* $k \to +\infty$ *for almost every* $s \in [0,1]$. *The latter looks like a measure turnpike result. However we did not exploit this result in our paper.*

Lemma 1.3.5.2 *: The optimal trajectory* $\widehat{y}_{\infty f}(\cdot)$ *of* $(\mathscr{P}^x_{\infty f})$ *satisfies*

$$\widehat{y}_{\infty f}(t) \longrightarrow \bar{y} \text{ as } t \to +\infty \tag{1.73}$$

Proof: From (1.62) we have

$$\int_0^{\mathrm{T}} \alpha\left(\left\| \begin{array}{c} \widehat{y}_{\infty f}(t)-\bar{y} \\ \widehat{u}_{\infty f}(t)-\bar{u} \end{array} \right\|\right) dt \leqslant \int_0^{\mathrm{T}} w(\widehat{y}_{\infty f}(t),\widehat{u}_{\infty f}(t))dt + \mathrm{S}(x) - \mathrm{S}(\widehat{y}_{\infty f}(\mathrm{T})) \tag{1.74}$$

the right-hand side of the inequality being bounded uniformly with respect to T one gets

$$\int_0^{\mathrm{T}} \alpha\left(\|\widehat{y}_{\infty f}(t)-\bar{y}\|\right) dt \leqslant \int_0^{\mathrm{T}} \alpha\left(\left\| \begin{array}{c} \widehat{y}_{\infty f}(t)-\bar{y} \\ \widehat{u}_{\infty f}(t)-\bar{u} \end{array} \right\|\right) dt \underset{\mathrm{T}\to+\infty}{=} \mathrm{O}(1) \tag{1.75}$$

which implies:

$$\Phi(\mathrm{T}) := \int_0^{\mathrm{T}} \alpha\left(\|\widehat{y}_{\infty f}(t)-\bar{y}\|\right) dt \underset{\mathrm{T}\to+\infty}{=} \mathrm{O}(1) \tag{1.76}$$

First, we remark that (1.76) and the positivity of $\alpha(\cdot)$ imply the convergence of $\Phi(\mathrm{T})$ as $\mathrm{T} \to +\infty$.

On the other hand, from (A_1) and (A_3) we know that f is of class C^1 on the compact set $\overline{\mathrm{B}}(0,b) \times \overline{\mathrm{B}}(0,c)$ thus bounded by a global constant, denoted by $k > 0$. Therefore $\widehat{y}_{\infty f}(\cdot)$ is globally Lipschitz continuous in time t, and consequently $t \mapsto \|\widehat{y}_{\infty f}(t)-\bar{y}\|$ as well.

From the boundedness of $\widehat{y}_{\infty f}(\cdot)$ (see (A_3)) and the continuity of $\alpha(\cdot)$, we deduce the uniform continuity of $t \mapsto \alpha(\|\widehat{y}_{\infty f}(t)-\bar{y}\|)$ over $[0+\infty)$. Indeed, $\alpha(\cdot)$ being continuous on a compact set, it is uniformly continuous (Heine theorem).

By applying Barbalat's lemma (see A.1.0.1), one has $\alpha(\|\widehat{y}_{\infty f}(t)-\bar{y}\|) \longrightarrow 0$ as $t \to +\infty$, which implies $\widehat{y}_{\infty f}(t) \to \bar{y}$ as $t \to +\infty$ and the proof is over ▫.

Corollary 1.3.5.1 *Lemma 1.3.5.2 remains true for the optimal trajectory of* $(\mathscr{P}^z_{\infty b})$ *problem (with the backward-in-time dynamics* $-f$*).*

1.3.6 Proof of the main result

For $T \geqslant T_0$, let us consider $(\widehat{y}_T(\cdot), \widehat{u}_T(\cdot))$, $(\widehat{y}_{\infty f}(\cdot), \widehat{u}_{\infty f}(\cdot))$ and $(\widehat{y}_{\infty b}(\cdot), \widehat{u}_{\infty b}(\cdot))$ the optimal solutions of respectively $\left(\mathscr{P}^{x,z}_{[0,T]}\right)$, $(\mathscr{P}^{x}_{\infty f})$ and $(\mathscr{P}^{z}_{\infty b})$.

We split the optimal cost $C_T(\widehat{u}_T, x, z)$ as

$$C_T(\widehat{u}_T, x, z) = \int_0^T w(\widehat{y}_T(t), \widehat{u}_T(t))\,dt \tag{1.77}$$

$$= \underbrace{\int_0^{t(T)} w(\widehat{y}_T(t), \widehat{u}_T(t))\,dt}_{C^f_T} + \underbrace{\int_{t(T)}^T w(\widehat{y}_T(t), \widehat{u}_T(t))\,dt}_{C^b_T} \tag{1.78}$$

where $t(T)$ is defined by (1.65).

We perform the proof in two steps. We first prove that

$$\textbf{Step 1:} \quad v_f(x) + v_b(z) \leqslant \liminf_{T\to+\infty} C_T(\widehat{u}_T, x, z) \tag{1.79}$$

Then we prove that

$$\textbf{Step 2:} \quad \limsup_{T\to+\infty} C_T(\widehat{u}_T, x, z) \leqslant v_f(x) + v_b(z) \tag{1.80}$$

which will prove the required result.

The real number r being defined in Assumption (A_8), we first remark that $(y,u) \mapsto w(y,u)$ is continuous on $\Omega_r := \overline{B}(\bar{y}, K_r) \times \overline{B}(\bar{u}, K_r)$ which is a compact set of $\mathbb{R}^n \times \mathbb{R}^p$. Consequently,

$$\exists M_r > 0 \quad | \quad \forall (y,u) \in \Omega_r, \quad |w(y,u)| \leqslant M_r \tag{1.81}$$

Let $\epsilon > 0$. The continuity of $\tau_f(\cdot)$ at $\bar{y}$ gives

$$\exists \eta > 0 \text{ s.t } \|x - \bar{y}\| \leqslant \eta \Rightarrow |\tau_f(x)| \leqslant \frac{\epsilon}{2.M_r} \tag{1.82}$$

The continuity of $\tau_{-f}(\cdot)$ at $\bar{y}$ gives

$$\exists \nu > 0 \text{ s.t } \|x - \bar{y}\| \leqslant \nu \Rightarrow |\tau_{-f}(x)| \leqslant \frac{\epsilon}{2.M_r} \tag{1.83}$$

We set $\gamma := \min(\eta, \nu, r) > 0$, and we denote by $B := B(\bar{y}, \gamma)$.

▻ **Step 1**: From Lemma 1.3.5.1, we know that

$$\exists T_1 \geqslant 0 \text{ s.t } \forall T \geqslant T_1, \quad \widehat{y}_T(t(T)) \in \overline{B} \tag{1.84}$$

We select a time horizon T such that $T \geqslant \max(T_0, T_1)$ and construct $\breve{u}(\cdot)$ an admissible control for the $(\mathscr{P}^{x}_{\infty f})$ problem as follows

$$\breve{u}(t) := \begin{cases} \widehat{u}_T(t) & \text{if } t \in [0, t(T)] \\ \widehat{u}_0(t) & \text{if } t \in [t(T), t(T) + \tau_0] \\ \bar{u} & \text{if } t \geqslant t(T) + \tau_0 \end{cases}$$

where $\tau_0 := \tau_f(\widehat{y}_T(t(T)))$ is the minimum time to reach $\bar{y}$ from $\widehat{y}_T(t(T))$ and $\widehat{u}_0(\cdot)$ the associated optimal control.

We infer from (1.82) and (1.84)

$$\begin{aligned} v_f(x) &\leqslant \int_0^{+\infty} w(\check{y}(t),\check{u}(t))\,dt \\ &\leqslant \int_0^{t(\mathrm{T})} w(\widehat{y}_{\mathrm{T}}(t),\widehat{u}_{\mathrm{T}}(t))\,dt + \int_{t(\mathrm{T})}^{t(\mathrm{T})+\tau_0} w(\underbrace{\widehat{y}_0(t),\widehat{u}_0(t)}_{\in\Omega_r})dt + \int_{t(\mathrm{T})+\tau_0}^{+\infty} \underbrace{w(\bar{y},\bar{u})}_{0}\,dt \\ &\leqslant \mathrm{C}_{\mathrm{T}}^f + \tau_0.\mathrm{M}_r \\ &\leqslant \mathrm{C}_{\mathrm{T}}^f + \frac{\epsilon}{2} \end{aligned} \tag{1.85}$$

For the second term $\mathrm{C}_{\mathrm{T}}^b$, we first remark that

$$\mathrm{C}_{\mathrm{T}}^b = \int_{t(\mathrm{T})}^{\mathrm{T}} w(\widehat{y}_{\mathrm{T}}(t),\widehat{u}_{\mathrm{T}}(t))\,dt = \int_0^{\mathrm{T}-t(\mathrm{T})} w((\widetilde{y}_{\mathrm{T}}(t),\widetilde{u}_{\mathrm{T}}(t))\,dt \tag{1.86}$$

where $(\widetilde{y}_{\mathrm{T}}(t),\widetilde{u}_{\mathrm{T}}(t)) := (\widehat{y}_{\mathrm{T}}(\mathrm{T}-t),\widehat{u}_{\mathrm{T}}(\mathrm{T}-t))$ is such that

$$\dot{\widetilde{y}}_{\mathrm{T}}(t) = -f(\widetilde{y}_{\mathrm{T}}(t),\widetilde{u}_{\mathrm{T}}(t)) \text{ with } \widetilde{y}_{\mathrm{T}}(0) = z \tag{1.87}$$

Noting that $\widetilde{y}_{\mathrm{T}}(\mathrm{T}-t(\mathrm{T})) = \widehat{y}_{\mathrm{T}}(t(\mathrm{T}))$, we construct $\check{u}(\cdot)$ an admissible control for the $(\mathscr{P}_{\infty b}^z)$ problem as follows

$$\check{u}(t) := \begin{cases} \widetilde{u}_{\mathrm{T}}(t) & \text{if } t\in[0,\mathrm{T}-t(\mathrm{T})] \\ \widehat{u}_1(t) & \text{if } t\in[\mathrm{T}-t(\mathrm{T}),\mathrm{T}-t(\mathrm{T})+\tau_1] \\ \bar{u} & \text{if } t\geqslant \mathrm{T}-t(\mathrm{T})+\tau_1 \end{cases}$$

where $\tau_1 := \tau_{-f}(\widetilde{y}_{\mathrm{T}}(\mathrm{T}-t(\mathrm{T})))$ is the minimum time to reach $\bar{y}$ from $\widetilde{y}_{\mathrm{T}}(\mathrm{T}-t(\mathrm{T}))$ and $\widehat{u}_1(\cdot)$ the associated optimal control.

We infer from (1.83) and (1.84)

$$\begin{aligned} v_b(z) &\leqslant \int_0^{+\infty} w(\check{y}(t),\check{u}(t))dt \\ &\leqslant \int_0^{\mathrm{T}-t(\mathrm{T})} w(\widetilde{y}_{\mathrm{T}}(t),\widetilde{u}_{\mathrm{T}}(t))dt + \int_{\mathrm{T}-t(\mathrm{T})}^{\mathrm{T}-t(\mathrm{T})+\tau_1} w(\underbrace{\widehat{y}_1(t),\widehat{u}_1(t)}_{\in\Omega_r})dt + \int_{\mathrm{T}-t(\mathrm{T})+\tau_1}^{+\infty} \underbrace{w(\bar{y},\bar{u})}_{0}\,dt \\ &\leqslant \mathrm{C}_{\mathrm{T}}^b + \tau_1.\mathrm{M}_r \\ &\leqslant \mathrm{C}_{\mathrm{T}}^b + \frac{\epsilon}{2} \end{aligned} \tag{1.88}$$

combining (1.85) and (1.88), we obtain

$$v_f(x) + v_b(z) \leqslant \mathrm{C}_{\mathrm{T}}^f + \mathrm{C}_{\mathrm{T}}^b + \epsilon = \mathrm{C}_{\mathrm{T}}(\widehat{u}_{\mathrm{T}},x,z) + \epsilon \tag{1.89}$$

and thus

$$v_f(x) + v_b(z) \leqslant \liminf_{\mathrm{T}\to+\infty} \mathrm{C}_{\mathrm{T}}(\widehat{u}_{\mathrm{T}},x,z) \tag{1.90}$$

▷ **Step 2**: From Lemma 1.3.5.2 and Corollary 1.3.5.1, we have $\widehat{y}_{\infty f}(t) \longrightarrow \bar{y}$ and $\widehat{y}_{\infty b}(t) \longrightarrow \bar{y}$ as $t\to+\infty$. Consequently

$$\exists \mathrm{T}_2 > 0 \text{ s.t } \forall \mathrm{T}\geqslant \mathrm{T}_2,\quad \left\|\widehat{y}_{\infty f}\left(\frac{\mathrm{T}}{2}-1\right)-\bar{y}\right\| \leqslant \gamma \tag{1.91}$$

and

$$\exists \mathrm{T}_3 > 0 \text{ s.t } \forall \mathrm{T}\geqslant \mathrm{T}_3,\quad \left\|\widehat{y}_{\infty b}\left(\frac{\mathrm{T}}{2}-1\right)-\bar{y}\right\| \leqslant \gamma \tag{1.92}$$

Take $\mathrm{T}\geqslant \max(\mathrm{T}_2,\mathrm{T}_3)$ and denote

- $\tau_3 := \tau_f\left(\widehat{y}_{\infty f}\left(\frac{T}{2}-1\right)\right)$ and $\widehat{u}_3(\cdot)$ the associated optimal control;
- $\tau_4 := \tau_{-f}\left(\widehat{y}_{\infty b}\left(\frac{T}{2}-1\right)\right)$ and $\widehat{u}_4(\cdot)$ the associated optimal control.

We construct the admissible control $\underline{u}_T(\cdot)$ admissible for $\left(\mathscr{P}_{[0,T]}\right)_{x,z}$ as follows (see Figure 1.6)

$$\underline{u}_T(t) := \begin{cases} \widehat{u}_{\infty f}(t) & \text{if } t \in \left[0, \frac{T}{2}-1\right] \\ \widehat{u}_3(t) & \text{if } t \in \left[\frac{T}{2}-1, \frac{T}{2}-1+\tau_3\right] \\ \bar{u} & \text{if } t \in \left[\frac{T}{2}-1+\tau_3, \frac{T}{2}+1-\tau_4\right] \\ \widehat{u}_4(T-t) & \text{if } t \in \left[\frac{T}{2}+1-\tau_4, \frac{T}{2}+1\right] \\ \widehat{u}_{\infty b}(T-t) & \text{if } t \in \left[\frac{T}{2}+1, T\right] \end{cases}$$

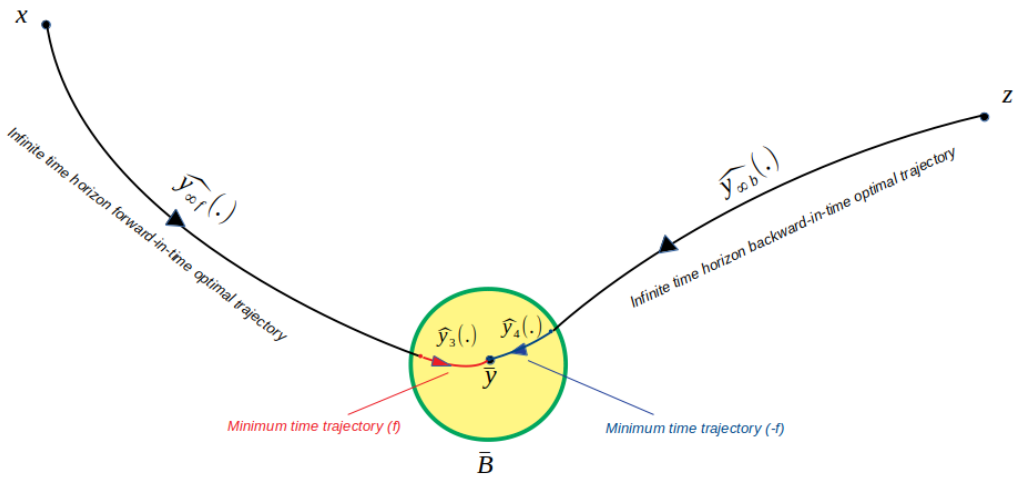

Figure 1.6: Construction of an admissible trajectory for $\left(\mathscr{P}^{x,z}_{[0,T]}\right)$

We have then the upper bound for the optimal cost

$$\begin{aligned} C_T(\widehat{u}_T, x, z) &\leqslant \int_0^T w(\underline{y}_T(t), \underline{u}_T(t))\,dt \\ &\leqslant A + B + C + D + E \end{aligned} \tag{1.93}$$

where:

$$A := \int_0^{\frac{T}{2}-1} w\left(\widehat{y}_{\infty f}(t), \widehat{u}_{\infty f}(t)\right) dt$$

$$\mathrm{E} := \int_{\frac{\mathrm{T}}{2}+1}^{\mathrm{T}} w\left(\widehat{y}_{\infty b}(\mathrm{T}-t), \widehat{u}_{\infty b}(\mathrm{T}-t)\right) dt = \int_{0}^{\frac{\mathrm{T}}{2}-1} w(\widehat{y}_{\infty b}(t), \widehat{u}_{\infty b}(t)) dt$$

$$\mathrm{B} := \int_{\frac{\mathrm{T}}{2}-1}^{\frac{\mathrm{T}}{2}-1+\tau_3} w(\underbrace{\widehat{y}_3(t), \widehat{u}_3(t)}_{\in \Omega_r}) dt \leqslant \tau_3.\mathrm{M}_r \leqslant \frac{\epsilon}{2}$$

$$\mathrm{C} := \int_{\frac{\mathrm{T}}{2}-1+\tau_3}^{\frac{\mathrm{T}}{2}+1-\tau_4} \underbrace{w(\bar{y}, \bar{u})}_{0} dt = 0$$

$$\mathrm{D} := \int_{\frac{\mathrm{T}}{2}+1-\tau_4}^{\frac{\mathrm{T}}{2}+1} w\left(\widehat{y}_4(\mathrm{T}-t), \widehat{u}_4(\mathrm{T}-t)\right) dt = \int_{\frac{\mathrm{T}}{2}-1}^{\frac{\mathrm{T}}{2}-1+\tau_4} w(\underbrace{\widehat{y}_4(t), \widehat{u}_4(t)}_{\in \Omega_r}) dt \leqslant \tau_4.\mathrm{M}_r \leqslant \frac{\epsilon}{2}$$

Finally, we obtain

$$\mathrm{C}_\mathrm{T}(\widehat{u}_\mathrm{T}, x, z) \leqslant \int_{0}^{\frac{\mathrm{T}}{2}-1} w\left(\widehat{y}_{\infty f}(t), \widehat{u}_{\infty f}(t)\right) dt + \int_{0}^{\frac{\mathrm{T}}{2}-1} w(\widehat{y}_{\infty b}(t), \widehat{u}_{\infty b}(t)) dt + \epsilon \tag{1.94}$$

Noting that the integrals A and E converge, we take the limit superior as $\mathrm{T} \to +\infty$ of the above inequality and we obtain

$$\limsup_{\mathrm{T}\to+\infty} \mathrm{C}_\mathrm{T}(\widehat{u}_\mathrm{T}, x, z) \leqslant v_f(x) + v_b(z) \tag{1.95}$$

▻ **Conclusion**: Combining (1.90) and (1.95), we obtain the required result

$$\lim_{\mathrm{T}\to+\infty} \mathrm{C}_\mathrm{T}(\widehat{u}_\mathrm{T}, x, z) = v_f(x) + v_b(z) \tag{1.96}$$

Chapter 2

Missile guidance problem

“ Doing nothing is very hard to do. You never know when you’re finished. ”

Leslie Nielsen

Sommaire

2.1 Introduction . . . 42
2.2 Guidance principles . . . 42
2.3 Surface to air missile . . . 43
2.4 Cruise missile . . . 43
2.4.1 Presentation . . . 43
2.4.2 Mission data preparation . . . 44
2.5 Equations of the motion and environment model . . . 44
2.5.1 Assumptions and Coordinate systems . . . 44
2.5.2 Kinematic equations . . . 45
2.5.3 Dynamic equations . . . 46
2.5.4 Flight in the vertical plane . . . 47
2.5.5 Discussion of the equations of motion . . . 48
2.5.6 Atmosphere model . . . 49
2.6 Context of the study . . . 50
2.7 Global trajectory optimization . . . 51
2.8 Mathematical setting . . . 51
2.9 Numerical values . . . 52

2.1 Introduction

Missiles can roughly be divided into two categories: guided missiles (or *tactical missiles*) and unguided missiles (or *strategic missiles*).

A tactical missile can be defined as an endo-atmospheric aerospace vehicle with varying guidance capabilities (means by which it steers, or is steered to a target), that is self-propelled through the atmosphere for the purpose of inflicting damage on a designated target. The vehicle is able to control its velocity through the thrust and its 3-D trajectory through the aerodynamic lift created by the rotation of its the movable surfaces (wings, fins). It is usually launched in the direction approximately towards that of a designated target and subsequently receives steering commands from the ground guidance system or its own onboard guidance system to improve its accuracy.

A strategic missile, for instance a ballistic missile, is an exo-atmospheric aerospace vehicle powered and guided for only a brief initial part of its flight after which it follows the natural laws of motion under gravity to establish a ballistic trajectory.

Figure 2.1: Artist view of the M 51 ballistic missile

Within the framework of this study, we are interested in the guidance of tactical missiles.

2.2 Guidance principles

Tactical missiles may either home to the target, or follow a nonhoming course. The nonhoming course can be either inertially guided or pre-programmed. When the firing range is beyond the seeker's detection range, the missiles usually combine both of above mentioned guidance modes. The nonhoming phase, also known as *mid-course guidance*, starts after the launch and aims at steering the missile to the vicinity of the target in the optimal conditions before engaging the homing phase. Just before the end of this stage, the onboard seeker locks on the target.

The homing phase, also known as *terminal guidance*, starts with the locking on of the seeker and ends at the interception of the target. During this stage, the seeker sends all the relevant target information to the missile computer in order to shape the trajectory till the interception.

Many studies solve the terminal guidance problem with various guidance laws amongst which the most famous being the Proportional Navigation and its variants (see [51]). In this thesis, we treat the overall trajectory guidance.

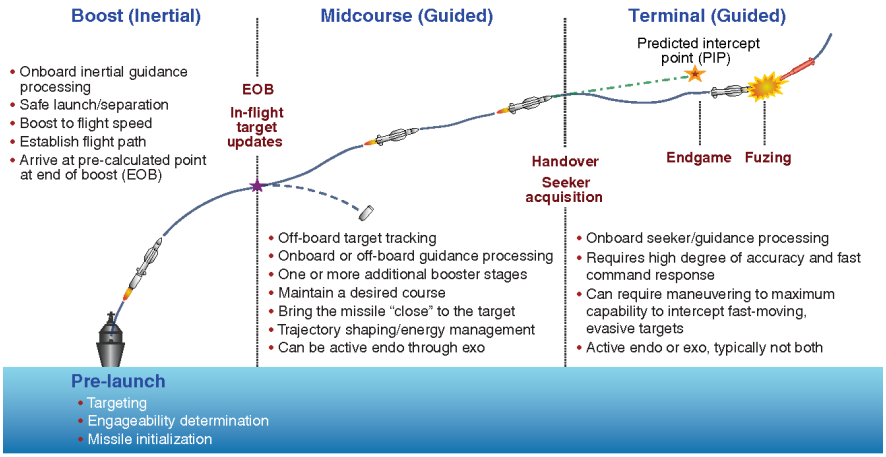

Figure 2.2: Guidance principle

2.3 Surface to air missile

The surface-to-air missile aims at intercepting highly maneuverable targets (fighters, enemy missiles) including at high altitudes (up to 20 km). Hence, the required maneuverability has to be great enough to fullfill the mission.

It is usually powered by an all boost rocket motor that provides thrust across the wide Mach number range and causes high peak velocities. The longitudinal acceleration is great during the propulsive phase after which the missile gradually decelerates due to the drag force. The propulsive phase duration is relatively short with respect to the flight time. The suitable aerodynamic configuration ensures high normal load factor capability.

During the mid-course guidance, the target trajectory is predicted by specific algorithms using its current state (position and velocity) returned by a radar. The position where the interception is supposed to happen is known as the Predicted Interception Point (PIP). The PIP can be sent periodically from the radar to the interceptor using a communication channel. From its current position and the updated target information, the missile computer calculates the optimal trajectory with respect to the target. When the interceptor approaches the PIP, the seeker locks on the target to perform the terminal guidance.

2.4 Cruise missile

2.4.1 Presentation

A cruise missile can be defined as a self guided, pilotless, continuously powered air-breathing vehicle that flies like airplane, supported by aerodynamic surfaces. Launched from air, sea or land, it aims at treating land or sea targets.

The typical range of a cruise missile is extremely variable and may depend on multiple factors amongst which the launch platform (a missile launched from a fighter will likely have longer range than a missile launched from a ship), the performance & autonomy of the propeller and of course of the assignated mission. Roughly speaking the typical range can vary between 10 km up to 750 km.

The mid course guidance is generally inertial (Global Positionning System (GPS) & Inertial Navigation Unit (INU)) with terrain correlation (periodical update with stored ground maps) and/or some waypoints. In practice, the guidance information delivered by the sensors is processed in real time by the onboard computer which adjusts the trajectory if needed. At the very end of this phase, the seeker switches on, searches for the target before locking on it. From the instant of lock on until the collision, the missile is guided in the autonomous way exploiting the information

provided by the seeker.

The guidance is crucial and continuous for cruise missiles since both the velocity and the direction of its flight can be unpredictably altered, for example, by local weather conditions.

2.4.2 Mission data preparation

The Mission Data Preparation (MDP) is a prelaunch design phase which aims (amongst other tasks) at calculating a reference trajectory that will be followed by the missile during the major part of its flight. The shaping of the trajectory starts at the theoretical launch point and ends at the target location (with possibly heading & pitch angles terminal constraints). The design of an acceptable trajectory has to respect several criteria:

- the dynamics has to comply with the vehicle capabilities (speed, load factor, fuel autonomy)
- the trajectory has to respect path constraints: avoidance of "forbidden zones" (enemy radar coverage zones) or flight within prescribed air corridors.
- minimization of the time of flight.

Within the context of multi-missile cooperative action, issues like collision avoidance may have to be suitably treated. May the meteorological report be available prior to the mission, one could optimize the time of flight with respect to the wind profile.

In the framework of this thesis, we consider the guidance of a cruise missile.

2.5 Equations of the motion and environment model

The equations of motion are derived by using the Newton's law. Newton's laws are valid when written relative to an inertial reference frame, that is, a reference frame which is not accelerating or rotating. If the equations of motion are derived relative to an accurate inertial reference frame and if approximations characteristic of missile motion are introduced into these equations, the resulting equations are those for flight over a nonrotating flat earth. Within our study, we restrict ourselves to the maximum range up to $50km$. Under this restriction, the flat earth assumption remains reasonable.
The equations of motion are composed of translational (force) equations ($F = m.a$) and rotational (moment) equations ($M = I.\alpha$) and are called the six degree of freedom (6-DOF) equations of motion. In our analysis, the translational equations are uncoupled from the rotational equations by assuming that the vehicle rotational rates are relatively small and that control surface deflections do not affect forces. Classically, the translational equations are referred to as the three degree of freedom (3-DOF) equations of motion.

2.5.1 Assumptions and Coordinate systems

In deriving the equations of motion for the flight of a cruise missile, the following physical model is assumed:

- The earth is flat, nonrotating, and an approximate inertial reference frame. The acceleration of gravity is constant and perpendicular to the surface of the earth. This is known as the flat earth model.
- The atmosphere is at rest relative to the earth, and atmospheric properties are functions of altitude only.
- The missile is a "classical" cruise missile type with fixed engine, an and a right-left plane of symmetry. It is modeled as a variable-mass particle.

- The forces acting on the vehicle in symmetrical flight are the thrust, the aerodynamic force, and the weight. They act at the center of gravity of the vehicle.

The derivation of the equations of motion is clarified by defining a number of coordinate systems. The three coordinate systems used here are the following, all of them being direct and orthonormal (see figure 2.3):

1. The local earth frame $\mathscr{R}_{ned} := (\mathrm{E}, \mathbf{i}_e, \mathbf{j}_e, \mathbf{k}_e)$ is fixed to the surface of the earth at mean sea level: $\mathbf{i}_e$ is oriented towards the local North, $\mathbf{j}_e$ towards the East and $\mathbf{k}_e$ is down oriented . This referential is usually called "North-East Down" (NED).

2. The body frame $\mathscr{R}_b := (\mathrm{G}, \mathbf{i}_b, \mathbf{j}_b, \mathbf{k}_b)$ is conventional to the body of the vehicle. The center of this frame is at the center of gravity of the vehicle, and its components are forward, out of the right side, and down. The orientation is calculated from the $\mathscr{R}_{ned}$ frame through three successive rotations: ψ-heading angle around z axis, θ-pitch angle around y axis and μ-roll angle around x axis.

3. The air frame $\mathscr{R}_a : (\mathrm{G}, \mathbf{i}_a, \mathbf{j}_a, \mathbf{k}_a)$ centered at the center of gravity and where $\mathbf{i}_a$ is coincident with the velocity vector $\mathbf{v}$. The orientation is obtained from the body frame through two successive rotations: α-angle of attack around y axis, β-sideslip angle around z axis.

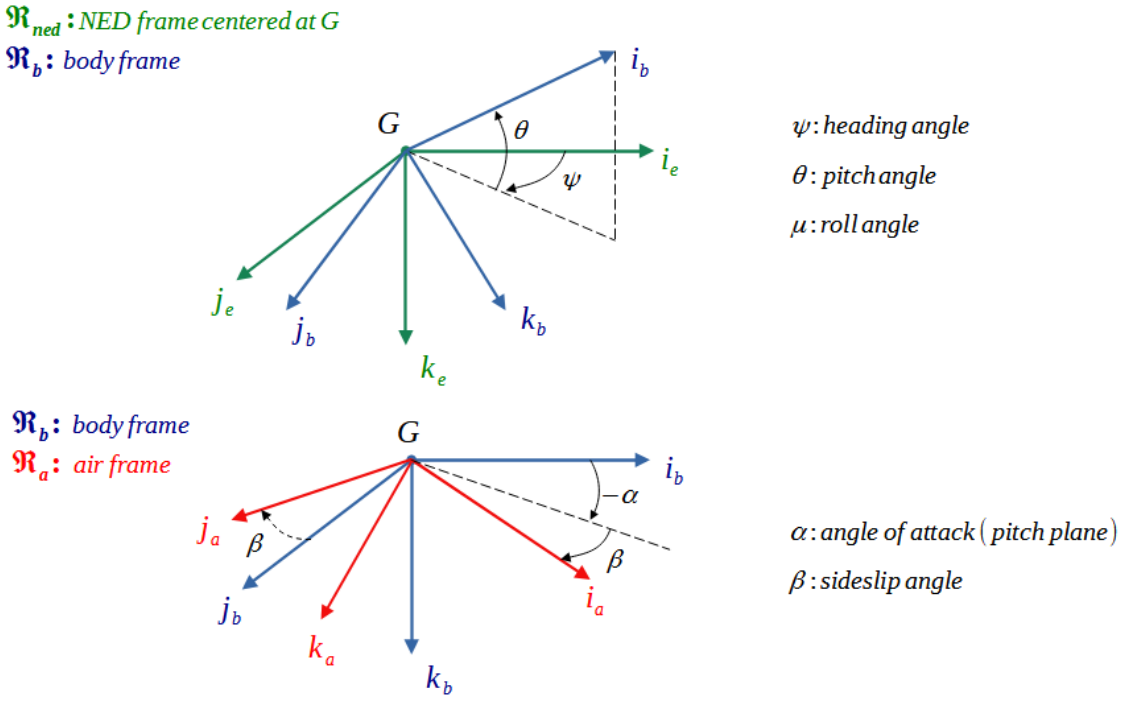

Figure 2.3: Coordinate systems

Remark 2.5.1.1 *: As one wants the angle of attack to be positive when the body is above the velocity in the pitch plane, we change the sign convention accordingly (see the figure 2.3).*

2.5.2 Kinematic equations

Kinematics is used to derive the differential equations for the coordinates of G, denoted by $(x, y, -h)$ h being the altitude of the vehicle above the sea level. The basic relation is:

$$\frac{d\mathbf{EG}}{dt} = \dot{x}\mathbf{i}_e + \dot{y}\mathbf{j}_e - \dot{h}\mathbf{k}_e = \mathbf{V} = v.\mathbf{i}_a \tag{2.1}$$

The coordinates of the vector $\mathbf{X}$ in the air frame $\mathscr{R}_a$ can be expressed in the NED frame $\mathscr{R}_{ned}$ as follows:

$$\mathbf{X}|_{\mathscr{R}_{ned}} = \mathrm{P}_{\mathscr{R}_{ned}/\mathscr{R}_a}.\mathbf{X}|_{\mathscr{R}_a} \tag{2.2}$$

$$= \mathrm{P}_3(\psi).\mathrm{P}_2(\theta).\mathrm{P}_1(\mu).\mathrm{P}_2(-\alpha).\mathrm{P}_3(\beta).\mathbf{X}|_{\mathscr{R}_a} \tag{2.3}$$

where:

$$\mathrm{P}_1(\mu) := \begin{pmatrix} 1 & 0 & 0 \\ 0 & \cos\mu & \sin\mu \\ 0 & -\sin\mu & \cos\mu \end{pmatrix}, \mathrm{P}_2(\theta) := \begin{pmatrix} \cos\theta & 0 & \sin\theta \\ 0 & 1 & 0 \\ -\sin\theta & 0 & \cos\theta \end{pmatrix}$$

$$\mathrm{P}_3(\psi) := \begin{pmatrix} \cos\psi & -\sin\psi & 0 \\ \sin\psi & \cos\psi & 0 \\ 0 & 0 & 1 \end{pmatrix}$$

With our notations, (2.1) reads:

$$\cdot \begin{pmatrix} \dot{x} \\ \dot{y} \\ -\dot{h} \end{pmatrix} = \mathrm{P}_3(\psi).\mathrm{P}_2(\theta).\mathrm{P}_1(\mu).\mathrm{P}_2(-\alpha).\mathrm{P}_3(\beta). \begin{pmatrix} v \\ 0 \\ 0 \end{pmatrix} \tag{2.4}$$

2.5.3 Dynamic equations

Dynamics is used to derive the differential equations for $\mathbf{V}$ and attitude angles. Newton's second law states that:

$$m.\dot{\mathbf{V}} + \dot{m}.\mathbf{V} = \mathbf{T} + \mathbf{L} + \mathbf{D} + \mathbf{W} \tag{2.5}$$

where $\mathbf{T}$ is the thrust, $\mathbf{D}$ is the aerodynamic drag, $\mathbf{L}$ is the aerodynamic lift and $\mathbf{W}$ is the weight.

Weight: The weight is given by $\mathbf{W} = m.g.\mathbf{k}_e$. Moreover, by introducing the specific fuel consumption denoted by C_s, the mass equation reads:

$$\dot{m} = -\mathrm{C}_s.\mathrm{T} \tag{2.6}$$

where T is the magnitude of the thrust force.

Drag and Lift: The drag on the vehicle is the friction force exerted on it by the air directed opposite to the velocity vector $\mathbf{V}$. Usually, the effect of the drag force is lumped into one coefficient $\mathrm{C_D}$ called drag coefficient which depends on the overall angle of attack (angle between the velocity of the vehicle $\mathbf{V}$ and its principal body axis $\mathbf{i}_b$), the Mach number and the aerodynamic configuration of the vehicle. The drag force is defined as follows:

$$\mathbf{D} = -\mathrm{D}.\,\mathbf{i}_a \text{ with } \mathrm{D} = \bar{q}(h,v).\mathrm{S}.\mathrm{C_D}(h,v,\alpha,\beta) \tag{2.7}$$

with $\mathrm{S} = \dfrac{\pi d^2}{4}$ being the vehicle section reference area, $\bar{q}(h,v) = \frac{1}{2}.\rho(h).v^2$ is the dynamical pressure, with ρ the air density.

The lift is defined as the aerodynamic force that acts orthogonally to the velocity vector. The analytical expression of the lift is provided as:

$$\mathbf{L} = \mathrm{L}.\mathbf{i}_a \wedge (\mathbf{i}_b \wedge \mathbf{i}_a) \text{ with } \mathrm{L} = \bar{q}(h,v).\mathrm{S}.\mathrm{C_L}(h,v,\alpha,\beta) \tag{2.8}$$

The scalar coefficient $\mathrm{C_L}$ called lift coefficient has the same dependancies than the drag coefficient $\mathrm{C_D}$.

Thrust: In terms of direction, the thrust vector is colinear to the vehicle body directed towards, thus $\mathbf{T} = \mathrm{T}.\mathbf{i}_b$. It is also known that thrust and specific fuel consumption C_s satisfy functional relations of the form:

$$\mathrm{T} = \mathrm{T}(h,v,\eta), \qquad \mathrm{C}_s = \mathrm{C}_s(h,v,\eta) \tag{2.9}$$

where η is the thrust throttle coefficient.

2.5.4 Flight in the vertical plane

Within the frame of our study, we restrict ourselves to the flight of the vehicle in the vertical plane. Consequently, from now on, the heading, the roll and the sideslip angles are such that $\psi = 0$, $\mu = 0$ and $\beta = 0$.

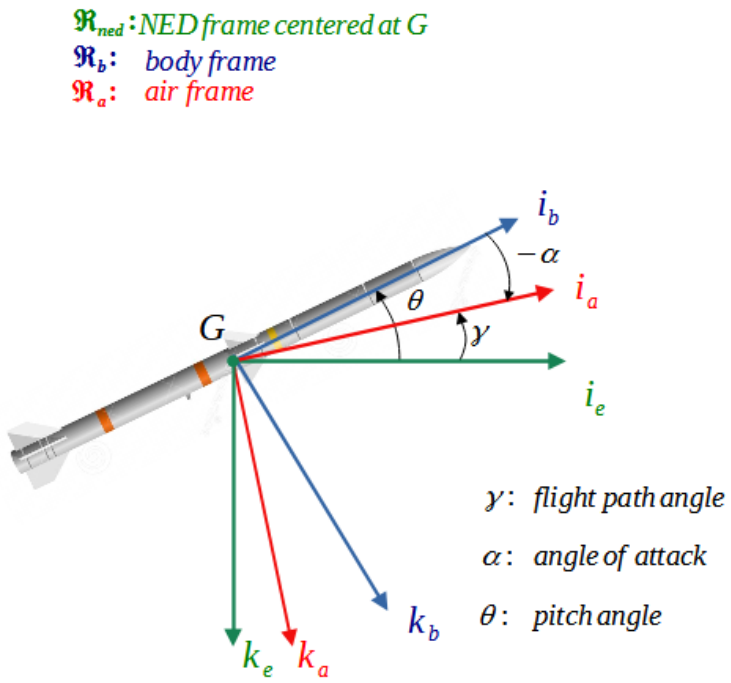

Figure 2.4: Forces acting on the vehicle in flight

With previous assumptions, by introducing the flight path angle $\gamma := \theta - \alpha$, (2.4) reduces to:

$$\dot{x} = v.\cos\gamma \tag{2.10}$$
$$\dot{h} = v.\sin\gamma \tag{2.11}$$

Remark 2.5.4.1 *: The flight path angle γ is classically the angle between the velocity vector and the horizontal reference in the vertical plane.*

By projecting (2.5) respectively on $\mathbf{i}_a$ and $\mathbf{i}_b$, one obtains after arrangement:

$$\dot{v} = \frac{T.\cos\alpha - D - \dot{m}.v}{m} - g.\sin\gamma \tag{2.12a}$$
$$\dot{\gamma} = \frac{L + T.\sin\alpha}{m.v} - \frac{g.\cos\gamma}{v} \tag{2.12b}$$

2.5.5 Discussion of the equations of motion

By regrouping (2.6), (2.10) and (2.12), one obtains:

$$\dot{x} = v.\cos\gamma \tag{2.13a}$$

$$\dot{h} = v.\sin\gamma \tag{2.13b}$$

$$\dot{v} = \frac{T(h,v,\eta).\cos\alpha - D(h,v,\alpha) - \dot{m}.v}{m} - g.\sin\gamma \tag{2.13c}$$

$$\dot{\gamma} = \frac{L(h,v,\alpha) + T(h,v,\eta).\sin\alpha}{m.v} - \frac{g.\cos\gamma}{v} \tag{2.13d}$$

$$\dot{m} = -C_s.T \tag{2.13e}$$

Consequently, the state variables are x, h, v, γ and m whereas the the thrust throttle η and the angle of attack α appear naturally as the control variables.

Actually, the coefficients C_D et C_L are not directly available: they are determined by using the axial force coefficient C_A and the normal force coefficient C_N (in the body frame $\mathscr{R}_b$, refer to [74, 35, 87]). The relation connecting them reads:

$$C_D = C_N(h,v,\alpha).\sin\alpha + C_A(h,v,\alpha).\cos\alpha \tag{2.14}$$

$$C_L = C_N(h,v,\alpha).\cos\alpha - C_A(h,v,\alpha).\sin\alpha \tag{2.15}$$

The coefficients C_N and C_A are experimentally measured during the wind tunnel trials. Their dependance on h, v and α is in general complex to estimate analytically as it depends on intrinsic aerodynamic characteristics of the missile body (length, wingspan, caliber...). However, some empirical formulas are available for instance in [74, 35, 87].

On the other hand, considering endo-atmospheric applications, the vehicle can be stabilized only if the angle of attack α remains lower than a critical threshold α_{max}, which is assumed to be quite low for the cruise missiles (typically, $\alpha_{max} \approx 15^\circ$). In this case, a Taylor development of the aerodynamic coefficients allows to obtain the following parabolic drag polar approximation:

$$C_D = C_{D_0} + k_c.C_L^2 \tag{2.16}$$

where C_{D_0} is the zero-lift drag coefficient, $k_c.C_L^2$ is the induced drag coefficient and k_c is the induced-by-the-lift drag factor. Theoretically, C_{D_0} and k depend of the Mach number. However, as the Mach number range covered by a cruise missile is reduced, we assume that the latter coefficients are constant.

With the drag polar approximation (2.16), one remarks that the aerodynamic forces D and L can now be expressed as functions of C_L, as the angle of attack α "disappears". Moreover, as the average value of α remains low during the flight, we make the assumption that $\cos\alpha \approx 1$ and $\sin\alpha \approx 0$ in the equations of motion (2.13). Consequently, the lift coefficient C_L becomes naturally the control in place of the angle of attack α.

Related to the thrust, the dependance on the parameters h, v can be quite intricate; indeed the produced thrust is function of the altitude, Mach number, surface and geometry of the air inlet entrance and outlet exit, the compressor pressure ratio... An overview of the existing technology and some empirical formulas to estimate the thrust performance is available for instance in [35]. In our study, we consider the following (somehow idealized) formula:

$$T = T_{max}.\eta \tag{2.17}$$

where the throttle coefficient $\eta \in [\eta_{min}, 1.0]$, and T_{max} is the maximum available thrust that can be delivered by the engine.

2.5.6 Atmosphere model

In order to compute the aerodynamical interactions between the vehicle and its environment, one needs to estimate, as functions of altitude, the air temperature, pressure, density and speed of sound. The function detailed below follow the ARDC (Air Research and Development Command, of the U.S Air Force) atmosphere model.

The atmosphere is divided into three layers within which the ambient temperature T_a [K] and pressure P_a [N.m^{-2}] are modelled as follows:

$$T_a = \begin{cases} T_0 - 6.5.h, & h \in [0\text{ km}, 11\text{ km}] \text{ (troposphere)} \\ 216.667, & h \in]11\text{ km}, 25\text{ km}] \text{ (lower stratosphere)} \\ 216.667 + 3.(h-25), & h > 25\text{ km (upper stratosphere)} \end{cases} \tag{2.18}$$

where T_0 is the ambient temperature at sea level, $T_0 = 288.2$ K.

$$P_a = \begin{cases} P_0(1 - 0.02256.h)^{5.2561}, & h \in [0\text{ km}, 11\text{ km}] \\ 0.223.P_0 \exp(-0.1577.(h-11)), & h \in]11\text{ km}, 25\text{ km}] \\ 2489.773.\exp(-0.1577.(h-25)), & h > 25\text{ km} \end{cases} \tag{2.19}$$

where P_0 is the ambient pressure at sea level, $P_0 = 101314.6$ N.m^{-2}.

We recover the air density $\rho = \dfrac{P_a}{R.T_a}$ [kg.m^{-3}] and the speed of sound $c = \sqrt{k.R.T_a}$ [m.s^{-1}] where k is the ratio of specific heat of the air ($k = 1.4$) and R is the gas constant (R = 287 J.kg^{-1}.K^{-1}).

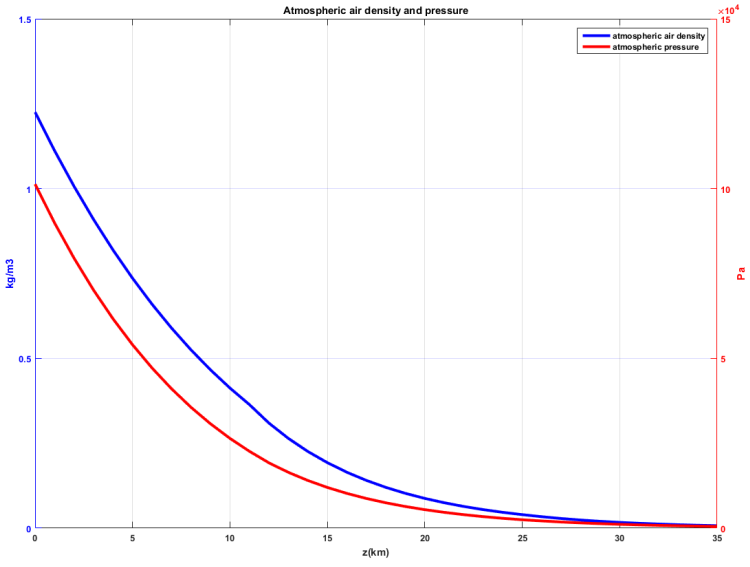

Figure 2.5: Atmospheric air density and pressure function of h

We highlight that for values of $h \in [0m, 20km]$, the above detailed formula of the air density ρ can be approximated as follows:

$$\rho(h) = \rho_0.\exp\left(-\frac{h}{h_r}\right) \tag{2.20}$$

where ρ_0 the air density of the standard atmosphere at the sea level and h_r is a fixed reference altitude. We will use this approximation of the atmosphere in this work. For more details on the atmosphere model, refer for instance to [74].

2.6 Context of the study

As explained previsously, we are interested in the cruise missile guidance problem restricted to the vertical plane. The trajectory of a such a vehicle is pre-programmed off-line prior to the mission depending on the relief on the path. For sake of simplicity, one can define two typical flight profiles (although somehow caricatural) in the vertical plane as follows:

- A-Profile: the relief being typically the sea, the vehicle flies most of the time at very low height with respect to the sea ("sea skimming") in order to minimize the exposure to enemy sensors (radars). The reference flight altitude is usually called cruise altitude, will be denoted by $h_c \in [100m, 500m]$. This flight profile is typically applicable to the anti-ship cruise missiles.

- B-Profile: the relief is mountainous, the missile can fly at higher ("safety") altitude in order to reduce any risk of collision prior to the end of the mission.

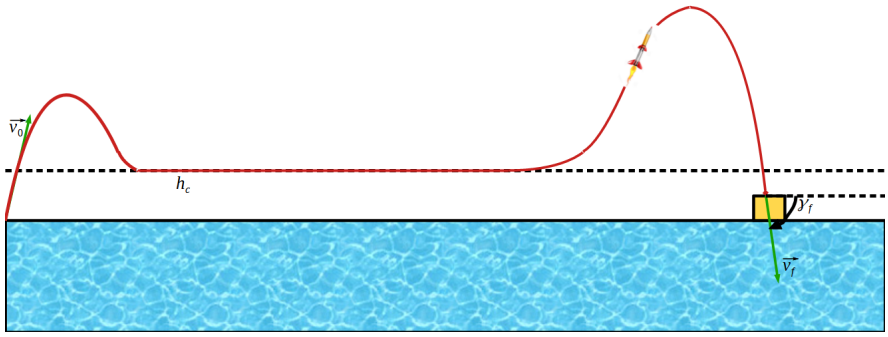

Figure 2.6: A-Profile typical trajetory

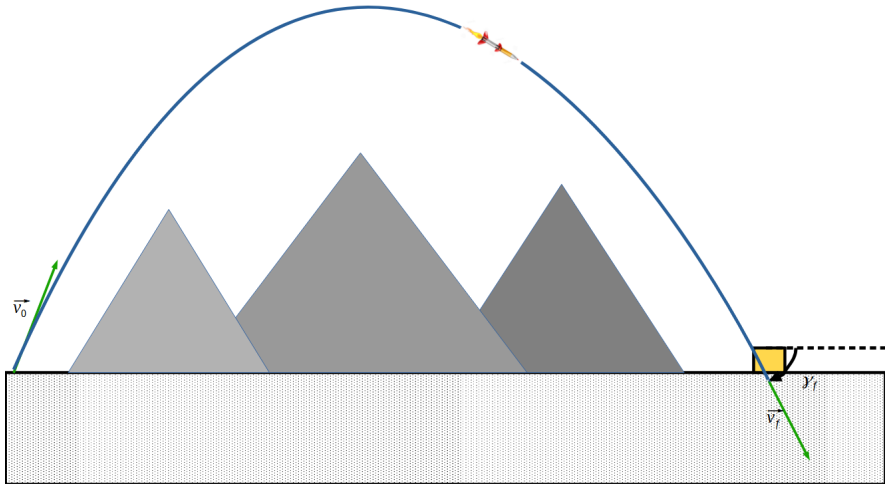

Figure 2.7: B-Profile typical trajetory

We consider hereafter the global guidance problem of such a vehicle starting from the launch and finishing at the impact with the target.

2.7 Global trajectory optimization

We consider a target modelled as a point of coordinates (x_f, h_f) with respect to the local earth frame $\mathscr{R}_{ned}$. The objective is to reach the target with prescribed flight path angle γ_f. The final speed $v_f > 0$ can be either prescribed or let free. In what follows, we assume that the launch and the final point are located on the Earth surface at sea level altitude thus one sets, for sake of simplicity: $(h_0, h_f) := (0,0)$.

For the A-profile mission, given the visibility constraint to be respected, one can intuitively expect the missile to remain "stuck" to the cruise altitude h_c most of its flight time. Consequently, the typical A profile trajectory can be divided into three pieces:

1. "initial transitory phase": the missile joins the cruise altitude starting from its initial position.
2. "cruise phase": the missile altitude remains close to h_c.
3. "bunt phase": the vehicle leaves the cruise altitude et climbs up to the peak of the trajectory before "diving" onto the target. Intuitively, the maximum altitude will be function of the desired terminal angle of attack (and velocity, if prescribed). This leads to a typical "parabolic shape" of the terminal trajectory, as illustrated on the figure 2.6.

Remark 2.7.0.1 *The A-profile trajectory will be called "bunt case" in the rest of the thesis.*

2.8 Mathematical setting

By taking into account (2.16) and (2.17), the dynamics (2.13) can be written as follows:

$$\dot{x} = v.\cos\gamma \tag{2.21a}$$
$$\dot{h} = v.\sin\gamma \tag{2.21b}$$
$$\dot{v} = \frac{T_{max}.(1+C_s.v).\alpha_1 - D(h,v,\alpha_2)}{m} - g.\sin\gamma \tag{2.21c}$$
$$\dot{\gamma} = \frac{L(h,v,\alpha_2)}{m.v} - \frac{g.\cos\gamma}{v} \tag{2.21d}$$
$$\dot{m} = -C_s.T_{max}.\alpha_1 \tag{2.21e}$$

where $\alpha_1 = \eta$ the thrust throttle and $\alpha_2 = C_L$ the lift coefficient. Clearly speaking $\alpha := \begin{pmatrix} \alpha_1 \\ \alpha_2 \end{pmatrix}$ is the control of the dynamical system given by (2.21). At the first order, we have:

- the thrust throttle $\alpha_1(\cdot)$, controlling the velocity
- the lift coefficient $\alpha_2(\cdot)$, controlling the "shape" of the trajectory. Physically, it plays the role of the angle of attack.

The controls are bounded due to the vehicle aerodynamic limitations: $\alpha_1(t) \in [\eta, 1]$, with $\eta \in]0,1[$ and $|\alpha_2(t)| \leqslant \alpha_2^m$. In what follows, we denote $\xi := (x \;\; h \;\; v \;\; \gamma \;\; m)^T$ and $A := [\eta, 1] \times [-\alpha_2^m, \alpha_2^m]$.

Now we have to model the constraints and the performance corresponding to each profile through an adequate index. An efficient way (but not the unique one!) to do so is to consider a Lagrange cost made of two terms which correspond respectively to the time of flight and the penalization of the the cruise altitude h_c. The optimal control problem can be formulated as follows:

$$(\mathbf{OCP})_0 \begin{cases} \min\limits_{(t_f, \alpha \in \mathscr{A})} J_0(t_f, \alpha) := \displaystyle\int_0^{t_f} \left(k_0 + k_1.\frac{(h(s)-h_c)^2}{h_c^2} \right) ds \\ \dot{\xi}(s) = f(\xi(s), \alpha(s)) \qquad \forall s \in [0, t_f] \\ \alpha(.) \in \mathscr{A} \\ \xi(0) = \xi_0, \;\; \xi(t_f) = \xi_f \end{cases} \tag{2.22}$$

where:

- $\mathscr{A}$ is a set of admissible control strategies defined as $\mathscr{A} := \{\alpha : [0, +\infty[\to A\}$ with A compact subset of $\mathbb{R}^p$
- $f(\xi,\alpha) := \begin{pmatrix} v.\cos\gamma \\ v.\sin\gamma \\ \dfrac{T_{max}.(1+C_s.v).\alpha_1 - D(h,v,\alpha_2)}{m} - g.\sin\gamma \\ \dfrac{L(h,v,\alpha_2)}{m.v} - \dfrac{g.\cos\gamma}{v} \\ -C_s.T_{max}.\alpha_1 \end{pmatrix}$ is the dynamics
- $\xi_0 = (x_0 \;\; h_0 \;\; v_0 \;\; \gamma_0 \;\; m_0)^T$ and $\xi_f = \left(x_f \;\; h_f \;\; v_f \text{ or} * \;\; \gamma_f \;\; *\right)^T$ are the prescribed initial and final states.
- $(k_0, k_1) \in \mathbb{R}^+ \times \mathbb{R}^+$ is the weight couple in the performance index. k_0 and k_1 weight respectively the time of flight and the deviation to the cruise altitude.

If one chooses $k_0 > 0$ and $k_1 = 0.0$, then $(\mathbf{OCP})_0$ is the time minimum problem and the optimal trajectory is expected to "resemble" to the B-profile (see fig. 2.7). If $k_1 > 0$ and large enough, then the cruise altitude constraint becomes active and the optimal trajectory should correspond rather to the A-profile (see fig. 2.6). This point will be discussed from the mathematical point of view in the chapter 3.

In the rest of this thesis (except in the chapter 4), we slightly simplify the original problem by assuming the induced-by-the-lift drag factor k_c is negligible thus $k_c \approx 0$. Indeed, in practice, the coupling between the lift and drag force can be neglected at first order.

Moreoever, in the chapter 3 we consider that the thrust remains at its maximum value (i.e, $\forall t \in [0, t_f]$, $\alpha_1(t) = 1$). In the chapter 4 and the Annex A, we will consider it as an active control.

Remark 2.8.0.1 *Under the last assumptions, the ODE (2.21c) governing the state variable $v(\cdot)$ depends only (at the second order) on the flight path angle γ, as the drag D does not depend anymore on α_2.*

Finally, the lift coefficient α_2 remains the unique control of our system and will be denoted by α.

2.9 Numerical values

The following table sums up the numerical values considered in our setting:

Variable	Value	Unit
d	0.65	m
C_d	0.4	n.a
T_{max}	5000	N
C_s	4.10^{-4}	$kg.s^1.N^{-1}$
g	9.81	$m.s^{-2}$
ρ_0	1.225	kg/m^3
h_r	7314	m
α_{max}	2	n.a
h_c	250	m
(k_0, k_1)	(var, var)	$n.a$

Table 2.1: Numerical values for the guidance problem

We consider the following boundary conditions:

$$(x_0, h_0, v_0, \gamma_0, m_0) = (0\text{m}, 0\text{m}, 300\text{m/s}, 80^\circ, 600\text{kg}) \tag{2.23a}$$

$$(x_f, h_f, v_f, \gamma_f, m_f) = (25000\text{m}, 0\text{m}, *, -80^\circ, *) \tag{2.23b}$$

Remark 2.9.0.1 *As the thrust control $\alpha_1(\cdot)$ has been set to 1, then we have to let the terminal velocity v_f free. Obviously if we consider the thrust $\alpha_1(\cdot)$ as active, then the velocity of the system can be controlled and we could specify a desired value for v_f. An example of the two dimensional control case is treated in the Annex section A.5.*

Chapter 3

Numerical solving of the guidance problem

"It is better to be hated for what you are than be loved for what you are not."

André Gide

Sommaire

3.1 Optimal control in finite dimension . . . 57
3.1.1 General setting . . . 57
3.1.2 Pontryagin maximum principle . . . 58
3.2 Numerical methods in optimal control . . . 59
3.2.1 Context . . . 59
3.2.2 Direct methods . . . 60
3.2.3 Indirect methods . . . 60
3.2.4 Methods implemented in the thesis . . . 61
3.3 Continuation methods . . . 62
3.3.1 Existence results and discrete continuation . . . 62
3.3.2 Numerical tracking of the zero paths . . . 62
3.4 Dubins-Fuller problem . . . 64
3.4.1 Motivation and definition of the model . . . 64
3.4.2 Dubins case $(k_0, k_1) = (1, 0)$ . . . 65
3.4.2.1 State of the art . . . 65
3.4.2.2 Direct method . . . 66
3.4.2.3 Shooting method . . . 67
3.4.2.4 Numerical implementation . . . 68
3.4.2.5 Numerical tests . . . 68
3.4.3 Fuller case $(k_0, k_1) = (0, 1)$ . . . 69
3.4.3.1 Direct method . . . 69
3.4.3.2 Comments . . . 70
3.4.3.3 Optimal synthesis in the Fuller case . . . 71
3.4.4 Dubins-Fuller case, $k_0 > 0$, $k_1 > 0$ . . . 72
3.4.4.1 Formal analysis . . . 72
3.4.4.2 Direct method . . . 73
3.4.4.3 Numerical solving strategy: L^2 regularization and shooting method 76

3.4.4.4 Continuation at step 1 . . . 78
3.4.4.5 Well posedness of the shooting method . . . 78
3.4.4.6 Optimal solution for $\lambda_1 = 1.0$ . . . 79
3.4.4.7 Continuation at step 2 . . . 80
3.4.4.8 Comments . . . 81
3.5 The missile guidance problem . . . 82
3.5.1 Parametrized dynamics . . . 82
3.5.2 Numerical solving strategy . . . 82
3.5.3 The minimum time problem . . . 83
3.5.4 The "bunt" case . . . 85
3.5.4.1 Continuation at step 1 . . . 86
3.5.4.2 Continuation at step 2 . . . 88
3.5.4.3 Comments and perspectives . . . 90
3.5.5 Computation of a quasi optimal trajectory by a reduced shooting method . 90

3.1 Optimal control in finite dimension

The term finite dimension refers to the fact that the state vector $\xi(\cdot)$ belongs to the finite dimensional space $\mathbb{R}^n$. However, it is important to keep in mind that solving an optimal control problem like (2.22) in finite dimension requires being able to solve an infinite dimensional optimization problem.

3.1.1 General setting

In this section, we consider the following general control problem: given $\mathscr{M}_0$ and $\mathscr{M}_1$ two submanifolds of $\mathbb{R}^n$ we aim at controlling the autonomous nonlinear system:

$$\dot{\xi}(t) = f(\xi(t), \alpha(t)) \text{ on } [0, t_f] \tag{3.1}$$

while minimizing the cost:

$$C(t_f, \alpha) := \int_0^{t_f} f^0(\xi(t), \alpha(t))\, dt + g(t_f, \xi(t_f)) \tag{3.2}$$

and such that:

$$\xi(0) \in \mathscr{M}_0 \text{ and } \xi(t_f) \in \mathscr{M}_f \tag{3.3}$$

In the above definition, we assume $f : \mathbb{R}^n \times \mathbb{R}^p \to \mathbb{R}^n$, $f^0 : \mathbb{R}^n \times \mathbb{R}^p \to \mathbb{R}$ and $g : \mathbb{R} \times \mathbb{R}^n \to \mathbb{R}$ are of class C^1. The control $\alpha(\cdot)$ belongs to the set $L^\infty([0, t_f], A)$ where A is a subset of $\mathbb{R}^p$. In the following, t_f can be free or fixed. We denote $\mathscr{A}$ the set of *admissible controls* i.e. such that the corresponding trajectories steer the system from an initial point of $\mathscr{M}_0$ to a final point of $\mathscr{M}_f$.

Remark 3.1.1.1 *It is far from obvious that there exists a solution to the previous optimal control problem. However, if one assumes, in addition to the above mentioned regularity assumptions on f, f^0 and g that the following asumptions hold:*

(i) A *is a compact subset of* $\mathbb{R}^p$

(ii) there exists $b > 0$ such that any admissible trajectory $\xi_\alpha(\cdot)$ and the associated time t_f are bounded by b:

$$\exists b > 0 \;\mid\; \forall \alpha \in \mathscr{A},\ \forall t \in [0, t_f],\ t_f + \|\xi_\alpha(t)\|_\infty \leqslant b \tag{3.4}$$

(iii) for any $\mu \in \mathbb{R}^n$, the set V *defined by:*

$$V(\mu) := \left\{ \left(f^0(\mu, a) + \gamma, f(\mu, a) \right) \mid a \in A,\ \gamma \geqslant 0 \right\} \tag{3.5}$$

is a convex subset of $\mathbb{R}^{n+1}$.

Then there exists a solution $\alpha^\star(.)$ defined on an interval $[0, t(\alpha^\star)]$ to the optimal control problem. The above mentioned assumptions ensure usual existence results, even if some of them could be weakened. For a survey of existence results in optimal control problems, refer to [19] for instance.

Definition 3.1.1.1 (End point mapping) *Let $\alpha(.) \in \mathscr{A}$ be an admissible control. For given $t \in [0, t_f]$, and $\xi_0 \in \mathbb{R}^n$, the end-point mapping E_{t,ξ_0} is defined as below*

$$E_{t,\xi_0} : \mathscr{A} \longrightarrow \mathbb{R}^n \tag{3.6a}$$

$$\alpha \mapsto \xi(t, \xi_0, \alpha) \tag{3.6b}$$

where $t \mapsto \xi(t, \xi_0, \alpha)$ is the value at time t of the solution to (3.1) such that $\xi(0) = \xi_0$.

It is well known that, if one endowes $\mathscr{A}$ with the standard L^∞ topology, then the end point mapping is C^1 on $\mathscr{A}$ and the optimal control problem (3.1)-(3.2)-(3.3) can be formulated in terms of end point mapping as follows:

$$\min\{C(t_f, \alpha),\ \xi(0) \in \mathscr{M}_0,\ E_{t_f,\xi_0}(\alpha) \in \mathscr{M}_f,\ \alpha \in \mathscr{A}\} \tag{3.7}$$

In next paragraph, we give a statement of the PMP. It expresses necessary conditions for a pair $(\xi^\star(\cdot), \alpha^\star(\cdot))$ to be optimal for (3.1)-(3.2)-(3.3).

3.1.2 Pontryagin maximum principle

By the PMP (see [55], [82]), there exists $p^0 \leqslant 0$ and an absolutely continuous mapping $p^\star(.) : [0, t_f] \to \mathbb{R}^n$, called *adjoint vector*, such that, for almost every $t \in [0, t_f]$

$$\dot{\xi}^\star(t) = \frac{\partial \mathrm{H}}{\partial p}(\xi^\star(t), p^\star(t), p^0, \alpha^\star(t)) \tag{3.8a}$$

$$\dot{p}^\star(t) = -\frac{\partial \mathrm{H}}{\partial \xi}(\xi^\star(t), p^\star(t), p^0, \alpha^\star(t)) \tag{3.8b}$$

where the Hamiltonian H is defined by:

$$\mathrm{H}(\xi, p, p^0, \alpha) := \langle p, f(\xi, \alpha)\rangle + p^0 f^0(\xi, \alpha) \tag{3.9}$$

For almost every $t \in [0, t_f]$, the control $\alpha^\star$ maximizes the Hamiltonian H:

$$\mathrm{H}(\xi^\star(t), p^\star(t), p^0, \alpha^\star(t)) = \max_{\nu \in \mathrm{A}} \mathrm{H}(\xi^\star(t), p^\star(t), p^0, \nu) \tag{3.10}$$

The adjoint vector satisfies the *transversality conditions* at both extremities (or just one of them):

$$p^\star(0) \perp \mathrm{T}_{\xi(0)}\mathscr{M}_0 \tag{3.11a}$$

$$p^\star(t_f) - p^0 \frac{\partial g}{\partial \xi}(t_f, \xi^\star(t_f)) \perp \mathrm{T}_{\xi(t_f)}\mathscr{M}_f \tag{3.11b}$$

where $\mathrm{T}_\xi \mathscr{M}$ is the notation for the tangent space of the submanifold $\mathscr{M}$ at ξ. If the final time t_f is free, there is an additional transversality condition:

$$\max_{\nu \in \mathrm{A}} \mathrm{H}(\xi^\star(t_f), p^\star((t_f)), p^0, \nu) = -p^0 . \frac{\partial g}{\partial t}(t_f, \xi^\star(t_f)) \tag{3.12}$$

Remark 3.1.2.1 (Autonomous case) *In the case where the final time is free and the dynamics f and the cost f^0 are autonomous (ie do not depend on t) one has:*

$$\max_{\nu \in \mathrm{A}} \mathrm{H}(\xi^\star(t), p^\star((t)), p^0, \nu) = \mathrm{C}ste \tag{3.13}$$

An *extremal* of the optimal control problem is a fourth-tuple $(\xi(\cdot), p(\cdot), p^0, \alpha(\cdot))$ solution of (3.8) and (3.10). If $p^0 = 0$, the extremal is said to be *abnormal*, if $p^0 < 0$, then the extremal is said to be *normal*.

Remark 3.1.2.2 (Sufficient conditions for optimality) *We emphasize once more that the PMP gives a set of necessary conditions. For clarity, let us simplify the optimal control problem (3.1)-(3.2)-(3.3) by taking $\mathrm{A} = \mathbb{R}^p$. If the strong Legendre condition holds along a given extremal $(\xi(\cdot), p(\cdot), p^0, \alpha(\cdot))$, that is, there exists $r > 0$ such that:*

$$\frac{\partial^2 \mathrm{H}}{\partial \alpha^2}(\xi(\cdot), p(\cdot), p^0, \alpha(\cdot))(\nu, \nu) \leqslant -r.\|\nu\|^2, \quad \forall \nu \in \mathbb{R}^p \tag{3.14}$$

then there exists $\epsilon > 0$ so that the trajectory $\xi(.)$ is locally optimal in L^∞ topology on $[0, \epsilon]$. If the extremal is moreover normal, i.e. $p^0 \neq 0$, then $\xi(\cdot)$ is locally optimal in C^0 topology on $[0, \epsilon]$. For more details on second order optimality conditions, refer for instance to [2] or [13].

Definition 3.1.2.1 (Singular arc) *Assume $\mathscr{M}_0 = \{\xi_0\}$. A control $\alpha_s(\cdot)$ defined on $[0, t_f]$ is said to be singular if and only if the Fréchet differential $d\mathrm{E}_{t_f, \xi_0}(\alpha_s)$ is not surjective. The associated trajectory $\xi_s(\cdot)$ is called singular trajectory.*

We recall the following two standard characterizations of singular controls (see [14], [55]). A control $\alpha_s \in \mathscr{A}$ is singular if and only if the linearized system along the trajectory $\xi_s(\cdot, \xi_0, \alpha_s)$ is not controllable. This is also equivalent to the existence of an absolutely continuous mapping $p_s : [0, t_f] \to \mathbb{R}^n \backslash \{0\}$ such that, for almost every $t \in [0, t_f]$,

$$\dot{\xi}_s(t) = \frac{\partial \mathrm{H}_s}{\partial p}(\xi_s(t), p_s(t), \alpha_s(t)) \tag{3.15a}$$

$$\dot{p}_s(t) = -\frac{\partial \mathrm{H}_s}{\partial \xi}(\xi_s(t), p_s(t), \alpha_s(t)) \tag{3.15b}$$

$$\frac{\partial \mathrm{H}_s}{\partial \alpha}(t, \xi_s(t), p_s(t), \alpha_s(t)) = 0 \tag{3.15c}$$

where the Hamiltonian H_s of the system is defined by:

$$\mathrm{H}_s(\xi, p, \alpha) := \langle p, f(\xi, \alpha) \rangle \tag{3.16}$$

Note that singular trajectories coincide with projections of abnormal extremals for which the maximization condition (3.10) reduces to $\partial \mathrm{H}/\partial \alpha = 0$. In case when the dynamics f and the cost f^0 are linear in the control α, a singular arc (restriction of an extremal to a subinterval I) corresponds to an arc along which one is unable to compute the control directly from the maximization condition of the PMP (at the contrary of bang-bang situation). Indeed, in this case, the above condition $\partial \mathrm{H}/\partial \alpha = 0$ along the arc means that some function (called switching function) vanishes identically along the arc. Then, it is well known that, in order to derive an expression of the control along such an arc, one has to differentiate this relation until the control appears explicitly. It is as well known that such singular arcs, whenever they occur, may be optimal. Their optimal status may be proved using generalized Legendre-Clebsch type conditions or the theory of conjugate points (see [72]-[39] or see [2]-[13] for a complete second-order optimality theory of singular arcs).

Remark 3.1.2.3 *In case when* A *is compact* ($\alpha(\cdot)$ *is constrained), the characterization* (3.15) *remains valid as soon as the control values remain in* Å.

3.2 Numerical methods in optimal control

3.2.1 Context

Let us first recall that there are mainly two kinds of numerical approaches in optimal control: direct and indirect methods.

On the one hand, direct methods consist of discretizing the state and the control so as to reduce the problem to a constrained nonlinear optimization problem in finite dimension. The process is straightforward and it can be applied in systematic way to any optimal control problem. Another great advantage of the direct methods is that they do not require any prior information on the structure of the control. New variables or constraints can be added easily. However, the convergence may be difficult due to the large number of variables.

On the other hand, indirect methods are based on the PMP which provides a set of necessary conditions for a local minimum. The problem is then reduced to a nonlinear system that is generally solved by a shooting method using a Newton-like algorithm. An advantage of such methods is their great accuracy when they converge. The drawbacks are the narrow radius of convergence and in some cases (presence of singular arcs, state constraints...) a prior theoretical work is necessary in order to identify the structure of the control. For more complete comparison between direct and indirect methods, refer to [83]. The principles of both direct and indirect methods are recalled hereafter.

3.2.2 Direct methods

Direct methods consist of discretizing both the state and the control. After discretizing, the optimal control problem is reduced to a nonlinear optimization problem in finite dimension, or nonlinear programming problem, of the form:

$$\min_{Z \in C} F(Z) \tag{3.17}$$

where $Z := (\xi_1, \xi_2, ..., \xi_N, \alpha_1, \alpha_2, ..., \alpha_N)$ and:

$$C := \left\{ Z \mid g_i(Z) = 0,\ i \in [[1, r]];\quad g_j(Z) \leqslant 0, j \in [[r+1, N]] \right\} \tag{3.18}$$

There exists an infinite number of variants, depending on the choice of finite-dimensional representations of the control and of the state, of the discretization of the extremal differential equations, and of the discretization of the cost functional. The discretization may be carried out in many ways, depending on the problem features. As an example, we may consider a subdivision $0 = t_0 < t_1 < .. < t_N = t_f$ of the interval $[0, t_f]$. We discretize the controls such that they are piecewise constant on this subdivision with values in A. Meanwhile, the differential equations may be discretized by an explicit Euler method, by setting $h_i := t_{i+1} - t_i$, we get $\xi_{i+1} = \xi_i + h_i.f(\xi_i, \alpha_i)$. The cost may be discretized by a quadrature procedure. We refer to [16] for a thorough description of many direct approaches in optimal control.

Then, to solve the optimization problem (3.17) under the constraints (3.18), there is also a large number of possible methods: gradient methods, penalization, quad-Newton, dual methods... We refer the reader to any good textbook of numerical optimization. In the frame of our study, we use the optimization routine **I**nterior **P**oint **OPT**imizer (IPOPT) combined with the automatic differentiation code A Mathematical Programming Language (AMPL) on a standard desktop machine. For more information, refer to [70]-[10]. Alternative variants of direct methods are the collocation methods, the spectral or pseudo-spectral methods, the probabilistic approaches, etc.

Another approach to optimal control problems that can be considered as a direct method, consists in solving the Hamilton Jacobi Bellman equation satisfied (in the viscosity sense) by the value function which is of the form:

$$\frac{\partial v}{\partial t} + H\left(\xi, \frac{\partial v}{\partial \xi}\right) = 0 \tag{3.19}$$

The value function v is the optimal cost for the optimal control problem starting from a given point (t, ξ). Once the value function estimated, optimal controls can be deduced from the DPP. This approach will be explored in the chapter 4 of this thesis.

3.2.3 Indirect methods

In indirect approaches, the PMP (first order necessary conditions for optimality) is applied to the optimal control problem. This reduces the problem to a nonlinear system of n equations with n unknowns generally solved by Newton-like methods. The indirect methods are also called shooting methods. The principle of the simple shooting and of the multiple shooting method is recalled herafter.

Simple shooting method: By setting $z(t) := (\xi(t), p(t))$, assume that, by using (3.10), the optimal control can be expressed as a function of the state and the adjoint variable. Then the extremal system (3.8a)-(3.8b) can be written under the form: $\dot{z}(t) = F(z(t))$. The initial and final conditions (3.3), the transversality conditions on the adjoint (3.11) and Hamiltonian (3.12) can be written as $R(z(0), z(t_f), t_f) = 0$. Finally, we obtain a two boundary value problem

$$\dot{z}(t) = F(t, z(t)),\ \ R(z(0), z(t_f), t_f) = 0 \tag{3.20}$$

Let $z(t, z_0)$ be the solution of the Cauchy problem:

$$\dot{z}(t) = \mathrm{F}(t, z(t)), \quad z(0) = z_0 \tag{3.21}$$

The two boundary problem (3.20) consists in finding a zero of the equation:

$$\mathrm{R}(z(0), z(t_f, z_0), t_f) = 0 \tag{3.22}$$

This problem can be solved by Newton-like or other other iterative methods.

Multiple shooting method: The drawback of the single shooting method is the sensitivity of the Cauchy problem to the initial condition z_0. The multiple shooting aims at a better numerical stability by dividing the time interval $[0, t_f]$ into N subintervales $[t_i, t_{i+1}]$ and considering as unknowns the values of $z_i = (\xi(t_i), p(t_i))$ at the beginning of each subinterval. The application of the PMP to the optimal control problem yields a multi-point boundary value problem, which consists in finding $\mathrm{Z} = (p(0), t_f, z_i)$ for $i = 1..,\mathrm{N}-1$ such that the differential equation:

$$\dot{z}_i(t) = \mathrm{F}(t, z(t)) = \begin{cases} \mathrm{F}_0(t, z(t)), & t_0 \leqslant t \leqslant t_1 \\ \mathrm{F}_1(t, z(t)), & t_1 \leqslant t \leqslant t_2 \\ ...., & \\ \mathrm{F}_{\mathrm{N}-1}(t, z(t)), & t_{\mathrm{N}-1} \leqslant t \leqslant t_{\mathrm{N}} \end{cases} \tag{3.23}$$

and the constraints:

$$\begin{aligned} &\xi(0) \in \mathscr{M}_0,\ \xi(t_f) \in \mathscr{M}_f,\ p^\star(0) \perp \mathrm{T}_{\xi(0)}\mathscr{M}_0 \\ &p^\star(t_f) - p^0 \frac{\partial g}{\partial \xi}(t_f, \xi^\star(t_f)) \perp \mathrm{T}_{\xi(t_f)}\mathscr{M}_f \\ &z_i(t_i^-) = z_i(t_i^+),\ i = 1, ..., \mathrm{N}-1,\ \mathrm{H}(t_f) = 0 \end{aligned}$$

are satisfied. The nodes of the multiple shooting may involve the switching times (at which the switching function changes sign) and the junction times (entry, contact or exit times) with boundary arcs for instance. In this case, an a priori knowledge of the solution structure is required.

3.2.4 Methods implemented in the thesis

Even though the direct methods will be implemented and evaluated, the shooting method based on the application of the PMP will be privileged in this thesis. The reasons for this choice are the following: the first one is the enhanced accuracy which is crucial in the applications of the optimal control to the aerospace field. Another reason is the possibility to adapt this method to a specific problem: indeed, if adequately initialized, the shooting method can provide a quasi instantaneous solution compliant with the real time implementation. Moreover, in case of deviation with respect to the optimal solution, one is able to compute online a new one. These requirements are important for the applications in the aerospace field and cannot, in general, be satisfied by direct methods as soon as the problem becomes too much complex. However, as explained previously the initialization is in general a hard and intricate task, which requires a detailed study of the optimal problem structure and sometimes additional mathematical tools coming for instance from the geometric optimal control (refer for instance to [83]).

As it is well known, the main issue of the shooting methods based on the Newton-like method is the initialization: indeed, due to the small convergence radius, the first guess shall be "close enough" to the solution. In recent years, the numerical continuation has become a powerful tool to overcome this difficulty. The section 3.3 recalls some mathematical concepts of the continuation approaches, with a focus on the numerical implementation of these methods.

3.3 Continuation methods

3.3.1 Existence results and discrete continuation

The basic idea of continuation (also called homotopy) method is to solve a difficult problem step by step starting from a simpler problem by parameter deformation. The theory and practice of the continuation methods are well-spread (see, e.g., [31], [71], [85]). Combined with the shooting method derived from the PMP, a continuation methods consists in deforming the problem into a simpler one (that can be easily solved) and then solving a series of shooting problems step by step to "come back" to the original problem.

One difficulty of the homotopy methods lies in the choice of a sufficiently regular deformation that allows the convergence along the path. The starting problem should be easy to solve and the path between this starting problem and the original problem should be easy to model. Another difficulty is to numerically follow the path between the starting problem the original problem. This path is parametrized by a parameter denoted usually by λ.

The choice of the homotopic parameter may require considerable physical insight into the problem. This parameter may be defined either artificially according to some intuition, or naturally by choosing physical parameters of the system, or by combination of both.

Assume one has to solve a system of N nonlinear equations in N dimensional variable Z:

$$\mathrm{F}(\mathrm{Z}) = 0 \tag{3.25}$$

where $\mathrm{F} : \mathbb{R}^n \longrightarrow \mathbb{R}^n$ is a smooth map. We define a deformation $\mathrm{G} : \Omega \times [0,1] \longrightarrow \mathbb{R}^n$ such that:

$$\mathrm{G}(\mathrm{Z},0) = \mathrm{G}_0(\mathrm{Z}), \quad \mathrm{G}(\mathrm{Z},1) = \mathrm{F}(\mathrm{Z}) \tag{3.26}$$

where $\mathrm{G}_0 : \mathbb{R}^n \longrightarrow \mathbb{R}^n$ is a smooth map having known zeros.

A zero path is a curve $c(s) \in \mathrm{G}^{-1}(0)$ where s represents the arc length. We would like to trace a zero path starting from a point Z_0 such that $\mathrm{G}(\mathrm{Z}_0,0) = 0$ and ending at a point Z_f such that $\mathrm{G}(\mathrm{Z}_f,1) = 0$. The first question to address is the existence of zero paths, since the feasability of the continuation method relies on this assumption.

Actually, it has been proved in [83]-[58], that the local feasability of the continuation method is closely related to the three following conditions:

1. there are no minimizing abnormal extremals
2. there are no minimizing singular controls, meaning the mapping $d\mathrm{E}_{t_f,\xi_0}(\alpha)$ is surjective (see definition 3.1.2.1).
3. there are no conjugate points: for precise definition of conjugate points, refer to [83]-[58]. Actually the absence of conjugate points can be numerically tested (see [13]).

Finally, it has to be noticed that, despite of local feasability, the zero paths may not be globally defined for any $\lambda \in [0,1]$. The path could cross some singularity or diverge to infinity before reaching $\lambda = 1$. The first possibility can be discarded by assuming (2) and (3) over all the domain Ω and for every $\lambda \in [0,1]$. The second possibility is related to some properness properties of the exponential mapping (see [12]-[81]).

3.3.2 Numerical tracking of the zero paths

There exists many numerical algorithms to track a zero path. Among these algorithms, the simplest one is called the *simple continuation* procedure.

Basic continuation: The continuation parameter λ is discretized by $0 = \lambda_0 < \lambda_1 < .. < \lambda_n = 1$ and the sequence of problems $\mathrm{G}(\mathrm{Z},\lambda_i) = 0$ is solved to end up with a zero point of $\mathrm{F}(\mathrm{Z})$. If the

increment $\Delta\lambda = \lambda_{i+1} - \lambda_i$ is small enough, then the solution Z_i associated to λ_i to $G(Z_i, \lambda_i) = 0$ is generally close to the solution of $G(Z, \lambda_{i+1}) = 0$. An implicit assumption is made that we are able to compute the solution at the first step of the continuation procedure, namely a zero Z_0 for $G(Z, 0) = 0$. The simple continuation algorithm is detailed below:

Algorithm 1 Simple continuation procedure

Initialization: $\lambda = 0$, $Z = Z_0$, $\Delta\lambda \in (\Delta\lambda_{\min}, \Delta\lambda_{\max})$
while $\Delta\lambda \in (\Delta\lambda_{\min}, \Delta\lambda_{\max})$ and $\lambda \leqslant 1$ **do**
  $\Delta\lambda = \min(\Delta\lambda, 1 - \lambda)$
  $\tilde{\lambda} = \lambda + \Delta\lambda$
  Look for $\widetilde{Z}$ zero of $G(\widetilde{Z}, \tilde{\lambda}) = 0$
  if success **then**
    $Z = \widetilde{Z}$
    $\lambda = \tilde{\lambda}$
    $\Delta\lambda = 2.\Delta\lambda$
  else
    $\lambda = \tilde{\lambda} - \Delta\lambda$
    $\Delta\lambda = \Delta\lambda/2$
  end if
end while
if success **then**
  The continuation procedure is successful
else
  The continuation procedure has failed
end if

Continuation with linear prediction: Behind this procedure is the idea that we can do better than just using Z_λ to approximate $Z_{\lambda+\Delta\lambda}$. Assume that we have already made two resolutions, yielding Z_{λ_1} and Z_λ, for two values λ_1 and λ such that $\lambda_1 < \lambda$. Assuming some regularity on the path of zeros, an approximation of $Z_{\lambda+\Delta\lambda}$ for a new value $\lambda + \Delta\lambda$ is given by

$$Z_{\lambda+\Delta\lambda} = Z_\lambda + \frac{\Delta\lambda}{\lambda - \lambda_1}\left(Z_\lambda - Z_{\lambda_1}\right) \tag{3.27}$$

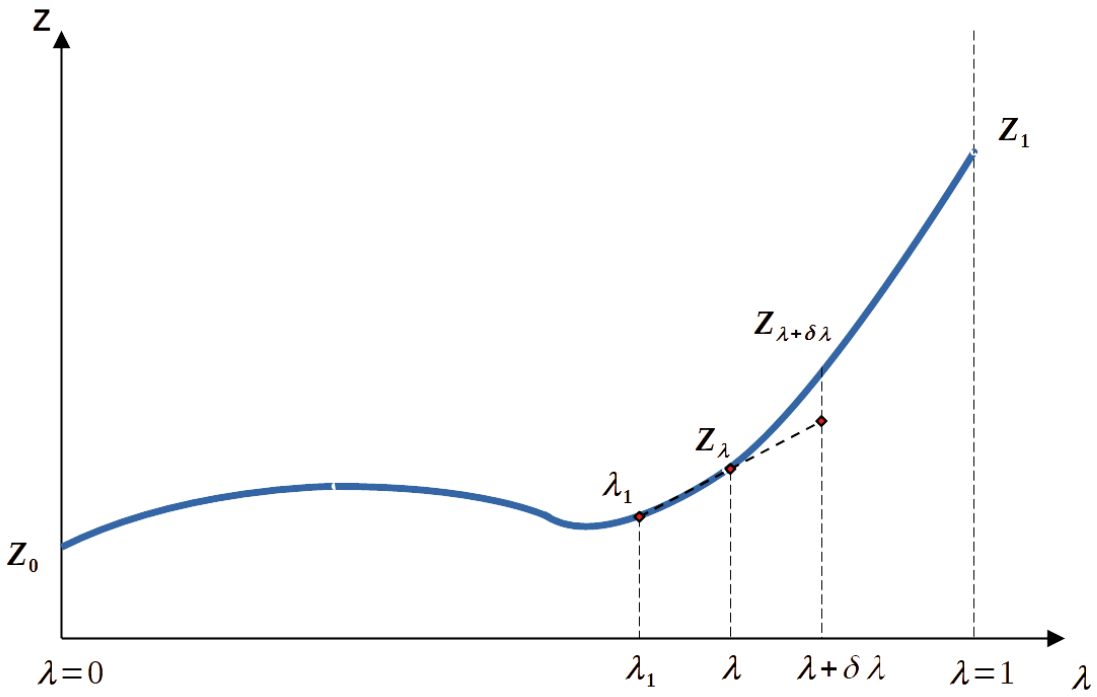

Figure 3.1: Continuation with linear prediction

This is the procedure we implemented throughout this article each time a continuation is performed, and we could experimentally witness an improvement in the runtime of the algorithm.

3.4 Dubins-Fuller problem

3.4.1 Motivation and definition of the model

Let us consider the following kinematic equations for an aerial vehicle in the vertical plane:

$$\dot{x} = v.\cos\gamma \tag{3.28a}$$
$$\dot{h} = v.\sin\gamma \tag{3.28b}$$
$$\dot{\gamma} = \alpha \tag{3.28c}$$

where $v > 0$ is the longitudinal speed, assumed to be fixed. (x, h, γ) are the state variables defining respectively the position and the pitch angle of the vehicle. α designates the pitch angular rate, which enables to maneuver and thus will be considered as a control variable. The rate is limited and $|\alpha| \leqslant 1$. Suppose that the vehicle has to move from the initial state $\mu_0 = (x_0, h_0, \gamma_0)$ to the final state $\mu_f = (x_f, h_f, \gamma_f)$ while minimizing the following cost:

$$J_{k_0,k_1}(t_f, \alpha) := \int_0^{t_f} k_0 + k_1.\left(\frac{h(s) - h_c}{h_c}\right)^2 ds \tag{3.29}$$

where h_c is a prescribed altitude, $k_0 \geqslant 0$ and $k_1 \geqslant 0$ are the weight coefficients. The final time t_f is let free.

Actually, the dynamics (3.28) can be understood as a simplified version of the missile dynamics as it can be obtained from (2.21) by making the following assumptions:

- neglect the gravity g and the variation of the air density $\rho(\cdot)$ with respect to the height h

- consider that the speed v and the mass m remain constant (at first order) during the flight. This can be achieved by setting $\dot{v} = 0$ and $C_s = 0$ in (2.21). Notice that these assumptions are far from being unrealistic in the case of a cruise missile where the covered speed range is relatively small and the mass variation limited provided that the time interval remains reasonable.

By denoting the reduced dynamics $f_r(\mu,\alpha) := \begin{pmatrix} v.\cos\gamma \\ v.\sin\gamma \\ \alpha \end{pmatrix}$, (3.28) can be written as $\dot{\mu} = f_r(\mu,\alpha)$, with $\mu(0) = \mu_0$ and $\mu(t_f) = \mu_f$.

Our goal hereafter is to first study the family of optimal control problems (3.28)-(3.29) and then link them to the missile guidance problem. We discuss the numerical solving strategy of (3.28)-(3.29) for various values of the couple (k_0, k_1). More precisely, we distinguish the following cases:

1. The (D) case corresponding to the dynamics (3.28) and the cost $J_{1,0}$, i.e. with $(k_0, k_1) = (1,0)$
2. The (F) case corresponding to the dynamics (3.28) and the cost $J_{0,1}$ i.e. with $(k_0, k_1) = (0,1)$. We explain in paragraph 3.4.3 why the cost $J_{0,1}$ leads to the well known Fuller phenomenon.
3. The so called (DF) case corresponding actually to the dynamics (3.28) and the *family* of costs J_{k_0,k_1} indexed by $k_0 > 0$ and $k_1 > 0$. This case is the weighted interpolation between the (D) and the (F) cases, the weight being determined by the ratio k_1/k_0. By setting $k_0 = 1$ and increasing gradually k_1 from 0 to $+\infty$, this family of optimal control problems can be understood as a continuation from the (D) case up to the (F) case.

We state that, if we are able to numerically solve (3.28)-(3.29), we will be able to solve the missile guidance problem. We will precise the link between the two problems later on in this thesis.

In what follows, we assume that $v = 1$, $h_c = 1/2$ and consider the following boundary conditions:

$$(x_0, h_0, \gamma_0) = (0,0,\pi/2) \text{ and } (x_f, h_f, \gamma_f) = (15,0,-\pi/2) \tag{3.30}$$

3.4.2 Dubins case $(k_0, k_1) = (1,0)$

3.4.2.1 State of the art

The optimal control problem (3.28)-(3.29) is actually known as the *Dubins path* problem which consists in finding the shortest C^1 2D curve joining two points in the two dimensional eucledian plane with prescribed initial and final tangents and limited curvature. The problem of finding such a path was initially raised by Markov in 1889 and solved by Lest Dubins in 1957 ([25]); since it was apparently impossible to give an explicit formula for the shortest path, Dubins gives a sufficient set of paths, i.e., a set which always contains what he called an R-geodesic, or optimal path. In 1990, Reeds and Sheep extended Dubins' result for a car that goes both forward and backward [41], allowing the presence of cusps in the path. Other variants of the Dubins problem such as an angular acceleration control ([76]) or the three dimensional space ([77]) case have as well been studied.

In the basic case (planar with angular rate control) it has been shown that the optimal path is the sequence of concatenated arcs of type CSC, CCC, or any subset of these (we denote with C a circular arc and S a straight line segment in the (x,h) plane).

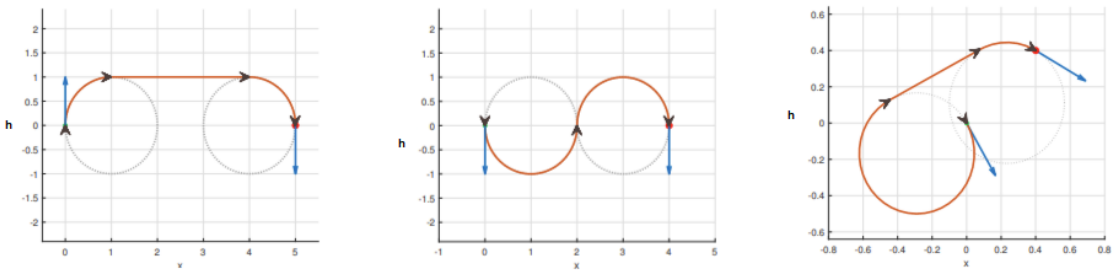

Figure 3.2: Illustration of optimal paths

The circular arcs correspond to the Bang controls ($\alpha = \pm 1$) and the straight line segment arc ($\alpha = 0$) is actually a singular control in the sense of 3.1.2.1.

Remark 3.4.2.1 *The straight line (singular) control can be obtained from* (3.46) *by setting* $k_1 = 0$.

Remark 3.4.2.2 *It is interesting to note that the Dubins case exhibits a turnpike phenomenon. Indeed, as mentioned above, a deep theoretical result states that the global optimal synthesis is of the form bang-singular-bang, where the initial and final bang arcs are circular arcs of curvature 1, and the middle singular arc is a segment (of course, according to the specific terminal conditions, some of those three arcs may be of zero length). The turnpike phenomenon is then clear: if the initial and final states are far one from each other, then necessarily the middle singular arc has to be long, while the initial and final bang arcs are short. Seen from afar, the optimal trajectory approximately looks as a segment. This is exactly the turnpike property. The turnpike set is the middle singular arc. Contrarily to [29, 84] where the turnpike set is never reached but the optimal trajectory remains close to it, here the turnpike is "exact" in the sense that the optimal trajectory coincides with the turnpike set on the long middle time interval. The wording of "exact turnpike" has been introduced and used in [79]. The recent work [84] does not apply to the Dubins case because the turnpike set consists of a singular arc, along which the linearized control system fails to be controllable, but as explained above the turnpike property is evident from the global optimal synthesis.*

The singular nature of the central arc is crucial from the numerical point of view as it implies that the continuation based on the "standard" shooting method will likely fail to numerically solve the (D) problem, as explained in the paragraph 3.3.1. Hereafter, we illustrate the optimal solution in our case with a direct method.

3.4.2.2 Direct method

We discretize (3.28)- (3.29) by using a simple implicit Crank Nicholson method with N = 500 time steps, and we use the optimization routine IPOPT (see [10]) combined with the automatic differentiation code AMPL (see [70]) on a standard desktop machine. The results are presented hereafter:

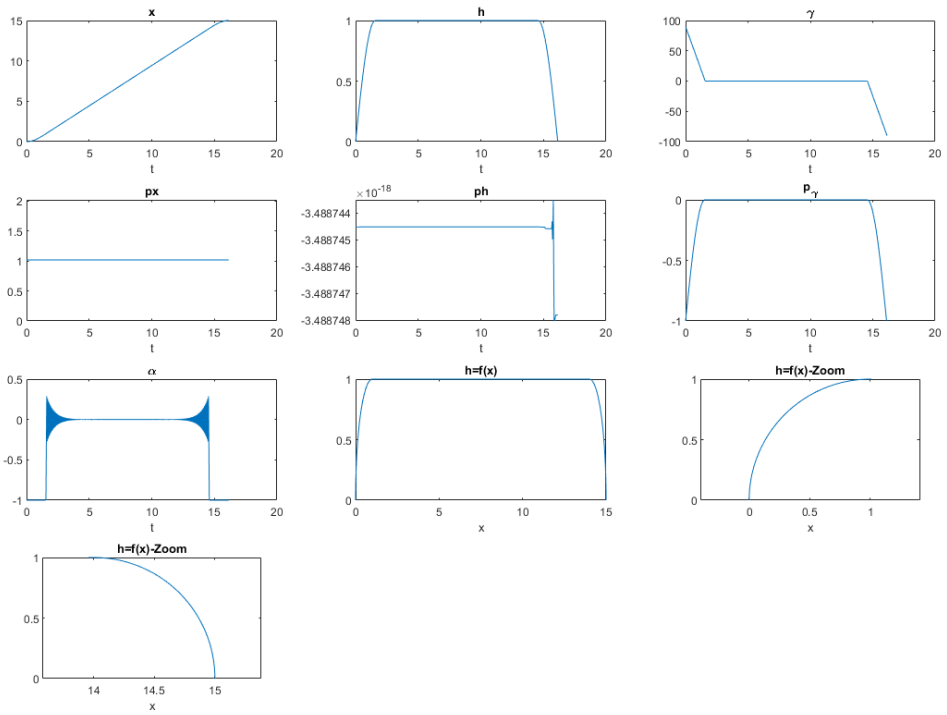

Figure 3.3: Optimal state, costate & control for $(k_0, k_1) = (1, 0)$

As expected, the optimal structure is: bang min- -singular- -bang min, and the switching function p_γ vanishes along the straight line arc.

If the global accuracy seems satisfactory, the computed control possesses oscillations at the beginning and the end of the central arc: this is a typical numerical artifact observed when a singular arc is computed through a direct method.

To overcome this issue, the classical idea is to solve the problem by implementing the shooting method. In the (D) case, the natural idea is to "split" the trajectory into three pieces corresponding to the subarcs identified previously. The three pieces are then integrated separately and the jonction conditions are implemented at the frontier of each arc. Herafter, we implement the classical shooting method (with computation of the adjoint state). However, it should be emphasized that, as the optimal structure is theoretically known, a reduced shooting on the switching times and based only on the state dynamics would converge easily.

3.4.2.3 Shooting method

When implementing a shooting method (see for instance [16]), the structure of the trajectory has to be known a priori. The structure of the control must be prescribed here by assigning a fixed number of interior switching times that correspond to junctions between nonsingular and singular arcs. These times $(t_i)_{i=1\ldots n}$ are part of the shooting unknowns and must satisfy some switching conditions. Each arc is integrated separately, and matching conditions must be verified at the switching times.

The switching conditions indicate a change of structure which corresponds in our case to an extremity of a singular arc. Along such a singular arc, it is required that the switching function vanishes which implies in our case: $p_\gamma = 0$. This relation implies $\dot{p}_\gamma = 0$ (refer to [32] for proof). The control is computed using the relation $\ddot{p}_\gamma = 0$. Therefore, using this expression of the control, switching conditions consist in imposing either $p_\gamma = 0$ at the extremities of the singular arc, or

$p_\gamma = \dot{p}_\gamma = 0$ at the beginning of the arc. In our simulations, we choose the latter solution which happens to provide better and more stable results.

To successfully initialize the shooting method, we deform the final state in order to ensure an easy convergence with a simple initial guess. We used the direct method AMPL & IPOPT to calculate the first guess as they offer the possibility to recover the Lagrange multipliers corresponding, up to a scaling, to the costate $p(\cdot)$ used in the PMP extremal equations. Then, we implement a continuation over the x coordinate of the final state to reach the desired boundary conditions. More precisely, the shooting function, denoted by $S_\lambda : \mathbb{R}^6 \mapsto \mathbb{R}^6$ is defined as follows:

$$S_\lambda : \begin{pmatrix} p(0) \\ t_1 \\ t_2 \\ t_f \end{pmatrix} \longmapsto \begin{pmatrix} x(t_f) - x_c(\lambda) \\ h(t_f) - h_f \\ \gamma(t_f) - \gamma_f \\ p_\gamma(t_1) \\ \dot{p}_\gamma(t_1) \\ H_d\left(\mu(t_f), p(t_f), -1, \alpha(t_f)\right) \end{pmatrix} \tag{3.31}$$

where $H_d(\mu, p, p^0, \alpha) := \langle p, f_r(\mu, \alpha)\rangle + p^0$, t_1 (resp. $t_2 > t_1$) correspond to the beginning (resp. end) instants of the singular arc.

The intermediate final state is given by: $x_c(\lambda) = x_0^f + \lambda.(x_f - x_0^f)$, where $x_0^f = 5.0$ and $\lambda \in [0,1]$ is the homotopy factor increasing from 0 to 1. The first guess provided by the direct method is given by: $(p(0), t_1, t_2, t_f) = (1.0, 0.0, -1.0, 1.5, 4.5, 6.0)$.

3.4.2.4 Numerical implementation

The shooting method and the continuation algorithm have been implemented in Python language on a standard desktop computer. The integration of the differential system is done using the numerical integrator *DOP853*. It consists in an explicit Runge-Kutta method with adaptative step comparing the methods *RK8*, *RK5* and *RK3*. The description of the solver options can be found for instance in [27].

3.4.2.5 Numerical tests

The computing time is around 10 sec on a standard desktop computer. The output are displayed hereafter:

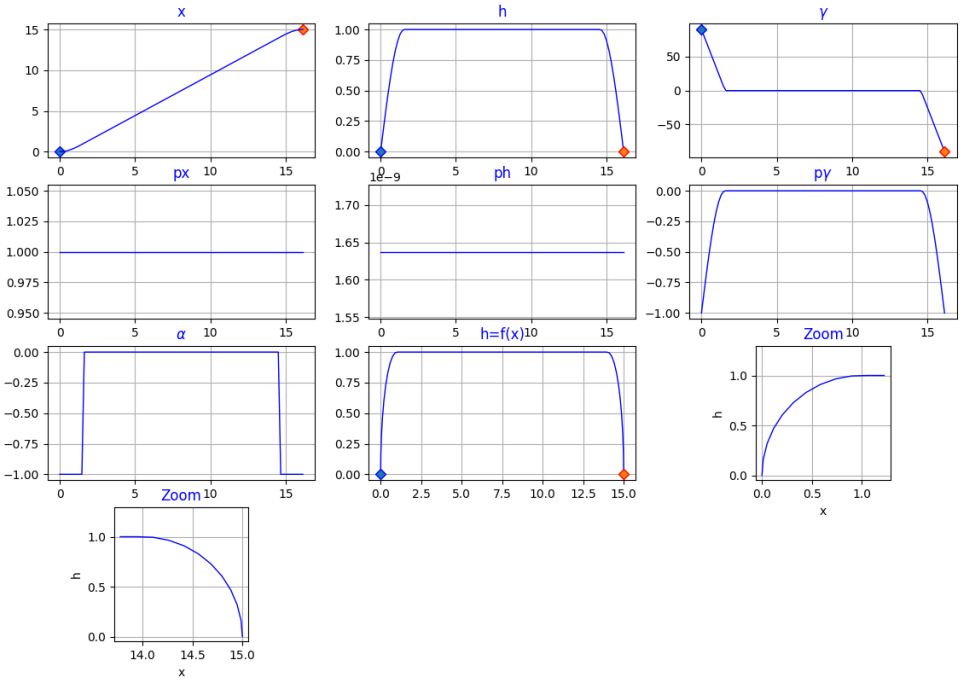

Figure 3.4: Optimal solution

This example illustrates the improvement of the accuracy obtained through the shooting method. Moreover, the stability of the optimal structure along the continuation path is theoretically guaranteed in the (D) case.

3.4.3 Fuller case $(k_0, k_1) = (0, 1)$

3.4.3.1 Direct method

First, we provide a direct method (AMPL & IPOPT) simulation for $(k_0, k_1) = (0, 1)$ in order to have an insight into the structure of the optimal solution.

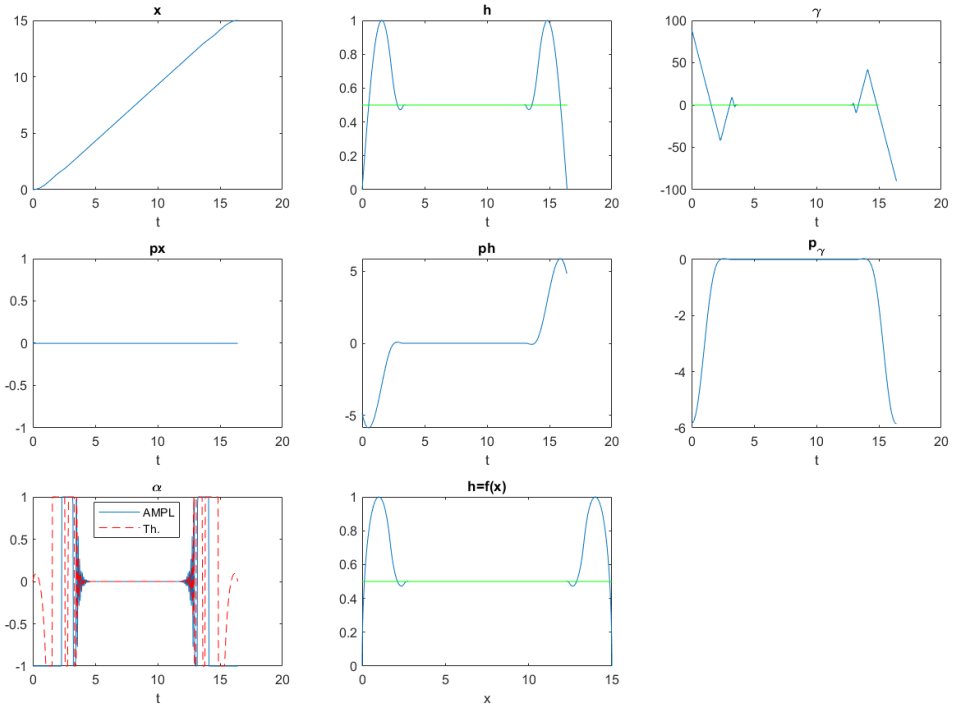

Figure 3.5: Optimal state, costate & control for $(k_0, k_1) = (0, 1)$

3.4.3.2 Comments

The optimal trajectory remains essentially "stuck" to $h = h_c$ except at the beginning and the end. Consequently, one has as well $\gamma(t) \simeq 0$ during the main part of the trajectory. Actually, when the time horizon is great enough, a turnpike phenomenon appears on (h, γ) state variables in the optimal synthesis. Formally speaking, the situation resembles to the linear turnpike (see paragraph 1.1.1 and [84]):

- the dynamics can be uncoupled as in (1.7) by setting $x := (h, \gamma)$ and $y := x$ (by using the notations of the Chapter 1)
- the solution of the "turnpike static" problem (1.8) is given by: $(\bar{x}(.), \bar{h}, \bar{\gamma}, \bar{u}) := (v.t, h_c, 0, 0)$.

However, contrary to the assumptions in the linear turnpike theorem, the linearized system at the turnpike is not controllable. Indeed, it can be easily proved by linearizing the dynamics along $(\bar{x}(.), \bar{h}, \bar{\gamma}, \bar{u})$ and verifying that the Kalman condition is not satisfied (the linearized system is time invariant). In other words, as in the Dubins case the turnpike arc is singular.

Moreover, one can remark that the theoretical control is chattering at the junction with the central arc. At this stage, we infer that we observe the so called *Fuller phenomenon*, widely studied in the literature. The Fuller problem is characterized by the chattering phenomenon which occurs when the optimal control switches an infinite number of times over a compact time interval.

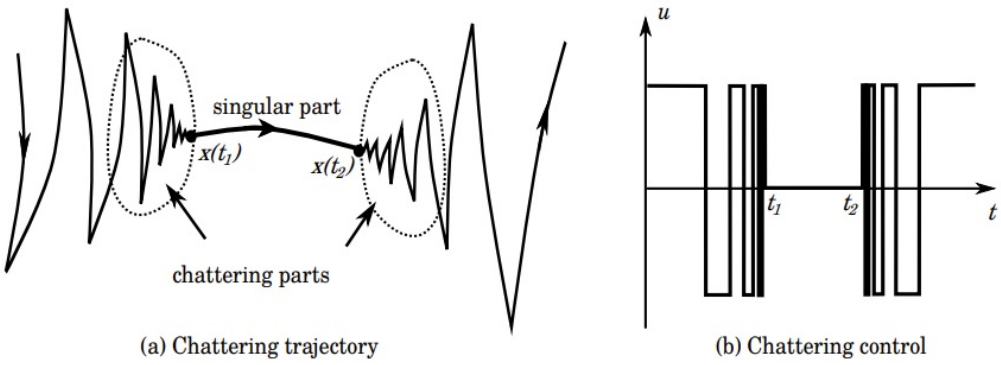

Figure 3.6: Chattering phenomenon

We provide now the explanation for the Fuller phenomenon: let us consider the initial condition $(x(0), h(0), \gamma(0)) = (x_0, h_0, \gamma_0)$ and the control $\alpha(t) := 0$. There exists a unique trajectory solution of (3.28) with the initial condition and associated to the control $\alpha(\cdot)$ (Cauchy problem). It is given by:

$$\begin{aligned} x(t) &= x_0 + v.t.\cos\gamma_0 \\ h(t) &= h_0 + v.t.\sin\gamma_0 \\ \gamma(t) &= \gamma_0 \end{aligned}$$

Without loss of generality, by taking $(x_0, h_0, \gamma_0) = (0,0,0)$, the above solution becomes: $x(t) = v.t$, $h(t) = 0$ and $\gamma(t) = 0$.

There exists a tubular neighbourhood of the above trajectory and a C^∞ diffeomorphism such that in this neighbourhood and in the new coordinates denoted by $(\tilde{x}, \tilde{h}, \tilde{\gamma})$ the differential system can be written as follows:

$$\begin{aligned} \dot{\tilde{x}}(t) &= v.(1-\tilde{\gamma}^2) \\ \dot{\tilde{h}}(t) &= \tilde{\gamma}(t) \\ \dot{\tilde{\gamma}}(t) &= \alpha(t) \end{aligned}$$

The above differential system associated to the cost $\int \tilde{h}(t)^2 dt$ is precisely the *Fuller* problem along $(\tilde{h}, \tilde{\gamma})$ state coordinates (plus an integrator coordinate x). We recall hereafter the Fuller's problem.

3.4.3.3 Optimal synthesis in the Fuller case

To better explain the chattering phenomenon, we recall the well-known Fuller's problem, which is the optimal control problem:

$$\min \int_0^{t_f} x_1^2(t)dt,\ \dot{x}_1(t) = x_2(t),\ \dot{x}_2(t) = u(t),\ |u(t)| \leqslant 1 \tag{3.32}$$

$$x_1(0) = x_{10},\ x_2(0) = x_{20},\ x_1(t_f) = x_2(t_f) = 0,\ t_f \text{ free} \tag{3.33}$$

We define $\xi := \left(\frac{\sqrt{33}-1}{24}\right)^{1/2}$ as the unique positive root of the equation $\xi^4 + \xi^2/12 - 1/18 = 0$ and we define the sets:

$$\Gamma_+ := \{(x_1, x_2) \in \mathbb{R}^2,\ x_1 = \xi.x_2^2,\ x_2 < 0\} \tag{3.34}$$

$$R_+ := \{(x_1, x_2) \in \mathbb{R}^2,\ x_1 < \text{sgn}(x_2).\xi.x_2^2\} \tag{3.35}$$

$$\Gamma_- := \{(x_1, x_2) \in \mathbb{R}^2,\ x_1 = -\xi.x_2^2,\ x_2 > 0\} \tag{3.36}$$

$$R_- := \{(x_1, x_2) \in \mathbb{R}^2,\ x_1 > -\text{sgn}(x_2).\xi.x_2^2\} \tag{3.37}$$

Then the optimal control is given in feedback form by:

$$u^\star = 1 \text{ if } x \in \mathrm{R}_+ \cup \Gamma_+ \text{ and } u^\star = -1 \text{ if } x \in \mathrm{R}_- \cup \Gamma_- \tag{3.38}$$

The control switches from $u = 1$ to $u = -1$ at points on Γ_- and from $u = -1$ to $u = 1$ at points on Γ_+. The corresponding trajectories crossing the switching curves $\Gamma_\pm$ transversally are chattering arcs with an infinite number of switchings that accumulate with a geometric progression at the final time $t_f > 0$.

The optimal synthesis for the Fuller's problem is drawn below. The solutions of the Fuller's problem are chattering solutions since they switch transversally on the switching curves $\Gamma_\pm$ until finally reaching the target point on the singular surface defined by the union of all singular solutions.

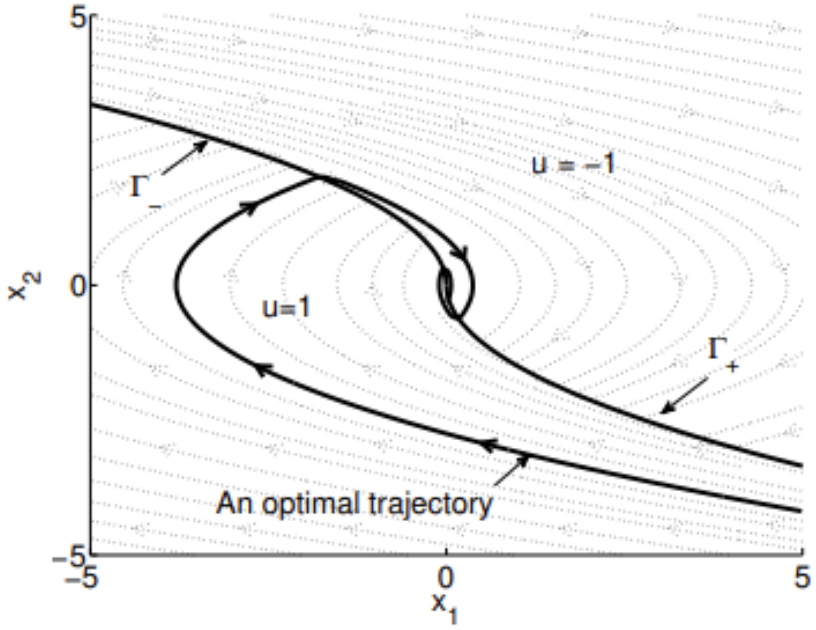

Figure 3.7: Optimal synthesis for the Fuller's problem

In fact, the optimal control of the Fuller's problem, denoted as $u^\star$ contains a countable set of switchings of the form

$$u^\star(t) = \begin{cases} 1 \text{ if } t \in [t_{2k}, t_{2k+1}) \\ -1 \text{ if } t \in [t_{2k+1}, t_{2k+2}] \end{cases} \tag{3.39}$$

where $(t_k)_{k\in\mathbb{N}}$ is a set of switching times that satisfies $(t_{i+2} - t_{i+1}) < (t_{i+1} - t_i)$, $i \in \mathbb{N}$ and converges to $t_f < +\infty$. This means that the chattering arcs contain an infinite number of switchings within a finite time interval $t_f > 0$. For more detailed analysis, refer to [37]-[61].

3.4.4 Dubins-Fuller case, $k_0 > 0$, $k_1 > 0$

As stated before, it corresponds actually to a family of costs J_{k_0,k_1} with $k_0 > 0$ and $k_1 > 0$.

3.4.4.1 Formal analysis

We apply the PMP reminded in 3.1.2. By denoting $\langle , \rangle$ the usual scalar product in $\mathbb{R}^3$ and the adjoint vector by:

$$p = \begin{pmatrix} p_x \\ p_h \\ p_\gamma \end{pmatrix} \tag{3.40}$$

the Hamiltonian of the optimal control problem (3.28)-(3.29) is given by:

$$\begin{aligned} H_0 &:= \langle p, f_r(\mu,\alpha)\rangle + p^0.f^0(\mu,\alpha) \\ &= p_x.v.\cos\gamma + p_h.v.\sin\gamma + p_\gamma.\alpha + p^0.\left(k_0 + k_1.\left(\frac{h-h_c}{h_c}\right)^2\right) \end{aligned}$$

As previously, we assume hereafter that the optimal state is not abnormal thus we take $p^0 = -1$. The adjoint equations can then be derived and one obtains:

$$\dot{p}_x = 0, \quad \dot{p}_h = 2.k_1.\frac{h-h_c}{h_c^2} \text{ and } \dot{p}_\gamma = v.(p_x.\sin\gamma - p_h.\cos\gamma) \tag{3.41}$$

The maximization condition (3.10) reads:

$$\alpha \in \underset{|r|\leqslant 1}{\arg\max}\,(p_\gamma.r) \tag{3.42}$$

which leads to following optimal policy:

$$\alpha(t) = \begin{cases} \dfrac{p_\gamma(t)}{|p_\gamma(t)|} \text{ if } p_\gamma(t) \neq 0 \\ \text{to be determined} \quad \text{if } p_\gamma(t) = 0 \end{cases} \tag{3.43}$$

Finally in our case (no terminal cost, free final time and autonomous dynamics and cost), (3.12)-(3.13) lead to:

$$\forall t \in [0, t_f], \quad H_0(\mu(t), p(t), -1, \alpha(t)) = 0 \tag{3.44}$$

As stated in (3.43), $\alpha(\cdot)$ remains undetermined in the case where $p_\gamma = 0$. Let us assume such a possibility over a subinterval of time denoted by I, and let us denote $\alpha_s(\cdot)$ the corresponding control. In this situation, as explained before, the computation of $\alpha_s(\cdot)$ requires to derivate the switching function p_γ as many times as necessary (that is to say until the control appears explicitly), twice in our case and one obtains:

$$\ddot{p}_\gamma = 0 \implies \alpha_s.(p_x.\cos\gamma + p_h.\sin\gamma) = \frac{2.k_1.(h-h_c).\cos\gamma.}{h_c^2} \tag{3.45}$$

It is not possible to have $p_x.\cos\gamma + p_h.\sin\gamma = 0$ over a subinterval of I. If it was true, then from $\dot{p}_\gamma = 0$, one would deduce that $p_x = p_h = 0$. Consequently, one would have $\dot{p}_h = 0$ leading to $h = h_c$. This would imply along this arc $H_0 = -k_0 < 0$ which contradicts the transversality condition on Hamiltonian (3.44).

Consequently, the control along the arc reads, almost everywhere:

$$\alpha_s = \frac{2.k_1.(h-h_c).\cos\gamma}{h_c^2.(p_x.\cos\gamma + p_h.\sin\gamma)} \tag{3.46}$$

Hereafter, we illustrate numerically how the optimal solution of (DF) case evolves with increasing values of k_1 coefficient (with $k_0 = 1$).

3.4.4.2 Direct method

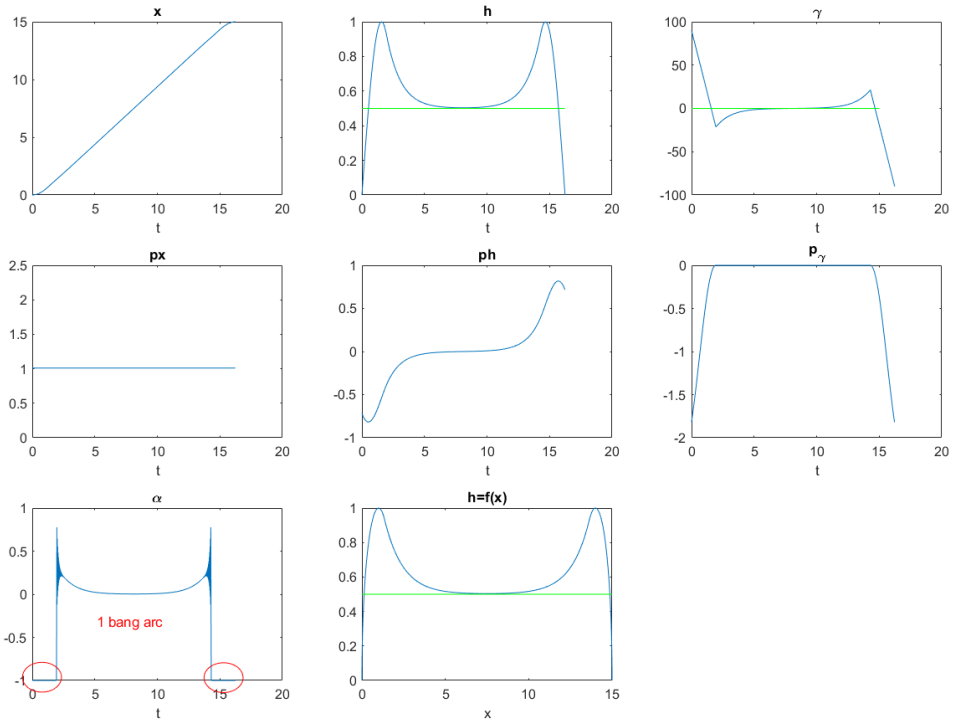

Figure 3.8: Optimal state, costate & control for $k_0 = 1$, $k_1 = 0.1$

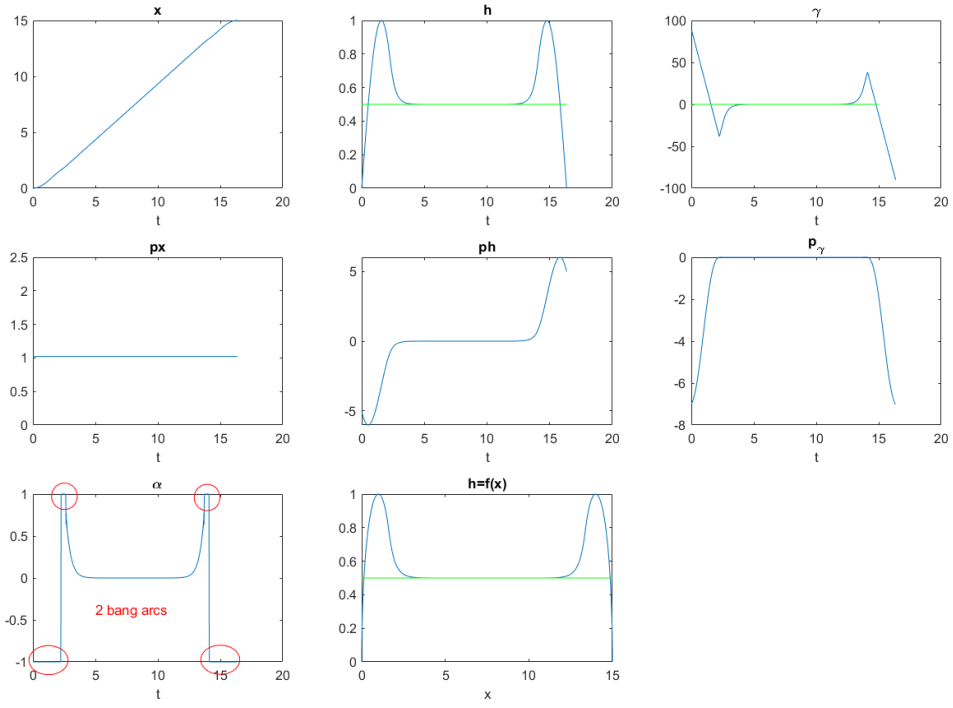

Figure 3.9: Optimal state, costate & control for $k_0 = 1$, $k_1 = 1$

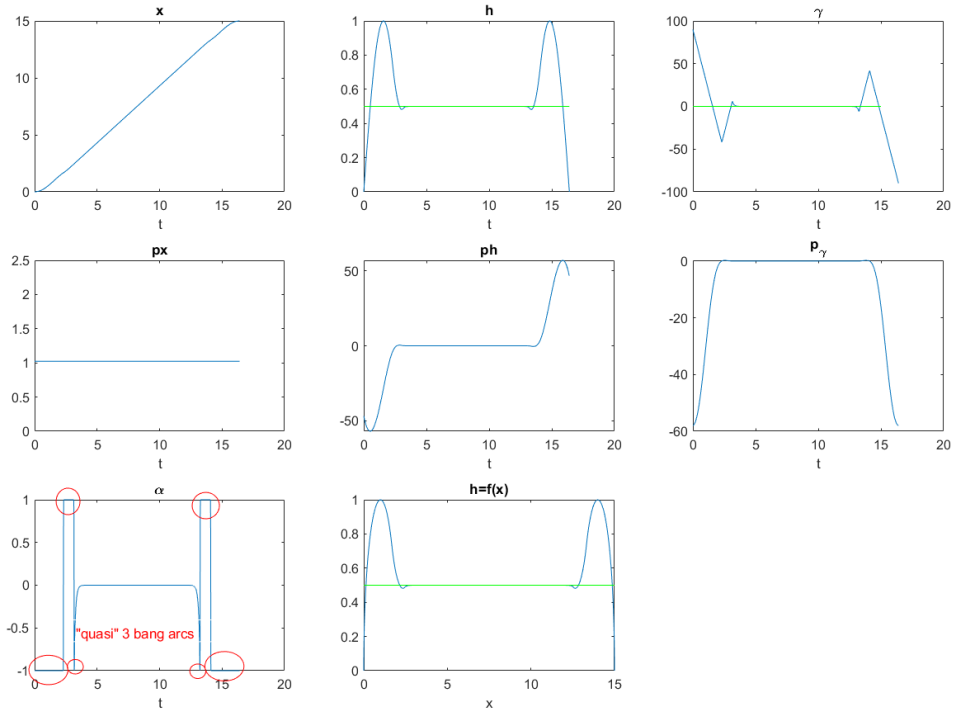

Figure 3.10: Optimal state, costate & control for $k_0 = 1$, $k_1 = 10$

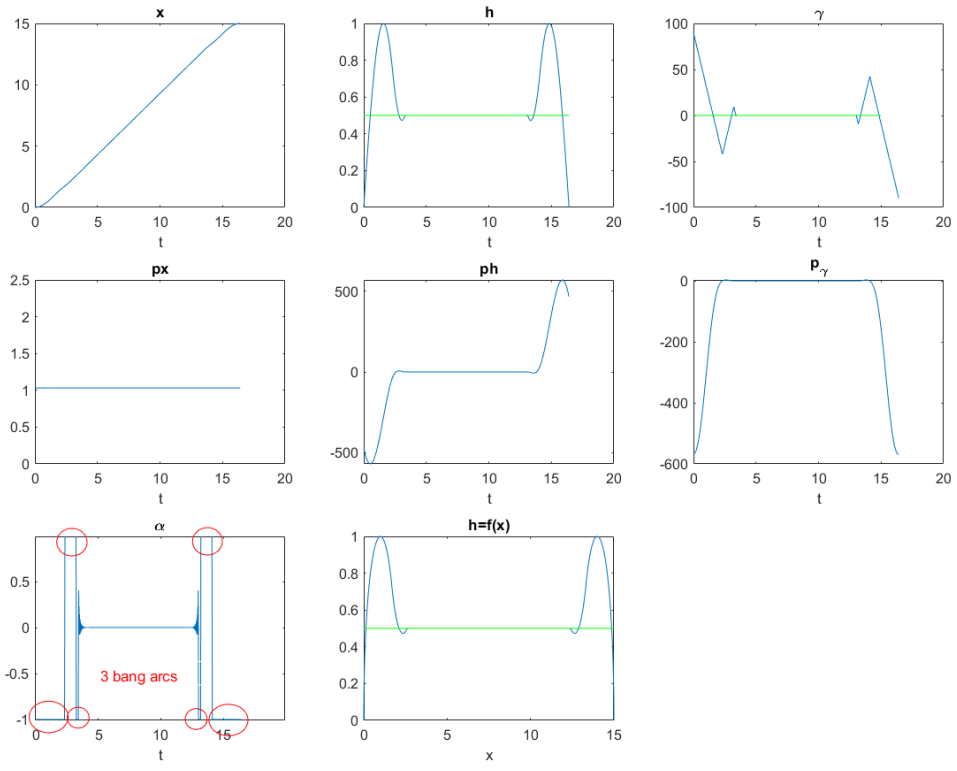

Figure 3.11: Optimal state, costate & control for $k_0 = 1$, $k_1 = 100$

As expected, when the k_1 coefficient tends formally to infinity, the number of optimal bang arcs before and after the central arc increase and should tend (at least theoretically) to infinity (which is of course not numerically observable). As stated previously, when $k_1 = 0$, one is in the (D) case whereas when $k_1 \to +\infty$, one is in the (F) case.

From now on, in order to solve numerically (3.28)-(3.29), we focus on the case $(k_0, k_1) = (1, 1)$.

3.4.4.3 Numerical solving strategy: L^2 regularization and shooting method

Even though the trajectory obtained by the direct method seems to be satisfactory, our objective is to solve the problem by using the shooting method. The natural strategy would consist in proceeding in the same way than in the (D) case. Indeed, from the results displayed on the figure 3.9, we infer that the optimal control structure is bang-bang- -singular- -bang-bang. However, numerical tests show that the convergence of the shooting implemented by splitting the trajectory is extremely difficult to obtain even for very small values of the continuation parameter. We infer that the instability of the optimal control structure leads to the failure of such a numerical approach. To overcome this difficulty, a classical method consists in regularizing the original problem by adding a quadratic term either to the dynamics or to the cost. This method has been widely used in the literature: in [32], in the Goddard's problem, the authors implement the homotopic approach based on the quadratic regularization of the cost in order to tackle with the nonsmoothness of the optimal control. In [80], the maximum mass orbital transfer problem for a low thrust propulsion system is solved. In particular, the authors discover the complex structure of the optimal control (with multiple bang arcs) without any a priori assumptions thanks to the identical strategy. Note that this type of approach has been as well adopted in [67] or [62].

In the sequel, we solve the Dubins-Fuller case precisely by adding a L^2 norm of the control α to the cost function. Such a problem has a strongly concave Hamiltonian with respect to α, with a continuous optimal control and is much easier to solve than the original one.

Let us consider the following cost:

$$J^r_{1,1}(t_f, \alpha) := \int_0^{t_f} f^0_r(\mu(s), \alpha(s))ds := \int_0^{t_f} \left(1 + \frac{(h(s) - h_c)^2}{h_c^2} + k_2.\alpha(s)^2\right) ds \tag{3.47}$$

where $k_2 \geqslant 0$ is a regularization parameter, penalizing the L^2-norm of the control α.

The regularized Hamiltonian is given by:

$$\begin{aligned} H^r_0(\mu, p, p^0, \alpha) &:= \langle p, f_r(\mu, \alpha)\rangle + p^0 f^0_r(\mu, \alpha) \\ &= \langle p, f_r(\mu, \alpha)\rangle + p^0.\left(1 + \left(\frac{h - h_c}{h_c}\right)^2 + k_2.\alpha^2\right) \end{aligned}$$

We maintain the assumption of normality here by taking $p^0 = -1$. Of course, as stated previously, one discards the abnormal case because it is identified. The adjoint equations in p_x, p_h and p_γ remain identical to (3.41). Following the maximization condition (3.10), the optimal control α is now given by:

$$\alpha \in \underset{|r|\leqslant 1}{\arg\max} \left(-k_2.r^2 + p_\gamma.r\right) \tag{3.48}$$

which leads to the following expression:

$$\alpha(t) = \max\left(\min\left(\frac{p_\gamma}{2.k_2}, 1\right), -1\right) \tag{3.49}$$

The Hamiltonian transversality conditions remain:

$$\forall t \in [0, t_f], \quad H^r_0(\mu(t), p(t), -1, \alpha(t)) = 0 \tag{3.50}$$

The basic idea behind the regularization is to smoothen the original optimal control problem by increasing k_2, then to solve the regularized problem and finally to carefully decrease k_2 by continuation in order to converge towards the initial problem.

First, we recall that, as the optimal control (3.49) can be expressed in function of the state and the adjoint state, we are, up to the saturation, in the context of the paragraph 3.2.3 . In order to avoid to activate the latter, we increase the saturation value from $\alpha_{\max} := 1$ up to $\alpha^0_{\max} = 5$. We perform a numerical continuation on boundary conditions. To ensure successful initialization, we deform the initial and final conditions in such a way that they are close and that the optimal trajectory is simple to compute: in this case the convergence is obtained with a trivial initial guess (in our case, the adjoint state $p(0)$ and final time t_f).

Moreover, as the expected final time is $t_f \simeq 15s$ (based on minimum time problem, see paragraph 3.4.4.2), we need to increase sufficiently the regularization coefficient k_2 in order to make the continuation converge. After performing numerical tests for various values of k_2, we set $k_2^{\max} = 10$. We highlight that the values lower than $k_2 = 5$ do not allow the continuation to successfully reach the terminal conditions (3.30). Roughly speaking, when the value of k_2 parameter is too close to zero, then the central arc of the optimal solution becomes close to the singular arc, a straight line in the (x,h) plane, and consequently makes the shooting method fail. Clearly speaking, this means that the determinant of the Jacobian matrix (3.54) of the shooting function tends to zero (see paragraph 3.4.4.5 and inside it the figure 3.12). The k_2 parameter can be considered as a "singular perturbation" in our optimal control problem.

Once the boundary conditions reached, we implement a simultaneaous decreasing continuation on the regularization coefficient k_2 and the control saturation $\alpha_{\max}$. To do so, we implement a variant of the shooting method, which we will formally call "shooting from the middle" (refer to [29] for deeper description and an academic example). The shooting from the middle consists in choosing $z(t_f/2)$ as unknown and then:

- integrating backward in time the differential system over $[0, t_f/2]$ in order to get the value of $z(0)$
- integrating forward in time the differential system over $[0, t_f/2]$ in order to get the value of $z(t_f)$

This very simple variant appears to be very efficient for two main reasons:

- it divides the time horizon by a factor 2 by starting the shooting at time $t = t_f/2$
- it is extremely useful when initialized at the turnpike (which is our case) as it exploits the local stability of the solution.

Of course, "the price to pay" is the increase of the number of unknowns (and the conditions conditions to fullfill).

Consequently, in the light of what precedes, we implement two successive continuations:

1. **Step 1**: Simultaneous continuation on the prescribed coordinates of the final state and the corresponding ones of the initial state. We implement the standard shooting method. The shooting is performed on the initial adjoint state $p(0)$ and the time of flight t_f. At the end of this procedure, the initial and final states reach their prescribed values. This continuation is parametrized by $\lambda_1 \in [0,1]$.
2. **Step 2**: Simultaneous decreasing continuation on the regularization coefficient k_2 and the control saturation $\alpha_{\max}$. We implement the shooting from the middle. The shooting is performed on the state $\xi\left(\frac{t_f}{2}\right)$ and costate $p\left(\frac{t_f}{2}\right)$ taken at time $t_f/2$ and of course on the time of flight t_f. This continuation is parametrized by $\lambda_2 \in [0,1]$.

3.4.4.4 Continuation at step 1

During the first continuation procedure, the shooting function denoted $S_{\lambda_1} : \mathbb{R}^4 \mapsto \mathbb{R}^4$ is defined as follows:

$$S_{\lambda_1} : \begin{pmatrix} p(0) \\ t_f \end{pmatrix} \longmapsto \begin{pmatrix} x(t_f) - x_1^c(\lambda_1) \\ h(t_f) - h_1^c(\lambda_1) \\ \gamma(t_f) - \gamma_1^c(\lambda_1) \\ H_0^r\big(\mu(t_f), p(t_f), -1, \alpha(t_f)\big) \end{pmatrix} \tag{3.51}$$

One performs the diagonal continuation on the following coordinates:

$$\begin{aligned}
x_0^c(\lambda_1) &= x_0^i + \lambda_1.(x_0 - x_0^i) \\
h_0^c(\lambda_1) &= h_0^i + \lambda_1.(h_0 - h_0^i) \\
\gamma_0^c(\lambda_1) &= \gamma_0^i + \lambda_1.(\gamma_0 - \gamma_0^i) \\
x_1^c(\lambda_1) &= x_m^i + \lambda_1.(x_f - x_m^i) \\
h_1^c(\lambda_1) &= h_m^i + \lambda_1.(h_f - h_m^i) \\
\gamma_1^c(\lambda_1) &= \gamma_m^i + \lambda_1.(\gamma_f - \gamma_m^i)
\end{aligned}$$

where $\lambda_1 \in [0,1]$ is the homotopy factor increasing from 0 to 1. The starting triple of the initial state is $(x_0^i, h_0^i, \gamma_0^i) = (0, h_c, 0)$, the corresponding triple of the final state is $(x_m^i, h_m^i, \gamma_m^i) = (1, h_c, 0)$. The first guess is $z(0) := (p_x(0), p_h(0), p_\gamma(0), t_f) = (0.0, 1.0, 1.0, 2.0)$ and the convergence is immediate.

3.4.4.5 Well posedness of the shooting method

We explain hereafter how the well posedness of the shooting method is related to the k_2 coefficient. As detailed in the section 3.2.3, the shooting method consists in searching $(p(0), t_f)$ such that:

$$S_{\lambda_1}(p(0), t_f) = S(\lambda_1, p(0), t_f) = 0 \tag{3.52}$$

Let $(\bar{\lambda}_1, \bar{p}, \bar{t})$ be a zero of S. S being of class C^1, if its Jacobian matrix with respect to $(p(0), t_f)$, taken at the point $(\bar{\lambda}_1, \bar{p}, \bar{t})$ is invertible, then according to a usual implicit function argument, one can locally solve (3.52) and the solution $(p(0), t_f)$ depends in a C^1 way on the parameter λ_1. Notice that this is the standard argument which is at the basis of the well-known Lagrange–Newton method in optimization and as well a necessary condition for the local feasability of the continuation. For more details refer for instance to [58] and [83].

Based on the direct method results, we infer that, at least along the central arc:

$$H_0^r(\mu, p, -1, \alpha) \longrightarrow H_s(\mu, p, \alpha) \text{ as } k_2 \longrightarrow 0 \tag{3.53}$$

where H_s is given by (3.16) which means that the central arc of the regularized problem can be considered as a quasi-singular arc when k_2 decreases. This is precisely the case where the Jacobian of the shooting function becomes singular and consequently the continuation procedure fails. This is likely the reason why one needs to increase k_2 in order to make the continuation converge.

In order to support this conjecture, we compute numerically the family of Jacobian matrices:

$$dS := \left[\frac{\partial S}{\partial p(0)} \middle| \frac{\partial S}{\partial t_f} \right] \tag{3.54}$$

along the continuation path (parametrized by λ_1) and estimate the extreme singular values at each successfull iteration. We repeat what precedes for different values of k_2. The results are displayed hereafter:

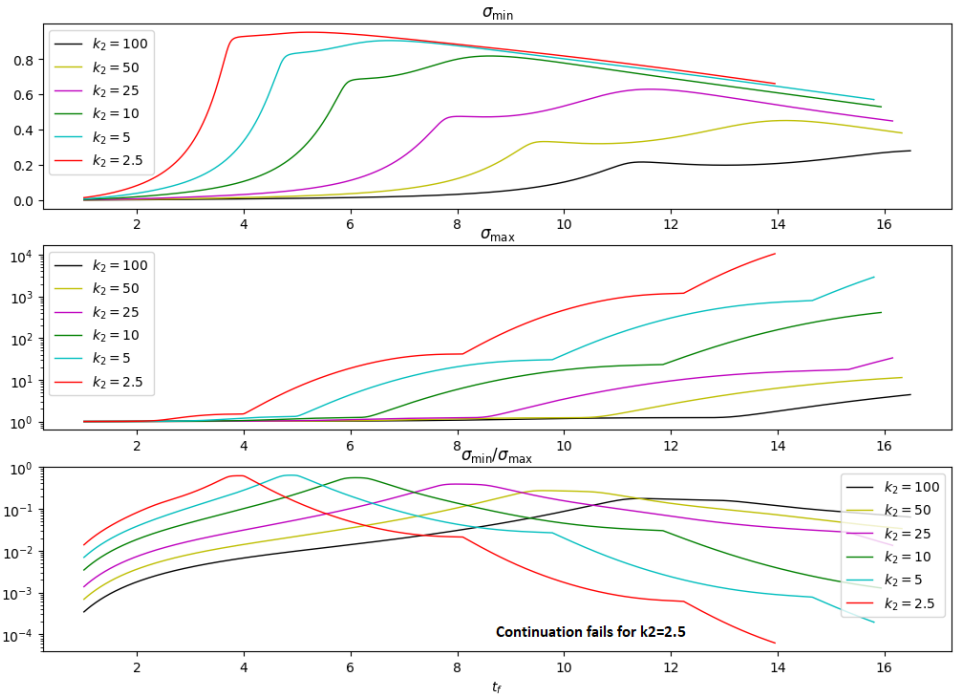

Figure 3.12: Singular values of the Jacobian for different values of k_2

One remarks that the ratio $\frac{\sigma_{min}}{\sigma_{max}}$ decreases as k_2 decreases. When this ratio drops below a threshold value, the solver likely declares the singularity of the Jacobian, and consequently the continuation is interrupted. For more details about the computation of the singular values, refer to the paragraph A.3.

3.4.4.6 Optimal solution for $\lambda_1 = 1.0$

The processing time is around 40 seconds. The computed state/costate/control are displayed hereafter ($k_2 = 10.0$):

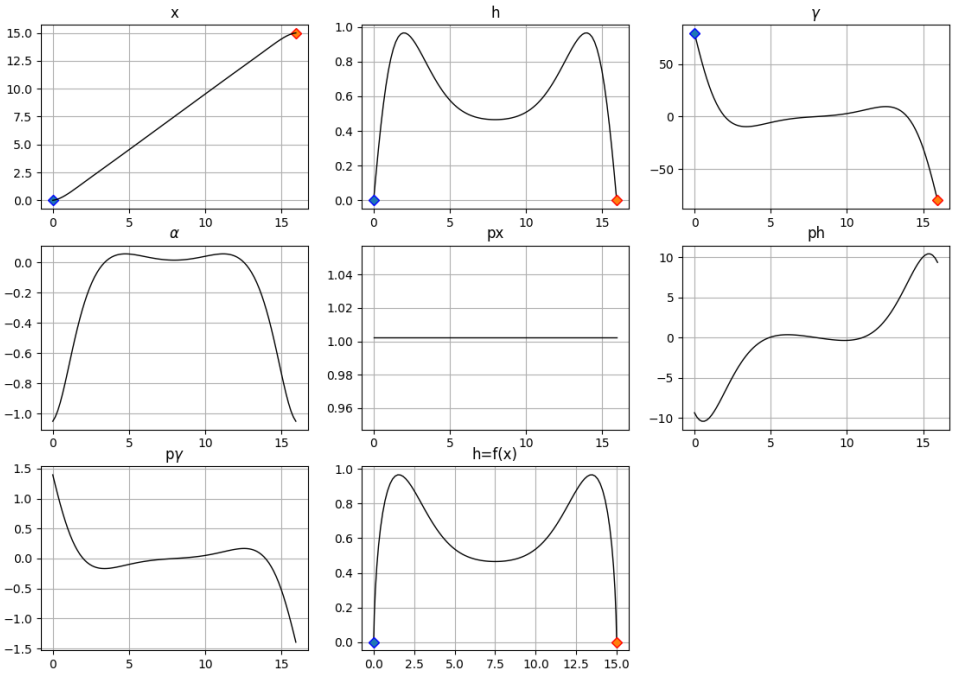

Figure 3.13: Optimal state, control and adjoint state for $\lambda_1 = 1$

The following table provides the terminal accuracy:

Shooting output	**Value**
$\lvert x(t_f) - x_f \rvert$	3.10^{-13}
$\lvert h(t_f) - h_f \rvert$	5.10^{-13}
$\lvert \gamma(t_f) - \gamma_f \rvert$	5.10^{-13}
$H_0^r(t_f)$	5.10^{-13}

Table 3.1: Final accuracy of the shooting (step 1)

As expected, the turnpike structure gradually appears on the state variables h and γ. This will be exploited in the following paragraph.

3.4.4.7 Continuation at step 2

The second continuation is based on the shooting function $S_{\lambda_2} : \mathbb{R}^{13} \mapsto \mathbb{R}^{13}$ defined hereafter:

$$S_{\lambda_2} : \begin{pmatrix} \mu^-\left(t_f/2\right) \\ \mu^+\left(t_f/2\right) \\ p^-\left(t_f/2\right) \\ p^+\left(t_f/2\right) \\ t_f \end{pmatrix} \longmapsto \begin{pmatrix} \mu(0) - \mu_0 \\ \mu(t_f) - \mu_f \\ H_0^r\left(\mu(t_f), p(t_f), -1, \alpha(t_f)\right) \\ \mu^-\left(t_f/2\right) - \mu^+\left(t_f/2\right) \\ p^-\left(t_f/2\right) - p^+\left(t_f/2\right) \end{pmatrix} \tag{3.55}$$

One performs the linear continuation on the coefficient k_2 and saturation value $\alpha_{\max}$:

$$k_2^c(\lambda_2) = k_2^{\max} + \lambda_2.(k_2^{\min} - k_2^{\max})$$
$$\alpha_{\max}^c(\lambda_2) = \alpha_{\max}^0 + \lambda_2.(\alpha_{\max} - \alpha_{\max}^0)$$

where $\lambda_2 \in [0,1]$ is the homotopy factor increasing from 0 to 1. The initial guess is obtained by extracting $(\mu(t_f/2), p(t_f/2))$ and t_f from the first step continuation for $\lambda_1 = 1.0$. After several

numerical tests, we set $k_2^{\min} = 0.25$ which is the minimum value for which one obtains the convergence when $\lambda_2 = 1.0$. We recall that $k_2^{\max} = 10.0$, $\alpha_{\max}^0 = 5.0$ and $\alpha_{\max} = 1.0$ (nominal value).
With the continuation step $\delta\lambda_2 = 0.01$, the processing time is around 40 sec.The computed optimal state/costate/control and the comparison with the non regularized direct method solution are displayed below:

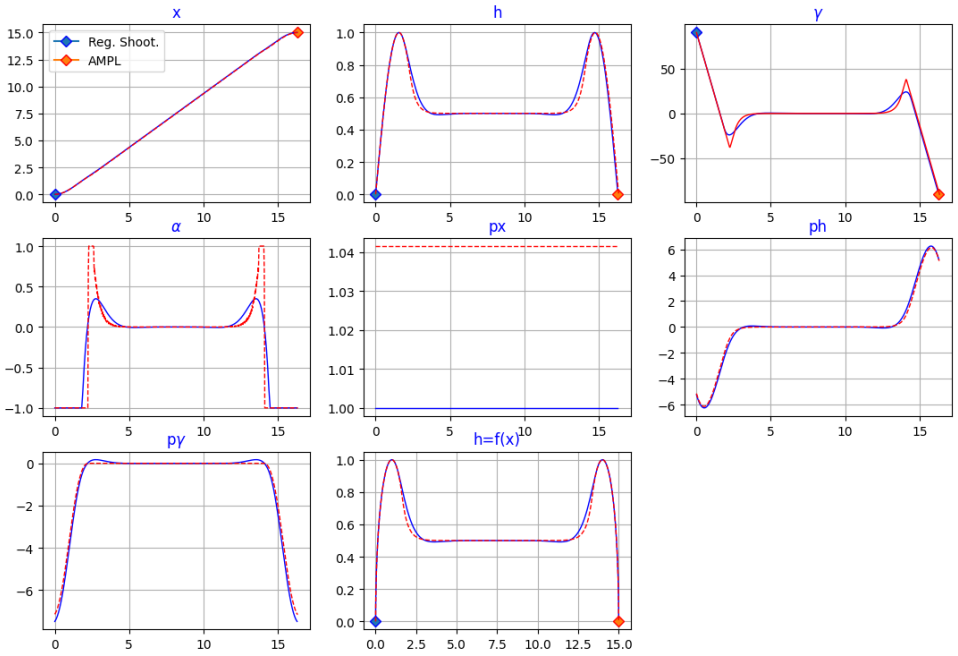

Figure 3.14: Optimal state, control and adjoint state for $\lambda_2 = 1$

The following table provides the accuracy for $\lambda_2 = 1.0$:

Shooting output	Value
$\lvert x(0) - x_0 \rvert$	1.10^{-9}
$\lvert h(0) - h_0 \rvert$	7.10^{-7}
$\lvert \gamma(0) - \gamma_0 \rvert$	2.10^{-6}
$\lvert x(t_f) - x_f \rvert$	1.10^{-8}
$\lvert h(t_f) - h_f \rvert$	1.10^{-6}
$\lvert \gamma(t_f) - \gamma_f \rvert$	10^{-6}
$H_0^r(t_f)$	7.10^{-8}

Table 3.2: Final accuracy of the shooting (step 2)

3.4.4.8 Comments

The L^2 regularization allows to compute the control without requiring prior knowledge of its structure. At step 2 of the solving procedure, we observed numerically that the continuation combined with the shooting from the middle allows to reach significantly lower value of k_2 than when combined with the standard shooting.

Remark 3.4.4.1 *An alternative to solve the non regularized problem is to implement the multiple shooting method in order to enhance the stability and accuracy. More precisely, one can proceed as follows:*

1. *Impose the control structure B-B-S-B-B and assume the stability of the latter along the continuation path.*
2. *Implement nodes on the control switching times.*
3. *Perform the shooting on the initial adjoint state, control switching times and the final time.*

We observed numerically that, in order to reach the prescribed boundary values, additional nodes need to be added, equally spaced one from each other, along the quasi-singular arc. The optimal solution is presented in appendix A.4.

In the next paragraph, we explain how the (D)/(DF) problems lead naturally to the missile guidance problem.

3.5 The missile guidance problem

Our objective is to solve numerically the optimal control problem (2.22) with the boundary conditions (2.23). As explained previously, we aim at computing the optimal solution in the minimum time case and the bunt case.

To do so, our goal is to deform the Dubins-Fuller problem into the missile guidance problem by performing a continuation over the dynamics and the boundary conditions.

Moreover, we highlight that, based on various numerical simulations the Dubins-Fuller problem appears to be very similar to the missile guidance problem in terms of global behavior of the optimal solutions. For this reason, we expect to successfully "transport" the optimal control structure from one to another.

Finally, the optimal synthesis in the missile guidance problem is actually a continuous deformation of the optimal synthesis in the Dubins-Fuller problem.

3.5.1 Parametrized dynamics

Let us consider the following 5D dynamical model: $\dot{\xi} = f_\lambda(\xi,\alpha)$ where $f_\lambda : \mathbb{R}^5 \longrightarrow \mathbb{R}^5$ is given by:

$$f_\lambda(\xi,\alpha) := \begin{pmatrix} v.\cos\gamma \\ v.\sin\gamma \\ \lambda.\left(\dfrac{T_{max}.(1+C_s.v)-D(h,v)}{m} - g.\sin\gamma\right) \\ a(\xi,\alpha).\lambda+\alpha \\ -\lambda.C_s.T_{max} \end{pmatrix} \tag{3.56}$$

with $a(\xi,\alpha) := \left(\dfrac{\bar{q}(h,v).S}{m.v} - 1\right).\alpha - g.\dfrac{\cos\gamma}{v}$. The dynamics is parametrized by the parameter $\lambda \in [0,1]$.

For $\lambda = 0$, one has the simplified dynamics (3.28) whereas for $\lambda = 1.0$, one has the full missile dynamics as defined in (2.21). Consequently, it seems natural to perform an increasing continuation over λ in order to "connect" both dynamics.

3.5.2 Numerical solving strategy

Similarly to the (DF) case, the missile guidance problem consists in steering the affine-in-control dynamical system from a fixed initial state to the partially fixed final state by minimizing a certain criterium. Consequently, we follow the same strategy as previously:

1. the minimum time problem: we implement an increasing continuation over λ and the boundary conditions in order to "transport" the optimal control structure from the Dubins problem up to the missile guidance problem.

2. the bunt problem: we first regularize the cost, then perform an increasing continuation over λ and boundary conditions in order to reach the desired ones. Then, we implement a decreasing continuation over the regularization parameter k_2 in order to get as close as possible to the original cost.

Remark 3.5.2.1 *The continuation will be simultaneously conducted on the dynamics and boundary conditions.*

3.5.3 The minimum time problem

We provide hereafter the state & costate equations arising from the application of the PMP to the minimum time problem with the parametrized missile dynamics (3.56). By denoting:

$$\mathrm{H}_\lambda(\xi, p, -1, \alpha) := \langle p, f_\lambda(\xi, \alpha)\rangle - 1 \tag{3.57}$$

The adjoint equations $\dot{p} = -\dfrac{\partial \mathrm{H}_\lambda}{\partial \xi}$ read along each coordinate (after arrangement):

$$\dot{p}_x = 0 \tag{3.58a}$$

$$\dot{p}_h = \lambda.\left(\frac{p_v}{m}.\frac{\partial \mathrm{D}}{\partial h}(h,v) - \frac{p_\gamma}{m.v}\frac{\partial \mathrm{L}}{\partial h}(h,v,\alpha)\right) \tag{3.58b}$$

$$\dot{p}_v = -p_x.\cos\gamma - p_h.\sin\gamma + \lambda.\left(\frac{p_v}{m}\frac{\partial \mathrm{D}}{\partial v}(h,v) - \frac{p_\gamma}{m}.\frac{\partial(\mathrm{L}/v)}{\partial v} - \frac{p_\gamma}{v^2}.g.\cos\gamma - \frac{p_v}{m}.\mathrm{C}_s.\mathrm{T}_{\max}\right) \tag{3.58c}$$

$$\dot{p}_\gamma = p_x.v.\sin\gamma - p_h.v.\cos\gamma + \lambda.p_v.g\cos\gamma - \lambda.\frac{p_\gamma}{v}g.\sin\gamma \tag{3.58d}$$

$$\dot{p}_m = \lambda.\frac{p_v}{m^2}\Big(\mathrm{T}_{\max}.(1+\mathrm{C}_s.v) - \mathrm{D}(h,v)\Big) + \lambda.\frac{p_\gamma}{v.m^2}.\mathrm{L}(h,v,\alpha) \tag{3.58e}$$

The control is derived in the same way than previously by derivating twice the switching function p_γ and its expression is:

$$\alpha_s(t) = \frac{1}{1-\lambda+\lambda.\dfrac{\bar{q}(h,v).\mathrm{S}}{m.v}}\left(\frac{\lambda.g.\cos\gamma}{v} + \frac{\mathrm{A}_\lambda(\xi,p)}{\mathrm{B}_\lambda(\xi,p)}\right) \tag{3.59}$$

where:

$$\mathrm{A}_\lambda(\xi,p) := \lambda.(p_h.\cos\gamma - p_x.\sin\gamma)\left(\frac{\mathrm{T}_{\max}.(1+\mathrm{C}_s.v)-\mathrm{D}(h,v)}{m} - g.\sin\gamma\right)$$
$$+\lambda.g.\cos\gamma.\left(p_x.\cos\gamma + p_h.\sin\gamma + \lambda.\frac{p_v.\mathrm{C}_s.\mathrm{T}_{\max}}{m} - \lambda.\frac{p_v}{m}\frac{\partial \mathrm{D}}{\partial v}\right) - \lambda.v.\cos\gamma.\frac{p_v.\mathrm{D}(h,v)}{m.h_r}$$

and

$$\mathrm{B}_\lambda(\xi,p) := v.(p_h.\sin\gamma + p_x.\cos\gamma) - \lambda.g.p_v.\sin\gamma$$

The adjoint transversality conditions (3.11) are:

$$p_v(t_f) = 0 \text{ and } p_m(t_f) = 0 \tag{3.60}$$

Finally, the transversality conditions on the Hamiltonian (3.12)-(3.13) lead to:

$$\forall t \in [0, t_f],\ \ \mathrm{H}_\lambda(\xi(t), p(t), -1, \alpha(t)) = 0 \tag{3.61}$$

Of course, one has to ingeniously select the variables/parameters over which the continuation should be performed in order to ensure the stability of the optimal structure. The choice proposed hereafter is based on the intuition and engineering experience.

Let us now consider the shooting function denoted by $S_\lambda : \mathbb{R}^8 \mapsto \mathbb{R}^8$ which is defined as follows:

$$S_\lambda : \begin{pmatrix} p(0) \\ t_1 \\ t_2 \\ t_f \end{pmatrix} \longmapsto \begin{pmatrix} x(t_f) - x_c(\lambda) \\ h(t_f) - h_f \\ \gamma(t_f) - \gamma_f \\ p_v(t_f) \\ p_m(t_f) \\ p_\gamma(t_1) \\ \dot{p}_\gamma(t_1) \\ H_\lambda\left(\xi(t_f), p(t_f), -1, \alpha(t_f)\right) \end{pmatrix} \tag{3.62}$$

where $0 \leqslant t_1 < t_2 \leqslant t_f$ are the instants corresponding to the beginning (resp. end) of the singular arc. Then one performs the diagonal continuation on the following parameters:

$$\begin{aligned} x_c(\lambda) &= x_f^i + \lambda.(x_f - x_f^i) \\ v_0(\lambda) &= v_0^i + \lambda.(v_0 - v_0^i) \\ \alpha_{\max}(\lambda) &= \alpha_{\max}^i + \lambda.\left(\alpha_{\max} - \alpha_{\max}^i\right) \end{aligned}$$

where $x_f^i = 5$, $v_0^i = 1$ and $\alpha_{\max}^i = 1.0$. The other parameters remain unchanged with respect to the table 2.1 and the boundary conditions (2.23). We display hereafter the samples of optimal trajectory, control and switching function along the continuation path with a step of $\delta\lambda = 0.05$.

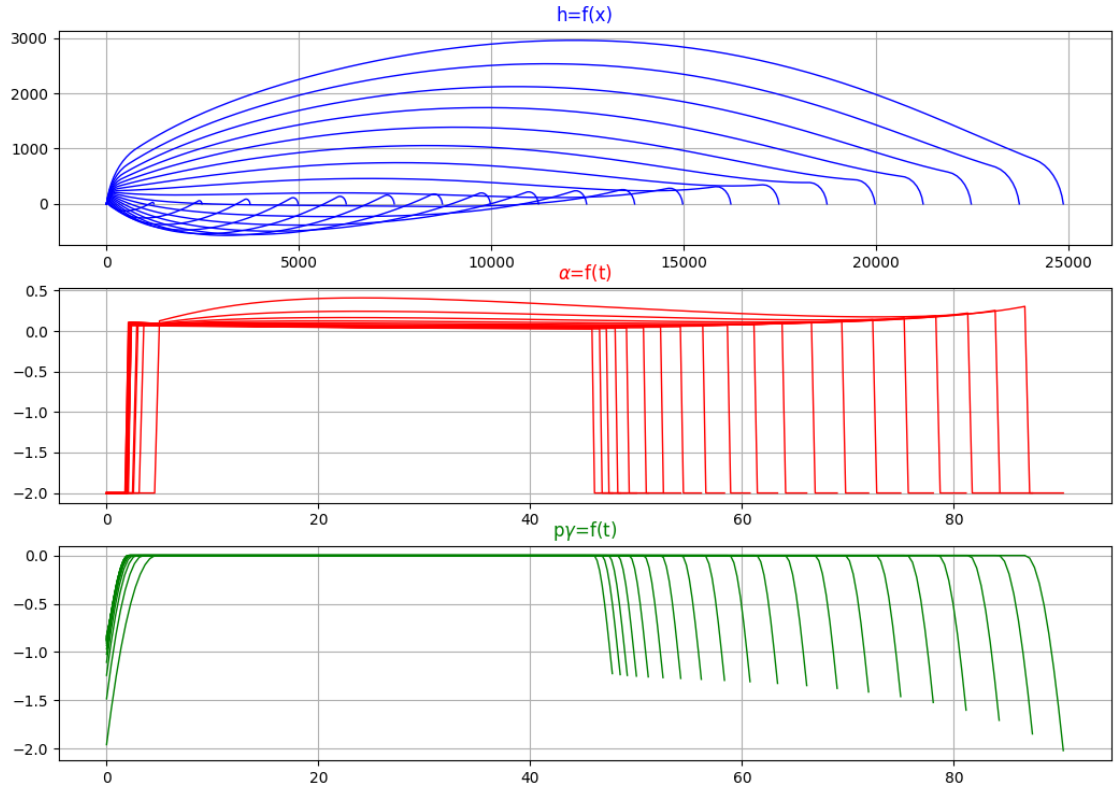

Figure 3.15: Trajectory, control & switching function samples

With the step $\delta\lambda = 0.0005$ and the maximum step $\delta\lambda^{\max} = 0.001$, the computing time is around 500 sec on a standard desktop computer. The final output are displayed hereafter (and compared to the output of the direct method):

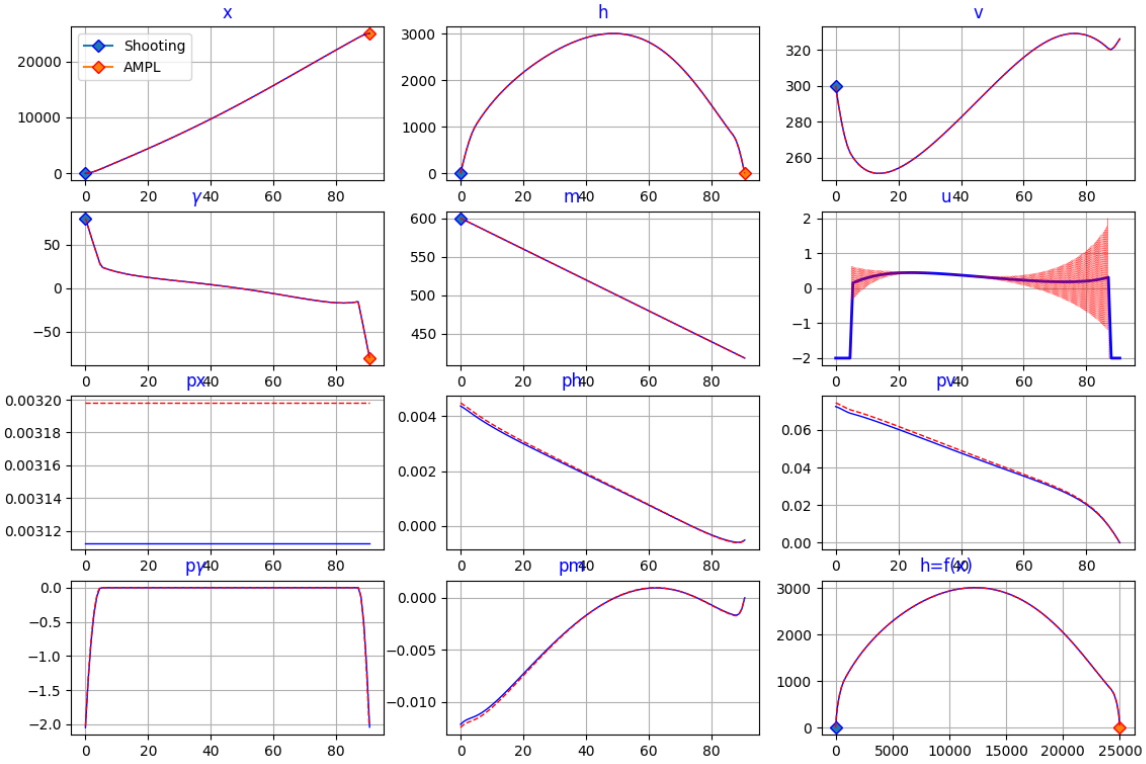

Figure 3.16: Shooting vs direct method comparison on minimum time problem

The following table provides the accuracy of the shooting method for $\lambda = 1.0$:

Shooting output	**Value**
$\lvert x(t_f) - x_f \rvert$	3.10^{-2}
$\lvert h(t_f) - h_f \rvert$	8.10^{-2}
$\lvert \gamma(t_f) - \gamma_f \rvert$	2.10^{-3}
$p_v(t_f)$	2.10^{-6}
$p_m(t_f)$	2.10^{-7}
$H_\lambda(t_f)$	2.10^{-14}

Table 3.3: Final accuracy

The switching instants are: $t_1 \approx 4.97$ sec, $t_2 \approx 87.05$ sec, and the time of flight $t_f \approx 90.7$ sec. By performing the continuation as detailed above, we implicitly made the assumption that the optimal structure remains unchanged over the range of the deformation parameter λ and final states. In practice, we did not prove it, but empirically inferred it by performing some AMPL/IPOPT simulations prior to the continuation.

3.5.4 The "bunt" case

We consider the regularized cost:

$$J_r(t_f, \alpha) := \int_0^{t_f} f_r^0(\xi(s), \alpha(s))ds := \int_0^{t_f} \left(1 + \frac{(h(s) - h_c)^2}{h_c^2} + k_2.\alpha(s)^2\right) ds \tag{3.63}$$

The regularized Hamiltonian is given by:

$$\begin{aligned} H_\lambda^r(\xi, p, p^0, \alpha) &:= \langle p, f_\lambda(\xi, \alpha)\rangle + p^0 f_r^0(\xi, \alpha) \\ &= \langle p, f_\lambda(\xi, \alpha)\rangle + p^0.\left(1 + \left(\frac{h - h_c}{h_c}\right)^2 + k_2.\alpha^2\right) \end{aligned}$$

We maintain the assumption of normality here by taking $p^0 = -1$. The adjoint equations in p_x, p_v, p_γ and p_m remain identical to (3.58). An additional term appears in p_h equation as:

$$\dot{p}_h = -\frac{\partial \mathrm{H}_\lambda}{\partial h} + \frac{2}{h_c^2}.(h - h_c) \tag{3.64}$$

Following the maximization condition (3.10), the optimal control α is now given by:

$$\alpha \in \underset{|r| \leqslant \alpha_{\max}}{\arg\max} \left(\beta_2.r^2 + \beta_1.r\right) \tag{3.65}$$

where:

$$\beta_2 := -k_2 \tag{3.66}$$

$$\beta_1 := p_\gamma.\left(1 + \lambda.\left(\frac{\rho(h).\mathrm{S}.v}{2.m} - 1\right)\right) \tag{3.67}$$

The transversality and Hamiltonian conditions remain unchanged:

$$\forall t \in [0, t_f], \quad \mathrm{H}_\lambda^r(\xi(t), p(t), -1, \alpha(t)) = 0 \tag{3.68}$$

and

$$p_v(t_f) = 0 \text{ and } p_m(t_f) = 0 \tag{3.69}$$

3.5.4.1 Continuation at step 1

During the first continuation procedure, the shooting function denoted by $\mathrm{S}_\lambda : \mathbb{R}^6 \mapsto \mathbb{R}^6$ is defined hereafter:

$$\mathrm{S}_\lambda : \begin{pmatrix} p(0) \\ t_f \end{pmatrix} \longmapsto \begin{pmatrix} x(t_f) - x_1^c(\lambda) \\ h(t_f) - h_1^c(\lambda) \\ \gamma(t_f) - \gamma_1^c(\lambda) \\ p_v(t_f) \\ p_m(t_f) \\ \mathrm{H}_\lambda^r\left(\xi(t_f), p(t_f), -1, \alpha(t_f)\right) \end{pmatrix} \tag{3.70}$$

One performs the diagonal continuation on the following coordinates:

$$\begin{aligned}
h_c^c(\lambda) &= h_c^i + \lambda.(h_c - h_c^i) \\
h_0^c(\lambda) &= h_c^c(\lambda) + \lambda.(h_0 - h_c^c(\lambda)) \\
v_0^c(\lambda) &= v_0^i + \lambda.(v_0 - v_0^i) \\
\gamma_0^c(\lambda) &= \gamma_0^i + \lambda.(\gamma_0 - \gamma_0^i) \\
x_1^c(\lambda) &= x_m^i + \lambda^2.(x_f - x_m^i) \\
h_1^c(\lambda) &= h_c^c(\lambda) + \lambda.(h_f - h_c^c(\lambda)) \\
\gamma_1^c(\lambda) &= \gamma_m^i + \lambda.(\gamma_f - \gamma_m^i)
\end{aligned}$$

where $\lambda \in [0, 1]$ is the homotopy factor increasing from 0 to 1. The initalization values are the following: $h_c^i = 0.5$, $x_m^i = 5$, $\gamma_0^i = 0$, $\gamma_m^i = 0$. The remaining coordinates are unchanged with respect to their numerical values (2.23). The first guess is $z(0) := (p_x(0), p_h(0), p_v(0), p_\gamma(0), p_m(0), t_f) = (0.5, 1.0, 1.0, 1.0, 1.0, 6.0)$ and the convergence is immediate.

After several numerical trials, we had to adjust the continuation step to the value $\delta\lambda = 0.001$. Moreover, we set the regularization coefficient to $k_2^{\max} = 50$. We highlight that values of k_2 lower than $k_2^{\max}$ combined with the continuation step greater than $\delta\lambda$ slow down significantly (or make fail) the algorithm .The observation on the k_2 was expected in the light of the paragraph 3.4.4.5: indeed, when k_2 tends to zero (precisely when $k_2 \leqslant k_2^{\max}$), then the central arc becomes too close to a

singular arc (that is along which the linearized system is not controllable, see 3.1.2.1). For this reason, the determinant of the Jacobian of the shooting function becomes close to zero which makes the shooting method fail. Clearly speaking, there exists an infimum of the k_2 values below which the continuation method fails to converge. As in the Dubins- Fuller case (see paragraph 3.4.4), k_2 parameter can be considered as a "singular perturbation" in our optimal control problem.

Under the previous settings, the processing time is around 500 seconds. We display hereafter the samples of optimal trajectory and control along the continuation path and the final solution:

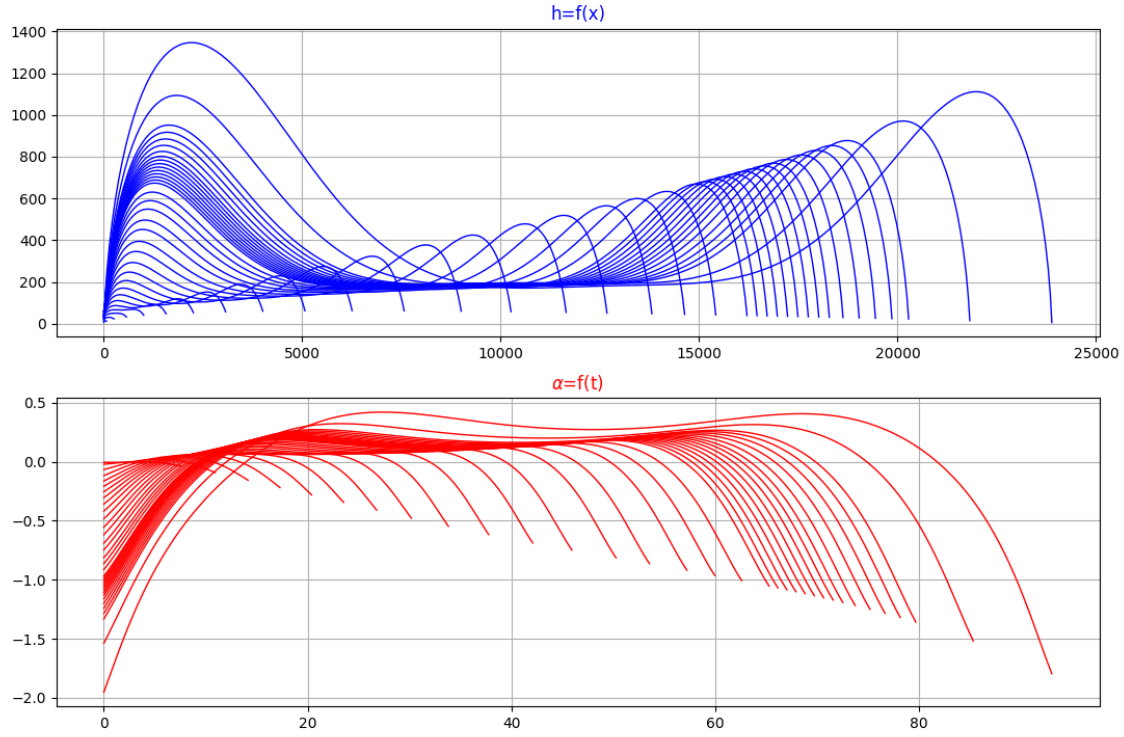

Figure 3.17: Samples of optimal trajectory and control

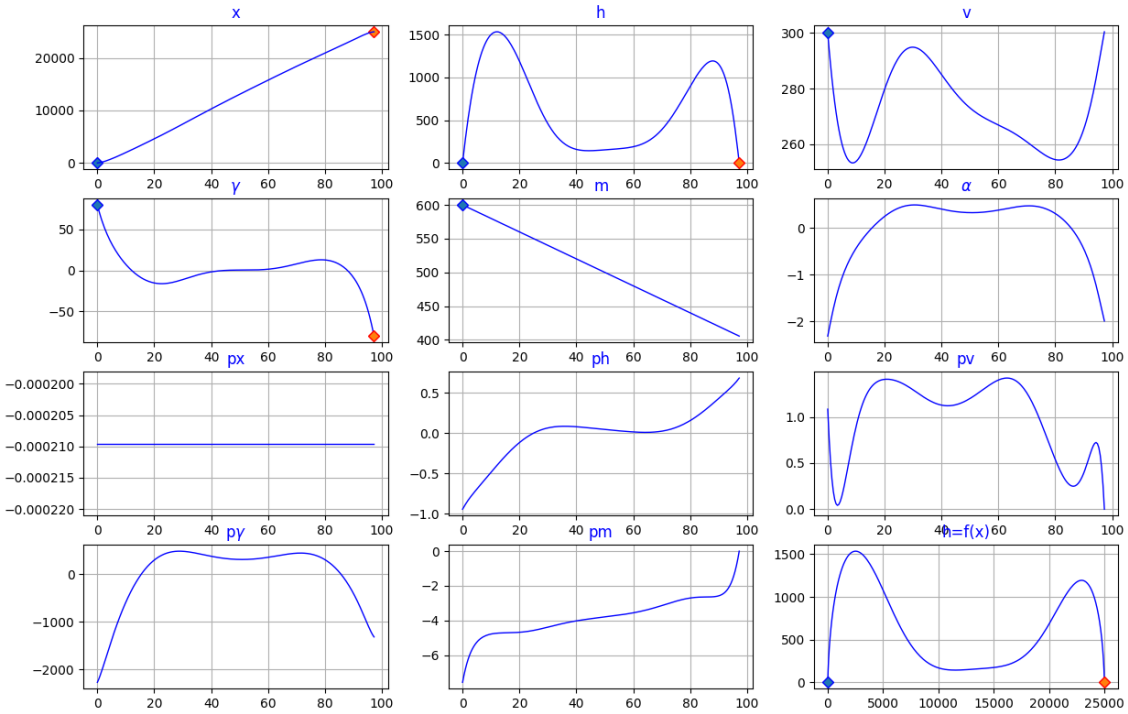

Figure 3.18: Optimal state, control and adjoint state for $\lambda = 1$

The following table provides the terminal accuracy:

Shooting output	**Value**
$\lvert x(t_f) - x_f \rvert$	7.10^{-10}
$\lvert h(t_f) - h_f \rvert$	2.10^{-10}
$\lvert \gamma(t_f) - \gamma_f \rvert$	5.10^{-11}
$p_v(t_f)$	2.10^{-11}
$p_m(t_f)$	2.10^{-11}
$\mathrm{H}_1^r(t_f)$	5.10^{-13}

Table 3.4: Final accuracy of the shooting (step 1)

3.5.4.2 Continuation at step 2

During the second continuation, the shooting function $S_\delta : \mathbb{R}^{21} \mapsto \mathbb{R}^{21}$ is defined hereafter:

$$S_\delta : \begin{pmatrix} \xi^-\left(t_f/2\right) \\ \xi^+\left(t_f/2\right) \\ p^-\left(t_f/2\right) \\ p^+\left(t_f/2\right) \\ t_f \end{pmatrix} \longmapsto \begin{pmatrix} \xi(0) - \xi_0 \\ x(t_f) - x_f \\ h(t_f) - h_f \\ \gamma(t_f) - \gamma_f \\ p_v(t_f) \\ p_m(t_f) \\ \mathrm{H}_1^r\left(\xi(t_f), p(t_f), -1, \alpha(t_f)\right) \\ \xi^-\left(t_f/2\right) - \xi^+\left(t_f/2\right) \\ p^-\left(t_f/2\right) - p^+\left(t_f/2\right) \end{pmatrix} \tag{3.71}$$

Identically to the (DF) case, one performs the decreasing continuation over k_2 and α_{max}:

$$k_2^c(\delta) = k_2^{max} + \delta.(k_2^{min} - k_2^{max})$$
$$\alpha_{max}^c(\delta) = \alpha_{max}^0 + \delta.(\alpha_{max} - \alpha_{max}^0)$$

where $\delta \in [0,1]$ is the homotopy factor increasing from 0 to 1. The initial guess is obtained by extracting $(\xi(t_f/2), p(t_f/2))$ and t_f from the first step continuation for $\lambda = 1.0$. After several numerical tests, we set $k_2^{min} = 0.75$ which is the minimum value for which one obtains the convergence for $\lambda_2 = 1.0$. We recall that $\alpha_{max}^0 = 20.0$ and $\alpha_{max} = 2.0$ (nominal value).

We set the continuation step $\delta\lambda_2 = 0.005$ which ensures a reasonable compromise between the computation time (300 sec) and the algorithm accuracy. The solution obtained with the shooting method is presented hereafter and compared to the non regularized solution obtained with the direct method:

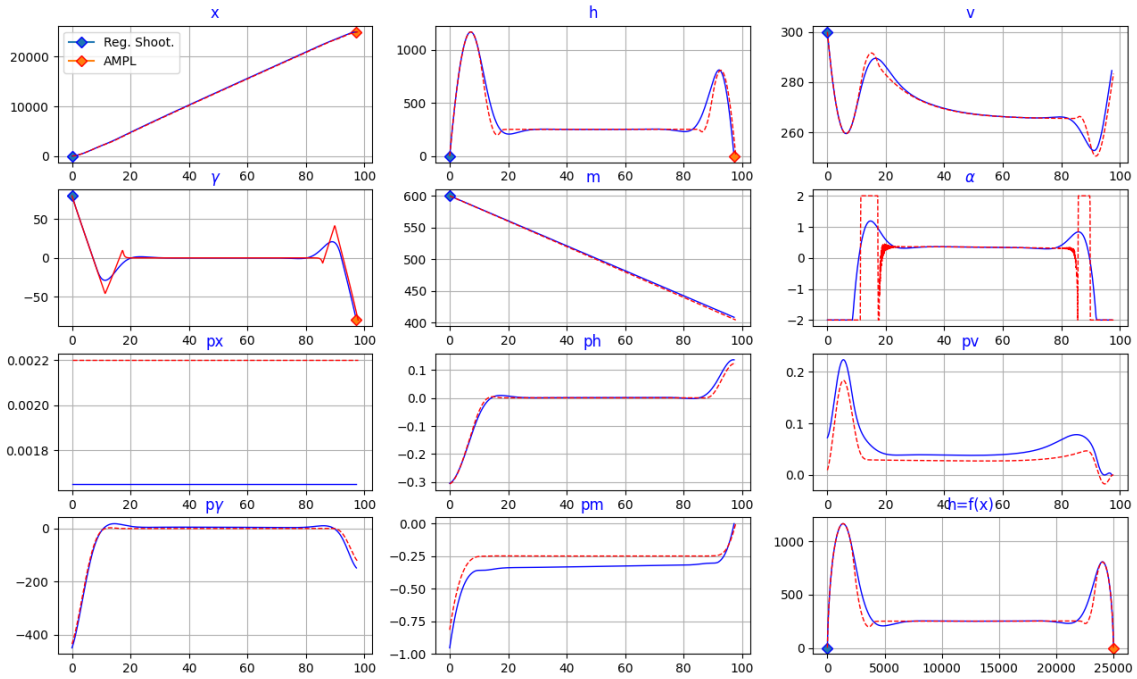

Figure 3.19: Optimal state, control and adjoint state for $\delta = 1$

The following table provides the accuracy of the continuation for $\delta = 1.0$:

Shooting output	Value
$\lvert x(0)-x_0\rvert$	1.10^{-7}
$\lvert h(0)-h_0\rvert$	7.10^{-7}
$\lvert v(0)-v_0\rvert$	3.10^{-8}
$\lvert \gamma(0)-\gamma_0\rvert$	2.10^{-8}
$\lvert m(0)-m_0\rvert$	1.10^{-13}
$\lvert x(t_f)-x_f\rvert$	3.10^{-6}
$\lvert h(t_f)-h_f\rvert$	5.10^{-7}
$\lvert \gamma(t_f)-\gamma_m\rvert$	2.10^{-7}
$p_v(t_f)$	7.10^{-9}
$p_m(t_f)$	4.10^{-7}
$\mathrm{H}_1^r(t_f)$	9.10^{-10}
$\lvert \xi^-\left(t_f/2\right)-\xi^+\left(t_f/2\right)\rvert$	0.0
$\lvert p^-\left(t_f/2\right)-p^+\left(t_f/2\right)\rvert$	0.0

Table 3.5: Final accuracy of the shooting (step 2)

3.5.4.3 Comments and perspectives

The regularization of the initial control problem allows to successfully compute an acceptable solution. The key idea behind this is the increase of the regularization coefficient k_2 which enhances the well posedness of the shooting method and consequently ensures the convergence of the algorithm. The other advantage is that, contrary to the minimum time problem, one does not need to know the structure of the optimal trajectory prior to the implementation, which simplifies the analysis and the computation of the algorithm.

On the other side, the (usual) drawback of the regularization is that one does not exactly solve the initial control problem due precisely to the coefficient k_2. However, in our case, the regularized solution is relatively close to the original one and totally acceptable from the operational point of view (see figure 3.19).

Additional numerical experiments show that the minimum value of the k_2 coefficient (meaning the minimum value of k_2 allowing the convergence of the continuation) increases with values of x_f. Consequently, the regularized problem becomes less representative of the original one: indeed the altitude peaks (during the first and last phase of flight) become higher which extends the exposure of the vehicle and the cruise altitude constraint is no more respected with acceptable tolerance.

3.5.5 Computation of a quasi optimal trajectory by a reduced shooting method

To overcome this issue and in order to compute an acceptable solution for even larger time horizons, one can exploit the partial turnpike phenomenon observed on h and γ. A pragmatic approach consists in replacing the central arc by a level flight arc during which one has rigorously $h(t)=h_c$ and $\gamma(t)=0$. The last equality leads from (2.21d) to a control in the form of a feedback of the state:

$$\gamma(t)\simeq 0 \Longrightarrow \dot{\gamma}(t)\simeq 0 \Longrightarrow \bar{\alpha}(t)\simeq \frac{m(t).g}{\bar{q}(h_c.v(t)).\mathrm{S}} \tag{3.72}$$

A counterpart of the approximation is an a priori loss of optimality: indeed there is no reason that the PMP holds along such an arc.The convient method is to implement a *reduced shooting method* which consists in considering the state dynamics only.

More precisely, based on the direct method results (see figure 3.19) let us consider the following control structure:

1. $\alpha(t)=-\alpha_{\max}$ on time interval $[0,t_1]$

2. $\alpha(t) = \alpha_{\max}$ on time interval $[t_1, t_2]$
3. $\alpha(t) = \bar{\alpha}(t)$ on time interval $[t_2, t_3]$
4. $\alpha(t) = \alpha_{\max}$ on time interval $[t_3, t_4]$
5. $\alpha(t) = -\alpha_{\max}$ on time interval $[t_4, t_f]$

where $0 < t_1 < t_2 < t_3 < t_4 < t_f$ are the different switching times. As remarked above, $\bar{\alpha}$ is not optimal, but based on the turnpike phenomenon, we infer that it may be a quasi-optimal arc.

By assuming the stability of the control structure when x_f increases, one can implement a continuation based on a shooting on the switching times only. More precisely, let us define the shooting function $S_\delta : \mathbb{R}^5 \mapsto \mathbb{R}^5$ defined as follows:

$$S_\delta : \begin{pmatrix} t_1 \\ t_2 \\ t_3 \\ t_4 \\ t_f \end{pmatrix} \longmapsto \begin{pmatrix} h(t_2) - h_c \\ \gamma(t_2) \\ x(t_f) - x_f^c(\delta) \\ h(t_f) - h_f \\ \gamma(t_f) - \gamma_f \end{pmatrix} \tag{3.73}$$

The two first components of $S_\delta(\cdot)$ impose that $\forall t \in [t_2, t_3],\ h(t) = h_c$ and $\gamma(t) = 0^\circ$. It suffices to perform the continuation on the x_f coordinate only:

$$x_f^c(\delta) = x_f^i + \delta.(x_f - x_f^i)$$

where $\delta \in [0,1]$ is the homotopy factor increasing from 0 to 1, $x_f^i = 25000m$ is the initial range value corresponding to the boundary value of the regularized problem. We set the new final range value at $x_f = 50000m$ and keep the other terminal conditions unchanged. The initialization of the shooting procedure can be easily done by choosing $(t_1, t_2, t_3, t_4, t_f) \simeq (11, 17, 86, 90, 100)$ deduced from the original regularized problem.

The principle of the shooting is analogous to the minimum time case as we integrate each of the five arcs separately. However, the main difference is that we do not consider the adjoint variables as we do not implement the PMP necessary optimality conditions as it is usually done in the shooting methods.

The optimal solution is displayed hereafter and compared to the one obtained with the direct method (AMPL & IPOPT):

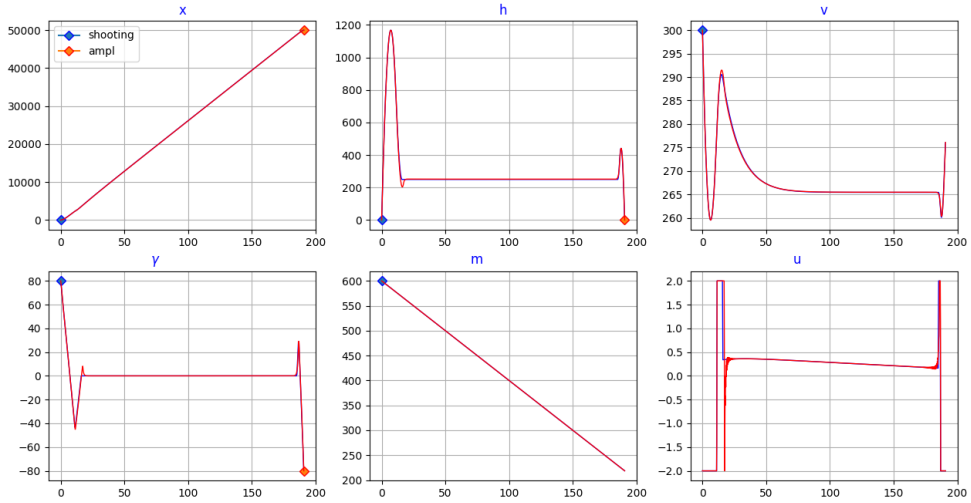

Figure 3.20: State and control: Shooting vs direct method

First, the output correspondence between the two approaches is satisfactory which validates the level flight approximation. Moreover, the cost obtained by the reduced shooting method is $C_{rs} \simeq 282.3$ whereas the cost obtained by the direct method is $C_{ampl} \simeq 281.7$. This observation confirms that the computed solution is quasi-optimal. Finally, we highlight that due to lower problem dimension (5 vs 10 for the standard shooting) the computation time of the shooting is significantly reduced.

Remark 3.5.5.1 *An alternative method to compute an optimal solution for great time horizons is to assume, as done before, a pre defined optimal control structure, with intermediate constraints (for instance, $h(t_2) = h_c$ and $\gamma(t_2) = 0$) and then to apply the Hybrid Maximum Principle ([21]-[22]). However, we did not test this approach within the frame of this thesis.*

Chapter 4

Hamilton Jacobi Bellman approach

"Tu sais que t'es physiquement intelligente toi?"

Brice de Nice

Sommaire

4.1 A global approach 94
4.1.1 Introduction 94
4.1.2 Dynamic Programming Principle 94
4.1.3 Theoretical elements related to the HJB approach 95
4.1.4 Minimum time trajectories reconstruction from the value function 96
4.2 An application: reachable sets for the vehicle in level flight 97
4.2.1 Minimum time problem 97
4.2.2 Numerical Hamiltonian 98
4.2.3 Spatial grid 98
4.2.4 Reachable sets 98
4.2.5 Minimum time trajectories 99
4.3 HJB approach for optimal control problems with state constraints 101
4.3.1 Motivation 101
4.3.2 Mathematical setting 101
4.3.3 Assumptions 101
4.3.4 General considerations and notations 102
4.3.5 Time variable change 102
4.3.6 State constrained case 104
4.3.7 A particular case: the target capture bassin 105
4.3.8 Optimal trajectories reconstruction from the value function 106
4.3.9 Numerical scheme 106
4.4 An application: optimisation of a glider trajectory 106
4.4.1 Setting 106
4.4.2 HJB equation 107
4.4.3 Numerical Hamiltonian 108
4.4.4 Computation domain and numerical results 108
4.4.5 Comments 110

4.1 A global approach

4.1.1 Introduction

The PMP can be used to find an optimal solution but it should be emphasized that there is no guarantee that this solution is the global optimal one because this approach deals only with necessary conditions of optimality.

Besides, the homotopy procedure being an iterative one, it raises the question of initialization and convergence. Finding a suitable initial guess can be tricky in particular, when dealing with duality and when the area of convergence is restricted as it is the case in the quasi Newton method.

With regard to local methods, the HJB approach has two major assets. First, the background theory ensures to obtain the global solution when it exists. Second, the implementation of the HJB approach doesn't require any iterative process, freeing the engineer from tricky tasks that are initialization and convergence.

Despite of these advantages, the approach suffers from some difficulties of computing the solution to the HJB equation in higher dimensions. The numerical simulations presented in the following sections show that the approximation of the HJB equations, even on coarse grids, provides solutions which depict well the qualitative structure of the optimal trajectories and may thus be used to guess the structure of optimal solutions. However, to get an accurate computation of the optimal trajectories, an important numerical effort is necessary to approach the solutions of the HJB equations on very fine grids.

4.1.2 Dynamic Programming Principle

Let us consider the following problem: look for the path starting from the point a and allowing reaching the point e in minimum time.

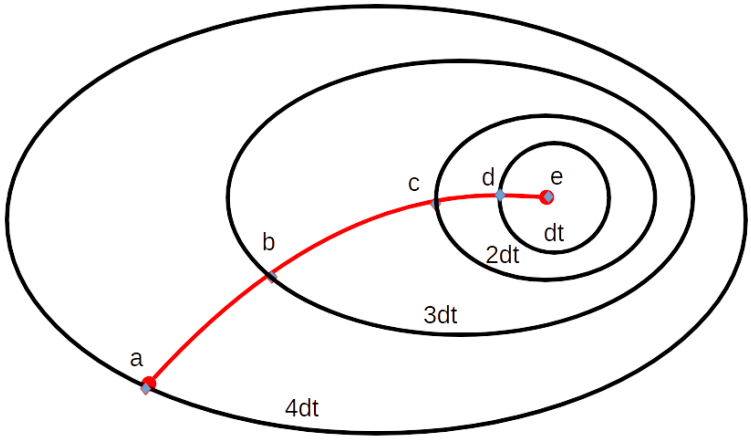

Figure 4.1: Illustration of the Dynamic Programming Principle

We assume the dynamics is such that at any time, the time of arrival depends only on the current state and on the control, in particular it is considered that the history of dynamics state prior to the curent state has no explicit influence on the future state. In this frame, the core idea at origin of the DPP can be expressed as follows: if the optimal trajectory from the point a to the point e goes through the point b, the portion of this trajectory linking the point b to the point e is also the quickest path between these latter points. If it was not, there would exist a quicker path between the points a and e. Now considering the quickest trajectory between the points b and e, this smaller optimization problem can be solved if we know that this trajectory goes through the point c for instance, and so on.

This simple-looking idea is at the origin of a powerful approach that can be used to solve an optimal control problem: starting from the target, one looks for the points being reachable in given time dt. The locus of this points may be understood as a level curve which is memorized. Starting from this curve, the location reachable in a given time dt is determined and memorized. This new level curve represents the locus of points reachable in $2dt$ and is memorized. This computation is running until the farthest level curve crosses the point a. Then this propagation phase, which is time backward, stops.

Now, starting from the point a, let us use the level curves which have been successively memorized dring the propagation phase to determine the quickest path, the time flowing forwards from 0 to dt, then from dt to $2dt$, and so on until reaching the point e. This is the so called reconstruction phase. Let us notice that not only the best path starting from the point a can be reconstructed, but all the paths starting from any point included inside the level curve croissing the point a.

4.1.3 Theoretical elements related to the HJB approach

As previously illustrated, the DPP proposes to solve an optimal control problem by considering it as a part of a family of optimal control problems: indeed, to find a path from the point a to the point e, one may find the optimal path from b to e and so on.

The HJB equation extends this approach, expressed in discrete domain, to continuous optimal control problem. Actually, solving HJB equation leads to the computation of a "value function" which associates the optimal cost of the control problem to the initial state. More precisely, the value function appears to be the solution of a first order nonlinear partial differential equation, the dimension of which being related to the number of variables involved in the problem.

Let us consider the following problem:

$$\begin{cases} \min t_f \\ \dot{\xi}(s) = f(\xi(s),\alpha(s)) \quad \forall s \in [0,t_f] \\ \alpha(s) \in \mathrm{A} \quad \text{for a.e. } s \in [0,t_f] \\ \xi(0) = x \\ \xi(t_f) \in \mathscr{C} \end{cases} \tag{4.1}$$

where $\mathscr{C}$ (target) is a smooth subset of $\mathbb{R}^n$, $f : \mathbb{R}^n \times \mathrm{A} \to \mathbb{R}^n$ is the dynamics, A is a compact set of $\mathbb{R}^p$. We denote by $\xi_x^\alpha(\cdot)$ the trajectory of the dynamical system starting from the initial position x and associated to the control α.

We recall some classical results related to the HJB approach of (4.1). Let us assume the continuity of f, the closedness and convexity of $f(x,\mathrm{A})$ for any $x \in \mathbb{R}^n$, the Lipschitz continuity of f in the state variable uniformely with respect to the control and the linear growth property.

Consider the minimal time function T which associates to any point $x \in \mathbb{R}^n$ the minimal time needed to reach the target $\mathscr{C}$ with an admissible trajectory $\xi_x^\alpha(\cdot)$:

$$\mathrm{T}(x) := \inf\{t \geqslant 0, \exists \alpha \in \mathscr{A}, \text{ s.t. } \xi_x^\alpha(t) \in \mathscr{C}\} \tag{4.2}$$

Many works have been devoted to the regularity of T. Under some controllability property around the target (typically the inward pointing qualification IPQ), the function T is the unique continuous viscosity solution of an HJB equation (see [56] for instance).

Unfortunately, in many control problems the IPQ condition is not satisfied at the boundary of the target $\mathscr{C}$. Thus the minimum time T may be discontinuous or even not real valued. Nevertheless, it can be shown ([4] for instance) that the epigraph of T can be characterized by an auxiliary value function which is Lipschitz continuous. What follows is borrowed from [4].
Let us first consider a Lipschitz continuous function $\psi : \mathbb{R}^n \to \mathbb{R}$ such that:

$$x \in \mathscr{C} \iff \psi(x) \leqslant 0 \tag{4.3}$$

Consider the value function $u : \mathbb{R}^+ \times \mathbb{R}^n \to \mathbb{R}$ such that:

$$u(t,x) := \inf\{\psi(\xi_x^\alpha(t)),\ \alpha \in \mathscr{A}\} \tag{4.4}$$

Let us now introduce the capture bassin (backward reachable set) at time t defined by:

$$Capt_{\mathscr{C}}(t) := \left\{x \in \mathbb{R}^n,\ \exists\ \alpha \in \mathscr{A} \,\middle|\, \xi_x^\alpha(t) \in \mathscr{C}\right\}. \tag{4.5}$$

The capture bassin and the minimal time function T can then be characterized as follows:

Proposition 4.1.3.1 *The capture bassin $Capt_{\mathscr{C}}(t)$ and the minimal time function T satisfy:*

$$Capt_{\mathscr{C}}(t) = \{x, u(t,x) \leqslant 0\} \tag{4.6a}$$

$$T(x) = \inf\{t \geqslant 0, x \in Capt_{\mathscr{C}}(t)\} = \inf\{t \geqslant 0, u(t,x) \leqslant 0\} \tag{4.6b}$$

Roughly speaking the value function u encodes the information to compute the capture bassin and the minimal time T. Moreover, as stated before, it satisfies the dynamical programming principle:

Proposition 4.1.3.2 (Dynamical Programming Principle)
Under adequate assumptions, for any $x \in \mathbb{R}^n$ and $0 < \tau \leqslant t$, one has:

$$u(t,x) = \inf_{\alpha \in \mathscr{A}} \{u(t-\tau, \xi_x^\alpha(\tau))\} \tag{4.7}$$

Finally, the value function u satisfies the following HJB equation:

Proposition 4.1.3.3 (Hamilton Jacobi Bellman Equation)
u is the unique continuous viscosity solution of the following HJB equation:

$$\partial_t u + \mathscr{H}_0(x, D_x u) = 0, \tag{4.8a}$$

$$u(0,x) = \psi(x) \tag{4.8b}$$

where the Hamiltonian is given by: $\mathscr{H}_0(x,p) := \sup_{a \in A}(-f(x,a).p)$.

In the above mentioned equation, $D_x u$ is the differential of u with respect to x in *the viscosity sense* which is weaker than the classical differentiability: indeed, expecting a value function to be differentiable is an unrealistic assumption in the HJB framework as we illustrate it later through an example. For more details on the need of viscosity solutions, please refer to A.2.

Remark 4.1.3.1 *: The precise assumptions leading to the DPP and HJB equations and the associated proofs will be detailed in the general case in the next section.*

Remark 4.1.3.2 *: It is easily proved that if one considers the Hamiltonian defined by:*

$$\mathscr{H}(x,p) := \max\left(0, \sup_{a \in A}(-f(x,a).p)\right) \tag{4.9}$$

*the negative level sets of the associated solution of (4.8) correspond to the capture bassins **before time t**. This is precisely what we implement in the next numerical example.*

4.1.4 Minimum time trajectories reconstruction from the value function

From a control viewpoint, the approximation of the value function u has a relatively lesser interest with respect to the construction of the (approximate) optimal control. We propose here a simple algorithm that leads, given an approximation of the value function, to construct quasi-optimal controls in feedback form.

Let us consider $(t_0 = 0 < t_1 < ... < t_n = T)$ a uniform partition of the time interval $[0,T]$ and $h = \frac{T}{n}$ be the time step. Let $\{\xi^n(\cdot)\}$ be the trajectory defined recursively on the time interval $(t_k, t_{k+1}]$ for $0 \leqslant k \leqslant n-1$ and let $\{\alpha^k(\cdot)\}$ be the corresponding sequence of controls.

Algorithm 2 Trajectory reconstruction algorithm for minimum time problem

Set $\xi^n(0) := x$

Step 1: Compute the optimal control $\alpha_k \in \mathrm{A}$ at t_k:

$$\alpha_k \in \underset{a\in\mathrm{A}}{\arg\min}\left(v^h(t_{n-k},\xi^n(t_k)),a\right)$$

Step 2: Define $\alpha_k(t)=\alpha_k$ be a constant control for $t\in(t_k,t_{k+1}]$ and $\xi^n(t)$ on $(t_k,t_{k+1}]$ be the solution to:

$$\dot{\xi}(t)=f(\xi(t),\alpha_k(t)) \text{ a.e } t\in(t_k,t_{k+1}], \text{ with the initial condition } \xi^n(t_k).$$

4.2 An application: reachable sets for the vehicle in level flight

Let us consider the bunt case in the missile guidance optimization problem (please refer to the chapter 3 for the precise setting): during "the turnpike arc", the missile is flying close to the cruise altitude h_c (refer to the figure 3.19). Then at first order, one has $h(t)\approx h_c$ which implies $\gamma(t)\approx 0$. Consequently, the dynamics can be reduced to the dimension 3.

4.2.1 Minimum time problem

Let us consider the minimum time problem for the reduced dynamical system where the thrust $\alpha_1(\cdot)$ is considered as active:

$$(\mathbf{OCP}_3)\begin{cases}\min\limits_{\alpha\in[\eta,1]} \ t_f\\ \dot{\phi}(s)=f_3(\phi(s),\alpha(s)) \qquad \forall s\in[0,t_f]\\ \phi(0)=\phi_0, \ \ \phi(t_f)=\phi_f\end{cases} \tag{4.10}$$

where:

- $\phi := (x \ \ v \ \ m)^{\mathrm{T}}$ is the state in dimension 3, the throttle $\alpha := \alpha_1$ is the control in dimension 1
- $f_3(\phi,\alpha) := \begin{pmatrix} v \\ \frac{\mathrm{T}_{\max}.(1+\mathrm{C}_s v)}{m}\alpha - \frac{\mathrm{D}_0(h_c,v)}{m} \\ -\mathrm{C}_s.\mathrm{T}_{\max}.\alpha \end{pmatrix}$ is the dynamics
- $\mathrm{D}_0(h,v) := \bar{q}(h,v).\mathrm{S}.\mathrm{C}_d$ is the first order drag force (the drag/lift coupling term in D has been neglected).
- $\phi_0 = (x_0 \ \ v_0 \ \ m_0)^{\mathrm{T}}$ and $\phi_f = \begin{pmatrix} x_f & v_f & * \end{pmatrix}^{\mathrm{T}}$ are the prescribed initial and final states.

We apply the forementioned theory to $(\mathbf{OCP}_3)$. We compute:

- the reachable sets starting from a given initial state
- the minimum time trajectories for a target problem

Remark 4.2.1.1 *: The dynamics f_3 is obtained from (2.21) by assuming $h=h_c$ and $\gamma=0^\circ$.*

Remark 4.2.1.2 *: Actually, the reachable set can be understood as the capture bassin of the initial state, propagating the value function negative levels forward in time.*

We highlight that, in order to improve the numerical efficiency, we proceed to some variable normalization in order to deal with comparable orders of magnitude between the state variables and the time: $\bar{t} := \frac{t}{10}$, $\bar{x} := \frac{x}{1000}$, $\bar{v} := \frac{v}{100}$, $\bar{m} := \frac{m}{100}$ and $\overline{\mathrm{T}}_{\max} := \frac{\mathrm{T}_{\max}}{1000}$.

4.2.2 Numerical Hamiltonian

The Lax Friedrich numerical approximation was implemented:

$$\mathscr{H}_{num}(\xi,(p_1^-,p_1^+),...,(p_n^-,p_n^+)) = \mathscr{H}\left(\xi,\frac{p^-+p^+}{2}\right) - \sum_{i=1}^{n} c_i \left(\frac{p_i^+ - p_i^-}{2}\right) \tag{4.11}$$

where $c_i = \sup_{(\xi,p)} \left|\frac{\partial \mathscr{H}}{\partial p_i}(\xi,p)\right|$ for $i \in [\![1,n]\!]$. Please see the next section for deeper explanations on the numerical schemes. In our example in dimension $n=3$, the maximized Hamiltonian can be analytically calculated and one obtains:

$$\mathscr{H}_0(\xi,p) = -p_x.v + \frac{5.\rho_0.S.v^2.C_d}{m}.p_v + T_{\max}.\left(\max(\Psi(\xi,p),0) + \min(\Psi(\xi,p),0).\eta\right)$$

where $\Psi(\xi,p) = 100.C_s.p_m - \frac{p_v}{m}(1+100.C_s.v)$.

4.2.3 Spatial grid

We consider the following time & space domain:

Variable	$t(das)$	$x(km)$	$v(hm/s)$	$m(hkg)$
min	0.0	-2.0	1.0	3.0
max	4.0	10.0	4.0	6.5

We used the $150 \times 120 \times 35$ nodes grid to discretize the spatial domain. This example was solved by exploiting the HJB-solver *ROC HJ* (refer to [1]) on a standard desktop computer. We use the finite difference scheme combined with Essentially Non Oscillatory (ENO) approximation and the Lax-Friedrichs numerical Hamiltonian.

The computation time of the value function is around 250 sec. We remind that the time consuming part of the simulation is the value function computation. Once this step finished, the reachable sets and optimum trajectories are obtained almost instantenously by postprocessing the value.

4.2.4 Reachable sets

In our example, the initial state is a parallelepiped in the state space defined by:

$$\psi(\phi) := \max(|x-x_a| - dx_a, |v-v_a| - dv_a) \tag{4.12}$$

where $(x_a,v_a) = (0.0,3.0)$ and $(dx_a,dv_a) = (0.25,0.05)$. On the following figure, we present the slice of the reachable sets for $m(0) = 6.0$. The sets are calculated from T = 0 das up to T = 3 das by step of 1 das.

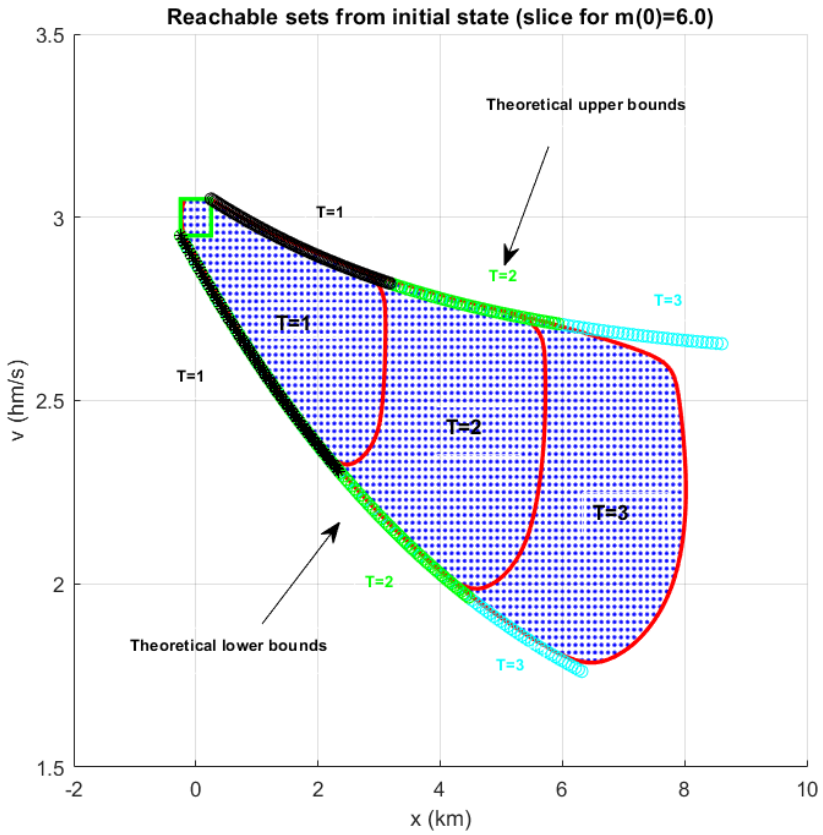

Figure 4.2: Reachable sets

In this particular case, it is possible to calculate analytically the theoretical lateral envelope. The numerical computation is coherent up to $T = 30sec$. For greater time horizons, the sets are in general underestimated which is likely due to the rising difficulty to efficiently propagate the negative level sets of the value function when the time horizon increases.

4.2.5 Minimum time trajectories

The target is a parallelepiped in the state space defined by:

$$\psi(\phi) := \max(|x - x_t| - dx_t, |v - v_t| - dv_t) \tag{4.13}$$

where $(x_t, v_t) = (7.25, 2.3)$ and $(dx_t, dv_t) = (0.25, 0.05)$. On the following figure, we give three examples of minimum time trajectories starting respectively from $\bar{\phi}_1(0) = (0.0, 3.0, 4.5)$ and $\bar{\phi}_2(0) = (1.0, 2.3, 6.0)$ and $\bar{\phi}_3(0) = (1.0, 1.5, 5.25)$. We use the Ultra Bee scheme combined with the Lax-Friedrichs numerical Hamiltonian on the *ROC-HJ* software. On the following figures the HJB and direct method (AMPL & IPOPT) approaches are displayed.

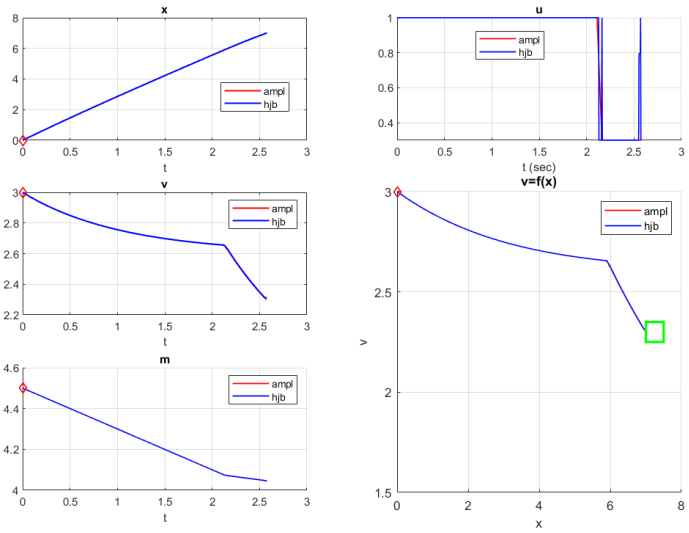

(a) Case 1

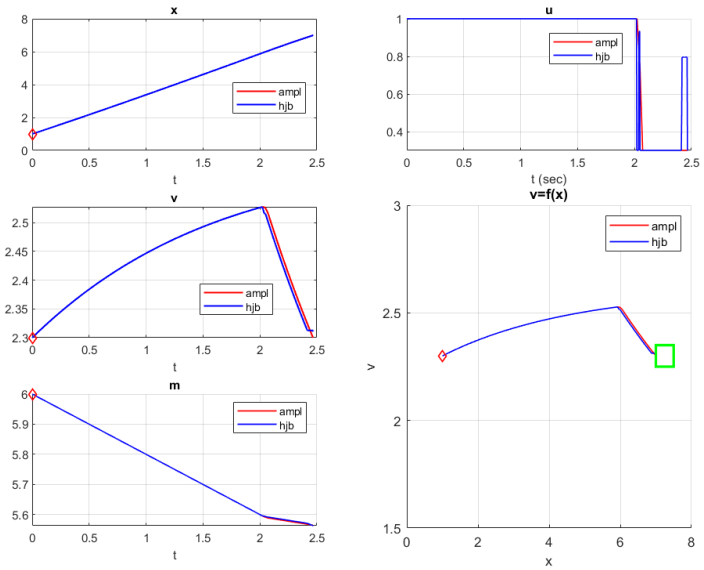

(b) Case 2

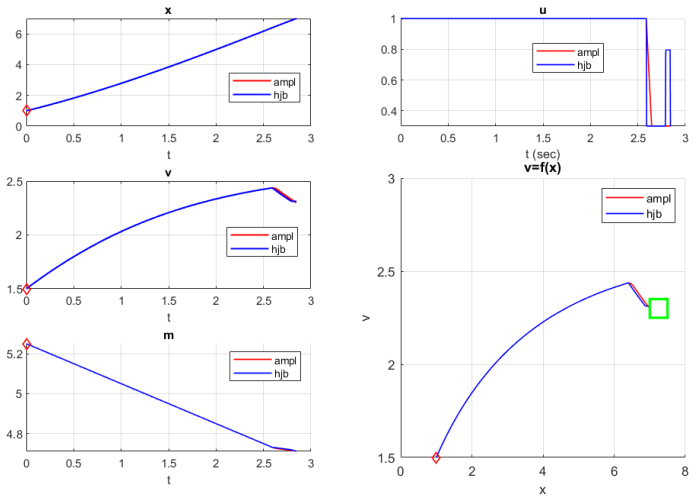

(c) Case 3

Based on the above examples, there is a satisfactory coherence between the two approaches. However, the accuracy of the control computation is likely better with the direct method.

4.3 HJB approach for optimal control problems with state constraints

4.3.1 Motivation

The optimal control problem (3.1)-(3.2)-(3.3) is actually not general enough to describe problems arising from real life and particularly from aeronautics. More specifically, it could be necessary to add constraints which involve control-state (mixed constraints) and/or state variables (pure state constraints) to the formulation. When this happens, the necessary conditions coming from the PMP presented previously must be carefully adapted.

The main difference with respect to the classical case is that the adjoint vector provided by PMP may not be an absolutely continuous function. Indeed, in presence of state constraints, the adjoint vector p may exhibit discontinuities. Moreover, a serious difficulty arises, that is, no knowledge concerning the evolution of the additional multipliers is provided, making impossible the integration of the new adjoint equations without further information. There exist several versions of PMP in this case ([7], [20] for instance).

In the light of what precedes, it is easily understood that adapting numerical methods such as shooting or multi-shooting algorithms becomes complicated when considering state constraints. For all these reasons, we will not tackle the constrained state case using the PMP, but using the HJB approach which offers a suitable framework.

As we have already motivated and introduced the HJB framework in the section 4.1.3, this section can be understood as a generalisation with a general cost in the Bolza form in presence of pure state constraints.

4.3.2 Mathematical setting

Consider the following optimal control problem with pure state constraints that is:

$$\begin{cases} \min\limits_{(t,\alpha)} \ \mathrm{J}(t,\mu,\alpha) \\ \dot{\xi}(s) = f(\xi(s),\alpha(s)) \quad \forall s \in [0,t] \\ \alpha(\cdot) \in \mathscr{A} \\ \xi(0) = \mu \\ \xi(s) \in \mathscr{K} \quad \text{for } s \in [0,t] \\ \xi(t) \in \mathscr{C} \end{cases} \tag{4.14}$$

where $\mathscr{A}$ is the set defined in section 3.1 and

$$\forall t \in [0,\mathrm{T}],\ \mathrm{J}(t,\mu,\alpha) := \int_0^t f^0(\xi(s),\alpha(s))ds + g(\xi(t)) \tag{4.15}$$

$\mathscr{K}$ and $\mathscr{C}$ are non empty closed subsets of $\mathbb{R}^n$. We denote by $\xi_\mu^\alpha(\cdot)$ the trajectory of the dynamical system starting from μ, associated to the control $\alpha(\cdot)$.

Hereafter we give the assumptions required in the HJB framework: we highlight that some of them are slightly weakened with respect to the ones presented in section 3.1.

4.3.3 Assumptions

We make the following assumptions:

$(\mathscr{H}_1)$: $f : \mathbb{R}^n \times \mathrm{A} \to \mathbb{R}^n$ is continuous. There exists $\mathrm{L}_f > 0$ such that for every $\alpha \in \mathscr{A}$:

$$\|f(\xi_1,\alpha) - f(\xi_2,\alpha)\| \leqslant \mathrm{L}_f.\|\xi_1 - \xi_2\|,\ \forall \xi_1,\xi_2 \text{ s.t. } \xi_1,\xi_2 \in \mathbb{R}^n \tag{4.16}$$

Moreover, $\exists c_f > 0 \mid \forall \mu \in \mathbb{R}^n,\ \max\{\|f(\mu,\alpha)\|, \alpha \in \mathscr{A}\} \leqslant c_f.(1+\|\mu\|)$.
$(\mathscr{H}_2)$: $f^0 : \mathbb{R}^n \times \mathrm{A} \to \mathbb{R}$ is continuous. Moreover, f^0 is Lipschitz continuous on the state variable uniformly with respect to the control:

$$\exists \mathrm{L}_0 > 0 \text{ s.t. } |f^0(\mu,a) - f^0(\mu',a)| \leqslant \mathrm{L}_0.|\mu-\mu'|, \forall \mu,\mu' \in \mathbb{R}^n,\ \forall a \in \mathrm{A} \tag{4.17}$$

$(\mathscr{H}_3)$: $g : \mathbb{R}^n \to \mathbb{R}$ is Lipschitz continuous:

$$\exists \mathrm{L}_g > 0 \text{ s.t. } |g(\mu) - g(\mu')| \leqslant \mathrm{L}_g.|\mu-\mu'|, \forall \mu,\mu' \in \mathbb{R}^n \tag{4.18}$$

$(\mathscr{H}_4)$: for any $\mu \in \mathbb{R}^n$, the set V defined by:

$$\mathrm{V}(\mu) := \left\{ \left(f^0(\mu,a) + \gamma, f(\mu,a) \right) \mid a \in \mathrm{A},\ \gamma \geqslant 0 \right\} \tag{4.19}$$

is a convex subset of $\mathbb{R}^n \times \mathbb{R}^m$.

4.3.4 General considerations and notations

For technical convienance, we denote:

$$\mathscr{P}_{t,\mu} := \left\{ (\xi,\alpha) : \dot{\xi}(s) = f(\xi(s),\alpha(s)), \text{ for } s \in [0,t];\ \xi(0) = \mu \right\} \tag{4.20a}$$

$$\mathscr{P}_{t,\mu}^{\mathscr{K},\mathscr{C}} := \{ (\xi,\alpha) \in \mathscr{P}_{t,\mu} : \xi(s) \in \mathscr{K} \text{ for } s \in [0,t],\ \xi(t) \in \mathscr{C} \} \tag{4.20b}$$

Under $(\mathscr{H}_1)$, $\mathscr{P}_{t,\mu}$ is a non empty set, while $\mathscr{P}_{t,\mu}^{\mathscr{K},\mathscr{C}}$ may be empty if there is no admissible control input that keeps the trajectory in the set $\mathscr{K}$ and reaches the target $\mathscr{C}$ at the final time t.

In the same way than in section 4.1.3, we introduce the "level set" functions $r : \mathbb{R}^n \to \mathbb{R}$ and $\psi : \mathbb{R}^n \to \mathbb{R}$ both Lipschitz continuous characterizing the sets of constraints as follows:

$$\mu \in \mathscr{K} \Leftrightarrow r(\mu) \leqslant 0, \quad \mu \in \mathscr{C} \Leftrightarrow \psi(\mu) \leqslant 0 \tag{4.21}$$

These functions exist as $\mathscr{K}$ and $\mathscr{C}$ are closed by assumption. For instance, if one denotes by $d_{\mathscr{K}}$ the signed distance to $\mathscr{K}$ ($d_{\mathscr{K}}(\mu) = d(\mu,\mathscr{K})$ if $\mu \notin \mathscr{K}$ and $d_{\mathscr{K}}(\mu) = -d(\mu,\mathbb{R}^n \backslash \mathscr{K})$ otherwise), then the function $r \equiv d_{\mathrm{K}}(\cdot)$ is Lipschitz continuous and satisfies (4.21).

Let us now fix an upper bound time horizon $\mathrm{T} > 0$ and introduce the value functions $u : [0,\mathrm{T}] \times \mathbb{R}^n \longrightarrow \overline{\mathbb{R}}$ such that:

$$u(t,\mu) := \inf \left\{ \mathrm{J}(t,\mu,\alpha),\ (\xi,\alpha) \in \mathscr{P}_{t,\mu}^{\mathscr{K},\mathscr{C}} \right\} \tag{4.22}$$

and $u_{\mathrm{T}} : \mathbb{R}^n \longrightarrow \overline{\mathbb{R}}$ such that:

$$u_{\mathrm{T}}(\mu) := \inf \left\{ \mathrm{J}(t,\mu,\alpha),\ (\xi,\alpha) \in \mathscr{P}_{t,\mu}^{\mathscr{K},\mathscr{C}},\ t \in [0,\mathrm{T}] \right\} \tag{4.23}$$

with the convention $\inf \varnothing = +\infty$ (indeed u and u_{T} can take unbounded values for instance if there's no admissible trajectory).

The main idea in what follows is to characterize u_{T} by introducing an auxiliary value function free of state constraints that is the unique solution of an HJB equation to be precised.

4.3.5 Time variable change

Before considering the state constraints, we turn the free final time problem (4.14) into a fixed final time problem. Let us operate the classical variable change: $t = \int_0^{\mathrm{T}} \lambda(\tau) d\tau$, with $\lambda(\cdot) \in \Lambda$, Λ being the space of measurable functions from $[0,\mathrm{T}]$ to $[0,1]$.

We introduce the following sets:

$$\widehat{\mathscr{P}}_{t,\mu} := \left\{(\xi,\alpha,\lambda) \mid \dot{\xi}(s) = \lambda(s) f(\xi(s),\alpha(s)),\ \text{for a.e } s\in[0,t],\ \xi(0)=\mu\right\}$$
$$\widehat{\mathscr{P}}^{\mathscr{K},\mathscr{C}}_{t,\mu} := \left\{(\xi,\alpha,\lambda) \mid (\xi,\alpha,\lambda)\in\widehat{\mathscr{P}}_{t,\mu},\ \xi(s)\in\mathscr{K} \text{ for } s\in[0,t],\ \xi(t)\in\mathscr{C}\right\}$$

Let us define the modified cost functional:

$$\forall t\in[0,\mathrm{T}],\ \widehat{\mathrm{J}}(t,\mu,\alpha,\lambda) := \int_0^t \lambda(s) f^0(\xi(s),\alpha(s))ds + g(\xi(t)) \tag{4.25}$$

and the value function:

$$v(\mathrm{T},\mu) := \inf\left\{\widehat{\mathrm{J}}(\mathrm{T},\mu,\alpha,\lambda) \;\middle|\; (\xi,\alpha,\lambda)\in\widehat{\mathscr{P}}^{\mathscr{K},\mathscr{C}}_{\mathrm{T},\mu}\right\} \tag{4.26}$$

Actually, the fixed final time problem (4.26) is in some sense equivalent to the free end time problem (4.23):

Proposition 4.3.5.1 $\forall\mu\in\mathscr{K},\ v(\mathrm{T},\mu) = u_{\mathrm{T}}(\mu)$.

Proof: Step 1 $v(\mathrm{T},\mu)\leqslant u_{\mathrm{T}}(\mu)$:

From (4.23), $\exists t^\star\in[0,\mathrm{T}]$, $\exists\alpha^\star:[0,t^\star]\to$ A such that $u_{\mathrm{T}}(\mu) = \mathrm{J}(t^\star,\mu,\alpha^\star)$, with $\xi^{\alpha^\star}_\mu(s)\in\mathscr{K}$ for $s\in[0,t^\star]$ and $\xi^{\alpha^\star}_\mu(t^\star)\in\mathscr{C}$. Let us define:

$$\lambda^\star(s) = \begin{cases} 1 \text{ if } s\in[0,t^\star] \\ 0 \text{ if } s\in[t^\star,\mathrm{T}] \end{cases}$$

We extend now (in a arbitrary way) the control $\alpha^\star(\cdot)$ over $[t^\star,\mathrm{T}]$ and the associated trajectory $\xi^{\alpha^\star}_\mu(\cdot)$ such that $\xi^{\alpha^\star}_\mu(s) = \xi^{\alpha^\star}_\mu(t^\star)$ for $s\in[t^\star,\mathrm{T}]$. Denoting by $(\xi^\star,\alpha^\star,\lambda^\star)$ the triple defined in such a way, it easy to check that $(\xi^\star,\alpha^\star,\lambda^\star)\in\widehat{\mathscr{P}}^{\mathscr{K},\mathscr{C}}_{\mathrm{T},\mu}$.
Moreover, one remarks that $\widehat{\mathrm{J}}(\mathrm{T},\mu,\alpha^\star,\lambda^\star) = u_{\mathrm{T}}(\mu)\geqslant v(\mathrm{T},\mu)$.

Step 2 $v(\mathrm{T},\mu)\geqslant u_{\mathrm{T}}(\mu)$:

From (4.26), $\exists\,(\xi^\star,\alpha^\star,\lambda^\star)\in\widehat{\mathscr{P}}^{\mathscr{K},\mathscr{C}}_{\mathrm{T},\mu}$ such that $v(\mathrm{T},\mu) = \widehat{\mathrm{J}}(\mathrm{T},\mu,\alpha^\star,\lambda^\star)$.
Let us denote $\mathrm{S} := \{s\in[0,\mathrm{T}] : \lambda^\star(s)\neq 0\}$, $\tau_0 = \displaystyle\int_0^{\mathrm{T}}\lambda^\star(s)ds = \int_{\mathrm{S}}\lambda^\star(s)ds$.
We define the change of variable $\sigma : s\to[0,\tau_0],\ \sigma : s\mapsto\tau = \displaystyle\int_0^s\lambda^\star(\theta)d\theta$.
If one defines $\widetilde{\xi}(\tau) := \xi^\star(\sigma^{-1}(s))$, $\widetilde{\alpha}(\tau) := \alpha^\star(\sigma^{-1}(s))$ then it is easy to see that $(\widetilde{\xi},\widetilde{\alpha})$ are defined on $[0,\tau_0]$ and satisfy:

$$\begin{cases} \dot{\widetilde{\xi}}(\tau) = f(\widetilde{\xi}(\tau),\widetilde{\alpha}(\tau)),\ \tau\in(0,\tau_0) \\ \widetilde{\alpha}\in\mathscr{A},\ \widetilde{\xi}(\theta)\in\mathscr{K},\ \forall\theta\in[0,\tau_0] \\ \widetilde{\xi}(0) = \xi^\star(0) = \mu,\ \widetilde{\xi}(\tau_0) = \xi^\star(\mathrm{T})\in\mathscr{C} \end{cases} \tag{4.27}$$

Moreover, one has:

$$\mathrm{J}(\tau_0,\mu,\widetilde{\alpha}) = \int_0^{\tau_0} f^0(\widetilde{\xi}(s),\widetilde{\alpha}(s))ds + g(\widetilde{\xi}(\tau_0)) \tag{4.28}$$
$$= \int_0^{\mathrm{T}}\lambda^\star(t)f^0(\xi^\star(t),\alpha^\star(t))dt + g(\xi^\star(\mathrm{T})) \tag{4.29}$$
$$= \widehat{\mathrm{J}}(\mathrm{T},\mu,\alpha^\star,\lambda^\star) = v(\mathrm{T},\mu) \tag{4.30}$$

which implies the desired inequality from the definition of u_{T}. □

4.3.6 State constrained case

We introduce the augmented dynamical system satisfying:

$$\begin{cases} \dot{\xi}(s) = \lambda(s) f(\xi(s), \alpha(s)) \ \forall s \in [0,t] \\ \dot{z}(s) = -\lambda(s) f^0(\xi(s), \alpha(s)) \ \forall s \in [0,t] \\ \alpha \in \mathscr{A}, \ \lambda \in \Lambda \\ \xi(0) = \mu, \ z(0) = \eta \end{cases} \tag{4.31}$$

A solution of (4.31) for a control law double (α, λ) will be denoted $\left(\xi_{t,\mu}^{\alpha,\lambda}(\cdot), z_{t,\eta}^{\alpha,\lambda}(\cdot)\right)$. The set of all admissible trajectories will be denoted by:

$$\widehat{\mathrm{S}}_{[0,t]}(\mu,\eta) := \left\{ \left(\xi_{t,\mu}^{\alpha,\lambda}(\cdot), z_{t,\eta}^{\alpha,\lambda}(\cdot)\right) \text{ satisfying (4.31) on } [0,t], (\alpha,\lambda) \in \mathscr{A} \times \Lambda \right\} \tag{4.32}$$

We recall that under $(\mathscr{H}_1) - (\mathscr{H}_4)$, $\widehat{\mathrm{S}}_{[0,t]}(\mu,\eta)$ is a compact subset of $\mathrm{W}^{1,1}([0,t];\mathbb{R}^n \times \mathbb{R})$ endowed with the C^0-topology.
Consider the augmented value function $\widehat{w} : [0,\mathrm{T}] \times \mathbb{R}^n \times \mathbb{R} \longrightarrow \mathbb{R}$:

$$\widehat{w}(\tau,\mu,\eta) = \inf_{(\xi,z) \in \widehat{\mathrm{S}}_{[0,\tau]}(\mu,\eta)} \left\{ (g(\xi(\tau)) - z(\tau)) \vee \sup_{\theta \in [0,\tau]} r(\xi(\theta)) \vee \psi(\xi(\tau)) \right\} \tag{4.33}$$

where $a \vee b = \max(a,b)$.
In the auxiliary value function (4.33), the term $\sup_{\theta \in [0,\tau]} r(\xi(\theta))$ is an exact penalization of the state constraints, the term $\psi(\xi(\tau))$ is penalizing the final time constraint (target).
Before concluding this section, we would like to stress on the fact that considering the auxiliary function $\widehat{w}$ allows to bypass all the regularity issues which arise when the control problem is in presence of state constraints. The proofs that follow are borrowed from [3].

Proposition 4.3.6.1 (Characterization of the epigraph of u_T) *:*
Assume $(\mathscr{H}_1)$-$(\mathscr{H}_4)$, then $\forall \mu \in \mathbb{R}^n$, $\forall \nu \in \mathbb{R}$, the following holds:

$$u_\mathrm{T}(\mu) \leqslant \nu \iff \widehat{w}(\mathrm{T},\mu,\nu) \leqslant 0 \tag{4.34a}$$

$$u_\mathrm{T}(\mu) = \nu^*(\mu) = \min\{\nu \in \mathbb{R} \mid \widehat{w}(\mathrm{T},\mu,\nu) \leqslant 0\} \tag{4.34b}$$

Proof: . Let us prove (4.34a): $\widehat{\mathrm{S}}_{[0,\mathrm{T}]}(\mu,\nu)$ being a compact set in $\mathrm{C}^0([0,t])$, $\widehat{w}(\mathrm{T},\mu,\nu) \leqslant 0$ implies that $\exists (\widehat{\xi},\widehat{z}) \in \widehat{\mathrm{S}}_{[0,\mathrm{T}]}(\mu,\nu)$ such that:

$$\widehat{w}(\mathrm{T},\mu,\nu) = \left(g(\widehat{\xi}(\mathrm{T})) - \widehat{z}(\mathrm{T})\right) \vee \sup_{\theta \in [0,\mathrm{T}]} r(\widehat{\xi}(\theta)) \vee \psi(\widehat{\xi}(\mathrm{T})) \tag{4.35}$$

which implies the negativity of the three terms of $\widehat{w}$. On the one hand, $\theta \in [0,\mathrm{T}]$, $\widehat{\xi}(\theta) \in \mathscr{K}$, $\widehat{\xi}(\mathrm{T}) \in \mathscr{C}$, and on the other hand:

$$u_\mathrm{T}(\mu) = v(\mathrm{T},\mu) \leqslant \int_0^\mathrm{T} \widehat{\lambda}(s) f^0(\widehat{\xi}(s), \widehat{\alpha}(s)) ds + g(\widehat{\xi}(\mathrm{T})) \leqslant \nu$$

Conversely, let us assume that $v(\mathrm{T},\mu) \leqslant \nu < +\infty$, then there exists a sequence of admissible triple $(\xi_n, \alpha_n, \lambda_n) \in \widehat{\mathscr{P}}_{\mathrm{T},\mu}$ such that:

$$\lim_{n \to +\infty} \int_0^\mathrm{T} \lambda_n(s).f^0(\xi_n(s), \alpha_n(s)) ds + g(\xi_n(\mathrm{T})) - \nu = v(\mathrm{T},\mu) - \nu \leqslant 0$$

The trajectories $\xi_n(\cdot)$ being admissible, one has $\sup_{\theta \in [0,\tau]} r(\xi_n(\theta)) \leqslant 0$ and $\psi(\xi_n(\mathrm{T})) \leqslant 0$. Finally we obtain:

$$\begin{aligned} \widehat{w}(\mathrm{T},\mu,\nu) &\leqslant \liminf_{n \to +\infty} \left(\widehat{\mathrm{J}}(\mathrm{T},\mu,\alpha_n,\lambda_n) - \nu\right) \vee \sup_{\theta \in [0,\tau]} r(\xi_n(\theta)) \vee \psi(\xi_n(\mathrm{T})) \\ &\leqslant 0 \end{aligned}$$

The proof of (4.34b) is the consequence of (4.34a) □.

Proposition 4.3.6.2 (Dynamic Programming Principle)
Under the assumptions $(\mathscr{H}_1)-(\mathscr{H}_4)$, $\widehat{w}$ *is locally Lipschitz continuous function on* $[0,\mathrm{T}]\times\mathbb{R}^n\times\mathbb{R}$ *and for any* $\tau\in[0,t[$ *the following holds:*

$$\widehat{w}(t,\mu,\eta)=\inf_{(\xi,z)\in\mathrm{S}_{[0,\tau]}(\mu,\eta)}\left(\widehat{w}\left(t-\tau,\xi(\tau),z(\tau)\right)\vee\sup_{\theta\in[0,\tau]}r(\xi(\theta))\right) \tag{4.37}$$

Proof: Let us denote $\mathscr{U}:=\mathscr{A}\times\Lambda$ and decompose $u\in\mathscr{U}_{[0,t]}=(u_1,u_2)$ with $u_1\in\mathscr{U}_{[0,\tau]}$ and $u_2\in\mathscr{U}_{[\tau,t]}$. Using the semigroup property: $\forall s\geqslant h,\ \xi_\mu^u(s)=\xi_{\xi_\mu^{u_1}(h)}^{u_2}(s-h)$, we obtain:

$$\begin{aligned}\widehat{w}(t,\mu,\eta)&=\inf_{u\in\mathscr{U}_{[0,t]}}\left(\left(g(\xi_\mu^u(t))-z_\eta^u(t)\right)\vee\sup_{\theta\in[0,t]}r(\xi_\mu^u(\theta))\vee\psi(\xi_\mu^u(t))\right)\\&=\inf_{u_1\in\mathscr{U}_{[0,\tau]}}\left(\widehat{w}(t-\tau,\xi_\mu^{u_1}(\tau),z_\eta^{u_1}(\tau))\vee\sup_{\theta\in[0,\tau]}r(\xi_\mu^u(\theta))\right)\end{aligned}$$

which proves the result. ▫

Proposition 4.3.6.3 (Hamilton Jacobi Bellman Equation)
Under the assumptions $(\mathscr{H}_1)-(\mathscr{H}_4)$, $\widehat{w}$ *is the unique viscosity continuous solution of the following HJB equation:*

$$\min\left(\partial_t\widehat{w}+\mathscr{H}(\mu,\mathrm{D}_\mu\widehat{w},\partial_\eta\widehat{w}),\widehat{w}(t,\mu,\eta)-r(\mu)\right)=0,\ t\in(0,\mathrm{T}] \tag{4.38a}$$

$$w(0,\mu,\eta)=(g(\mu)-\eta)\vee r(\mu)\vee\psi(\mu),\ \mu\in\mathbb{R}^n,\ \eta\in\mathbb{R} \tag{4.38b}$$

the Hamiltonian $\mathscr{H}(\mu,p,q)=\max\left(0,\sup_{a\in\mathrm{A}}(-f(\mu,a).p+f^0(\mu,a).q)\right)$.

Proof: Please refer to A.6.

4.3.7 A particular case: the target capture bassin

The capture bassin of the target $\mathscr{C}$ before the time $\mathrm{T}>0$, denoted by $\mathrm{C}apt_{\mathscr{C}}(\mathrm{T})$, is the subset of all initial positions from which it is possible to find an admissible trajectory that reaches $\mathscr{C}$ before the time T while lying in the set $\mathscr{K}$. It can be written mathematically as follows:

$$\mathrm{C}apt_{\mathscr{C}}(\mathrm{T})=\left\{\mu\in\mathscr{K}\ \middle|\ \exists\,\tau\in[0,\mathrm{T}],\exists\,(\xi,\alpha)\in\mathscr{P}_{\tau,\mu}^{\mathscr{K},\mathscr{C}}\right\}. \tag{4.39}$$

Under the notations of previous section, let us set $f^0\equiv 0$ and define the terminal cost g as the characteristic function of the target $\mathscr{C}$ that is: $\forall\mu\in\mathscr{C}\iff g(\mu)\leqslant 0$.

Now, we define a particular value function $\nu_\mathrm{T}:\mathbb{R}^n\longrightarrow\mathbb{R}$ such that:

$$\nu_\mathrm{T}(\mu)=\inf\left\{g(\xi(t))\ \middle|\ (\xi,\alpha)\in\mathscr{P}_{t,\mu}^{\mathscr{K},\mathscr{C}},\ t\in[0,\mathrm{T}]\right\} \tag{4.40}$$

We have the two following results:

$$\mu\in\mathrm{C}apt_{\mathscr{C}}(\mathrm{T})\iff\nu_\mathrm{T}(\mu)\leqslant 0 \tag{4.41a}$$

$$\nu_\mathrm{T}(\mu)\leqslant 0\iff\widehat{w}(\mathrm{T},\mu,0)\leqslant 0 \tag{4.41b}$$

where the function $\widehat{w}$ is the unique viscosity solution of (4.38) where the running cost $f^0\equiv 0$ and without the terminal state constraint function $\psi(\cdot)$.

Moreover, if there are no the state constraints (i.e $\mathscr{K}=\mathbb{R}^n$), the obtained HJB equation is the same than (4.8) associated to the Hamiltonian (4.9).

Consequently, the HJB equation (4.38) can be seen as a generalization of the one associated to the minimum time case studied in the section 4.1.3.

4.3.8 Optimal trajectories reconstruction from the value function

The trajectory reconstruction algorithms are well known by now and are available for instance in [45], [24] or [56].

4.3.9 Numerical scheme

The Hamilton Jacobi equation (4.38) can be numerically approximated by using the finite difference schemes (refer to the work of Crandall and Lions, [59]). In our case, we consider a slightly more precise scheme, an ENO scheme of second order (for details, refer to [60]).

For given positive mesh step h, $\Delta\xi = (\Delta\xi_i)_{1\leqslant i\leqslant n}$ and Δz, for a given multi-index $i = (i_1,...,i_n)$, let $\xi_i := \xi_{\min} + i.\Delta\xi \equiv (\xi_{k,\min} + i_k.\Delta\xi_k)_{1\leqslant k\leqslant n}$, $z_j = z_{\min} + j.\Delta z$ and $t_p = p.h$. Let us define the following grid of $\mathcal{K}\times[z_{\min}, z_{\max}]$:

$$\mathcal{G} := \{(\xi_i, z_j) \;\; i\in\mathbb{N}^n, \;\; j\in\mathbb{N}, \;\; (\xi_i, z_j)\in\mathcal{K}\times[z_{\min}, z_{\max}]\}$$

Let us denote $v^p_{i,j}$ an approximation of the solution $v(t_p,\xi_i,z_j)$.

Given $\mathscr{H}_{num} : \mathbb{R}^n\times\mathbb{R}^n\times\mathbb{R}^n \longrightarrow \mathbb{R}$, suitable numerical approximation of $\mathscr{H}$ involved in (4.38) (see the remark below), the following scheme is considered, as in [4]. First it is initialized with:

$$v^1_{i,j} = (g(\xi_i) - z_j)\vee r(\xi_i)\vee\psi(\xi_i) \tag{4.42}$$

Then for $p\in\{2,3,...,N-1\}$, $v^{p+1}_{i,j}$ is computed recursively as follows:

$$v^{p+1}_{i,j} = \max\left(v^p_{i,j} - \Delta t.\mathscr{H}_{num}\left(\xi_i, D^- v^p_{i,j}, D^+ v^p_{i,j}\right), r(\xi_i)\right), \;\; (\xi_i, z_j)\in\mathscr{G} \tag{4.43}$$

The scheme is equivalent to the following:

$$\min\left(\frac{v^{p+1}_{i,j} - v^p_{i,j}}{\Delta t} + \mathscr{H}_{num}\left(\xi_i, D^- v^p_{i,j}, D^+ v^p_{i,j}\right), v^{p+1}_{i,j} - r(\xi_i)\right) = 0 \tag{4.44}$$

The monotone finite difference approximation is obtained using $D^\pm v^p_{i,j} = (D^\pm_k v^p_{i_k,j})_{1\leqslant k\leqslant n}$ and:

$$D^\pm_k v^p_{i_k,j} = \pm\frac{v^p_{i_k\pm1,j} - v^p_{i_k,j}}{\Delta\xi_k}$$

The second order ENO scheme is used to estimate the terms $D^\pm_k v^p_{i_k,j}$.

4.4 An application: optimisation of a glider trajectory

4.4.1 Setting

We consider hereafter a maximum range problem for a glider flying in the vertical plane. The glider is considered as a mass particle moving in the atmosphere. Usually released from an aircraft at a given altitude and speed, the vehicle uses its aerodynamic surfaces in order to maximize the horizontal range. By doing so, some constraints shall be respected:

- the vehicle airspeed shall remain greater than a critical value $v_{\min}$ in order to minimize the risk of aerodynamic stall.
- the flight altitude shall remain greater than a minimal value $h_{\min}$.
- the final flight path angle shall remain lower than a given value γ_f.

The above mentioned flight conditions are mandatory in order to permit the pursue of the mission.

The dynamics is identical to (2.13) where the thrust is null (thus $T_{max} = 0$ and $\dot{m} = 0$). The lift coefficient remains the unique control denoted by α. We highlight that in this setting we conserved the induced drag-to-lift coefficient $k_c = 0.05$.

After variable normalization, the considered dynamics reads:

$$\dot{\bar{x}} = 0.1\,\bar{v}\cos\bar{\gamma} \tag{4.45a}$$

$$\dot{\bar{h}} = 0.1.\bar{v}\sin\bar{\gamma} \tag{4.45b}$$

$$\dot{\bar{v}} = \frac{-\mathrm{D}(1000\bar{h}, 10\bar{v}, \alpha)}{100m} - g.\sin\bar{\gamma} \tag{4.45c}$$

$$\dot{\bar{\gamma}} = \frac{\mathrm{L}(1000\bar{h}, 10\bar{v}, \alpha)}{100\bar{m}\bar{v}} - \frac{g\cos\bar{\gamma}}{\bar{v}} \tag{4.45d}$$

where: $\bar{t} := \dfrac{t}{10}$, $\bar{x} := \dfrac{x}{1000}$, $\bar{h} := \dfrac{h}{1000}$, $\bar{v} := \dfrac{v}{10}$, $\bar{\gamma} := \gamma$ and $\bar{m} := \dfrac{m}{100}$.

4.4.2 HJB equation

Consider the set of state constraints $\mathscr{K} := \{\bar{\xi} \in \mathbb{R}^4 \mid r(\bar{\xi}) \leqslant 0\}$, with:

$$r(\bar{\xi}) := \max\left(\bar{h}_{\min} - \bar{h}, \bar{v}_{\min} - \bar{v}\right)$$

where $\bar{h}_{\min} = \dfrac{h_{\min}}{1000} = 2$ and $\bar{v}_{\min} = \dfrac{v_{\min}}{100} = 22.5$. This set is representative of the permanent state constraints underwent by the glider.

The final flight path angle constraint plays the role of the target $\mathscr{C}$ and is represented by the function $\psi(\bar{\xi}) := \bar{\gamma} - \bar{\gamma}_f$, where $\bar{\gamma}_f = \gamma_f = -\dfrac{\pi}{6}$.

Under the notations of this section, the optimal control problem to be minimized can be written as follows:

$$u_{\mathrm{T}}(\mu) := \inf\left\{-\bar{x}(t),\ (\bar{\xi}, \alpha) \in \mathscr{P}_{t,\mu}^{\mathscr{K},\mathscr{C}},\ t \in [0, \mathrm{T}]\right\} \tag{4.46}$$

where $\mathrm{T} > 0$ is a fixed upper bound time horizon.

Actually, we are in the framework of the section 4.3.6 where $f^0(\mu, \alpha) \equiv 0$, $g(\mu) \equiv -\bar{x}$, the PDE to solve is given by (4.38) where the Hamiltonian is

$$\mathscr{H}(\mu, p, q) = \max(0, \sup_{a \in \mathrm{A}}(-f(\mu, a).p + \underbrace{f^0(\mu, a)}_{=0}.q)) \tag{4.47}$$

$$= \max(0, \mathscr{H}_0(\mu, p)) \tag{4.48}$$

where $\mathscr{H}_0(\mu, p) = \sup_{|a| \leqslant \alpha_m} (-f(\mu, a).p)$.

An explicit computation leads to:

$$\mathscr{H}_0(\mu, p) = -0.1\,p_{\bar{x}}\,\bar{v}\cos\bar{\gamma} - 0.1\,p_{\bar{h}}\,\bar{v}\sin\bar{\gamma} + p_{\bar{v}}\,g\sin\bar{\gamma} + \frac{p_{\bar{\gamma}}}{\bar{v}}\,g\cos\bar{\gamma}$$
$$+ \frac{p_{\bar{v}}}{100\bar{m}}\,\bar{q}.\mathrm{S}\mathrm{C}_d + \frac{\bar{q}.\mathrm{S}}{100\bar{m}} \max_{|a| \leqslant \alpha_m} \left(p_{\bar{v}}\,k_{cz}\,a^2 - \frac{p_{\bar{\gamma}}}{\bar{v}}\,a\right)$$

where $\bar{q} = \bar{q}(1000\bar{h}, 10\bar{v})$. The Hamiltonian being a quadratic function of the control, it reaches its maximum for $a \in \{-\alpha_m,\ \bar{a},\ \alpha_m\}$, where $\bar{a} := \dfrac{p_{\bar{\gamma}}}{2.k_{cz}.\bar{v}.p_{\bar{v}}}$

4.4.3 Numerical Hamiltonian

Let us define:

$$\mathscr{H}_a^{num}(\mu, p^-, p^+) := \sum_{i=1}^{n} \left(\max(-f_i(\mu, a), 0).p_i^- + \min(-f_i(\mu, a), 0).p_i^+ \right)$$

where $(f_i)_{1 \leqslant i \leqslant 4}$ are the components of the dynamics f.
If we define the numerical Hamiltonian $\mathscr{H}_0^{num}$ as:

$$\mathscr{H}_0^{num}(\mu, p^-, p^+) := \max\left(\mathscr{H}_{-\alpha_m}^{num}(\mu, p^-, p^+), \mathscr{H}_{\bar{a}}^{num}(\mu, p^-, p^+), \mathscr{H}_{\alpha_m}^{num}(\mu, p^-, p^+)\right)$$

then it satisfies the following properties:

- Lipschitz continuous on all its arguments
- consistent with $\mathscr{H}_0$ (ie $\mathscr{H}_0^{num}(\mu, p, p) = \mathscr{H}_0(\mu, p)$).
- monotone (ie $\dfrac{\partial \mathscr{H}_0^{num}}{\partial p_k^-}(\mu, p^-, p^+) \geqslant 0$ and $\dfrac{\partial \mathscr{H}_0^{num}}{\partial p_k^+}(\mu, p^-, p^+) \leqslant 0$)

Moreover, if the following Courant Friedrich Lax (CFL) is satisfied:

$$\Delta t. \sum_{i=1}^{n} \frac{1}{\Delta \xi_i} \left(\left| \frac{\partial \mathscr{H}_0^{num}}{\partial p_k^-} \right| + \left| \frac{\partial \mathscr{H}_0^{num}}{\partial p_k^+} \right| \right) \leqslant 1 \tag{4.49}$$

then it has been shown ([4]) that the numerical scheme defined in section 4.3.9 converges to the desired solution.

4.4.4 Computation domain and numerical results

We consider the following time & space domain:

Variable	$\bar{t}(ds)$	$\bar{x}(km)$	$\bar{h}(km)$	$\bar{v}(hm/s)$	$\bar{\gamma}(rad)$	$\bar{z}(km)$
min	0.0	-2.0	1.0	10.0	$-\pi/2$	-15.0
max	6.0	15.0	8.0	40.0	$\pi/2$	0.0

We used the $51 \times 28 \times 30 \times 36 \times 15$ nodes grid to discretize the spatial domain. This example was solved by exploiting the HJB-solver *ROC HJ* on a standard desktop computer.

The value is finally recovered by using $u_T(\mu) = \min(\nu \mid \widehat{w}(T, \mu, \nu) \leqslant 0)$ and the trajectories are reconstructed from the value function.

We give hereafter two optimal trajectories for the following initial conditions:

- Case 1: $(x_0, h_0, v_0, \gamma_0) = (0m, 5000m, 350m/s, 0)$
- Case 2: $(x_0, h_0, v_0, \gamma_0) = (0m, 3500m, 375m/s, \pi/6)$

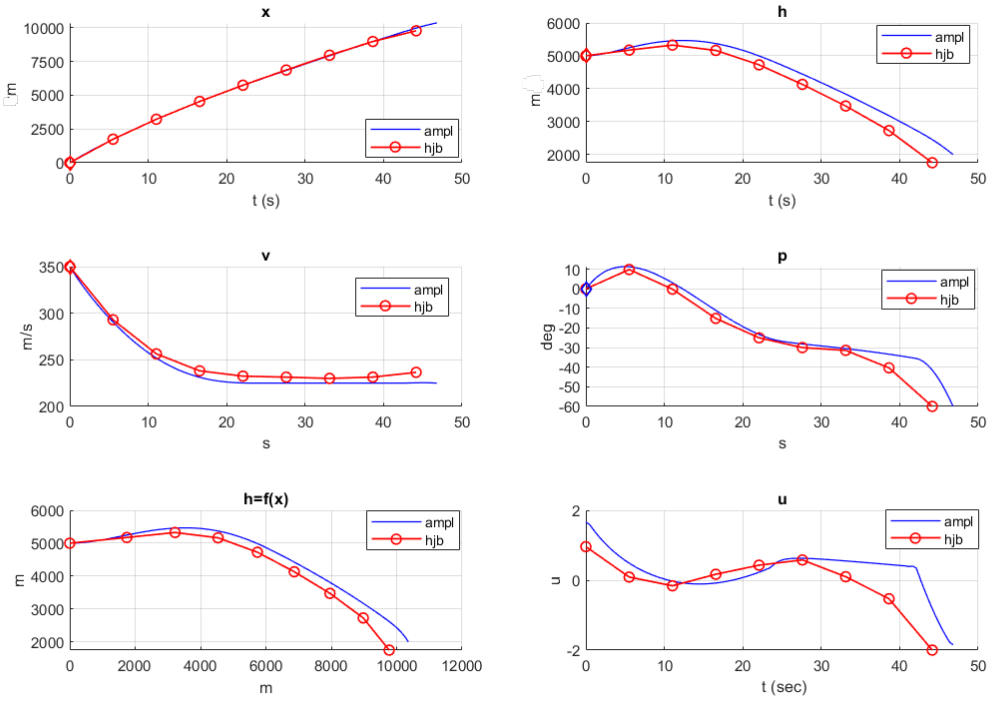

Figure 4.4: Glider range optimisation: case 1

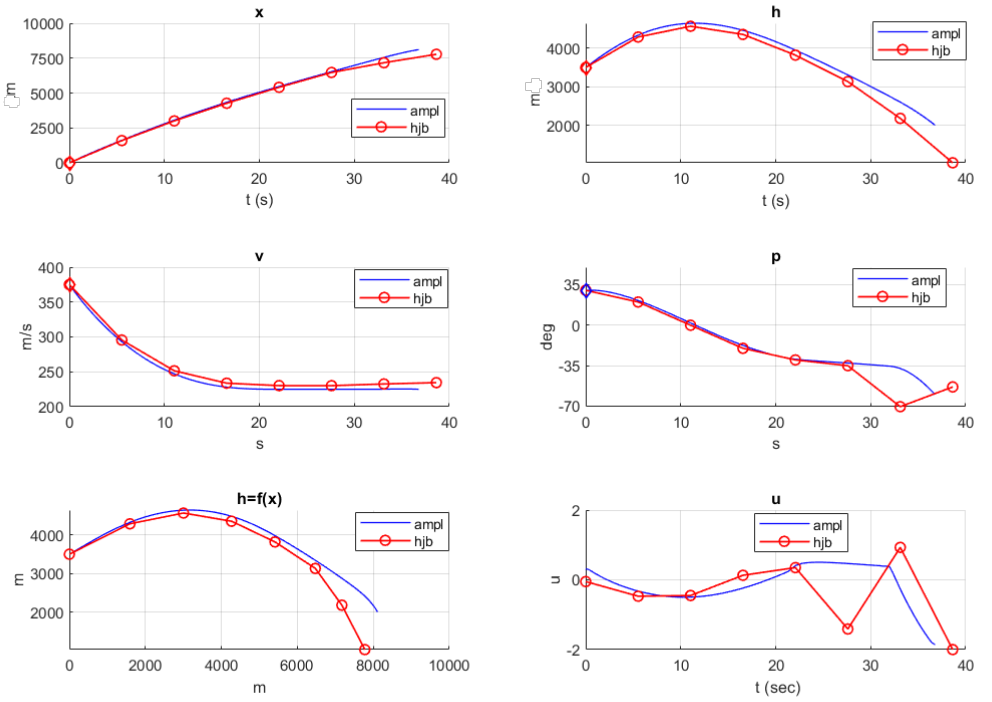

Figure 4.5: Glider range optimisation: case 2

4.4.5 Comments

We remark a global coherence between the direct method (AMPL & IPOPT) and HJB approach results. As commented before, the HJB approach lacks accuracy as soon as the spatial domain is wide. A more precise results could likely be obtained with finer grids but the counterpart would be an increase of the computation time.

We highlight here that, unlike the shooting method, the HJB approach does not require any prior knowledge of the optimal trajectory structure. Actually, it could be advantageously exploited in order to initialize the shooting method (for instance, see [26]).

Conclusion and perspectives

Contributions: this work was divided into two main parts: the first part was dedicated to the study of the asymptotic behavior in large time of the value function associated to an optimal control problem. In the second part, we studied numerical methods in optimal control with a focus on the shooting method combined with numerical continuations in order to solve the bunt problem.

In the first part of this thesis, we actually established two results, the second one being a generalization of the first one.

Large-time expansion of the value function in the LQ case: under the Kalman condition and using only basic results of LQ theory, we established a two-terms large-time expansion of $\frac{1}{T}v(T,.)$ in $1/T$ (as $T \longrightarrow +\infty$), T being the time horizon. The term of order zero is the minimal value of the associated static optimization problem. The term of order one includes the sum of two optimal costs of infinite time stabilization problems forward and backward in time. The originality is that all the terms of the expansion have been explicitly calculated as functions of the solutions of the Riccati algebric equation, initial/final states and the Lagrange multiplier of the static optimization problem.

Large-time expansion of the value function for dissipative nonlinear systems: assuming the strict dissipativity property and the uniqueness of the solution of the static optimization problem, we established a similar result as above. The term of order zero is identical to the LQ case. The term at order one is a sum of optimal costs of the infinite time problems with a shifted Lagrange cost forward and backward in time.

In the second part, our general objective was to evaluate exact numerical methods applied to a benchmark problem in the field of aerial vehicle guidance. To this end, we have established the physical model of the vehicle dynamics (dimension 5), and we have formulated the optimal control problem to be solved. The originality of the approach was to reduce the original problem to a simpler one in dimension 3, namely the Dubins-Fuller problem. Then, we studied the optimal synthesis of this reduced problem which is actually a weighted interpolation between two problems: the Dubins and the Fuller problem. Our contributions were the following:

Analysis and numerical solving of the reduced problem: by implementing the shooting method combined with continuations.

Analysis and numerical solving of the initial problem: by implementing continuations on the dynamics and the boundary conditions in order to "connect" the reduced problem with the original one.

In the last chapter, we evaluated numerically the HJB approach on two simplified problems. After recalling the theoretical background, we performed the following tasks:

Computation of reachable sets and time optimum trajectories: for a model of a propelled aerial vehicle in dimension 3.

Computation of range maximizing trajectories: for a model of a glider (non propelled aerial vehicle) in dimension 4 and in presence of pure state constraints.

Perspectives: Various aspects of this work raise subjects that are open or interesting to study. We list some of them hereafter, in a non exhaustive way, and we start with the ones related to the value function expansion:

1. The large-time expansion of the value function in the LQ case and infinite dimensional case has been established. An article related to this subject is currently in preparation and will be published in a dedicated paper.

2. Despite numerous works in the literature ([86], [15]) the strict dissipativity still remains, from our point of view, a "theoretical" notion and it would be interesting to "illustrate" it by, for instance, exhibiting nontrivial examples of nonlinear dynamical systems enjoying this property.

3. It would be interesting to establish the large-time expansion of the value function for nonlinear dynamical systems in presence of several turnpikes and/or state constraints.

Concerning the numerical part of our work, we mention hereafter some perspectives:

1. The potential improvement of the representativeness of the vehicle model. Indeed, as mentioned in chapter 2, the dynamical model could be enhanced in various ways, amongst which the following:

   - The dependencies on the Mach number and altitude could be modelled in the aerodynamic coefficients C_D, C_L and the thrust T.
   - The flight domain could be introduced: usually, it corresponds to a specified range of Mach number and altitude within which the vehicle can fly. From the optimal control point of view, it would introduce mixed and/or pure state constraints.
   - Generally, more representative model of the motion could be implemented by taking into account the moment equation of the Newton's law. The counterpart would be the increase of state variables.

2. Related to the numerical implementation in Python language, the associated computation time is not satisfactory. It could be significantly reduced by implementing the indirect method in compiled langages such as Fortran or C.

3. Another interesting perspective would be to couple the HJB approach with the shooting method in order to compute a solution to a more complex version of the optimal control problem, possibly including state constraints: in this case, one could first estimate the optimal structure of the solution on a reduced model by using HJB approach. Then, this information could be advantageously exploited to implement accurate solution on the full model by using the shooting method, combined with continuations.

Appendix A

Appendix

A.1 Some useful results

Proposition A.1.0.1 *: The LQ system* (1.11) *is strictly dissipative with respect to w and the storage function is* $S(r) := \langle \bar{\lambda}, r \rangle$.

Proof: Let us consider:

$$\mathscr{L}(y,u,\lambda) := \langle \lambda, f(y,u) \rangle + \lambda_0 f^0(y,u) \tag{A.1}$$

the Lagrangian associated to the steady optimisation problem, where we assume $\lambda_0 = -1$ as stated before. In the linear quadratic case one has:

$$\nabla^2_{(y,u)} \mathscr{L}(y,u,\bar{\lambda}) = \begin{bmatrix} -Q & 0 \\ 0 & -U \end{bmatrix}$$

remembering that $\nabla_{(y,u)} \mathscr{L}(\bar{y},\bar{u},\bar{\lambda}) = 0$, this implies:

$$\mathscr{L}(y,u,\lambda) = \mathscr{L}(\bar{y},\bar{u},\bar{\lambda}) - \frac{1}{2}\left(\|y-\bar{y}\|^2_Q + \|u-\bar{u}\|^2_U \right) \tag{A.2}$$

as $A\bar{y} + B\bar{u} = 0$ the latter leads to:

$$w(y,u) - \langle \bar{\lambda}, Ay + Bu \rangle = \frac{1}{2}\left(\|y-\bar{y}\|^2_Q + \|u-\bar{u}\|^2_U \right) \tag{A.3}$$

Q and U being symmetric positive definite matrices, there exists $\rho > 0$ such that:

$$\|y-\bar{y}\|^2_Q + \|u-\bar{u}\|^2_U \geqslant \rho \left\| \begin{array}{c} y-\bar{y} \\ u-\bar{u} \end{array} \right\|^2 \tag{A.4}$$

By injecting (A.4) in (A.3) and integrating with respect to the time t over $[0,T]$, one finally obtains:

$$\int_0^T w(y(t),u(t))dt + \langle \bar{\lambda}, x \rangle \geqslant \langle \bar{\lambda}, z \rangle + \int_0^T \alpha\left(\left\| \begin{array}{c} y(t)-\bar{y} \\ u(t)-\bar{u} \end{array} \right\| \right) dt$$

which is the strict dissipativity inequality with $S(r) := \langle \bar{\lambda}, r \rangle$ and $\alpha(x) := \frac{\rho}{2}\|x\|^2$ □.

Lemma A.1.0.1 (Barbalat's lemma) *Assume that* $f : [0,+\infty) \longrightarrow \mathbb{R}$ *is uniformly continuous and* $\lim_{t\to+\infty} \int_0^t f(\tau)d\tau$ *exists and is finite, then* $\lim_{t\to+\infty} f(t) = 0$.

Proof: A proof can be found for instance in [47]. By contradiction, take $\epsilon > 0$ and assume that $f(t)$ does not converge to 0 as $t \to +\infty$. In this case, there exists an increasing sequence $(t_n)_{n\in\mathbb{N}}$ in $\mathbb{R}^+$

such that $|f(t_n)| > \epsilon$. By the uniform continuity of f there exists $\delta > 0$ such that, for any $n \in \mathbb{N}$, and any $t \in \mathbb{R}$

$$|t - t_n| \leqslant \delta \Longrightarrow |f(t) - f(t_n)| \leqslant \frac{\epsilon}{2}.$$

So for any $t \in [t_n, t_n + \delta]$ and any $n \in \mathbb{N}$, one has

$$|f(t)| = |f(t_n) - (f(t_n) - f(t))| \geqslant |f(t_n)| - |f(t_n) - f(t)| \geqslant \frac{\epsilon}{2}.$$

Therefore,

$$\left| \int_0^{t_n+\delta} f(t)dt - \int_0^{t_n} f(t)dt \right| = \left| \int_{t_n}^{t_n+\delta} f(t)dt \right| = \int_{t_n}^{t_n+\delta} |f(t)|dt \geqslant \frac{\delta.\epsilon}{2}.$$

the latter inequality contradicts the convergence of $\int_0^t f(\tau)d\tau$ as $t \to +\infty$ and the lemma follows. □.

Lemma A.1.0.2 *The optimal trajectory of* $(\mathscr{P}_{0,T}^{\bar{y},\bar{y}})$ *is such that for any* $t \in [0,T]$, $y(t) = \bar{y}$ *and* $u(t) = \bar{u}$.

Proof: From the dissipativity property, for any admissible couple $(y(\cdot), u(\cdot))$ such that $y(0) = y(T) = \bar{y}$, we have

$$\int_0^T w(y(t), u(t))dt \geqslant 0. \tag{A.5}$$

The particular admissible solution $(\widehat{u}(\cdot), \widehat{y}(\cdot)) \equiv (\bar{u}, \bar{y})$ zeroes the above cost, thus this is an optimal solution and it is unique by assumption. □.

Lemma A.1.0.3 *The optimal couple* $(\widehat{y}_{\infty f}(\cdot), \widehat{u}_{\infty f}(\cdot))$ *of* $(\mathscr{P}_{\infty f}^{\bar{y}})$ *is such that for any* $t \geqslant 0$, $\widehat{y}_{\infty f}(t) = \bar{y}$ *and* $\widehat{u}_{\infty f}(t) = \bar{u}$. *Consequently* $v_f(\bar{y}) = 0$.

Proof: Consider the value function $v_f(\cdot)$ defined by (1.58). From the assumptions, all the admissible trajectories and controls are bounded and f & f^0 are C^1, thus from the mean value inequality, we conclude that f and w are globally Lipschitz continuous in the state and control. Moreover, the cost w remains bounded. These observations ensure the boundedness and the continuity of v_f (see [56], Chapter 3, Proposition 2.1).

The DPP implies:

$$v_f(\bar{y}) = \int_0^t w(\widehat{y}_{\infty f}(s), \widehat{u}_{\infty f}(s))ds + v_f(\widehat{y}_{\infty f}(t)), \quad \forall t \geqslant 0 \tag{A.6}$$

If we let $t \to +\infty$ in the above equality, from the continuity of $v_f(\cdot)$ and the fact that $\widehat{y}_{\infty f}(t) \longrightarrow \bar{y}$ as $t \to +\infty$ (see lemma 1.3.5.2), we deduce that $\int_0^{+\infty} w(\widehat{y}_{\infty f}(t), \widehat{u}_{\infty f}(t))ds = 0$. As the "steady" couple $(y(t), u(t)) \equiv (\bar{y}, \bar{u})$ zeroes the infinite time cost, from the uniqueness argument we conclude that $(\widehat{y}_{\infty f}(t), \widehat{u}_{\infty f}(t)) \equiv (\bar{y}, \bar{u})$.

Corollary A.1.0.1 *: The lemma A.1.0.3 remains true for the infinite backward-in-time problem* $(\mathscr{P}_{\infty b}^{\bar{y}})$. *Consequently* $v_b(\bar{y}) = 0$.

A.2 On the need of viscosity solutions in the HJB framework

Consider the 1-D scalar system for $t \in [0,T]$:

$$\dot{y}(s) = \alpha(s) \in A := [-1,1] \qquad \forall s \in [t,T] \tag{A.7a}$$
$$y(t) = x \tag{A.7b}$$

and the functional $J(t,x,\alpha) = \exp\left(-(y^{\alpha}_{t,x}(T))^2\right)$. Defining $\mathscr{A} := L^{\infty}([0,T],A)$, the value function $v(t,x) = \inf_{\alpha \in \mathscr{A}} J(t,x,\alpha)$ can be analytically calculated and is given by:

$$\forall (x,t) \in \mathbb{R} \times [0,T] \quad v(t,x) = \exp\left(-(T-t+|x|)^2\right)$$

It can be easily checked that for any $x \in \mathbb{R}$ where v is the differentiable, it the solution of the HJB equation:

$$-\frac{\partial v}{\partial t}(t,x) + |\nabla_x v(t,x)| = 0 \quad \forall t \in [0,T] \tag{A.8}$$

Actually, v is a classical solution of (A.8) for $x \neq 0$ but cannot be defined as such for $x = 0$ as it is not differentiable at this point. Therefore (A.8) has no classical meaning at $x = 0$.

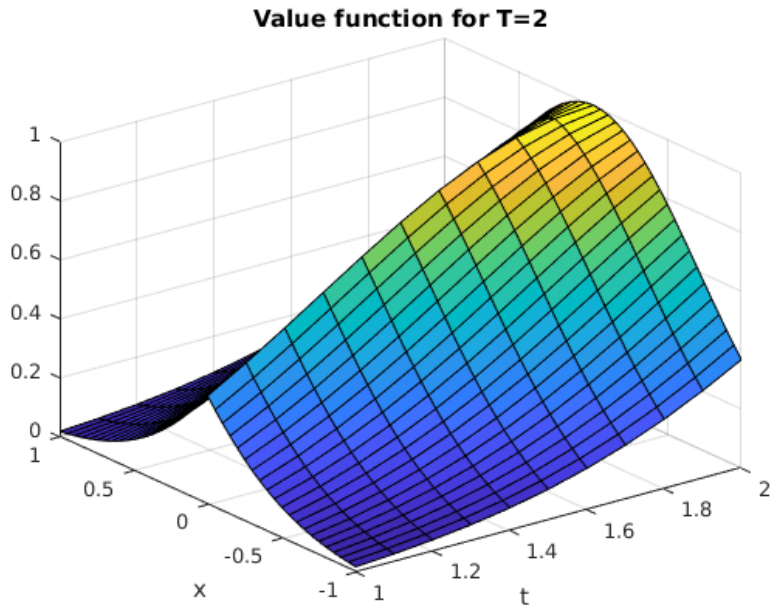

Figure A.1: Value function

To overcome the problem of defining not differentiable solutions for the HJB equations, Kruzkow introduced in the 60 the idea of generalized solutions, i.e. solutions which satisfies the equation almost everywhere. This is a powerful idea and a lot of results have been obtained under different set of assumptions (for a complete description see [52] and references therein). However we can easily build equations in the framework of optimal control problems where we have a lack of uniqueness and stability for the generalized solution. For instance, consider the the following HJB equation in dimension 1 with prescribed boundary conditions:

$$|u'(x)| - 1 = 0 \text{ for } x \in [-1,1] \tag{A.9a}$$
$$u(-1) = u(1) = 0 \tag{A.9b}$$

Actually, this PDE admits infinitely many piecewise affine (slope ± 1) generalized solutions, as illustrated hereafter:

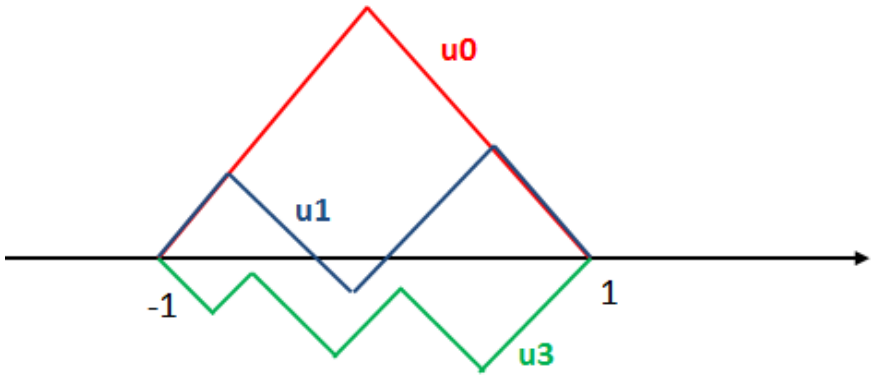

Figure A.2: Non uniqueness of lipschitzian solutions

The main point of the viscosity theory is to select among all the generalized solutions the "correct one" from the optimal control theory point of view, which will ensure the stability and uniqueness properties.

A.3 Computation of the Jacobian of the shooting function

We precise the principle of the computation of the Jacobian of the shooting function (3.51) along the continuation path. As explained before, if one has $\alpha = \alpha(\mu, p)$ then the extremal system arising from the PMP equations can be written as:

$$z(t) = \mathrm{F}(z(t)) \tag{A.10}$$
$$z(0) = z_0 \tag{A.11}$$

where $z(t) = (\mu(t), p(t))$ is the optimal state-costate couple associated to the initial condition $z(0) = (\mu_0, p_0)$.

In the Dubins-Fuller case, $d\mathrm{S}$ can be expressed as follows:

$$d\mathrm{S} = \begin{pmatrix} \frac{\partial x(t_f)}{\partial p_x(0)} & \frac{\partial x(t_f)}{\partial p_h(0)} & \frac{\partial x(t_f)}{\partial p_\gamma(0)} & \frac{\partial x(t_f)}{\partial t_f} \\ \frac{\partial h(t_f)}{\partial p_x(0)} & \frac{\partial h(t_f)}{\partial p_h(0)} & \frac{\partial h(t_f)}{\partial p_\gamma(0)} & \frac{\partial h(t_f)}{\partial t_f} \\ \frac{\partial \gamma(t_f)}{\partial p_x(0)} & \frac{\partial \gamma(t_f)}{\partial p_h(0)} & \frac{\partial \gamma(t_f)}{\partial p_\gamma(0)} & \frac{\partial \gamma(t_f)}{\partial t_f} \\ \frac{\partial \mathrm{H}(t_f)}{\partial p_x(0)} & \frac{\partial \mathrm{H}(t_f)}{\partial p_h(0)} & \frac{\partial \mathrm{H}(t_f)}{\partial p_\gamma(0)} & \frac{\partial \mathrm{H}(t_f)}{\partial t_f} \end{pmatrix}$$

To estimate the components of $\frac{\partial \mathrm{S}}{\partial p(0)}$ involving the state variables, one has to numerically compute the Jacobi fields $\delta z_i(\cdot) := (\delta\mu_i(\cdot), \delta p_i(\cdot))$ along the optimal extremal $z(t)$ which are solutions of the following variational system:

$$\dot{\delta z_i}(t) = \mathrm{DF}(z(t)).\delta z_i(t) \tag{A.12}$$
$$\delta z_i(0) = (\delta\mu_i(0), \delta p_i(0)) \tag{A.13}$$

where $(\delta\mu_i(0), \delta p_i(0)) = (0,0,0,..e_i,...0)$ with $(e_i)_{1\leqslant i\leqslant 3}$ representing the canonical basis of $\mathbb{R}^3$. Then the $\frac{\partial \mathrm{S}}{\partial p(0)}$ is the concatenation the required state components of $\delta z_i(t_f)$.

The component of $\frac{\partial S}{\partial p(0)}$ involving the Hamiltonian is given by $\frac{\partial H(t_f)}{\partial p(0)} = \frac{\partial H(0)}{\partial p(0)} = F(z(0))$.

Finally, to compute $\frac{\partial S}{\partial t_f}$, its suffices to remark that $\frac{dz(t_f)}{dt_f} = F(z(t_f))$ and that from the fact that $H(t_f) = cst = H(0)$ one gets $\frac{H(t_f)}{dt_f} = 0$.

We give hereafter the details of the expressions of $F(\cdot)$ and $DF(\cdot)$.

$$F := \begin{pmatrix} F_1 & F_2 & \dots & F_6 \end{pmatrix}^\intercal \tag{A.14}$$

where:

$$\begin{aligned} F_1 &= v.\cos\gamma \\ F_2 &= v.\sin\gamma \\ F_3 &= \frac{p_\gamma}{2.k_2} \\ F_4 &= 0.0 \\ F_5 &= \frac{2.(h-h_c)}{h_c^2} \\ F_6 &= v.(p_x.\sin(\gamma) - p_h.\cos(\gamma)) \end{aligned}$$

The terms of the matrix $DF := \left(\frac{\partial F_i}{\partial z_j}\right)_{i,j\in[1,6]^2}$ are detailed hereafter:

$$\begin{aligned} &\frac{\partial F_1}{\partial x} = \frac{\partial F_2}{\partial x} = \dots = \frac{\partial F_6}{\partial x} = 0 \\ &\frac{\partial F_1}{\partial h} = \frac{\partial F_2}{\partial h} = \dots = \frac{\partial F_4}{\partial h} = 0 = \frac{\partial F_6}{\partial h},\ \frac{\partial F_5}{\partial h} = \frac{2}{h_c^2} \\ &\frac{\partial F_1}{\partial \gamma} = -v.\sin\gamma,\ \frac{\partial F_2}{\partial \gamma} = v.\cos\gamma,\ \frac{\partial F_3}{\partial \gamma} = \frac{\partial F_4}{\partial \gamma} = \frac{\partial F_5}{\partial \gamma} = 0,\ \frac{\partial F_6}{\partial \gamma} = v.(p_x.\cos\gamma + p_h.\sin\gamma) \\ &\frac{\partial F_1}{\partial p_x} = \frac{\partial F_2}{\partial p_x} = \dots = \frac{\partial F_5}{\partial p_x} = 0,\ \frac{\partial F_6}{\partial p_x} = v.\sin\gamma \\ &\frac{\partial F_1}{\partial p_h} = \frac{\partial F_2}{\partial p_h} = \dots = \frac{\partial F_5}{\partial p_h} = 0,\ \frac{\partial F_6}{\partial p_h} = -v.\cos\gamma \\ &\frac{\partial F_1}{\partial p_\gamma} = \frac{\partial F_2}{\partial p_\gamma} = 0\ \ \frac{\partial F_3}{\partial p_\gamma} = \frac{1}{2.k_2},\ \frac{\partial F_4}{\partial p_\gamma} = \frac{\partial F_5}{\partial p_\gamma} = \frac{\partial F_6}{\partial p_\gamma} = 0 \end{aligned}$$

A.4 Solving DF with multiple shooting

The optimal solution of the DF is presented on the figure below (coloured rounds on the control correspond to the nodes):

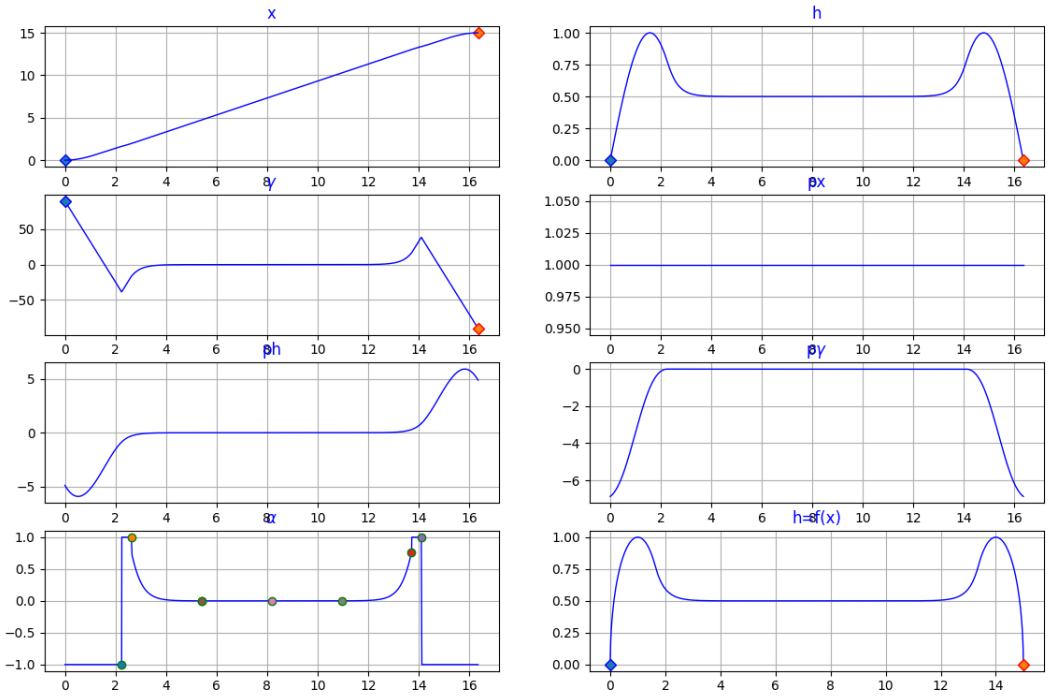

Figure A.3: Multiple shooting for the Dubins-Fuller problem

The following table provides the accuracy of the shooting:

Shooting output	Value
$\lvert x(t_f) - x_f \rvert$	3.10^{-15}
$\lvert h(t_f) - h_f \rvert$	3.10^{-16}
$\lvert \gamma(t_f) - \gamma_f \rvert$	2.10^{-14}

A.5 Guidance problem with the control in dimension 2

In this section, we propose to solve the initial optimal control problem with the cost (3.63) in the case where the thrust control $\alpha_1(\cdot)$ is active ($\alpha_2(.)$ already being active). Clearly speaking, the dynamics involves now a additional control as specified in (2.21). As explained previously, we prescribe the final value of the speed $v(t_f) = v_f$.

The Hamiltonian associated to the missile dynamics with the control in dimension 2 is now given by:

$$\begin{aligned} \mathrm{H} &:= \langle p, f(\xi,\alpha)\rangle + p^0.f^0(\xi,\alpha) \\ &= p_x.v.\cos\gamma + p_h.v.\sin\gamma + p_v.\left(\frac{\mathrm{T_{max}}.(1+\mathrm{C}_s.v)\,\alpha_1 - \mathrm{D}(h,v)}{m} - g\sin\gamma\right) \\ &\quad + \frac{p_\gamma}{v}\left(\frac{\mathrm{L}(h,v,\alpha_2)}{m} - g.\cos\gamma\right) - \mathrm{C}_s.\mathrm{T_{max}}.p_m.\alpha_1 + p^0.\left(k_0 + k_1.\left(\frac{h-h_c}{h_c}\right)^2 + k_2.\alpha_2^2\right) \end{aligned}$$

Assuming that $p^0 = -1$, the adjoint equations are, after arrangement:

$$\dot{p}_x = 0 \tag{A.15a}$$

$$\dot{p}_h = \frac{p_v}{m}.\frac{\partial \mathrm{D}}{\partial h}(h,v) - \frac{p_\gamma}{m.v}\frac{\partial \mathrm{L}}{\partial h}(h,v,\alpha_2) + \frac{2.k_1}{h_c^2}(h-h_c) \tag{A.15b}$$

$$\dot{p}_v = -p_x.\cos\gamma - p_h.\sin\gamma - \frac{p_v}{m}.\mathrm{C}_s.\mathrm{T_{max}}.\alpha_1 + \frac{p_v}{m}\frac{\partial \mathrm{D}}{\partial v}(h,v) - \frac{p_\gamma}{m}.\frac{\partial(\mathrm{L}/v)}{\partial v} - \frac{p_\gamma}{v^2}.g.\cos\gamma \tag{A.15c}$$

$$\dot{p}_\gamma = p_x.v.\sin\gamma - p_h.v.\cos\gamma + p_v.g\cos\gamma - \frac{p_\gamma}{v}g.\sin\gamma \tag{A.15d}$$

$$\dot{p}_m = \frac{p_v}{m^2}\left(\mathrm{T_{max}}.(1+\mathrm{C}_s.v).\alpha_1 - \mathrm{D}(h,v)\right) + \frac{p_\gamma}{v.m^2}.\mathrm{L}(h,v,\alpha_2) \tag{A.15e}$$

As the two controls are uncoupled, the optimal control $\alpha_2(\cdot)$ is still given by (3.65)-(3.66), whereas $\alpha_1(\cdot)$ reads:

$$\alpha_1 \in \underset{r\in[\eta,1]}{\arg\max}\ \Theta(t).r \tag{A.16}$$

where the switching function $\Theta(\cdot)$ is given by:

$$\Theta(t) = \mathrm{T_{max}}.\left(\frac{p_v.(1+\mathrm{C}_s.v)}{m} - \mathrm{C}_s.p_m\right) \tag{A.17}$$

The adjoint transversality conditions (3.11) now reduce to:

$$p_m(t_f) = 0 \tag{A.18}$$

while (3.12) still leads to:

$$\forall t \in [0,t_f],\ \ \mathrm{H}(\xi(t),p(t),-1,\alpha(t)) = 0 \tag{A.19}$$

As explained before, as the Hamiltonian is linear with respect to α_1, one requires the knowledge of the structure of the the latter prior to the implementation of the shooting method. However within the range of initial and final conditions, we infer that the thrust control structure is of bang max-bang min nature (we confirm it by running some direct method simulations).

We set the new boundary conditions:

$$(x_0,h_0,v_0,\gamma_0,m_0) = (0\mathrm{m},0\mathrm{m},250\mathrm{m/s},45^\circ,500\mathrm{kg}) \tag{A.20a}$$

$$(x_f,h_f,v_f,\gamma_f,m_f) = (15000\mathrm{m},0\mathrm{m},250\mathrm{m/s},-45^\circ,*) \tag{A.20b}$$

We solve numerically the problem by implementing the standard shooting method combined to the continuation over the boundary conditions. We set $k_0 = k_1 = 1$ and $k_2 = 2$. The samples of the optimal trajectory and control and the final optimal solution are displayed hereafter:

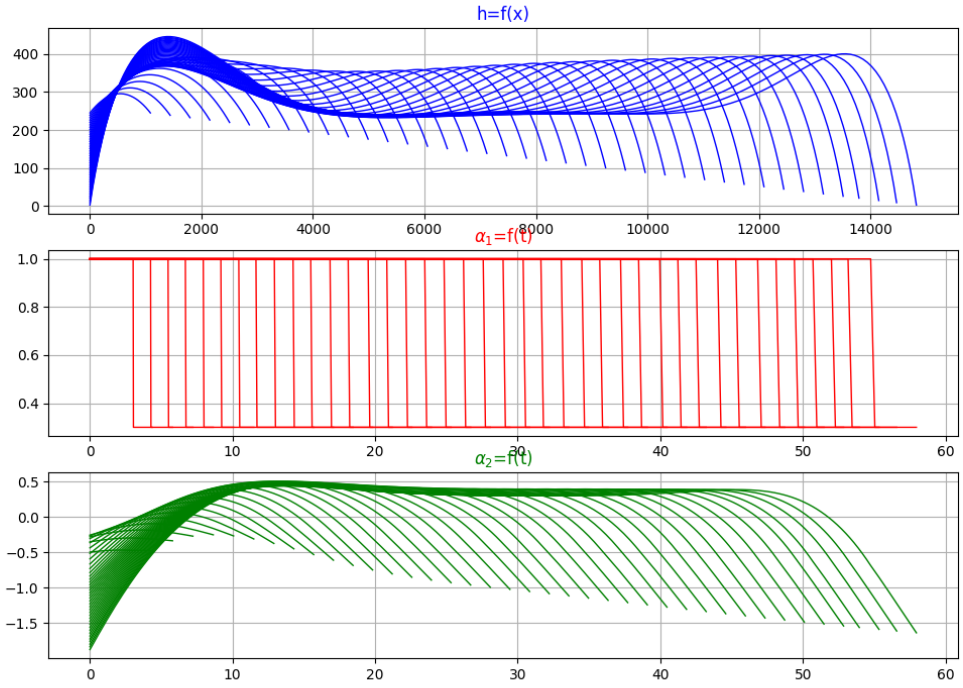

Figure A.4: Samples of optimal state & control (continuation)

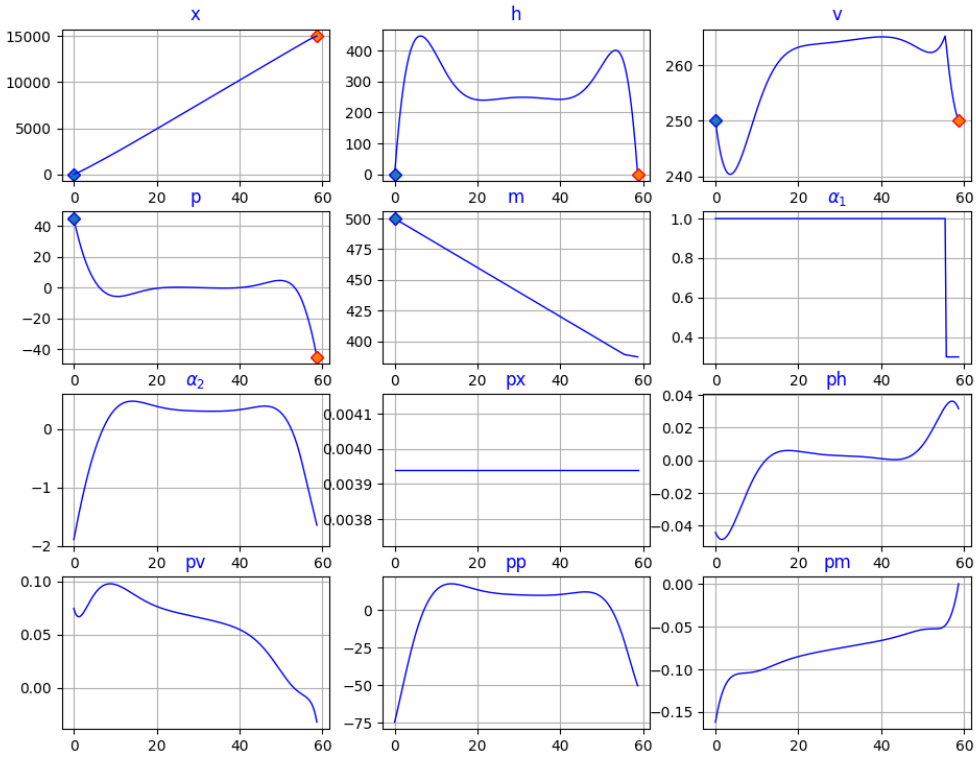

Figure A.5: Final optimal state, costate & control

The following table provides the final accuracy of the shooting:

Shooting output	**Value**
$\lvert x(t_f) - x_f \rvert$	10^{-6}
$\lvert h(t_f) - h_f \rvert$	10^{-6}
$\lvert v(t_f) - v_f \rvert$	10^{-7}
$\lvert \gamma(t_f) - \gamma_f \rvert$	10^{-7}
$p_m(t_f)$	10^{-10}
$\mathrm{H}(t_f)$	10^{-6}

Table A.1: Final shooting accuracy with the control in dimension 2

A.6 Existence, regularity and uniqueness of the solution to the HJB equation

In this section we prove the results of the proposition 4.3.6.3.

A.6.1 Definition

We recall the definition of the viscosity solution for HJB equation with obstacle term (4.38). Let $V:[0,T]\times\mathbb{R}^n\times\mathbb{R}\longrightarrow\mathbb{R}$ be a continuous function and $(t_0,\mu_0,\eta_0)\in(0,T)\times\mathbb{R}^n\times\mathbb{R}$.

1. V is a viscosity supersolution if for any $\phi\in C^1([0,T]\times\mathbb{R}^n\times\mathbb{R})$ such that $V-\phi$ attains a local minimum on (t_0,μ_0,η_0), we have

$$\min\left(\frac{\partial\phi}{\partial t}(t_0,\mu_0,\eta_0)+\mathscr{H}(\mu_0,D_\mu\phi(t_0,\mu_0,\eta_0),D_\eta\phi(t_0,\mu_0,\eta_0))\right)\geqslant 0$$

2. V is a viscosity subsolution if for any $\phi\in C^1([0,T]\times\mathbb{R}^n\times\mathbb{R})$ such that $V-\phi$ attains a local maximum on (t_0,μ_0,η_0), we have

$$\min\left(\frac{\partial\phi}{\partial t}(t_0,\mu_0,\eta_0)+\mathscr{H}(\mu_0,D_\mu\phi(t_0,\mu_0,\eta_0),D_\eta\phi(t_0,\mu_0,\eta_0))\right)\leqslant 0$$

3. V is a viscosity solution of (4.38) if it is both a supersolution and a subsolution and if it satisfies the final condition (4.38b).

A.6.2 Regularity

For sake of clarity, let us denote: $x=(\mu,\eta)$, $x'=(\mu',\eta')\in\mathbb{R}^n\times\mathbb{R}$, $\beta:=(\alpha,\lambda)\in\mathscr{B}$ where $\mathscr{B}:=\mathscr{A}\times\Lambda$, $y_x^\beta(\cdot):=(\xi_\mu^\beta(\cdot),z_\eta^\beta(\cdot))$ and $h(y):=g(\xi)-z$. By using the definition of $\widehat{w}$ and the following inequalities:

$$\max(A,B)-\max(C,D)\leqslant\max(A-C,B-D),\qquad \inf A_\alpha-\inf B_\alpha\leqslant\sup(A_\alpha-B_\alpha)\tag{A.21}$$

Then for $\tau\in[0,T]$, one has:

$$\begin{aligned}\widehat{w}(\tau,x)-\widehat{w}(\tau,x')&\leqslant\sup_{\beta\in\mathscr{B}}\left(\max\left(h(y_x^\beta(\tau))-h(y_{x'}^\beta(\tau)),\sup_{\theta\in[0,\tau]}(r(\xi_\mu^\beta(\theta))-r(\xi_{\mu'}^\beta(\theta)),\psi(\xi_\mu^\beta(\tau))-\psi(\xi_{\mu'}^\beta(\tau))\right)\right)\\&\leqslant\sup_{\beta\in\mathscr{B}}\left(\max\left(L_h.\|y_x^\beta(\tau)-y_{x'}^\beta(\tau)\|,L_r.\sup_{\theta\in[0,\tau]}\|\xi_\mu^\beta(\theta))-\xi_{\mu'}^\beta(\theta)\|,L_\psi.\|\xi_\mu^\beta(\tau))-\xi_{\mu'}^\beta(\tau)\|\right)\right)\end{aligned}$$

where L_h, L_r and L_ψ are respectively the Lipschitz constants of h, r and ψ. By the assumptions $(\mathscr{H}_1)-(\mathscr{H}_2)$ of the chapter 4, $\|y_x^\beta(\tau)-y_{x'}^\beta(\tau)\|\leqslant e^{L.T}\|x-x'\|$ (where $L>0$ is the Lipschitz constant of $\widehat{f}:=(\lambda.f,-\lambda.f^0)$) and for any $\theta\in[0,\tau]$, $\|\xi_\mu^\beta(\theta)-\xi_{\mu'}^\beta(\theta)\|\leqslant e^{L_f.T}\|\mu-\mu'\|$.

Consequently, one obtains: $\widehat{w}(\tau,x)-\widehat{w}(\tau,x')\leqslant\max(L_h,L_r,L_\psi).e^{L.T}\|x-x'\|$.

On the other hand, let us take $x=(\mu,\eta)$ and $\tau\in[0,t]$. By remarking that $\widehat{w}(t-\tau,x)\geqslant r(\mu)$ (from

the definition of $\widehat{w}$), we have, by using the DPP:

$$\begin{aligned}
\widehat{w}(t-\tau,x)-\widehat{w}(t,x) &= \inf_{\beta}(\widehat{w}(t-\tau,x)\vee r(\mu))-\inf_{\beta}(\widehat{w}(t-\tau,y_x^{\beta}(\tau))\vee \sup_{\theta\in[0,\tau]} r(\xi_{\mu}^{\beta}(\theta)))\\
&\leqslant \sup_{\beta}\left(\widehat{w}(t-\tau,x)\vee r(\mu)-\widehat{w}(t-\tau,y_x^{\beta}(\tau))\vee \sup_{\theta\in[0,\tau]} r(\xi_{\mu}^{\beta}(\theta))\right)\\
&\leqslant \sup_{\beta}\max\left(\widehat{w}(t-\tau,x)-\widehat{w}(t-\tau,y_x^{\beta}(\tau)),\ \sup_{\theta\in[0,\tau]}\left(r(\mu)-r(\xi_{\mu}^{\beta}(\theta))\right)\right)\\
&\leqslant \sup_{\beta}\max\left(\underbrace{\widehat{w}(t-\tau,x)-\widehat{w}(t-\tau,y_x^{\beta}(\tau))}_{=\mathrm{A}},\mathrm{K}_r.\sup_{\theta\in[0,\tau]}\left(\mu-\xi_{\mu}^{\beta}(\theta)\right)\right)
\end{aligned}$$

From what precedes, one has $\mathrm{A}\leqslant\max(\mathrm{L}_h,\mathrm{L}_r,\mathrm{L}_\psi).e^{\mathrm{L}.\mathrm{T}}\|y_x^{\beta}(\tau)-x\|$. Furthermore, by denoting $\mathrm{C}:=\max_{\beta\in\mathscr{B}}\|\widehat{f}(0,\beta)\|$, we have $\|\widehat{f}(x,\beta)\|\leqslant \mathrm{C}+\mathrm{L}.\|x\|$ and then from the Gronwall estimate, $\|y_x^{\beta}(\tau)-x\|\leqslant (\mathrm{C}+\mathrm{L}.\|x\|)e^{\mathrm{L}.\mathrm{T}}.\tau$. We have the same type of upper bound for the other term. Therefore, we can conclude that $\widehat{w}(t',x)-\widehat{w}(t,x)\leqslant \mathrm{C}.(1+\|x\|).|t'-t|$ for some constant $\mathrm{C}>0$. Finally, combining all the inequalities above, we get:

$$\widehat{w}(t,x)-\widehat{w}(t',x')\leqslant \mathrm{R}.(1+\|x\|).(\|x'-x\|+|t'-t|) \tag{A.24}$$

for some $\mathrm{R}>0$ which ends the proof.

A.6.3 Existence

First we prove that $\widehat{w}$ is a super-solution of (4.38a):
Let us consider a test function $\phi\in\mathrm{C}^1([0,\mathrm{T}]\times\mathbb{R}^n\times\mathbb{R})$ such that $\widehat{w}-\phi$ attains a local minimum at (t,μ,η). This implies that for some $r>0$:

$$\widehat{w}(t,\mu,\eta)-\widehat{w}(t',\mu',\eta')\leqslant\phi(t,\mu,\eta)-\phi(s,\mu',\eta') \tag{A.25}$$

for $|t-t'|\leqslant r$, $|\mu-\mu'|\leqslant r$ and $|\eta-\eta'|\leqslant r$.
For any $\epsilon>0$, from the inequality "$\geqslant$", in the DPP, we have:

$$\widehat{w}(t,\mu,\eta)\geqslant \inf_{(\xi,z)\in\widehat{\mathrm{S}}_{[0,\tau]}(\mu,\eta)}\widehat{w}\left(t-\tau,\xi(\tau),z(\tau)\right)\text{ for any }\tau\in[0,t[\tag{A.26}$$

There exist an ϵ-optimal couple $\bar{\alpha}=\bar{\alpha}(\epsilon,\tau)$ and $\bar{\lambda}=\bar{\lambda}(\epsilon,\tau)$ such that:

$$\widehat{w}(t,\mu,\eta)\geqslant \widehat{w}\left(t-\tau,\bar{\xi}(\tau),\bar{z}(\tau)\right)-\epsilon.\tau \tag{A.27}$$

For $\tau>0$ small enough, we have $\|\bar{\xi}(\tau)-\mu\|\leqslant r$ and $|\bar{z}(\tau)-\eta|\leqslant r$ and consequently:

$$-\epsilon.\tau\leqslant\widehat{w}(t,\mu,\eta)-\widehat{w}(t-\tau,\bar{\xi}(\tau),\bar{z}(\tau))\leqslant\phi(t,\mu,\eta)-\phi(t-\tau,\bar{\xi}(\tau),\bar{z}(\tau)) \tag{A.28}$$

By denoting $h(\tau):=\phi(t-\tau,\bar{\xi}(\tau),\bar{z}(\tau))$ and dividing the above inequality by $\tau>0$ we obtain:

$$\frac{h(0)-h(\tau)}{\tau}\geqslant-\epsilon \tag{A.29}$$

Now we express h as follows:

$$h(\tau)=h(0)+\int_0^{\tau}h'(\theta)d\theta \tag{A.30a}$$

$$=h(0)+\int_0^{\tau}\left(\bar{\mathrm{A}}(\theta)+\bar{\lambda}(\theta).(\bar{\mathrm{B}}(\theta)+\bar{\mathrm{C}}(\theta))\right)d\theta \tag{A.30b}$$

where:

$$\begin{aligned}
\bar{A}(\theta) &:= -\frac{\partial \phi}{\partial t}\left(t-\theta, \bar{\xi}(\theta), \bar{z}(\theta)\right) \\
\bar{B}(\theta) &:= D_{\mu}\phi\left(t-\theta, \bar{\xi}(\theta), \bar{z}(\theta)\right).f\left(\bar{\xi}(\theta), \bar{\alpha}(\theta)\right) \\
\bar{C}(\theta) &:= -D_{\eta}\phi\left(t-\theta, \bar{\xi}(\theta), \bar{z}(\theta)\right).f^{0}\left(\bar{\xi}(\theta), \bar{\alpha}(\theta)\right)
\end{aligned}$$

By denoting:

$$\begin{aligned}
\bar{B}^{\alpha}(\theta) &:= D_{\mu}\phi\left(\star-\theta, \bar{\xi}(\theta), \bar{z}(\theta)\right).f\left(\bar{\xi}(\theta), \alpha\right) \\
\bar{C}^{\alpha}(\theta) &:= -D_{\eta}\phi\left(\star-\theta, \bar{\xi}(\theta), \bar{z}(\theta)\right).f^{0}\left(\bar{\xi}(\theta), \alpha\right)
\end{aligned}$$

one obtains:

$$\begin{aligned}
\frac{h(0)-h(\tau)}{\tau} &= \frac{1}{\tau}\int_{0}^{\tau} -\bar{A}(\theta)d\theta + \frac{1}{\tau}\int_{0}^{\tau} \bar{\lambda}(\theta)\left(-\bar{B}(\theta)-\bar{C}(\theta)\right)d\theta \\
&\leqslant \frac{1}{\tau}\int_{0}^{\tau} -\bar{A}(\theta)d\theta + \frac{1}{\tau}\int_{0}^{\tau} \sup_{(\lambda,\alpha)}\left[\lambda(\theta).\left(-\bar{B}^{\alpha}(\theta)-\bar{C}^{\alpha}(\theta)\right)\right]d\theta \\
&\leqslant \frac{1}{\tau}\int_{0}^{\tau} -\bar{A}(\theta)d\theta + \frac{1}{\tau}\int_{0}^{\tau} \max\left(0, \sup_{\alpha}\left(-\bar{B}^{\alpha}(\theta)-\bar{C}^{\alpha}(\theta)\right)\right)d\theta
\end{aligned}$$

Now by letting $\tau \to 0$, as $\bar{\xi}(\theta) \to \mu$ and $\bar{z}(\theta) \to \eta$, one obtains:

$$-\epsilon \leqslant \frac{\partial \phi}{\partial t}(t,\mu,\eta) + \mathscr{H}\left(\mu, D_{\mu}\phi(t,\mu,\eta), D_{\eta}\phi(t,\mu,\eta)\right) \tag{A.34}$$

where $\mathscr{H}(\mu,p,q) := \max\left(0, \sup_{a\in A}\left(-f(\mu,a).p + f^{0}(\mu,a).q\right)\right)$.

By arbitrariness of $\epsilon > 0$, we obtain the following inequality:

$$\frac{\partial \phi}{\partial t}(t,\mu,\eta) + \mathscr{H}\left(\mu, D_{\mu}\phi(t,\mu,\eta), D_{\eta}\phi(t,\mu,\eta)\right) \geqslant 0 \tag{A.35}$$

in the viscosity sense. Moreover, by definition of $\widehat{w}$, we have:

$$\widehat{w}(t,\mu,\eta) \geqslant \inf_{(\xi,z)\in\widehat{S}_{[0,t]}(\mu,\eta)} \sup_{s\in[0,t]} r(\xi(s)) \geqslant r(\mu) \tag{A.36}$$

Combining the two last inequalitites, we obtain:

$$\min\left(\partial_{t}\widehat{w} + \mathscr{H}\left(\mu, D_{\mu}\widehat{w}, D_{\eta}\widehat{w}\right), \widehat{w} - r\right) \geqslant 0 \tag{A.37}$$

Second we prove that $\widehat{w}$ is a sub-solution of (4.38a):

We remark that is $\widehat{w}(t,\mu,\eta) \leqslant r(\mu)$, then we have easily:

$$\min\left(\partial_{t}\widehat{w} + \mathscr{H}\left(\mu, D_{\mu}\widehat{w}, D_{\eta}\widehat{w}\right), \widehat{w} - r\right) \leqslant 0 \tag{A.38}$$

Now, assume that $\widehat{w}(t,\mu,\eta) > r(\mu)$. By continuity of $\widehat{w}$ and r, there exists $\tau > 0$ such that for any $(\xi,z) \in \widehat{S}_{[0,\tau]}(\mu,\eta)$, $\widehat{w}(t-\theta,\xi(\theta),z(\theta)) > r(\xi(\theta))$, for all $\theta \in [0,\tau]$ (as $\xi(\theta)$ and $z(\theta)$ will remain in the neighborhood of respectively μ and η). Hence by exploiting the DPP (4.37), we get that:

$$\widehat{w}(t,\mu,\eta) = \min_{(\xi,z)\in\widehat{S}_{[0,\tau]}(\mu,\eta)} \widehat{w}\left(t-\tau, \xi(\tau), z(\tau)\right) \tag{A.39}$$

Let us now consider a test function $\phi \in C^1([0,T]\times\mathbb{R}^n\times\mathbb{R})$ such that $\widehat{w}-\phi$ attains a local maximum at (t,μ,η). This implies that for some $r>0$:

$$\phi(t,\mu,\eta)-\phi(t',\mu',\eta') \leqslant \widehat{w}(t,\mu,\eta)-\widehat{w}(t',\mu',\eta') \tag{A.40}$$

for $|t-t'|\leqslant r$, $|\mu-\mu'|\leqslant r$ and $|\eta-\eta'|\leqslant r$.
Let us take $(\alpha,\lambda)\in\mathscr{A}\times\Lambda$, such that $\alpha\equiv a$, $\lambda\equiv l$. For τ small enough, one has $\|\xi(\tau)-\mu\|\leqslant r$ and $|z(\tau)-\eta|\leqslant r$, thus:

$$\phi(t,\mu,\eta)-\phi(t-\tau,\xi(\tau),z(\tau)) \leqslant \widehat{w}(t,\mu,\eta)-\widehat{w}(t-\tau,\xi(\tau),z(\tau)) \leqslant 0$$

by exploiting the DPP. By dividing by τ and using the previous notations we obtain:

$$\frac{1}{\tau}\int_0^\tau -A(\theta)\,d\theta+\frac{1}{\tau}\int_0^\tau \lambda(\theta).(-B(\theta)-C(\theta))\,d\theta\leqslant 0 \tag{A.41}$$

if we let $\tau\to 0$, we obtain:

$$\frac{\partial\phi}{\partial t}(t,\mu,\eta)+l.\left(-D_\mu\phi(t,\mu,\eta).f(\mu,a)+D_\eta\phi(t,\mu,\eta).f^0(\mu,a)\right)\leqslant 0 \tag{A.42}$$

By taking the supremum over $(a,l)\in A\times[0,1]$ on the left side of the above inequality, one gets:

$$\frac{\partial\phi}{\partial t}(t,\mu,\eta)+\mathscr{H}\left(\mu,D_\mu\phi(t,\mu,\eta),D_\eta\phi(t,\mu,\eta)\right)\leqslant 0 \tag{A.43}$$

with $\mathscr{H}(\mu,p,q):=\max\left(0,\sup_{a\in A}(-f(\mu,a).p+f^0(\mu,a).q)\right)$.

This is the desired inequality in the viscosity sense.

Finally, one checks easily that by definition (4.33), $\widehat{w}$ checks the initial condition (4.38b) which ends the proof.

A.6.4 Uniqueness

The proof of the uniqueness of the solution can be found for instance in [3].

Appendix B

Acronym List

AMPL A Mathematical Programming Language. 60, 66, 68, 69, 85, 91, 99, 110

D Dubins. 18, 65–67, 69, 76, 81

DF Dubins-Fuller. 17, 18, 65, 73, 81, 82, 89

DPP Dynamic Programming Principle. 34, 60, 94–96, 114

ENO Essentially Non Oscillatory. 98, 106

F Fuller. 18, 65, 76

GPS Global Positionning System. 43

HJB Hamilton Jacobi Bellman. 7, 13, 18, 93–96, 98, 99, 101, 102, 105, 107, 108, 110–112, 115, 121

INU Inertial Navigation Unit. 43

IPOPT **I**nterior **P**oint **OPT**imizer. 60, 66, 68, 69, 85, 91, 99, 110

KKT Karush Kuhn Tucker. 25, 31

LQ Linear Quadratic. 5, 14, 15, 24, 26, 34, 111, 112

MDP Mission Data Preparation. 44

PDE Partial Differential Equations. 13, 107, 115

PIP Predicted Interception Point. 43

PMP Pontryagin Maximum Principle. 13–15, 17, 21, 26, 31, 57–62, 68, 72, 82, 90, 91, 94, 101, 116

Bibliography

[1] Roc-hj solver: reachability and optimal control solver. http://itn-sadco.inria.fr/itn-sadco.inria.fr/software/ROC-HJ.html. 18, 98

[2] Y. Sachkov A. Agrachev. *Control theory and optimization, II, Control Theory from the Geometric Viewpoint*. Encyclopaedia of Mathematical Sciences, vol. 87. Springer, Berlin, 2004. 58, 59

[3] H. Zidani A. Altarovici, O. Bokanowski. *A general Hamilton Jacobi framework for non linear state-constrained control problems*. ESAIM Control, optimisation and Calculus of Variation. 1999. 18, 104, 125

[4] H. Zidani A. Altarovici, O. Bokanowski. *Reachability and minimal times for state constrained nonlinear problems without any controllability assumption*. SIAM J. Control and Optim., 48 (2010), pp. 4292-4316. 1999. 18, 95, 106, 108

[5] P. F. Gath A. Calise. *Optimization of launch vehicle ascent trajectories with path constraints and coast arcs*. vol. 2, no. 24, p. 296-304. Journal of Guidance, Control, and Dynamics, 2001. 17

[6] S. Lee A. Calise, N. Melamed. *Design and evaluation of a three-dimensional optimal ascent guidance algorithm*. Vol. 21, No. 6, p. 867-875. Journal of Guidance, Control, and Dynamics, 1998. 17

[7] Y. C. Cho A. E. Bryson. *Applied optimal control*. Hemisphere Publishing Corp. Washington, D.C, 1975. 101

[8] E. Zuazua A. Porretta. *Long time versus steady state optimal control*. 51(6):4242–4273. SIAM J. Control Optim, 2013. 14

[9] E. Zuazua A. Porretta. *Remarks on long time versus steady state optimal control*. volume 15 of Springer INdAM Ser pages 67–89. Mathematical paradigms of climate science, 2016. 14

[10] L. T. Biegler A. Wächter. *On the implementation of the interior point filter-line search algorithm for large scale nonlinear programming*. Math. Program., 106. 2006. 60, 66

[11] M. Arisawa. *Ergodic problem for the Hamilton Jacobi-Bellman equation i. existence of the ergodic attractor*. vol. 14, Elsiever, 415-438. Annales de l'Institut Henri Poincaré, Nonlinear Analysis, 1997. 13, 20

[12] E. Trélat B. Bonnard. *On the role of abnormal minimizers in SR-geometry*. Ann. Fac. Sci. Toulouse (6), 10(3), 405-491. 2001. 62

[13] E. Trélat B. Bonnard, J-B. Caillau. *Second order optimality conditions in the smooth case and applications in optimal control*. 13(2), 207-236. ESAIM Control Optim. Calc. Var., 2007. 58, 59, 62

[14] M. Chyba B. Bonnard. *Singular trajectories and their role in control theory*. vol. 40. Mathématiques et Applications, 2003. 59

[15] B. Maschke B. Brogliato, R. Lozano and O. Egeland. *Dissipative systems analysis and control.* Springer-Verlag London, Ltd, 2006. 34, 112

[16] J. T. Betts. *Practical methods for optimal control and estimation using nonlinear programming.* Adv. Des. Control, vol. 19, second edition. SIAM, Philadelphia, PA, 2010. 17, 60, 67

[17] H. Brezis. *Functional analysis, Theory and applications.* Dunod, 2005. 35

[18] D. Pighin E. Zuazua C. Esteve, H. Kouhkouh. *On the turnpike property and the long time behavior of the Hamilton-Jacobi equation.* HAL-02873544v1, 2020. 14

[19] L. Cesari. *Optimization – theory and applications. Problems with ordinary differential equations.* Applications of Mathematics. Springer-Verlag, 1983. 31, 57

[20] F. Clarke. *Optimisation and nonsmooth analysis.* Canadian Mathematical Society Series of monographs and advanced texts. John Wiley & Sons, Inc., New York, 1983. 101

[21] A. V. Dmitruk and A. M. Kaganovich. *The Hybrid Maximum Principle is a consequence of Pontryagin Maximum Principle.* 57:964–970. Systems and Control Letters, 2008. 92

[22] A. V. Dmitruk and A. M. Kaganovich. *Maximum Principle for optimal control problems with intermediate constraints.* 22. Computational Mathematics and Modeling, 2011. 92

[23] P.V. Kokotovic .D.O. Anderson. *Optimal control problems over large time intervals.* 23 (3) 355-363. Automatica J. IFAC, 1987. 20, 21

[24] I. Capuzzo Dolcetta. *On a Discrete Approximation of the Hamilton-Jacobi Equation of Dynamic Programming.* 10, 367-377. Applied Mathematics & Optimization, 1983. 106

[25] L. E. Dubins. *On Curves of Minimal Length with a Constraint on Average Curvature, and with Prescribed Initial and Terminal Positions and Tangents.* Vol. 79, No. 3. American Journal of Mathematics, 1957. 18, 65

[26] P. Martinon E. Christiani. *Initialization of the shooting method via the Hamilton-Jacobi-Bellman approach.* 146, p. 321–346. Journal of Optimization Theory and Applications, 2010. 110

[27] G. Wanner E. Hairer, S.P. Norsett. *Solving Ordinary Differential Equations I : Nonstiff Problems.* Springer Series in Computational Mathematics. Springer Berlin Heidelberg, 2008. 68

[28] C. Zhang E. Trélat. *Integral and measure-turnpike properties for infinite-dimensional optimal control systems.* 30(1):Art. 3, 34. Math. Control Signals Systems, 2018. 14, 16

[29] E. Zuazua E. Trélat. *The turnpike property in finite-dimensional nonlinear optimal control.* Journal of Differential Equations, **258** no.1, 81-114. 2015. 14, 17, 20, 21, 25, 28, 66, 77

[30] E. Zuazua E. Trélat, C. Zhang. *Steady-state and periodic exponential turnpike property for optimal control problems in Hilbert spaces.* 56(2):1222–1252. SIAM J. Control Optim, 2018. 14

[31] K. Georg E.Allgower. *Numerical Continuation Methods.* Springer, Berlin, 1990. 62

[32] E. Trélat F. Bonnans, P. Martinon. *Singular arcs in the generalized Goddard problem.* J. Opt. Theory Appl. 139(2), 439–461. 2008. 16, 17, 18, 67, 76

[33] R.B. Vinter F.H. Clarke. *The relationship between the maximum principle and dynamic programming.* 25, pp. 1291–1311. SIAM J. Control Optim, 1987. 33

[34] R.B. Vinter F.H. Clarke. *Semiconcave Functions, Hamilton-Jacobi Equations and Optimal Control.* 25, pp. 1291–1311. Progr. Nonlinear Differential Equations Appl. 58, Birkhauser Boston, 2004. 33

[35] E. L. Fleeman. *Missile Design and System Engineering.* 2012. 48

[36] H. Frankowska. *Value Function in Optimal Control.* Summer School on Mathematical Control Theory, 2001. 33

[37] A.T. Fuller. *Study of an Optimum Non-Linear Control System.* vol. 15, no. 1, p 63-71. International Journal of Electronics, 1963. 18, 72

[38] P. Sougadinis G. Barles. *On the Large Time Behavior of Solutions of Hamilton-Jacobi Equations.* SIAM J. Math. Ana, 2000. 13, 20

[39] B.S Goh. *Necessary conditions for singular extremals involving multiple control variables.* vol. 40, 716-731. J. SIAM Control, 1966. 59

[40] L. N. Nguyen H. Frankowska. *Local Regularity of the Minimum Time Function.* 164, 68-91. Journal of Optimal Theory applications, 2015. 33

[41] L. A. Sheep J. A. Reeds. *Optimal Paths for a Car that goes both Forwards and Backwards.* Vol. 142; No 2. Pacific Journal of Mathematics, 1990. 65

[42] J. Gergaud J.-B. Caillau, O. Cots. *Differential pathfollowing for regular optimal control problems.* 27 (2), pp.177-196. Optimization Methods and Software, 2012. 17

[43] T. Haberkorn J. Gergaud. *Homotopy method for minimum consumption orbit transfer problem.* 12, pp.294-310. Optimisation and Calculus of Variations, 2006. 17

[44] H. Frankowska J-P. Aubin. *Set-Valued Analysis.* Birkhauser, Boston, Inc., Boston, MA, 1990. 33

[45] R.B. Vinter J.D.L. Rowland. *Construction of optimal feedback controls.* 16, 357-367. Systems & Control Letters, 1991. 106

[46] J.W. Hardtla J.E. Bradt, M.V. Jessick. *Optimal guidance for future space applications.* p. 87-2401. AIAA, 1987. 17

[47] H. K. Khalil. *Nonlinear Systems.* Prentice Hall, Upper Saddle River, 2016. 113

[48] A. Schiela L. Grune, M. Schaller. *Exponential sensitivity and turnpike analysis for linear quadratic optimal control of general evolution equations.* 2018. 14

[49] M.A. Müller L. Grüne. *On the relation between strict dissipativity and turnpike properties.* 90, 45-53. Systems Control Lett., 2016. 16, 32

[50] R. Guglielmi L. Grüne. *Turnpike properties and strict dissipativity for discrete time linear quadratic optimal control problems.* 56 no2, 1282-1302. SIAM J. Control Optim., 2018. 14, 16, 32

[51] C.F. Lin. *Modern navigation guidance and control processing.* Prentice Hall, Englewood Cliffs, 1991. 42

[52] P.L. Lions. *Generalized Solutions of Hamilton Jacobi Equations.* Springer Series in Computational Mathematics. Pitman, Boston, 1982. 115

[53] E. Trélat L.Rifford. *Morse-Sard type results in sub-Riemannian geometry.* 332, pp. 145–159. Math. Ann., 2005. 33

[54] E. Trélat L.Rifford. *On the stabilization problem for nonholonomic distributions.* 11 (2009), pp. 223–255. J. Eur. Math. Soc (JEMS), 2009. 33

[55] R.V. Gamkrelidze E.F. Mishchenko L.S. Pontryagin, V.G. Boltyanskii. *The mathematical theory of optimal processes.* J. Wiley & Sons, 1962. 26, 31, 58, 59

[56] I. Capuzzo-Dolcetta M. Bardi. *Optimal Control and Viscosity Solutions of Hamilton-Jacobi-Bellman Equations*. Modern Birkhäuser Classics, 1997. 13, 18, 20, 33, 95, 106, 114

[57] E. Trélat M. Cerf, T. Haberkorn. *Continuation from a flat to a round Earth model in the coplanar orbit transfer problem*. vol. 33, no. 6, p. 654-675. Optimal Control Appl. Methods, 2012. 17

[58] J. Zhu M. Cerf, E. Trélat. *Geometric optimal control and applications to aerospace*. Pacific Journal of Mathematics for Industry, 9(1):8. 2017. 18, 62, 78

[59] P.L. Lions M. Crandall. *Viscosity solutions of Hamilton Jacobi equations*. SOc, 277(1):1-42. Trans. Amer. Math, 1983. 106

[60] P.L. Lions M. Crandall. *High essentially non oscillatory schemes for Hamilton-Jacobi equations*. 28(4):907-922. SIAM J, Numer. Anal, 1991. 106

[61] C. Marcha. *Chattering arcs and chattering controls*. vol. 11, p. 441-468. Journal of Optimization Theory and Applications, 1973. 18, 72

[62] P. Martinon. *Numerical resolution of optimal control problems by a piecewise linear continuation method*. Ph.D. thesis. Institut National polytechnique de Toulouse, 2005. 76

[63] L. W. McKenzie. *Turnpike theorems for a generalized leontief model*. 31(1/2):165–180. Econometrica, 1963. 14

[64] V.F. Borisov M.I. Zelikin. *Optimal chattering feedback control*. vol. 114, p. 1227-1344. Journal of Mathematical Sciences, 2003. 18

[65] M. Bardi O. Alvarez. *Ergodic Problems in Differential Games*. AISDG,vol. 9. Annals of the International Society of Dynamic Games, 2000. 13, 20

[66] H. Frankowska P. Cannarsa. *Local regularity of the value function in optimal control*. 62, 791-794. System and Control Letters, 2013. 33

[67] J. Gergaud P. Martinon. *Using switching detection and variational equations for the shooting method*. 28, no. 2, 95–116. Optimal Cont. Appl. Methods, 2007. 17, 18, 76

[68] R. Dorfman P.A. Samuelson and R.M. Solow. *Linear Programming and Economic Analysis*. McGraw-Hill, New York, 1958. 14, 20

[69] J. Renault R. Buckdahn, M. Quincampoix. *On Representation Formulas for Long Run Averaging Optimal Control Problem*. 2015. 13

[70] B.W. Kerninghan R. Fourer, D.M. Gay. *AMPL: A modelling language for mathematical programming, second edition*. Encyclopaedia of Mathematical Sciences, vol. 87. Duxbury Press, 2002. 60, 66

[71] W. C. Rheinboldt. *Numerical continuation methods: a perspective*. J. Comput. Appl. Math 1(124), 229-244. 2000. 62

[72] H. M. Robbins. *A generalized Legendre-Clebsch condition for the singular case of optimal control*. Dev. 11, 361-372. IBM J Res., 1967. 59

[73] P. Kokotovic R.R. Wilde. *A dichotomy in linear control theory*. 17 (3) 382-383. IEEE Trans. Automat. Control, 2020. 25

[74] G. Siouris. *Missile Guidance and Control Systems*. 2003. 48, 49

[75] G. Stefani. *Regularity properties of the minimum time map*. Nonlinear Synthesis, Birkhauser, 1991. 33

[76] H. Sussmann. *The Markov-Dubins problem with angular acceleration control.* 2639–2643. Conf. Dec. Contr., San Diego, LA, USA, 1997. 65

[77] H. Sussmann. *Shortest 3-dimensional paths with a prescribed curvature bound.* 3306–3312. Conf. Dec. Contr., New Orleans, LA, USA, 1997. 65

[78] M. Stieler K. Worthmann T. Damm, L. Grüne. *An exponential turnpike theorem for dissipative discrete time optimal control problems.* 52, 1935-1957. SIAM J. Control Optim., 2014. 14, 16, 32

[79] C. Jones D. Bonvin T. Faulwasser, M. Korda. *On turnpike and dissipativity properties of continuous time optimal control problems.* 81, 297-304. Automatica J. IFAC, 2017. 14, 16, 32, 66

[80] J. Gergaud T. Haberkorn, P. Martinon. *Low thrust minimum-fuel orbital transfer: a homotopic approach.* 27, 6 (2004), 1046–1060. J. Guidance Cont. Dyn., 2004. 17, 18, 76

[81] E. Trélat. *Some properties of the value function and its level sets for affine control systems with quadratic cost.* J. Dyn. Control Systems 6(4), 511-541. 2000. 62

[82] E. Trélat. *Contrôle optimal: théorie et applications.* Concrètes. Mathématiques Concrètes, 2008. 16, 26, 31, 58

[83] E. Trélat. *Optimal control and applications to aerospace: some results and challenges.* J. optim. Theory, Appl. 3(154), 713-758. 2012. 17, 59, 61, 62, 78

[84] E. Trélat. *Linear turnpike theorem.* Math. Control Sign. Systems, 2023. 21, 22, 35, 66, 70

[85] L. T. Watson. *Theory of globally convergent probability-one homotopies for nonlinear programming.* SIAM. J. Optim 3(11), 761-780. 2001. 62

[86] J.C. Willems. *Dissipative dynamical systems, Part I: General Theory.* 45, 321-351. Arch. Ration. Mech. Anal., 1972. 15, 32, 112

[87] P. Zarchan. *Tactical and strategic missile guidance.* American Institute of Aeronautics and Astronautics, 2012. 48

[88] A. J. Zaslavski. *Turnpike theory of continuous-time linear optimal control problems.* vol. 104. Springer Optimization and Its Applications, 2015. 14